

**BARYON EFFECTIVE THEORIES AND PHENOMENOLOGY IN
THE $1/N_C$ EXPANSION**

A Dissertation

by

ISHARA PRIYASAD FERNANDO

Submitted to the Graduate College of Hampton University in
partial fulfillment of the requirements for the degree of

DOCTOR OF PHILOSOPHY

December 2017

This dissertation submitted by Ishara Priyasad Fernando in partial fulfillment of the requirements for the degree of Doctor of Philosophy at Hampton University, Hampton, Virginia is hereby approved by the committee under whom the work has been completed.

José L. Goity, Ph.D.
Committee Chair

Alberto Accardi, Ph.D.

Michael Kohl, Ph.D.

David Richards, Ph.D.

Christian Weiss, Ph.D.

Michelle Penn-Marshall, Ph.D.
Dean, The Graduate College

Date

Copyright by
ISHARA PRIYASAD FERNANDO
2017

ABSTRACT

Baryon Effective Theories and Phenomenology in the $1/N_c$ Expansion

(December 2017)

Ishara Priyasad Fernando, B.S., University of Colombo

Chair of Thesis Committee: Prof. José L. Goity

Chiral perturbation theory (ChPT) and the $1/N_c$ expansion provide systematic frameworks to investigate the strong interaction at low energy. There are two main focuses of this dissertation. First, analyzing the masses of baryons in the framework of the $1/N_c$ expansion, using the available physical masses and masses calculated in lattice QCD. Second, combining both ChPT and the $1/N_c$ expansion into a single framework and applying it to the phenomenology of baryons with three light-quark flavors. In the first focus, the baryon states are organized into irreducible representations of $SU(6) \times O(3)$, where the $[56, \ell^P = 0^+]$ contains the ground state and radially excited baryons, and the $[56, 2^+]$ and $[70, 1^-]$ contain orbitally excited states are analyzed. The analyses are carried out to $\mathcal{O}(1/N_c)$ and first order in the quark masses. The issue of state identifications is discussed. Numerous parameter independent mass relations and the famous Gell-Mann-Okubo (GMO) and Equal-Spacing (ES) relations are tested. Also, the quark mass dependence of the operator coefficients for baryon mass is discussed. In the second focus, a small scale expansion of the combined approach is defined as the ξ -expansion, in which the power counting of $1/N_c$ and chiral expansions are linked as $\mathcal{O}(p) = \mathcal{O}(1/N_c) = \mathcal{O}(\xi)$. A calculation of one-loop corrections to the ground state baryon masses, vector and axial-vector currents up to $\mathcal{O}(\xi^3)$ is presented. Moreover, the physical and lattice QCD masses are considered in order to understand the quark mass dependence, along with an analysis of the violations to GMO, ES and Gürsey-Radicati (GR) mass relations, and their dependence on N_c .

Dedicated to my parents.

ACKNOWLEDGEMENTS

First of all, I would like to express my heartfelt appreciation and gratitude to the chair of my committee, and my thesis advisor Professor José Goity for his guidance, encouragement, mentorship and support throughout this work. His enthusiasm and inspiration helped encourage my hard work, and helped develop my interest in hadronic physics in general, and in particular in effective theories.

I would like to thank my committee members, Dr. Alberto Accardi, Dr. Michael Kohl, Dr. David Richards and Dr. Christian Weiss for serving on my committee during their busy schedules. Their effort spent reading and providing valuable comments on the manuscript, is most appreciated. Special thanks are extended to Dr. Alvero Calle Cordón, Dr. Rubén Flores-Mendieta, Dr. Enrique Ruiz Arriola and Dr. José Manuel Alarcón Soriano for their collaboration and fruitful discussions. I would also like to thank my friend, Colin Egerer (graduate student from the College of William & Mary) for useful comments on the manuscript.

My special thanks are given to Dr. Paul Gueye (chair, Physics department), Dr. Donald Whitney (former chair) and everyone in the Hampton University (HU) Physics family. I am grateful for Dr. Michelle Penn-Marshall, Mrs. Kristie Cansler, and Mrs. Karen Rankin for their guidance and help with all the graduate college paperwork. It was a great privilege to be a “user” at the Thomas Jefferson National Accelerator Facility (JLab). I would like to thank everyone who mentored and supported me both at JLab and HU.

I cannot forget the international community at HU associated with the HU international office. I would like to thank all the staff members (current and former) at the

HU international office: Ms. Angela Boyd, Ms. Ebony Majeed, Mrs. Leah Pfitzinger, Mr. Nikola Mundzic, Mrs. Lisa Shroyer and Mrs. Georgiana Lau.

I am grateful for the Physics family at the University of Colombo. Their help and guidance while I was an undergraduate student was extremely valuable. In particular, I would like to thank Dr. S. R. D. Rosa, Dr. J. K. D. S. Jayanetti and Dr. K. A. I. L. Gamalath for their eminent guidance towards my higher studies in Physics. Moreover, I extend gratitude to all my teachers from my school, Prince Of Wales' College.

I am grateful for my colleagues and friends for their contribution, friendship and empathy through the happiest and saddest of times. Finally, and most importantly, I wish to thank my parents and my sister for standing by me throughout my academic career. Their patience and encouragement supported me in difficult times during this long journey, and helped empower me to achieve my goals. Their unconditional love, dedication and courage contributed greatly to the completion of this work.

This work was supported in part by DOE Contract No. DE-AC05-06OR23177 under which JSA operates the Thomas Jefferson National Accelerator Facility (J. L. G.), and by the National Science Foundation (USA) through grants PHY-0855789, PHY-1307413, and PHY-1613951 (I. P. F. and J. L. G.).

TABLE OF CONTENTS

Chapter		Page
1	INTRODUCTION	1
I	BARYON MASSES IN THE $1/N_c$ EXPANSION	6
2	$1/N_c$ EXPANSION AS AN EFT IN QCD	7
2.1	Introduction	7
2.2	Feynman diagrams for large N_c	11
2.3	Large N_c mesons	16
2.4	Large N_c baryons	19
2.5	Meson-baryon coupling	20
3	THE BARYON WAVE FUNCTION IN LARGE N_c	23
3.1	Introduction	23
3.2	Baryon wave function for three quarks	24
3.2.1	The spin-flavor part ($\psi_{\text{spin}}\psi_{\text{flavor}}$) of three quarks	24
3.2.2	The spatial wave function of three quarks	27
3.3	Generalization to large N_c with the Hartree picture	31
3.4	Ground state baryons in large N_c	36
3.5	Excited state baryons in large N_c	38
4	SPIN-FLAVOR SYMMETRY IN LARGE N_c BARYONS	41
4.1	Introduction	41
4.2	Large N_c consistency condition	42
4.3	Contracted spin-flavor algebra	44

Chapter	Page
4.4 Large N_c baryon multiplets	45
4.5 $1/N_c$ corrections	48
4.5.1 $1/N_c$ corrections to axial currents	49
4.5.2 $1/N_c$ corrections to baryon masses	51
5 BARYON OPERATORS IN THE $1/N_c$ EXPANSION	55
5.1 Introduction	55
5.2 Baryon operator expansion	56
5.3 Quark operator classification	59
5.4 Operator identities	62
5.5 An application : Baryon mass operator	66
5.5.1 Baryon masses in the $SU(3)$ symmetric limit	66
5.5.2 Baryon masses in the $SU(3)$ breaking limit	67
6 BARYON MASSES IN THE $1/N_c$ EXPANSION FRAMEWORK 70	70
6.1 Introduction	70
6.2 Baryon mass operators for spin-flavor multiplets in the $1/N_c$ expansion	73
6.3 $[56, 0^+]$ multiplet : ground states and excited states	76
6.3.1 Introduction to $[56, 0^+]$ multiplet	76
6.3.2 Mass operators in $[56, 0^+]$ multiplet	77
6.3.3 Mass relations for $[56, 0^+]$ multiplet	78
6.3.4 Fit results for $[56, 0^+]$ multiplet masses to data	80
6.4 $[56, 2^+]$ excited states	83
6.4.1 Introduction to $[56, 2^+]$ multiplet	83
6.4.2 Mass operators in $[56, 2^+]$ multiplet	83
6.4.3 Mass relations for $[56, 2^+]$ multiplet	84
6.4.4 Fit results for $[56, 2^+]$ multiplet masses to data	87

Chapter	Page
6.4.5	Mass predictions 89
6.5	$[\mathbf{70}, 1^-]$ excited states 90
6.5.1	Introduction to $[\mathbf{70}, 1^-]$ multiplet 90
6.5.2	Mass operators in $[\mathbf{70}, 1^-]$ multiplet 93
6.5.3	Mass relations for $[\mathbf{70}, 1^-]$ multiplet 97
6.5.4	Fit results for $[\mathbf{70}, 1^-]$ multiplet masses to data 100
6.6	Summary of the fits to baryon masses 108
6.7	Conclusions and discussion 111

II COMBINED EFT APPROACH: ChPT AND THE $1/N_c$ EXPANSION 113

7	CHIRAL PERTURBATION THEORY AS AN EFT IN QCD . . 114
7.1	Introduction 114
7.2	Symmetries of \mathcal{L}_{QCD} 115
7.2.1	Global $U(1)_V$ symmetry 115
7.2.2	Global $U(1)_A$ symmetry 116
7.2.3	Isospin $SU(2)_f$ symmetry 116
7.2.4	$SU(3)_f$ symmetry 117
7.2.5	Chiral symmetry 118
7.2.6	Symmetry breaking due to quark mass 121
7.2.7	QCD in the presence of external fields and PCAC 123
7.3	Construction of effective field theories 125
7.4	Meson Chiral Perturbation Theory 127
7.4.1	Construction of the effective Lagrangian 131
7.4.2	The lowest-order effective Lagrangian 133

Chapter	Page
7.4.3	Explicit symmetry breaking due to quark mass 135
7.4.4	Higher order effective Lagrangians 138
7.4.5	The chiral effective Lagrangian at order $\mathcal{O}(p^4)$ 140
7.4.6	Application : Goldstone boson masses to $\mathcal{O}(p^4)$ 141
7.5	Baryon Chiral Perturbation Theory 147
7.5.1	The leading order meson-baryon chiral Lagrangian 150
7.5.2	An application at tree level : Goldberger-Treiman relation . . 152
7.6	Heavy Baryon Approach 154
7.6.1	Power counting scheme in HBChPT 154
7.6.2	Octet baryons in HBChPT 155
7.6.3	Decuplet baryons in HBChPT 158
7.6.4	Most general Lagrangian at lowest order 160
8	COMBINED EFFECTIVE THEORY OF THE $1/N_c$ AND CHIRAL EXPANSIONS 161
8.1	Introduction 161
8.2	Foundation of the Effective Lagrangian 163
8.2.1	Building blocks of the effective Lagrangian 164
8.2.2	Properties of the effective Lagrangian 166
8.3	Interactions from the effective Lagrangians 167
8.3.1	Meson Lagrangian 167
8.3.2	Baryon effective Lagrangians of $\mathcal{O}(\xi)$, $\mathcal{O}(\xi^2)$ and $\mathcal{O}(\xi^3)$. . . 168
8.4	ξ power counting 172
8.5	One-loop correction to the baryon self-energy 175
8.6	One-loop corrections to the baryon currents 181

9 GROUND STATE BARYON MASSES FROM THE COMBINED FRAMEWORK	186
9.1 Introduction	186
9.2 Baryon mass at leading order	187
9.3 One-loop correction to the baryon mass	188
9.4 Corrections to baryon mass relations	191
9.4.1 Gell-Mann-Okubo (GMO) relation	191
9.4.2 Equal Spacing (ES) relation	193
9.4.3 Gürsey-Radicati (GR) relation	194
9.5 Fits to the baryon spectrum	196
9.5.1 Individual fits : physically (experimentally) measured masses .	197
9.5.2 Individual fits : LQCD baryon masses	198
9.5.3 Combined fits to the lattice QCD masses	201
9.6 Predictions on sigma terms	205
9.7 Conclusions and discussion	206
10 BARYON CURRENTS (VECTOR AND AXIAL-VECTOR) FROM THE COMBINED APPROACH	208
10.1 Introduction	208
10.2 Vector currents: charges	210
10.3 Axial couplings	214
10.3.1 Fits to LQCD Results	219
11 CONCLUSIONS AND PERSPECTIVES	224
REFERENCES	228

APPENDICES

A	SPIN-FLAVOR ALGEBRA AND OPERATOR BASES	242
A.1	Matrix elements of spin-flavor generators	243
A.2	Bases of spin-flavor composite operators	244
B	BUILDING BLOCKS FOR THE EFFECTIVE LAGRANGIANS	247
C	LOOP INTEGRALS	249
C.1	Specific integrals	250
D	USEFUL OPERATOR REDUCTION FORMULAS	253
	VITA	255

LIST OF TABLES

Table	Page
2.1 Quark masses in the $\overline{\text{MS}}$ renormalization scheme at a scale of $\mu = 2 \text{ GeV}$.	8
3.1 Symmetric flavor states of three quarks : baryon decuplet.	26
3.2 Mixed-symmetric flavor states of three quarks : baryon octet.	26
3.3 Antisymmetric flavor state of three quarks : baryon singlet.	26
5.1 $SU(2N_f)$ identities : Transformation properties of the identities under $SU(2) \times SU(N_f)$ are given in the second column.	65
6.1 Ground state (left), and $[56, 0^+]$ excited Roper (right) baryon masses in MeV. The inversion in the ordering of the masses of the $\Xi_{1/2}$ and the Δ masses at and above $M_\pi = 391 \text{ MeV}$ is similar to that observed in other LQCD calculations.	78
6.2 Mass relations for the ground state octet and decuplet. The relations are valid up to corrections $\mathcal{O}(\epsilon^2/N_c)$ in the case of the GMO and EQS relations, and up to $\mathcal{O}(\epsilon/N_c^2)$ for the rest.	79
6.3 Mass relations for the Roper multiplet. The relations hold at the same orders as in the case of the ground state baryons.	79
6.4 Coefficients of the GR mass formula for the ground state baryons. The case $M_\pi = 702 \text{ MeV}$ corresponds to exact $SU(3)$ symmetry. χ_{dof}^2 is the χ^2 per degree of freedom.	81
6.5 Fit to the $[56, 0^+]$ excited Roper baryons. It is found that the $SU(3)$ breaking effects on the HF interactions can be neglected, thus $b_2 = 0$ throughout.	81
6.6 Predictions of physically unknown states in the Roper multiplet.	82
6.7 Matrix elements of $SU(3)$ singlet operators (top) and $SU(3)$ breaking operators (bottom). Here, $a_S = 1, -2/3$ for $S = 3/2, 5/2$, respectively and $b_S = 1, 2/3, 1/9, -2/3$ for $S = 1/2, 3/2, 5/2, 7/2$, respectively. . .	84

Table	Page
6.8 The input baryon masses (physical and LQCD) corresponding to the $[56, 2^+]$ multiplet. The experimental values are those for baryons with a three star or higher rating by the PDG.	85
6.9 Mass relations for the $[56, 2^+]$ multiplet. The relations hold at the same orders as in the case of the ground state baryons.	86
6.10 Two fits, with (second column) and without (third column) the operators B_2 and B_3 (see Table (6.7)). The second fit does not describe well the physical baryons.	88
6.11 Predictions of physically unknown states in the $[56, 2^+]$ multiplet, and suggested identifications with PDG listed states. The first two GMO relations and the 12^{th} equation in Table (6.9), which is a large N_c parameter independent mass relation, were used to predict the above masses.	90
6.12 Mass operator basis and matrix elements for the $[20, 1^-]$ multiplet. . .	94
6.13 $SU(3)$ singlet basis of operators for the $[70, 1^-]$ masses.	95
6.14 $SU(3)$ octet basis of operators for the $[70, 1^-]$ masses.	96
6.15 $[70, 1^-]$ masses. The experimental values are those for baryons with a three star or higher rating by the PDG.	98
6.16 GMO and ES relations for the $[70, 1^-]$ multiplet. Due to the insufficient number of physically known states with three or more stars, the mass relations for physical states cannot be checked for the physical case. . .	99
6.17 Octet-Decuplet mass relations for the $[70, 1^-]$ multiplet. S_B is the mass splitting between the state B and the non-strange states in the $SU(3)$ multiplet to which it belongs. The results shown correspond to the relation divided by the sum of the positive coefficients in the relation (e.g., 163 for the first relation).	99
6.18 Fits to the non-strange $[20, 1^-]$ baryon masses. Unless the mixing angles are inputs to the fit, the operator O_8 is not necessary due to linear dependence as there are only seven mass inputs to fit. For the physical case with seven parameter fit (second column), the mixing angles from the global analysis ($\theta_{N_{1/2}}=0.49\pm0.29$, $\theta_{N_{3/2}}=3.01\pm0.17$) were used as inputs. For the minimal fit (third column) with c_1, c_5, c_6 , the mixing angles in the physical case are not inputs.	101

Table	Page
6.19 Fit to the $[70, 1^-]$ masses using a subset of operators chosen as a minimal subset such the χ^2_{dof} is acceptable for all input sets. For the physical case the mixing angles from the global analysis ($\theta_{N_{1/2}}=0.49\pm0.29$, $\theta_{N_{3/2}}=3.01\pm0.17$) were used as inputs.	103
6.20 Fit results with minimal set of mass operators for the $[70, 1^-]$. Only masses are used as inputs.	103
6.21 Mixing angles in the $[70, 1^-]$ predicted from the fit to the masses. . . .	104
6.22 Predictions of physically unknown states in the $[70, 1^-]$ multiplet from the fit in Table (6.19).	107
7.1 Renormalized LECs L_i^r (empirical values) at the scale $\mu = m_\rho$	141
8.1 Vertices from the lowest order effective Lagrangians.	171
8.2 β functions for mass renormalization.	179
8.3 Projection operators for operator products of irreps of $SU(2)$	180
8.4 Projection tensors for the operator products of irreps. of $SU(3)$	180
8.5 One loop diagrams for the vector currents. The subscript of δm refers to either the intermediate baryon propagator δm_n or the incoming/outgoing $\delta m_{in/out}$ baryon propagator with respect to the current-vertex.	183
8.6 Axial-Vector Currents (I).	184
8.7 Axial-Vector Currents (II).	185
9.1 Partial contributions to the one-loop correction of the self-energy. . . .	190
9.2 Baryon masses : The first row corresponds to the physical measurements. The rest are the masses from LQCD calculations by Alexandrou <i>et al.</i> , each column corresponds to a specific lattice spacing (or β value) given in accordance with the Table (9.3).	197
9.3 LQCD parameters and the values of M_π and M_K (from Alexandrou <i>et al.</i>).	198
9.4 Fit results for the physically observed baryons (the baryon mass for a given spin, hyper-charge and iso-spin is given in the Eq. (9.16)).	198

Table	Page
9.5	Fit results of LECs to individual sets of baryon masses from LQCD (the baryon mass for a given spin, hyper-charge and iso-spin is given in the Eq. (9.16)). 199
9.6	Baryon masses obtained from the fits to LQCD data. Each line contains a set of baryon masses corresponding to their pion mass scale from LQCD. 200
9.7	Deviations from the mass relations using LQCD data (in black) Vs fitted masses (in blue) from the combined effective theory. 200
9.8	Results for LECs : first row fit to LQCD octet and decuplet baryon masses by Alexandrou <i>et al.</i> including results for $M_\pi \leq 300$ MeV, and second row including also the physical masses. Throughout the renormalization scale is $\mu = m_\rho$ 202
9.9	Deviations from mass relations in MeV. Here, $\Delta_{\text{ES1}} = m_{\Xi^*} - 2m_{\Sigma^*} + m_\Delta$ and $\Delta_{\text{ES2}} = m_{\Omega^-} - 2m_{\Xi^*} + m_{\Sigma^*}$ 203
10.1	β functions for counter terms contributing to the axial-vector currents. 218
10.2	LECs obtained by fitting to the LQCD results from Alexandrou <i>et al.</i> : here the choices are $\Lambda = m_\rho$ MeV and for the full NLO fit $\mu = m_\rho$ as well. The independence of the χ^2 on the choice of μ has been checked. In the NLO full fits \hat{g}_A is an input; three different reasonable values are included as example. 221
A.1	2-body identities for the $SU(6)$ generators acting on the irreducible representation $(N_c, 0, 0, 0, 0, 0)$ 245
A.2	2-body basis operators. 246
A.3	Operators of interest in the 3-body basis up to $\ell = 1$ 246

LIST OF FIGURES

Figure	Page
2.1 Summary of measurements of α_s as a function of the energy scale Q . . .	9
2.2 Double line notation of a gluon field.	12
2.3 Gluon-vacuum polarization.	12
2.4 Quark-gluon, three-gluons and four-gluons vertices.	13
2.5 Two-loop diagram.	14
2.6 Three-loop diagram.	14
2.7 A non-planar diagram.	14
2.8 An internal-quark-loop diagram.	14
2.9 A quark-loop inside a gluon loop.	15
2.10 Two-point correlator $\langle JJ \rangle$ of $\mathcal{O}(N_c)$. (a) Free field correlator. (b) Corrections to free field correlator.	16
2.11 Non-leading corrections to the two-point correlator $\langle JJ \rangle$. Diagram (b) is the double line notation of diagram (a).	16
2.12 Intermediate state contributing to $\langle JJ \rangle$	17
2.13 The dominant three meson diagram. The diagram on right hand side is in double line notation of the diagram on left hand side.	18
2.14 (a) meson coupling to same quark line. (b) meson coupling to two different quark lines.	21
2.15 Baryon meson scattering of $\mathcal{O}(N_c^0)$	21
3.1 Young diagram for the symmetric representation of large N_c baryon. . .	36

Figure	Page
3.2 Weight diagram for the $SU(3)$ flavor representation of the spin $1/2$ baryons. The long side of the weight diagram contains $\frac{1}{2}(N_c+1)$ weights. The numbers denote the multiplicity of the weights.	37
3.3 Weight diagram for the $SU(3)$ flavor representation of the spin $3/2$ baryons. The long side of the weight diagram contains $\frac{1}{2}(N_c-1)$ weights. The numbers denote the multiplicity of the weights.	38
4.1 Dominant diagrams for pion-nucleon scattering amplitude.	42
4.2 $B + \pi \rightarrow B + \pi + \pi$ scattering amplitude.	49
4.3 Hyperfine mass splitting of large N_c baryons.	53
5.1 (a): single quark operator insertion. (b) : single quark operator insertion with a one-gluon-exchange.	57
6.1 Evolution of the coefficients with M_π for the ground state baryons (left panel) and the Roper baryons (right panel).	81
6.2 Evolution of the operator coefficients with M_π for the two fits of the $[56, 2^+]$ masses.	89
6.3 Evolution of the minimum set of operator coefficients with M_π in $SU(4) \times O(3)$	100
6.4 Evolution with respect to M_π of the coefficients of the basis operators used to fit both the physical and the LQCD $[70, 1^-]$ masses.	105
6.5 Evolution with respect to M_π of the coefficients in Table (6.20).	106
6.6 At $M_\pi=139$ MeV (physical) : green colored boxes represent the physically unidentified states which were calculated using the mass relations and, the red colored line represents the corresponding baryon mass from the fit. Light-blue color represents the octets and light-yellow color represents a singlet (for the case of Λ) or decuplet (for the cases of Σ, Ξ).	108
6.7 Baryon spectrum for $M_\pi=391$ MeV with LQCD input from Edwards <i>et al.</i> and the fits from $1/N_c$ expansion framework. Light-blue color represents the octets and light-yellow color represents a singlet (for the case of Λ) or decuplet (for the cases of Σ, Ξ).	109
6.8 Baryon spectrum for $M_\pi=524$ MeV with LQCD input from Edwards <i>et al.</i> and the fits from $1/N_c$ expansion framework. Light-blue color	

Figure	Page
represents the octets and light-yellow color represents a singlet (for the case of Λ) or decuplet (for the cases of Σ, Ξ).	110
7.1 Unrenormalized meson propagator (light-gray color) as a sum of irreducible self-energy diagrams (dark-gray color).	142
7.2 Lowest-order contribution to the single-nucleon matrix element of the pseudoscalar density.	153
8.1 One-loop contribution to the self-energy of a baryon field.	175
9.1 The deviation of GMO relation with N_c	192
9.2 The deviation of ES1 and ES2 relation with N_c	194
9.3 The deviation of Gürsey-Radicati (GR) relation with N_c	195
9.4 The evolution of baryon masses obtained from the combined fit result (second row of Table (9.8)) with respect to the pion mass. The 67% confidence interval is represented by the band of light blue, and 95% confidence interval is represented by the band of light green. The red points with error bars are the calculations from LQCD (Alexandrou <i>et al.</i>).	204
10.1 Diagrams contributing to the 1-loop corrections to the vector charges.	213
10.2 Diagrams contributing to the 1-loop corrections to the axial vector currents.	215
10.3 The effect of switching off the contribution of the Δ in the loops (Cordon & Goity).	223

CHAPTER 1

INTRODUCTION

“Quantum Chromodynamics” (QCD) is the fundamental theory of strong interaction which describes the phenomenology of quarks and gluons [1–6]. Because the strong coupling (α_s) experiences a running behavior at low energy [7, 8], the perturbative expansion in terms of α_s is only possible at high energies. This observation leads to the fact that quarks are always confined into bound states called *hadrons* at low energies. In nature, these hadrons have been observed as either quark-antiquark pairs (mesons) or, three-quark bound states (baryons). In order to describe the phenomenology of hadrons, the so-called *effective* field theory approach has been established. This allows one to perform perturbative expansion in the low energy regime by considering hadrons as the degrees of freedom.

The starting point of the effective field theory approach was proposed by S. Weinberg [9] in 1979. The idea is to build the most general effective Lagrangian containing all the possible terms associated with the symmetry principles. In this work, *chiral symmetry* and the *spin-flavor symmetry* are combined together to build an effective theory to explore the baryon phenomenology. One needs to extract an expansion parameter with a power counting scheme in order to systematically expand the theory up to any desired order. In Chiral Perturbation Theory (ChPT), the expansion parameter is the momentum of Goldstone bosons divided by an energy scale. This power counting scheme was first proposed by S. Weinberg. $1/N_c$ also can be used as an expansion parameter in QCD [10], where N_c is the number of colors (experimentally, $N_c = 3$). Because of the emergence of the spin-flavor symmetry in QCD [11–14]

at large N_c , $1/N_c$ expansion has become not only a qualitative but also a quantitative tool to describe the physical observables in powers of $1/N_c$. An application of this framework to baryons was initially done by E. Witten [15], introducing the large N_c counting rules.

In the baryon sector, the $1/N_c$ expansion is implemented as an effective theory built in terms of effective operators associated with the observable to be analyzed. This framework has been successfully applied in the analysis of baryon masses, magnetic moments, axial-couplings, etc. For example, the ground state baryon mass operator in the $1/N_c$ expansion satisfy several well known mass relations, namely Gell-Mann-Okubo relations [16], Coleman-Glashow relations [17–19], and also the spin-flavor breaking Gürsey Radicati mass-relations [20]. In the resonance domain of the baryon spectrum, the corresponding symmetry for the excited baryons is $SU(2N_f) \times O(3)$, where $O(3)$ governs the spatial rotations and $SU(2N_f)$ is the spin-flavor symmetry group [21]. From the group theory point of view and without any loss of generality, low-lying excited baryons may be considered to be comprised of a *core* of $(N_c - 1)$ quarks in the ground state and one excited quark [22].

In general, spin-flavor symmetry is not exact for excited baryons even in the $N_c \rightarrow \infty$ limit, because the spin-flavor $SU(2N_f)$ symmetry is broken at $\mathcal{O}(N_c^0)$ [21]. This is identified in the constituent quark picture by the coupling of orbital angular momentum, which phenomenologically couples very weakly. The decoupling approach is more convenient in analyzing the mixed-symmetric baryon excited states, which belong to the $[70, 1^-]$ multiplet [21, 23, 24]. However, for the analysis of symmetric states, such as baryons belonging to $[56', 0^+]$ and $[56, 2^+]$ multiplets, there is no need to decouple the baryon wave function into a core and an excited quark [25, 26]. In this work, ground-state baryons in the **56**-plet and excited-state baryons in the $[56', 0^+]$,

$[56, 2^+]$ and $[70, 1^-]$ multiplets are analyzed [27] with the physical masses and masses calculated from lattice QCD [28, 29].

The main focus of this work is to combine these two effective theories: ChPT and $1/N_c$ expansion into a single framework and apply it to gain insight into the phenomenology of baryons. Notably, this is the first application to the baryon masses and currents made out of three light-quark flavors, or the case of $SU(3)_{\text{flavor}}$. Since the two expansions do not commute [30], they are linked by considering the size of baryon mass splittings of $\mathcal{O}(1/N_c)$ which is of $\mathcal{O}(p)$. This is called the ξ -expansion. Calculations have been performed up to one-loop correction with the inclusion of both octet and decuplet intermediate baryon states in the loop, to improve the convergence of the chiral expansion [31–36]. Another remarkable feature of this combined effective approach is it allows one to calculate the violations to the mass relations such as Gell-Mann-Okubo (GMO) relation, Equal Spacing (ES) relation and Gürsey-Radicati (GR) relation explicitly up to $\mathcal{O}(\xi^2)$, whereas GMO and ES relations are exact at tree-level for any finite N_c . In addition to the application to baryon masses, this framework has been applied in calculating the vector charges and axial-vector couplings in the case of $SU(3)$, and fits have been performed to lattice QCD (LQCD) results [37, 38].

This dissertation is divided as follows. The first part includes Chapters 2-6, which cover the $1/N_c$ expansion framework and its application to baryon masses. The second part includes Chapters 7-10, which present the combined framework of ChPT and $1/N_c$ and its applications to baryon masses and currents. Lastly, conclusions with future perspectives are presented, followed by four appendices. **Part I** of the dissertation starts with Chapter two, which is dedicated to introducing the $1/N_c$ expansion. The foundations and the development of the $1/N_c$ expansion framework

is discussed with applications to mesons and baryons. Chapter 3 is devoted to the baryon wave function in the large N_c limit. Starting with the description of the structure of a baryon with three valence quarks, the generalization to N_c number of quarks in a baryon is discussed systematically. Chapter 4 is devoted to the spin-flavor symmetry in large N_c baryons. This gives a brief overview of the emergence of the spin-flavor symmetry by studying baryon-meson scattering amplitudes, which leads to a consistency condition resulting in the existence of an infinite tower of degenerate baryon states. This chapter covers the contracted spin-flavor algebra resulting from the large N_c consistency conditions. Also, large N_c baryon representations as well as $1/N_c$ corrections to the baryon observables, such as masses and axial currents are covered. Chapter 5 is dedicated to baryon operators in the $1/N_c$ expansion. In this chapter, the fundamental building blocks of baryon operators in large N_c and the quark operator classification are discussed in detail, followed by operator identities which can be used to perform the operator reduction. An application to baryon mass operators is discussed considering the $SU(3)$ -symmetric and $SU(3)$ -breaking limits.

Chapter 6 is dedicated to baryon masses in the $1/N_c$ expansion framework. This chapter covers the work done on the “baryon spin-flavor structure from an analysis of lattice QCD results of the baryon spectrum” [27]. Baryon multiplets including ground states in the **56**-plet and excited-states in $[\mathbf{56}', 0^+]$, $[\mathbf{56}, 2^+]$ and $[\mathbf{70}, 1^-]$ multiplets are analyzed using $1/N_c$ baryon mass operators. The quark mass dependence of the baryon states corresponding to the considered baryon multiplets and the mixing angles have been addressed in this calculation. The multiplets $[\mathbf{56}', 0^+]$, $[\mathbf{56}, 2^+]$ and $[\mathbf{70}, 1^-]$ are discussed in separate subsections, each containing a discussion of mass operators, mass relations and fit results to the data. A summary of the fits is also given with conclusions and discussions of the study in the last sections of Chapter 6.

Part II of this dissertation starts with Chapter 7. It covers the foundations of chiral perturbation theory, pedagogically organized by constructing the effective Lagrangian for heavy baryon ChPT, including applications. The Chapters 8, 9, and 10 are dedicated to the combined effective framework of ChPT and the $1/N_c$ expansion. Chapter 8 covers the building blocks of the combined framework, whereas Chapters 9 and 10 cover the application of the combined framework to ground-state baryon masses and baryon currents, respectively. All the calculations are performed up to one-loop correction, and fits are performed to the available physical and LQCD data for masses, vector charges and axial-currents. The results of these analyses for baryon masses, vector charges and axial-couplings are discussed separately at the end of Chapters 9 and 10. The last chapter is dedicated to conclusions and discussions of the current study, and perspectives for future research are discussed. Any analytical or technical details related to some chapters are shown in the appendices.

Part I

BARYON MASSES IN THE $1/N_c$ EXPANSION

CHAPTER 2

1/N_C EXPANSION AS AN EFT IN QCD

2.1 Introduction

The fundamental degrees of freedom in QCD are quarks and gluons; which represent the *matter-field* and *force-field* of the strong interaction, respectively. To date, six flavors of quarks have been discovered: up- u , down- d , charm- c , strange- s , top- t , bottom- b . These flavors are organized into three types of families under weak interactions. First family: u & d , second family: c & s , third family: t & b . Quarks contain fractional electric charge: u, c, t quarks are $+2/3$, and d, s, b quarks are $-1/3$. The mass of a quark is just a parameter in the Lagrangian of the theory. The quark masses cannot be measured directly because they are not observed physically, this is due to the phenomena called “*confinement*”. Confinement is the property where quarks tend to bind themselves so strong at low energies into “*hadrons*”, although at very high energies quarks tend to interact less. They are determined indirectly through their influence on hadronic properties. The quark mass parameter behaves like a coupling constant in quantum field theory, depending on the momentum scale and the renormalization scheme to render finite values for the quark masses. In this work, the considered quark masses values were evaluated using the *dimensional regularization* method with the *modified minimal subtraction* (or $\overline{\text{MS}}$) scheme. The three quark flavors, up- u , down- d , strange- s quarks are identified as “*light quarks*”, and charm- c , top- t , bottom- b quarks can be identified as “*heavy quarks*” by comparing their masses in Table (2.1).

Table 2.1. Quark masses in the $\overline{\text{MS}}$ renormalization scheme at a scale of $\mu = 2 \text{ GeV}$.

Quark flavor:	up	down	charm	strange	top	bottom
Mass:	1.5-4 MeV	4-8 MeV	$\sim 1.25 \text{ GeV}$	$\sim 100 \text{ MeV}$	$\sim 175 \text{ GeV}$	$\sim 4.25 \text{ GeV}$
Electric charge:	$+2/3$	$-1/3$	$+2/3$	$-1/3$	$+2/3$	$-1/3$

Quarks carry an additional quantum number called, “color”. The color quantum number was initially suggested by Greenberg, *et al.* [5]. Color serves as the charge of QCD. The behavior of the color charge is very different than the electric charge. The electric charge is a scalar quantity in the sense that the total charge of an electric system is simply the algebraic sum of individual charges, whereas the color charge is a quantum vector charge (a concept similar to spin angular momentum in quantum mechanics). The total color charge of a system must be obtained by combining the individual color charges of the constituents according to group theoretic rules (analogous to combining angular momenta in quantum mechanics).

Gluons are the quanta of the color field that binds quarks into baryons and mesons. Chromodynamics is then a theory like electrodynamics, but with eight gluons instead of a single photon. As the gluons themselves carry a color charge, they can directly interact with each other. Theories in which field quanta may interact with each other are called non-Abelian. The local non-Abelian $SU(3)_{\text{color}}$ symmetry describes the interactions among quarks and gluons. Local $SU(3)_{\text{color}}$ symmetry transformations leave the theory invariant, which leads QCD to be identified as a “gauge” theory. Quarks behave asymptotically free at very short distances (at high energy), and they are confined to colorless hadrons at large distances (at low energy).

The phenomenology of quarks and gluons is described by the QCD Lagrangian,

$$\mathcal{L}_{\text{QCD}} = \sum_{f=1}^{N_f} \bar{\psi}_{\alpha,f}^c(x) \left(i\gamma^\mu D_\mu^{cc'} - m_f \delta^{cc'} \right) \psi_{\alpha,f}^{c'}(x) - \frac{1}{4} \mathcal{G}_{\mu\nu}^a \mathcal{G}_a^{\mu\nu}, \quad (2.1)$$

where $\psi_{\alpha,f}^c(x)$ and $\bar{\psi}_{\alpha,f}^c(x)$ represent the quark and anti-quark fields with Dirac index (α), color index (c), flavor index (f), and N_f the number of flavors. The covariant derivative $D_\mu = \partial_\mu - igA_\mu$ includes the dynamics of quarks and their coupling to gluons, whereas the gluon field-strength tensor $\mathcal{G}_{\mu\nu}(x) = \frac{i}{g}[D_\mu, D_\nu] = \partial_\mu A_\nu - \partial_\nu A_\mu - ig[A_\mu, A_\nu]$ describes the dynamics of gluons. Since $\mathcal{G}_{\mu\nu}(x)$ is also an element of the $SU(3)_{\text{color}}$ algebra, one can write $\mathcal{G}_{\mu\nu}(x) = \mathcal{G}_{\mu\nu}^a(x)T^a$. Gluons are flavor-blind and each gluon field $A_\mu^a(x)$ is associated with its generator T^a in the fundamental representation of $SU(3)$. The generators of $SU(3)_{\text{color}}$ $T^a = \lambda^a/2$ with $a = \{1, \dots, 8\}$, and λ^a are the Gell-Mann matrices. One can show that only the color-trace form of $\mathcal{G}_{\mu\nu}\mathcal{G}^{\mu\nu}$ which is $\mathcal{G}_{\mu\nu}^a\mathcal{G}_a^{\mu\nu}$ can appear in the Lagrangian. The non-Abelian nature of $SU(3)_{\text{color}}$ and the nonlinear self-interacting gluon fields, make the Lagrangian more complicated than Quantum Electrodynamics (QED).

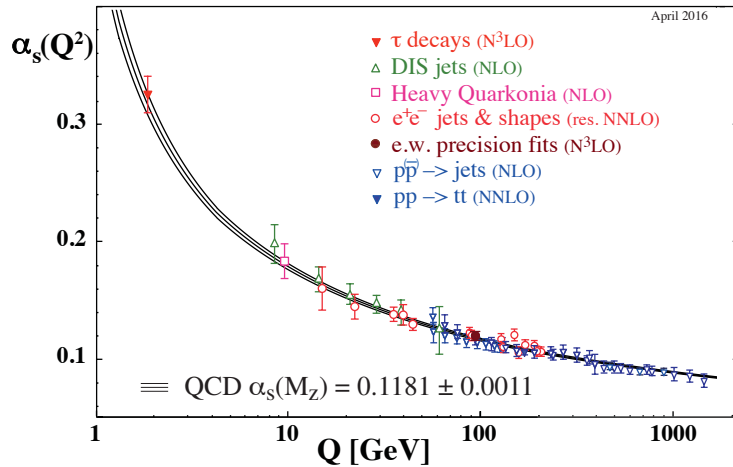


Figure 2.1. Summary of measurements of α_s as a function of the energy scale Q [39].

To understand the dynamical properties of QCD, one necessarily has to understand the behavior of the strong coupling constant as a function of distance. QCD has two distinct properties: asymptotic freedom and confinement [40]. Asymptotic freedom means that the strong coupling becomes small in very high energy reactions. This is due to the phenomenon called anti-screening, in which the charge is small at short distances, and grows at larger distances [40]. In non-Abelian gauge theories, the existence of asymptotic freedom depends on the gauge group and the number of flavors of interacting particles. The asymptotically free behavior in QCD was first discovered by David Gross, Frank Wilczek and David Politzer [7, 8]. This strange behavior of α_s has been verified in high-energy experiments to very high precision, as illustrated in Fig. (2.1) .

Asymptotic freedom implies that the theory becomes simple at short distance or high energy, while the coupling becomes very strong at large distances or low and intermediate energies. Therefore, the fundamental fields (i.e. quarks and gluons), do not appear in the physical spectrum as asymptotic states [40]. All physical states with finite energy appear to be color singlet combinations of quarks and gluons, which are always confined at rather short distances of order 1 fm. This phenomena is known as color confinement, which means that the force between quarks does not diminish as they are separated [40]. This implies that in the low energy regime of QCD, the degrees of freedom are no longer quarks and gluons, but rather color singlet hadrons.

The idea of generalizing the $SU(3)$ color gauge theory to $SU(N_c)$ gauge theory was initially proposed in 1974 by 't Hooft [10], introducing N_c number of colors. The expectation of this approach was to solve the theory with the color gauge group $SU(N_c)$ at large N_c limit ($N_c \rightarrow \infty$), and to have qualitatively and quantitatively close results to the $N_c = 3$ theory. Therefore in $SU(N_c)$ QCD, we have N_c number

of quark colors for each flavor, and $N_c^2 - 1$ number of gluons, where three colors for each quark flavor and eight gluons in $SU(3)_c$ QCD is a special case. 't Hooft realized that $1/N_c$ is a hidden expansion parameter, which can be used to implement a perturbative expansion in powers of $1/N_c$ to QCD at low and high energies.

In 1979 E. Witten [15] applied the $1/N_c$ framework for mesons as well as for baryons. He derived that mesons become free and non-interacting at large N_c , because the meson-meson coupling scales as $\mathcal{O}(1/N_c)$. Therefore, QCD becomes a weakly coupled theory for mesons at large N_c . One may be puzzled about how a theory with $N_c \rightarrow \infty$ can approximate the theory with $N_c = 3$. It has been proven that the results are in good agreement with experiment, if one considers the next to leading order terms in the $1/N_c$ expansion. In order to understand the large N_c limit, one has to first identify the $1/N_c$ order of quark-gluon diagrams. Then, one can introduce hadrons in large the N_c limit and study their interactions.

2.2 Feynman diagrams for large N_c

“Planar diagrams” are a special class of Feynman diagrams identified by 't Hooft [10], as the dominant diagrams in the $1/N_c$ expansion. In large N_c QCD, there are N_c possible colors for the quark fields during processes. The “double line notation” replaces the gluon gauge field A_μ^a by a double line corresponding to a tensor field $(A_\mu)^{ij}$, where the indices i, j belong to the fundamental representation of the color group $SU(N_c)$. This is illustrated in Fig. (2.2), where the gluon field has one upper index like the quark field q^i and one lower index like the anti-quark field q_j . Each line represents N_c number of colors. Therefore, the sum over all intermediate states gives large combinatoric factors, and leads to the suppression of contributions from some

Feynman diagrams.



Figure 2.2. Double line notation of a gluon field.

Let's consider the gluon vacuum polarization diagram with its double line representation (see Fig. (2.3)). The color quantum number of the initial and final states are specified, but the intermediate state has a loop specified by an index k which gives N_c possibilities, leading to a combinatoric factor N_c for this Feynman diagram. Therefore in the limit $N_c \rightarrow \infty$ the diagram is infinite.

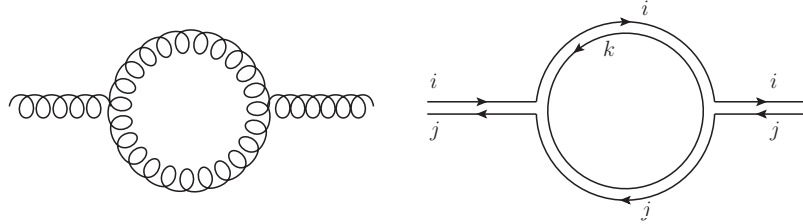


Figure 2.3. Gluon-vacuum polarization.

In order to have a finite limit for the gluon vacuum polarization, one can rescale the coupling constant g of the large N_c QCD lagrangian as [10, 15],

$$g \rightarrow \frac{g_0}{\sqrt{N_c}} \quad (2.2)$$

where g_0 is a new coupling fixed in the large N_c limit, known as the *'t Hooft coupling*. Therefore, considering both rescaled coupling and the color combinatoric factor together lead to N_c independence,

$$\left(\frac{g_0}{\sqrt{N_c}} \right)^2 N_c = g_0^2 \quad (2.3)$$

to the order of the Feynman diagram in Fig. (2.3). With this rescaling scheme, the quark-gluon and three-gluon vertices are of order $1/N_c$ and four-gluon vertices are of order $1/N_c$ (see Fig. (2.4)).

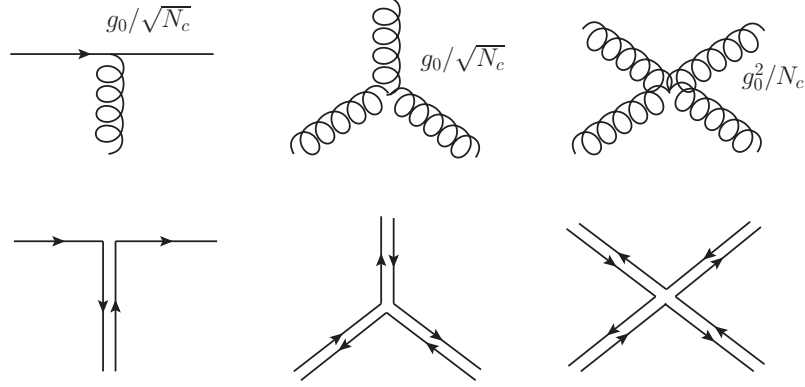


Figure 2.4. Quark-gluon, three-gluons and four-gluons vertices.

Now we can focus on a couple of examples of determining the $1/N_c$ order of a given Feynman diagram. Let's consider the two-loop diagram given in Fig. (2.5). There are four vertices $(1/\sqrt{N_c})^4$, and two internal loops (each contributing with a factor of N_c). Therefore the order of the two-loop contribution to the gluon propagator is $(1/\sqrt{N_c})^4 \times N_c^2 = 1$. Similarly, the three-loop contribution to the gluon propagator (see Figure (2.6)) is $(1/\sqrt{N_c})^6 \times N_c^3 = 1$, since there are six vertices and three internal loops. Therefore in general, m -loop contribution to the gluon propagator will be $(1/\sqrt{N_c})^{2m} \times N_c^m = 1$, also independent of N_c . In other words, adding an extra gluon to a given planar diagram while preserving it's planar nature, would only creates an additional two interaction vertices with one closed color loop giving a contribution $(1/\sqrt{N_c})^4 \times N_c^2 = 1$ to the overall diagram.

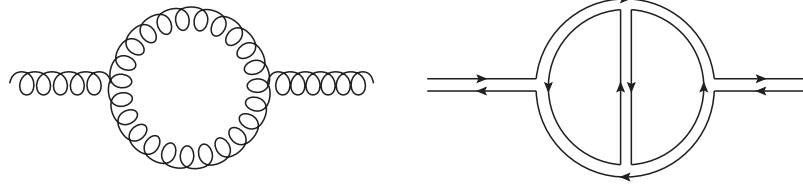


Figure 2.5. Two-loop diagram.

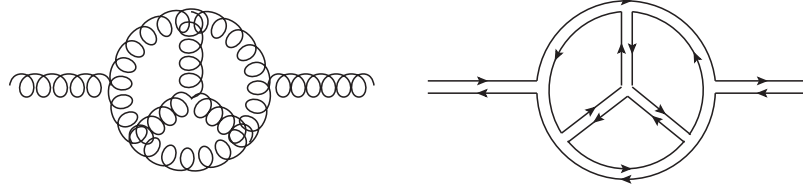


Figure 2.6. Three-loop diagram.

However, this is different for non-planar diagrams. For instance, in the diagram in Fig. (2.7) has six vertices and one closed color loop where the overall order is $(1/\sqrt{N_c})^6 \times N_c = 1/N_c^2$, which leads to be suppressed at large N_c limit. Also, it is possible to show that the maximum contribution from a non-planar Feynman diagram would be of order $1/N_c^2$ so they vanish in the large N_c limit [15].

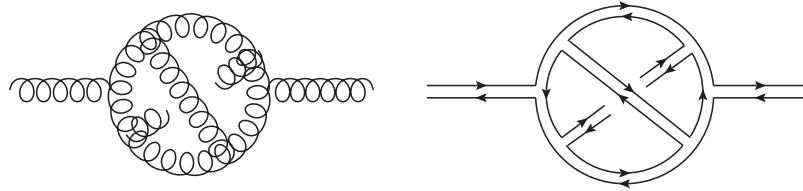


Figure 2.7. A non-planar diagram.

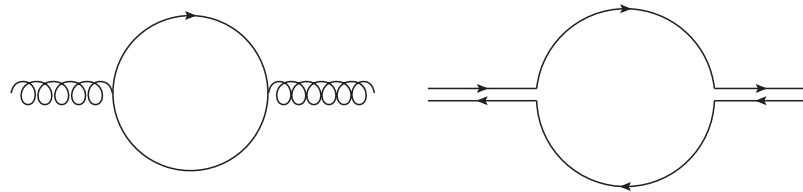


Figure 2.8. An internal-quark-loop diagram.

One may want to consider a quark loop as in the Fig. (2.8). Since the color indices for the initial and final state are specified, there will be no combinatoric factor contributions, but each vertex contributes with a factor of $1/\sqrt{N_c}$ and the overall order is $1/N_c$ which also vanishes at large N_c limit. If one wants to consider an internal quark loop as represented in Fig. (2.9) also vanishes at large N_c limit since it is of order $(1/\sqrt{N_c})^6 \times N_c^2 = 1/N_c$.

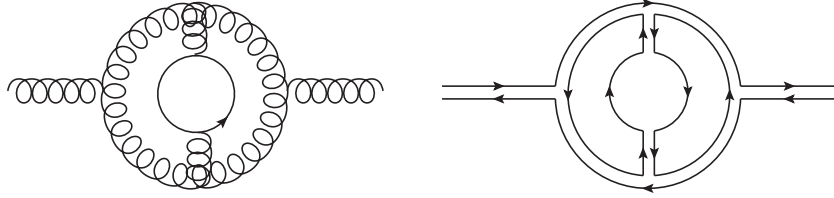


Figure 2.9. A quark-loop inside a gluon loop.

Let's summarize the large N_c counting rules for Feynman diagrams :

- Planar gluon insertion doesn't affect the order of the diagram since it is of $\mathcal{O}(1)$.
- Non-planar gluon line insertion leads to suppress the diagram by a factor of $1/N_c^2$.
- Insertion of an internal quark loop leads to suppress the diagram by a factor of $1/N_c$.

As a conclusion, planar Feynman diagrams which contain the minimum number of non-planar gluons and internal quark loops will be the most important diagrams in large N_c limit.

Let's consider matrix elements of quark bilinears. For example, the two-point function $\langle J(x)J(y) \rangle$ of a current correlation function J , where $J(x)$ creates a meson at point x and annihilates the meson at point y . In free field theory, a two-point

function is represented by closed loop as shown in Fig. (2.10(a)), which is order N_c in color. There are arbitrary planar gluon insertions possible as shown in Fig. (2.10(b)), which would not affect the N_c order. However the diagrams in Fig. (2.11) are also planar, and are of order $1/N_c$, which leads to suppression by a factor of $1/N_c^2$ compare to the diagrams in Fig. (2.10). Therefore, the leading order dependence of N_c of quark bilinear matrix elements is governed by not only the planarity but also the fact that quark lines are at the edge.



Figure 2.10. Two-point correlator $\langle JJ \rangle$ of $\mathcal{O}(N_c)$. (a) Free field correlator. (b) Corrections to free field correlator.



Figure 2.11. Non-leading corrections to the two-point correlator $\langle JJ \rangle$. Diagram (b) is the double line notation of diagram (a).

2.3 Large N_c mesons

The main motivation of discussing mesons is some results in the expansion of mass operator of baryons depend on the baryon-meson scattering. Large N_c meson states are color singlet bound states consist of quark and an anti-quark. Therefore

the composite meson operator can be written as, [41].

$$\frac{1}{\sqrt{N_c}} \sum_{i=1}^{N_c} \bar{q}_i q^i, \quad (2.4)$$

where, the summation over N_c possible colors gives an order $\sqrt{N_c}$ to the meson state.

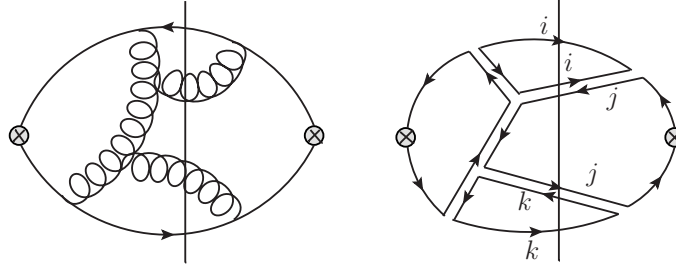


Figure 2.12. Intermediate state contributing to $\langle JJ \rangle$.

Let's consider creation and annihilation of a meson. This process is associated with matrix elements of operator $J(x)$ which correspond to quark bilinear such as $\bar{q}q$ or $\bar{q}\gamma^\mu q$. Consider the Fig. (2.12), which illustrates a two-point function of a quark bilinear. If we cut the diagram in a typical way, then we have an intermediate state with one quark, one anti-quark and two gluons. So, if one consider the color structure, then the intermediate state,

$$\bar{q}_i A_j^i A_k^j q^k \quad (2.5)$$

is a color singlet, which is a one meson in the confining theory. This is true when we have planar diagrams for the two-point function with only a single quark loop running at the edge. Because if we look at possible non-planar diagrams like in Fig. (2.11), then the intermediate state is a product of two color singlet states,

$$\bar{q}_i A_j^i q^j A_m^l A_l^m. \quad (2.6)$$

These intermediate states can be interpreted as one meson $\bar{q}_i A_j^i q^j$ and one color singlet gluon bilinear $A_m^l A_l^m$. As we discussed, non-planar diagrams are suppressed in the large N_c limit.

Therefore, meson states are one-particle intermediate state of a two-point function of J ,

$$J(k)J(-k) = \sum_n \frac{\langle 0|J|n\rangle^2}{k^2 - M_n^2} \quad (2.7)$$

where, J creates a meson with amplitude $\langle 0|J|n\rangle$ which propagates with a propagator $1/(k^2 - M_n^2)$, also we sum over all possible intermediate (color singlet) meson states to obtain the two-point function. We need to determine the N_c order of the matrix element $\langle 0|J|n\rangle$ which determines the dependence in N_c in the right hand side of Eq. (2.7). The leading order two-point function is order N_c , and all planar diagrams with quarks at the edges have the same order. Therefore, the matrix element $\langle 0|J|n\rangle$ which corresponds to the meson decay constant is of order $\sqrt{N_c}$.

$$f_M \sim \langle 0|J|n\rangle \sim \mathcal{O}(\sqrt{N_c}) \quad (2.8)$$

Now, consider a typical three point function as in Figure 2.13. E. Witten [15] illustrated systematically how to obtain the order of the three meson vertex. But if we use the fact that each meson creation/annihilation is order $\sqrt{N_c}$, then we can simply obtain the three meson vertex is of order $1/\sqrt{N_c}$, because the diagram is of order N_c .

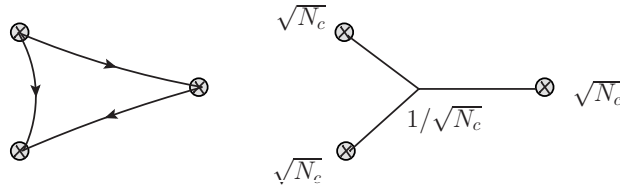


Figure 2.13. The dominant three meson diagram. The diagram on right hand side is in double line notation of the diagram on left hand side.

Therefore, for an n -point function the n -meson vertex is,

$$(\sqrt{N_c})^n \times \left(\frac{1}{N_c}\right)^{n-2} = N_c \quad (2.9)$$

of order $1/N_c^{n-2}$. Let's summarize the properties of large N_c mesons.

- The meson decay constant f_M (eg: pion decay constant f_π) is of $\mathcal{O}(\sqrt{N_c})$.
- The meson mass is of $\mathcal{O}(N_c^0)$.
- The amplitude of meson decay in to two mesons is of $\mathcal{O}(1/\sqrt{N_c})$.
- The n-meson coupling is of $\mathcal{O}(1/N_c^{n-2})$.

2.4 Large N_c baryons

In large N_c picture, baryons are colorless bound states which consist of N_c valence quarks, anti-symmetric in color indices. In order to form the color singlet state, these color indices of the N_c quarks are contracted with the $SU(N_c)$ invariant ϵ -symbol.

$$\epsilon_{i_1 i_2 i_3 \dots i_{N_c}} q^{i_1} q^{i_2} q^{i_3} \dots q^{i_{N_c}} \quad (2.10)$$

The number of colors N_c must be odd, because the baryon state has to be a fermionic bound state. At leading order, a large- N_c baryon can be represented using N_c valence quark lines. There are arbitrary number of planar and non-planar gluon exchanges between quark lines at higher orders in $1/N_c$. For example, the interaction between two quarks by exchanging one gluon is of order $1/N_c$ because each quark gluon vertex is of order $1/\sqrt{N_c}$. But the interaction of a quark with all the rest $N_c - 1$ quarks adds coherently to give an interaction energy per quark which is order N_c^0 .

The baryon mass is of order N_c . Because the number of quarks in a large N_c baryon grows with N_c , baryons become infinitely heavy in the large N_c limit ($N_c \rightarrow \infty$).

$$M_{\text{Baryon}} = \mathcal{O}(N_c) \quad (2.11)$$

The size and the shape of a baryon is independent of N_c . Because of the confinement property of quarks, the size of a baryon is fixed by the scale of $\Lambda_{QCD}^{-1} \approx 1$ fm. Thus, the quark density of a baryon increases with N_c . E. Witten [15] realized the applicability of the Hartree approximation since the average potential for each quark will be the same, in the large N_c limit of a baryon.

According to Witten's large N_c power counting, the key properties of large N_c baryons can be summarized as follows.

- Baryon mass is of $\mathcal{O}(N_c)$
- Baryon size is of $\mathcal{O}(N_c^0)$

2.5 Meson-baryon coupling

Studying the meson-baryon couplings is very important to explain the interactions at low energy QCD. Gervais with Sakita [11], and Dashen with Manohar [12] performed a pioneering study on meson-baryon couplings, and they independently discovered the spin-flavor symmetry of meson-baryon couplings at the large N_c limit. A detailed discussion on this spin-flavor symmetry of baryons is given in Chapter 4.

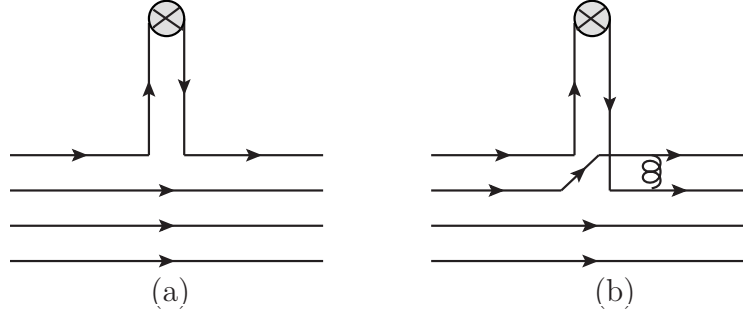


Figure 2.14. (a) meson coupling to same quark line. (b) meson coupling to two different quark lines.

Using the knowledge of determining the N_c order of planar diagrams, one can think about the N_c order of meson-baryon couplings. Let's consider the two diagrams given in Fig. (2.14). In diagram Fig. (2.14(a)), a meson is coupled to a single quark line of the baryon, with N_c possibilities. Therefore, the meson wave function's normalization factor $1/\sqrt{N_c}$ combines with the factor of N_c corresponds to the number of quark lines will combine together determine that the order of a meson-baryon coupling is $\mathcal{O}(\sqrt{N_c})$. Now, consider the case where meson is coupled to two different quarks with an exchange of a gluon between those quark lines (see Fig. (2.14(b))). Each quark-gluon vertex is $\mathcal{O}(1/\sqrt{N_c})$, each meson wave function has a factor of $1/\sqrt{N_c}$ and there are N_c^2 possibilities of selecting two quarks. Therefore, generally the order of the meson-baryon coupling is $\mathcal{O}(\sqrt{N_c})$.

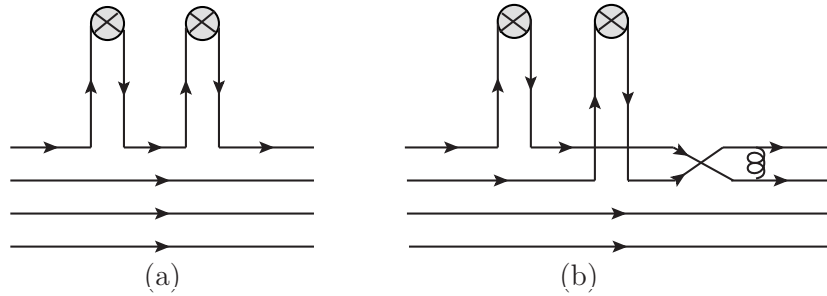


Figure 2.15. Baryon meson scattering of $\mathcal{O}(N_c^0)$.

Let's consider the scattering process of baryon + meson \rightarrow baryon + meson shown in Figure (2.15). There are four quark-gluon vertices giving a factor of $(1/\sqrt{N_c})^4$. Then the sum over the color indices c', c, c'' give a factor of $(N_c)^3$. Also, a factor of $(1/\sqrt{N_c})^2$ comes from two meson wave functions. Therefore, the order of the diagram is,

$$\left(\frac{1}{\sqrt{N_c}}\right)^4 (N_c)^3 \left(\frac{1}{\sqrt{N_c}}\right)^2 = 1.$$

CHAPTER 3

THE BARYON WAVE FUNCTION IN LARGE N_c

3.1 Introduction

In the simple quark-shell model picture, the general form of a baryon wave function can be written as,

$$\Psi = \psi_{\text{spatial}} \psi_{\text{spin}} \psi_{\text{flavor}} \psi_{\text{color}}. \quad (3.1)$$

As the baryons are fermions, the total wave function of a baryon has to be antisymmetric under the permutation of quarks. Since nature requires that the ψ_{color} has to be $SU(N_c)$ singlet (or colorless) because of the color confinement, then the color part leaves the remaining part of the wave function to be always symmetric. In this work, only the ordinary baryons with quantum numbers provided by N_c valence quarks of u, d, s flavors are considered.

The objective of this chapter is to give an idea about the combined role of the group theoretical contribution and the Hartree approximation of the complete baryon state. Since the real physical QCD is the theory when $N_c = 3$, the second section of this chapter will focus on the structure of baryon states with three quarks. In the third section, the idea will be generalized into the case of N_c number of quarks. Also, the third section is more focused on the ψ_{spatial} part considering the Hartree approximation for non-relativistic and relativistic limits. Then the fourth and fifth sections illustrate about the ground state baryons and excited state baryons respectively.

3.2 Baryon wave function for three quarks

Since, the baryon wave function can be decomposed as in Eq. (3.1), let's consider the spin-flavor part and the spatial part separately.

3.2.1 The spin-flavor part ($\psi_{\text{spin}}\psi_{\text{flavor}}$) of three quarks

Each quark can be labeled using two possible spins (\uparrow and \downarrow) and six possible flavors (u, d, s, c, t, b). Since this study is more focused on the standard hadrons (baryons and mesons consisting of light quarks), let's take only u, d, s quarks in to the discussion. Therefore, each quark in a baryon has six degree of freedoms which can be denoted as, $u \uparrow, u \downarrow, d \uparrow, d \downarrow, s \uparrow, s \downarrow$. This corresponds to $SU(6)$ spin-flavor symmetry group. Therefore the direct product for three quarks, according to the Young tableaux can be represented as follows,

$$\begin{array}{ccccccc}
 6 & 6 & 6 & & 56 & 70 & 70 & 20 \\
 \square & \otimes & \square & \otimes & \square & = & \square\square\square & \oplus & \begin{array}{|c|} \hline \square & \square & \square \\ \hline \square & & \\ \hline \end{array} & \oplus & \begin{array}{|c|} \hline \square & \square & \square \\ \hline & \square & \\ \hline \end{array} & \oplus & \begin{array}{|c|} \hline \square \\ \hline \square \\ \hline \square \\ \hline \end{array}
 \end{array} \tag{3.2}$$

where the dimensions **56**, **70**, **20** of the irreducible representations (irreps.) are indicated with each diagram. **56** is symmetric, **70**'s are mixed-symmetric and mixed-antisymmetric respectively, and **20** is antisymmetric under permutations of quarks [20]. Therefore the light baryons belong to these multiplets in the $SU(6)$ spin-flavor representation.

If we considered only the spin degree of freedom of quarks, then the baryons (three-quark spin states) can be represented in irreps. of the $SU(2)$ subgroup:

$$\frac{1}{2} \otimes \frac{1}{2} \otimes \frac{1}{2} = \frac{3}{2}^{\text{S}} \oplus \frac{1}{2}^{\text{MS}} \oplus \frac{1}{2}^{\text{MA}}, \tag{3.3}$$

where **S**, **MS**, **MA** labels correspond to symmetric, mixed-symmetric and mixed-anti-symmetric representations respectively. Also it can be represented In $(2S+1)$ notation combined with the Young tableaux:

$$\begin{array}{c} 2 & 2 & 2 & & 4 & & 2 & & 2 \\ \square & \otimes & \square & \otimes & \square & = & \square & \square & \square & \oplus & \square & \square & \oplus & \square & \square \\ & & & & & & & & & & & & & & \end{array} , \quad (3.4)$$

where, **4** represents the total spin $3/2$ and **2**'s represent the total spin $1/2$ multiplets. Considering only the flavor degree of freedom, it is the $SU(3)$ representation.

$$\begin{array}{c} 3 & 3 & 3 & & 10 & & 8 & & 8 & & 1 \\ \square & \otimes & \square & \otimes & \square & = & \square & \square & \square & \square & \oplus & \square & \square & \oplus & \square & \square & \oplus & \square \\ & & & & & & & & & & & & & & & & \end{array} \quad (3.5)$$

Therefore one can decompose the $SU(6)$ multiplets into the $SU(3)_{\text{flavor}} \times SU(2)_{\text{spin}}$ representations by following the rules for combining the states of different permutation symmetries [42] to visualize the spin and flavor contributions separately.

$$\begin{aligned} \mathbf{56} &= \mathbf{10} \otimes \mathbf{4} \oplus \mathbf{8} \otimes \mathbf{2} \\ \mathbf{70} &= \mathbf{10} \otimes \mathbf{2} \oplus \mathbf{8} \otimes \mathbf{4} \oplus \mathbf{8} \otimes \mathbf{2} \oplus \mathbf{1} \otimes \mathbf{2} \\ \mathbf{20} &= \mathbf{8} \otimes \mathbf{2} \oplus \mathbf{1} \otimes \mathbf{4} \end{aligned} \quad (3.6)$$

Also we can write down the $SU(2)$ spin wave functions and the $SU(3)$ flavor wave functions [42] for baryons as given in Tables (3.1), (3.2) and (3.3).

Table 3.1. Symmetric flavor states of three quarks : baryon decuplet.

Baryon	ϕ^S
Δ^{++}	uuu
Δ^+	$\frac{1}{\sqrt{3}}(uud + udu + duu)$
Δ^0	$\frac{1}{\sqrt{3}}(udd + dud + ddu)$
Δ^-	ddd
Σ^+	$\frac{1}{\sqrt{3}}(uus + usu + suu)$
Σ^0	$\frac{1}{\sqrt{3}}(uds + dus + usd + sud + sdu + dsu)$
Σ^-	$\frac{1}{\sqrt{3}}(sdd + dsd + dds)$
Ξ^0	$\frac{1}{\sqrt{3}}(uss + sus + ssu)$
Ξ^-	$\frac{1}{\sqrt{3}}(dss + sds + ssd)$
Ω^-	sss

Table 3.2. Mixed-symmetric flavor states of three quarks : baryon octet.

Baryon	$\phi^{M,S}$	$\phi^{M,A}$
P	$-\frac{1}{\sqrt{6}}(udu + duu - 2uud)$	$\frac{1}{\sqrt{2}}(udu - duu)$
N	$\frac{1}{\sqrt{6}}(udd + dud - 2ddu)$	$\frac{1}{\sqrt{2}}(udd - dud)$
Σ^+	$\frac{1}{\sqrt{6}}(usu + suu - 2uus)$	$-\frac{1}{\sqrt{2}}(usu - suu)$
Σ^0	$-\frac{1}{\sqrt{12}}(2uds + 2dus - sdu - sud - usd - dsu)$	$-\frac{1}{\sqrt{2}}(usd + dsu - sdu - sud)$
Σ^-	$\frac{1}{\sqrt{6}}(dsd + sdd - 2dds)$	$-\frac{1}{\sqrt{2}}(dsd - sdd)$
Λ^0	$\frac{1}{2}(sud - sdu + usd - dsu)$	$\frac{1}{\sqrt{12}}(2uds - 2dus + sdu - sud + usd - dsu)$
Ξ^0	$-\frac{1}{\sqrt{6}}(uss + sus - 2ssu)$	$-\frac{1}{\sqrt{2}}(uss - sus)$
Ξ^-	$-\frac{1}{\sqrt{6}}(dss + sds - 2ssd)$	$-\frac{1}{\sqrt{2}}(dss - sds)$

Table 3.3. Antisymmetric flavor state of three quarks : baryon singlet.

Baryon	ϕ^A
Λ	$\frac{1}{\sqrt{6}}(sdu - sud + usd - dsu + dus - uds)$

For example, consider the $\Delta^+(uud)$ with spin $S_z = \frac{1}{2}|\uparrow\uparrow\downarrow\rangle$. The totally symmetric $SU(6)$ wave-function can be written as [42] :

$$\frac{1}{3} \left| \begin{array}{l} u\uparrow u\uparrow d\downarrow + u\uparrow d\uparrow u\downarrow + d\uparrow u\uparrow u\downarrow \\ + u\uparrow u\downarrow d\uparrow + u\uparrow d\downarrow u\uparrow + d\uparrow u\downarrow u\uparrow \\ + u\downarrow u\uparrow d\uparrow + u\downarrow d\uparrow u\uparrow + d\downarrow u\uparrow u\uparrow \end{array} \right\rangle, \quad (3.7)$$

where the $SU(2) \otimes SU(3)$ decomposition is:

$$\frac{1}{\sqrt{3}}|uud + udu + duu\rangle \frac{1}{\sqrt{3}}|\uparrow\uparrow\downarrow + \uparrow\downarrow\uparrow + \downarrow\uparrow\uparrow\rangle. \quad (3.8)$$

3.2.2 The spatial wave function of three quarks

According to QCD, a baryon is a color singlet object with three quarks and gluons. The exact picture of the interaction among these quarks and gluons is complicated and still an open question. In the chiral limit, quarks are massless. Because of the effect of spontaneous symmetry breaking of the QCD vacuum, quarks are dressed themselves by the quark-antiquark pairs (sea quarks) and gluons. Therefore, quarks acquire an effective mass of order Λ_{QCD} through these non-perturbative mechanisms. These effective quarks are the elementary excitations of the QCD vacuum, and they are identified as “constituent quarks” with the quantum numbers of an elementary quark.

The Hamiltonian of constituent quarks according to the simple quark-shell model can be written as,

$$H = \sum_{i=1}^{N_c} T_i + V_i, \quad (3.9)$$

which assumes the non-relativistic approximation. T_i is the kinetic energy and V_i is the potential energy due to the average confinement potential of the i^{th} quark in the baryon. This Hamiltonian will affect only the ψ_{spatial} part of the total wave function, while the $\psi_{\text{spin}} \otimes \psi_{\text{flavor}}$ part generates the spin-flavor baryon multiplets corresponding to the $SU(2N_f) \otimes O(3)$ group theoretical representation. Also note that the number

of quarks in the baryon is governed by the ψ_{color} part.

The spatial wave-function has two components namely, the radial and orbital components. Also, the spatial part of the baryon can be obtained using the variational principle with the Hartree-Fock approximation (Approximating ansatz to the Schrödinger equation of the baryon using symmetric quark wave functions, then the quark wave functions can be obtained by the variational principle). This approximation is exact in large N_c limit. Therefore, let's consider the non-relativistic picture of a baryon.

Simply, one can consider solving the Schrödinger equation for a single quark by assuming a central three dimensional harmonic oscillator potential for the purpose of illustration,

$$\left(\frac{p^2}{2m} + \frac{1}{2} m \omega^2 r^2 \right) \psi = E \psi. \quad (3.10)$$

The energy eigenvalues are

$$E = \left(2k + l + \frac{3}{2} \right) \hbar \omega, \quad (3.11)$$

where, l is the orbital angular momentum quantum number and $k = \{0, 1, 2, \dots\}$ is associated with the number of nodes in the radial wave-function. Therefore the general form of the spatial wave-function can be written as [43]

$$\psi_{nlm} = \mathcal{N} (\alpha r)^l L_k^{l+1/2} (\alpha^2 r^2) \exp^{-\alpha^2 r^2/2} Y_l^m(\theta, \phi) \quad (3.12)$$

where $\alpha^2 = m\omega$, $n = 2k + l$, L is a Laguerre polynomial and the normalization constant \mathcal{N} is given by,

$$\mathcal{N} = \frac{2\alpha^3 k!}{\sqrt{\pi} \left(k + l + \frac{1}{2}\right) \left(k + l - \frac{1}{2}\right) \cdots \frac{3}{2} \times \frac{1}{2}}. \quad (3.13)$$

Now, the shell-model Hamiltonian for three quarks at positions $r_j (j = \{1, 2, 3\})$ interacting through the harmonic oscillator potential is,

$$H = \sum_j \frac{p_j^2}{2m} + \frac{1}{2}m\omega^2 r_j^2, \quad (3.14)$$

so that the baryon spatial wave-function is obtained as a product of three independent quark wave-functions. The color component of the total wave function is integrated out, so that the spatial and the spin-flavor components have to have the same symmetry property in order for the spatial-spin-flavor part to be in a totally symmetric state. If the Jacobi coordinates R, λ, ρ are introduced to neglect the center of mass motion,

$$\begin{aligned} R &= \frac{1}{\sqrt{3}}(r_1 + r_2 + r_3) , \\ \lambda &= \frac{1}{\sqrt{6}}(r_1 + r_2 - 2r_3) , \\ \rho &= \frac{1}{\sqrt{2}}(r_1 - r_2) , \end{aligned} \quad (3.15)$$

then the Hamiltonian can be re-written in the form [43],

$$H = \frac{P^2}{6m} + \frac{3}{2}m\omega^2 R^2 + \left[\frac{1}{2m} (p_\lambda^2 + p_\rho^2) + \frac{1}{2}m\omega^2 (\lambda^2 + \rho^2) \right] \quad (3.16)$$

where, P, p_λ, p_ρ are canonically conjugate momenta to R, λ, ρ respectively. The eigenfunction to this Hamiltonian may be written in the form,

$$\Psi = \chi(R)\varphi(\lambda)\phi(\rho) \quad (3.17)$$

where χ, φ and ϕ are one-body harmonic oscillator wave-functions. The first part $\chi(R)$ describes the center-of-mass motion and it is constrained to be held in the ground state, whereas the excitations of the center-of-mass are referred to as being “spurious”. Since we require the overall wave function (except the color part) to be

symmetric, a spatial wave-function of symmetric, mixed symmetric or anti-symmetric type must combine with the **56**, **70** and **20** spin-flavor $SU(6)$ multiplets, respectively.

Also, the parity of the wave function is,

$$\mathcal{P} = (-1)^\ell, \quad \ell = \sum_i l_i \quad (3.18)$$

where l_i is the angular momentum of i^{th} quark. Therefore one can label the baryon multiplets $[\mathbf{X}, l^P]$ which are corresponding to $SU(6) \otimes O(3)$ irreducible representation, where \mathbf{X} is the dimension of $SU(6)$.

The lowest level is $n = 0$ and it is the ground state, where all three quarks are in s -wave $(0s)^3$ state. Since the orbital part is completely symmetric ($l^P = 0^+$), this is identified as $[\mathbf{56}, 0^+]$. This **56** multiplet in the $SU(6)$ representation can be decomposed into an octet and a decuplet as discussed in the previous section. The first excited level is when $n = 1$, where one of the quarks is excited to its p -wave and the other two quarks remain in the s -wave, In this $(0s)^2(0p)$ configuration with $l^P = 1^-$, it is possible to form both symmetric and mixed symmetric spatial wave-functions. However, the symmetric wave function is a spurious state (because it corresponds to the configuration in which the quarks are in the ground state but the center-of-mass motion is in the $(0p)$ state [43]) since it is proportional to the center-of-mass coordinate R . On the other hand the mixed symmetric spatial wave function is non-spurious. Therefore, the first excited state $n = 1$ belongs to the $[\mathbf{70}, 1^-]$ multiplet. The $n = 2$ level is more complicated and it has three possible spatial wave functions which are degenerate in energy, namely $(0s)^2(1s)$, $(0s)^2(0d)$ and $(0s)(0p)^2$. The possible spurious states (the center-of-mass motion) can be eliminated by taking appropriate linear combinations of shell-model wave functions and they are given in the

Appendix B of Faiman *et al* [43].

As a result, the baryon multiplets which are corresponding to a symmetric representation of $SU(6) \otimes O(3)$ can be constructed using their $SU(3)$ -flavor, $SU(2)$ -spin and $O(3)$ -orbital components as just illustrated.

3.3 Generalization to large N_c with the Hartree picture

The generalization of the baryon wave-function from three quarks to N_c quarks was originally done by E. Witten et al. [15]. As described in the previous chapter, large N_c picture of a baryon is a color singlet state consist of N_c quarks. Therefore the baryon number for large N_c baryons becomes,

$$\mathcal{B} = \frac{N_c}{3} \quad (3.19)$$

where for the physical case $N_c \rightarrow 3$ and the baryon number of a quark becomes $1/3$. Witten realized that the divergent behavior of perturbation theory does not mean that a large N_c limit for baryons does not exist, but only that the baryon mass is of $\mathcal{O}(N_c)$. Because one can write down an expression for the baryon mass,

$$M_B = N_c M + N_c T + \frac{1}{2} N_c^2 \left(\frac{1}{N_c} V \right) \quad (3.20)$$

where M is the quark mass, T is the kinetic energy of a quark and the last term corresponds to the overall average potential term since the interaction between one quark pair is of $\mathcal{O}(1/N_c)$ and there are $N_c^2/2$ quark pairs in the baryon.

Determining the large N_c limit for baryons is more subtle because of the combinatoric factors of N_c contributions from the planar diagrams leads the lowest order

diagram to diverge at large N_c . It is easy to see the divergent behavior of perturbation theory associated with the propagation of a N_c -quark state in a given time t . Because the amplitude $\exp^{-iN_c t f(g,M)}$ can be expanded in powers of the strong coupling g , each successive term in the expansion will be more divergent in N_c [15], where $f(g, M)$ is some function of the strong coupling and quark masses. In order to overcome this issue Witten considered the Hamiltonian and path integral methods in the limit of heavy quarks. Because if the quarks are very heavy, then the non-relativistic Schrödinger equation with a Coulomb type potential can be used to describe the N_c -quark state regardless of the size of the N_c . Thus, the Hamiltonian can be written as,

$$H = N_c M + \sum_i -\frac{\nabla_i^2}{2M} - \frac{g^2}{N_c} \sum_{i < j} \frac{1}{x_i - x_j} \quad (3.21)$$

where, the minus sign in the last term explains the attractiveness of the interaction. Although this Hamiltonian is not entirely realistic, one can extract some qualitative results that are valid for the case when quarks are not so heavy. An important remark is that the last term in Eq. (3.21) should not be considered as of $\mathcal{O}(1/N_c)$ since there is a combinatoric factor $\frac{1}{2}N_c^2$ when the sum over quark pairs is performed.

Witten et al. [15] described the large N_c limit using the Hartree approximation. The logic behind this approximation as follows : although the large N_c interaction between any pair of quarks is of $\mathcal{O}(N_c)$, the total potential experienced by one quark is of $\mathcal{O}(1)$. Therefore, each quark in the large N_c baryon interacts with the average potential produced by the other $N_c - 1$ quarks with strength of $\mathcal{O}(1/N_c)$. The Hartree approximation becomes exact in the large N_c limit.

Let's consider the ground state. The wave-functions are totally symmetric under the simultaneous interchange of coordinate and spin-flavor indices due to color antisymmetrization. Since the Hartree potential is spin-flavor independent, the large N_c ground state baryon wave-function can be written as [44],

$$\Phi(x_1, \xi_1; \dots; x_{N_c}, \xi_{N_c}) = \chi_S(\xi_1, \dots, \xi_{N_c}) \prod_{i=1}^{N_c} \phi(x_i) \quad (3.22)$$

where $\phi(x_i)$ is $l = 0$ quark wave-function with its position x_i of the i^{th} quark, and $\chi_S(\xi_1, \dots, \xi_{N_c})$ is a symmetric tensor of rank N_c in the spin-flavor space corresponding to the quantum numbers ξ_i . The most straight-forward method to determine ϕ is the variational principle associated with the time-independent Schrödinger equation. Also, the variational functional for N_c -quark system $\langle \Phi | H - E | \Phi \rangle$ can be considered as $\langle \Phi | H - N_c \mathcal{E} | \Phi \rangle$, since the total energy E is equivalent to $N_c \mathcal{E}$, where \mathcal{E} is the energy per quark. Therefore substituting the ansatz (Eq. (3.22)) in $\langle \Phi | H - N_c \mathcal{E} | \Phi \rangle$ gives,

$$\begin{aligned} \langle \Phi | H - N_c \mathcal{E} | \Phi \rangle &= N_c \left[M + \int d^3x \frac{\nabla \phi^* \nabla \phi}{2M} + \frac{g^2}{2} \int d^3x d^3y \frac{\phi^* \phi(x) \phi^* \phi(y)}{|x - y|} \right. \\ &\quad \left. - \mathcal{E} \int d^3x \phi^* \phi(y) \right]. \end{aligned} \quad (3.23)$$

Therefore the variational equation (or Hartree equation) for this case is,

$$-\frac{\nabla^2}{2M} \phi(x) - g^2 \phi(x) \int d^3y \frac{\phi^* \phi(y)}{|x - y|} = \mathcal{E} \phi(x) \quad (3.24)$$

and the ground state baryon corresponds to the lowest value of \mathcal{E} . Then the ansatz in Eq. (3.22) has to be generalized for the case of the time-dependent Hartree approximation

$$\Phi(x_1, \xi_1; \dots; x_{N_c}, \xi_{N_c}; t) = \chi_S(\xi_1, \dots, \xi_{N_c}) \prod_{i=1}^{N_c} \phi(x_i, t) \quad (3.25)$$

which is associated with the variational principle from the time-dependent Schrödinger equation. If the ansatz in Eq. (3.25) are exact in the large N_c limit, then instead of

varying the quantity

$$\int dt \left\langle \Phi \left| H - i \frac{\partial}{\partial t} \right| \Phi \right\rangle \quad (3.26)$$

with respect to Φ , one can vary only with respect to ϕ . Therefore, one can obtain the time-dependent Hartree equation:

$$-\frac{\nabla^2}{2M}\phi(x, t) - g^2\phi(x, t) \int d^3y \frac{\phi^*\phi(y, t)}{|x - y|} = i \frac{\partial}{\partial t}\phi(x) \quad . \quad (3.27)$$

This equation has many solutions including the simple form :

$$\phi(x, t) = \phi_0(x) \exp^{-i\mathcal{E}t}$$

when the baryon at rest, and the Galilean-boosted form :

$$\phi(x, t) = \phi_0(x - vt) \exp^{(iMv \cdot x)} \exp^{(-i\mathcal{E}t - \frac{1}{2}iMv^2t)}$$

when the baryon is moving with uniform velocity v . Therefore, one can obtain solutions for the time-dependent Hartree equation by integrating it using some arbitrary initial data for $\phi(x, 0)$. However, the Hartree approximation is exact in the large N_c limit. And the corrections to the true Hamiltonian are suppressed by the sub-leading orders of $1/N_c$.

The large N_c picture of the excited baryon consist of n quarks (of $\mathcal{O}(N_c^0)$) in the excited state, while the rest of $N_c - n$ quarks (of $\mathcal{O}(N_c)$) remain in the ground state (“core”) [21, 23, 25], where $n \ll N_c$. This is called the “decoupling picture”. These core quarks can be described by the same wave functions which are totally symmetric in both spatial and spin-flavor, corresponding to the baryon ground state. The states with only a single quark in the excited state (when $n = 1$) belong to spin-flavor either symmetric or mixed-symmetric states. The totally symmetric representation

is given by a row of N_c boxes, while the mixed-symmetric representation is given by $N_c - 1$ boxes in the first row and one separate box in the second row (representing the excited quark) in Young tableaux. Note that, both symmetric and mixed-symmetric representations contain N_c boxes in total. These excited states correspond to totally symmetric states can be represented as [44],

$$\Phi_S(x_1, \xi_1; \dots; x_{N_c}, \xi_{N_c}) = \frac{1}{2\sqrt{N_c}} \chi_S(\xi_1, \dots, \xi_{N_c}) \sum_j^{N_c} \left(\prod_{i \neq j}^{N_c} \phi(x_i) \right) \psi(x_j) \quad (3.28)$$

and the wave function for the mixed-symmetric state can be represented as,

$$\begin{aligned} \Phi_M(x_1, \xi_1; \dots; x_{N_c}, \xi_{N_c}) = & \frac{1}{\sqrt{N_c(N_c - 1)}} \sum_{i \neq j} \left[\left(\prod_{k \neq i, j}^{N_c} \phi(x_k) \right) \phi(x_i) \psi(x_j) \chi_M(\xi_1, \dots, \xi_{N_c}) \right. \\ & \left. - i \leftrightarrow j \right], \end{aligned} \quad (3.29)$$

where, χ_M is the irreducible rank N_c mixed symmetry tensor, and $\psi(x)$ represents the wave-function of the excited quark.

The generalization to arbitrary N_c of a symmetric state is trivial and unique as shown in Fig. (3.1). But the generalization of the mixed-symmetric state is not trivial and unique. This subtlety was solved by Matagne & Stancu [45] by considering the Jacoby coordinates for a system of N_c particles.

$$\dot{x}^{N_c} = \frac{1}{\sqrt{N_c}} \sum_{t=1}^{N_c} x^t \quad (3.30)$$

$$\dot{x}^s = \frac{1}{\sqrt{s(s+1)}} \left(\sum_{t=1}^s x^t - s x^{s+1} \right) \quad (3.31)$$

The center of mass coordinate given in Equation (3.30) is the basis vector for the symmetric representation $[\mathbf{N}_c]$, and the internal coordinates given in Equation (3.31) form an invariant subspace for the mixed-symmetric representation $[\mathbf{N}_c - \mathbf{1}, \mathbf{1}]$. A detailed study by Matagne & Stancu [45] suggested that the only possible solution

for the excited states is the irreducible representation $[\mathbf{N}_c - \mathbf{1}, \mathbf{1}]$ of the permutation group \mathcal{S}_{N_c} . Note that this solution is reduced to the mixed-symmetric irreducible representation [21] when $N_c = 3$ (see the Young diagram generalization).

So, we can generalize the ψ_{spatial} part of the baryon wave-function by large N_c Hartree approximation. On the other hand the spin-flavor structure of large N_c baryons (with N_f quark flavors) exhibits the $SU(2)_{\text{spin}} \otimes SU(N_f)_{\text{flavor}}$ symmetry and a detailed discussion is given in the next chapter. The only requirement is $\psi_{\text{spatial}} \otimes \psi_{\text{spin}} \otimes \psi_{\text{flavor}}$ has to be symmetric under the interchange of the corresponding indices between any two quarks.

3.4 Ground state baryons in large N_c

Let's consider the ground-state baryons. All the N_c quarks are populated in the ground state (s -wave). One can represent the ground state of the large N_c baryon using a Young diagram with N_c boxes, as shown in Figure (3.1). The baryon spin can vary from $S = 1/2$ to $S = N_c/2$, where N_c is an odd number. Since each quark contains two possible spin projections and N_f possible quark flavors, then the large N_c spin-flavor structure of ground state baryons correspond to the totally symmetric representation of the $SU(2N_f)$ group.

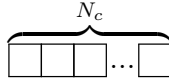


Figure 3.1. Young diagram for the symmetric representation of large N_c baryon.

In the case of two quark flavors ($N_f = 2$), the spin-flavor wave function transforms like totally symmetric $SU(4)$ representation which can be decomposed into

$SU(2)_{\text{spin}} \otimes SU(2)_{\text{flavor}}$. The baryon tower contains states with

$$S = I = \frac{1}{2}, \frac{3}{2}, \dots, \frac{N_c}{2}. \quad (3.32)$$

In the case of three quark flavors ($N_f = 3$), the spin-flavor wave function transforms like totally symmetric representation of $SU(6)$ which can be decomposed into $SU(2)_{\text{spin}} \otimes SU(3)_{\text{flavor}}$. This can be written in terms of Young diagrams as given in Equation (3.33) [46] where each Young tableaux consist of N_c number of boxes in total.

$$\overbrace{\square \square \square \dots \square}^{N_c} = \left(\begin{array}{|c|c|} \hline \square & \square \\ \hline \square & \square \\ \hline \end{array} \dots \begin{array}{|c|c|} \hline \square & \square \\ \hline \square & \square \\ \hline \end{array}, J = \frac{1}{2} \right) \oplus \left(\begin{array}{|c|c|} \hline \square & \square \\ \hline \square & \square \\ \hline \end{array} \dots \begin{array}{|c|c|c|c|} \hline \square & \square & \square & \square \\ \hline \square & & & \\ \hline \end{array}, J = \frac{3}{2} \right) \oplus \dots \oplus \left(\begin{array}{|c|c|c|} \hline \square & \square & \square \\ \hline \square & & \\ \hline \end{array} \dots \square, J = \frac{N_c}{2} \right) \quad (3.33)$$

Notice that, when $N_f \geq 3$, the dimension of the flavor representation of the baryon spin-flavor tower grows with N_c . This can be understood by studying the flavor weight diagrams for each spin ranging from $1/2$ to $N_c/2$. The flavor weight diagrams for spin $1/2$ and spin $3/2$ cases are shown in Figures (3.2) and (3.3).

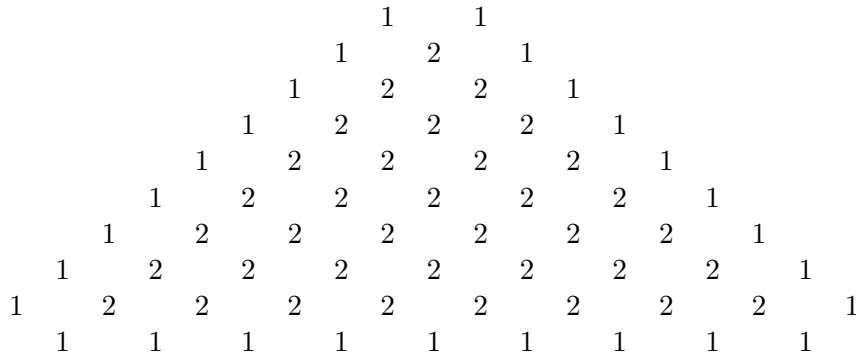


Figure 3.2. Weight diagram for the $SU(3)$ flavor representation of the spin $1/2$ baryons. The long side of the weight diagram contains $\frac{1}{2}(N_c + 1)$ weights. The numbers denote the multiplicity of the weights [47].

These flavor representations reduce to the baryon octet and decuplet when $N_c = 3$. For arbitrary N_c , the familiar spin 1/2 octet and spin 3/2 decuplet can be identified with the states at the top of each flavor representation, if the number of strange quarks N_s is of $\mathcal{O}(1)$ (not $\mathcal{O}(N_c)$). Also, the hypercharge Y of baryon states at the top of the flavor weight diagram is given by,

where, \mathcal{B} is the baryon number and \mathcal{S} is the strangeness ($\mathcal{S} = -N_s$) of $\mathcal{O}(1)$.

The large N_c picture of excited baryons is based on a picture similar to the quark-shell model, where the baryon is split into a symmetric core and an excited quark. If the spin-flavor dependence of the interactions are neglected, then the excited baryon spectrum contains degenerate spin-flavor towers. But, these orbital excitations of the single quark break the spin-flavor $SU(2N_f)$ symmetry in the large N_c limit, to the leading order in the $1/N_c$ expansion and first order in perturbation theory (in α_s) [44]. Therefore, the excited baryons can be classified in multiplets of the group

$SU(2N_f) \times O(3)$, because the zeroth order breaking in the $1/N_c$ expansion turns out to be small in the large N_c limit. For the case of $N_f = 3$, the excited baryons belong to the $SU(6) \times O(3)$ representation.

The spectrum of the p-wave baryons ($l = 1$) can be obtained in a similar way using the symmetry properties. In the real world with $N_c = 3$ the spin-flavor wave function of the $l = 1$ light baryons ($N_f = 3$) transforms according to the mixed symmetry representation **70** of $SU(6)$. Its decomposition into spin-flavor multiplets is,

$$\begin{array}{|c|c|} \hline \square & \square \\ \hline \square & \\ \hline \end{array} = \left(\mathbf{10}, S = \frac{1}{2} \right) \oplus \left(\mathbf{8}, S = \frac{3}{2} \right) \oplus \left(\mathbf{8}, S = \frac{1}{2} \right) \oplus \left(\mathbf{1}, S = \frac{1}{2} \right). \quad (3.35)$$

The generalization to arbitrary N_c for the case of $SU(6)$ with three flavors can be obtained by adding additional boxes to the first line of the Young diagram, as a product of $SU(6)$ representations.

$$\overbrace{\square \square \square \dots \square}^{N_c-1} \otimes \square = \overbrace{\square \square \square \dots \square}^{N_c} \oplus \overbrace{\begin{array}{|c|c|c|} \hline \square & \square & \square \\ \hline \square & & \end{array}}^{N_c-1} \dots \square \quad (3.36)$$

The decomposition of the symmetric representation on the left-hand side is already known from Figure (3.1). Subtracting from the product on the left-hand side the representations of $SU(3) \otimes SU(2)$ corresponding to the symmetric representation can be obtained [46].

$$\begin{aligned}
\overbrace{\begin{array}{|c|c|} \hline \square & \square \\ \hline \square & \square \end{array} \dots \begin{array}{|c|} \hline \square \\ \hline \end{array}}^{N_c-1} &= \left(\begin{array}{|c|c|} \hline \square & \square \\ \hline \square & \square \end{array} \dots \dots \begin{array}{|c|} \hline \square \\ \hline \end{array}, S = \frac{1}{2} \right) \oplus \left(\begin{array}{|c|c|} \hline \square & \square \\ \hline \square & \square \end{array} \dots \dots \begin{array}{|c|c|c|c|} \hline \square & \square & \square & \square \\ \hline \square & \square & \square & \square \end{array}, S = \frac{1}{2}, \frac{3}{2}, \frac{5}{2} \right) \\
&\oplus \left(\begin{array}{|c|c|} \hline \square & \square \\ \hline \square & \square \end{array} \dots \dots \begin{array}{|c|c|} \hline \square & \square \\ \hline \square & \square \end{array}, S = \frac{1}{2}, \frac{3}{2} \right) \oplus \left(\begin{array}{|c|c|} \hline \square & \square \\ \hline \square & \square \end{array} \dots \dots \begin{array}{|c|c|c|} \hline \square & \square & \square \\ \hline \square & \square & \square \end{array}, S = \frac{1}{2}, \frac{3}{2} \right) \oplus \dots \\
&\oplus \left(\overbrace{\begin{array}{|c|c|c|} \hline \square & \square & \square \\ \hline \square & \square & \square \end{array} \dots \begin{array}{|c|} \hline \square \\ \hline \end{array}}^{N_c}, S = \frac{N_c}{2} - 1 \right) \oplus \left(\overbrace{\begin{array}{|c|c|c|} \hline \square & \square & \square \\ \hline \square & \square & \square \end{array} \dots \begin{array}{|c|} \hline \square \\ \hline \end{array}}^{N_c-1}, S = \frac{N_c}{2} - 1, \frac{N_c}{2} \right)
\end{aligned} \tag{3.37}$$

The multiplets are labeled as $[\mathbf{X}, \ell^P]$, where \mathbf{X} represents the dimension of the irreducible representation of the spin-flavor group $SU(2N_f)$, and ℓ^P indicates the orbital angular momentum ℓ of the multiplet with its parity P . For $N_f = 3$ with $\ell = \{0, 1, 2\}$ cases, the excited baryon states correspond to $[\mathbf{56}, 0^+]$, $[\mathbf{70}, 1^-]$ and $[\mathbf{56}, 2^+]$ multiplets in the $SU(6) \times O(3)$ representation. Although the $[\mathbf{56}, 0^+]$ multiplet is identified as the ground state, but it is also identified as a multiplet which contains the radial excitations of the ground state s -wave baryons (Roper multiplet). Therefore the spin-flavor wave function transforms as a totally symmetric representation of $SU(6)$, which can be decomposed into $SU(2)_{\text{spin}} \otimes SU(3)_{\text{flavor}}$. The large- N_c Young tableaux representation is the same for the $[\mathbf{56}, 0^+]$ Roper multiplet baryons as in $\mathbf{56}$ -plet ground state baryons.

CHAPTER 4

SPIN-FLAVOR SYMMETRY IN LARGE N_c BARYONS

4.1 Introduction

An important advance in large N_c was made with the discovery of the existence of a spin-flavor symmetry for large N_c baryons by Gervais and Sakita [11, 13] and later by Dashen and Manohar [12, 14], from the study of pion-nucleon scattering process in the limit $N_c \rightarrow \infty$. That means, baryons satisfy a contracted $SU(2N_f)_c$ spin-flavor algebra where N_f is the number of flavors. The contracted spin-flavor symmetry of baryons implies that, the ground-state baryons form an infinite tower of degenerate states when $N_c \rightarrow \infty$. This contracted spin-flavor symmetry emerges from consistency conditions on baryon-meson scattering amplitudes in order for the theory to be unitary at $N_c \rightarrow \infty$ limit. One can use the $SU(2N_f)$ algebra, because the algebra used in the quark-shell model is $SU(2N_f)$ is equivalent to $SU(2N_f)_c$ in the limit $N_c \rightarrow \infty$ [48]. The spin-flavor symmetry of large N_c baryons is broken at $\mathcal{O}(1/N_c)$, thus the degenerate baryon states split at $\mathcal{O}(1/N_c)$. At finite N_c , the spin-flavor structure of baryons is given by the $1/N_c$ corrections to the large N_c limit. Since the consistency conditions constrain the form of sub-leading $1/N_c$ corrections, one can make definite predictions at sub-leading orders by calculating matrix elements of operator products of the baryon spin-flavor generators.

There are two natural ways to study the spin-flavor algebra of baryons for large N_c [49]. Both approaches are associated with constructing solutions to the large N_c consistency condition. First approach uses the irreducible representations of the contracted group $SU_c(2N_f)$ at the limit $N_c \rightarrow \infty$ [50], while the second approach uses the quark operators [12, 49, 50]. The first approach is closely related to the Skyrme

model [51], and the second approach is closely related to the non-relativistic quark model. The spin-flavor structure of the baryon states from the non-relativistic quark model and the Skyrme model are identical in the $N_c \rightarrow \infty$ [52] limit. The second approach gives an intuitive picture of baryons as quark bound states without assuming either the non-relativistic quark model is valid or the quarks in the baryons are non-relativistic. Thus, the $1/N_c$ counting is simply related to quark Feynman diagrams.

This chapter is organized as follows : In the next section, large N_c consistency conditions are discussed. The third section is about the contracted $SU(2N_f)_c$ spin-flavor algebra. In the fourth section, the large N_c baryon representations are introduced. Finally in the fifth section, the $1/N_c$ corrections to the large N_c consistency condition are discussed with applications.

4.2 Large N_c consistency condition

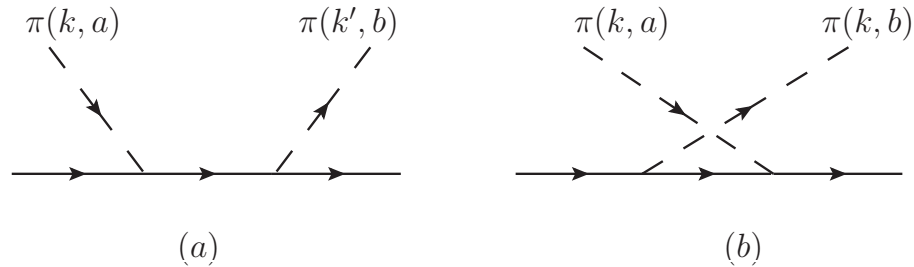


Figure 4.1. Dominant diagrams for pion-nucleon scattering amplitude.

Witten [15] showed that the baryon-meson scattering amplitudes at fixed energy is of $\mathcal{O}(1)$ by applying the large N_c power counting rules. This was explicitly discussed in chapter 2, by considering the two cases; incident and emitting pions are coupled to the same quark, and incident and emitting pions are coupled to different quarks with a gluon exchange between those two quarks (see Fig. (2.15)). Consider the dominant diagrams for the pion-nucleon scattering, as shown in Figure (4.1). At

low energy, baryon acts as a heavy static source for the scattering of mesons since the baryon mass is $\mathcal{O}(N_c)$. The large N_c counting rules show that the axial vector coupling g_A of a baryon is $\mathcal{O}(N_c)$, and the pion decay constant F_π is of $\mathcal{O}(\sqrt{N_c})$. Thus, the baryon-meson vertex $g_A \mathbf{q}/F_\pi$ grows as $\mathcal{O}(\sqrt{N_c})$, where \mathbf{q} is the meson momentum. Therefore, the total scattering amplitude grows as $\mathcal{O}(N_c)$ and violates unitarity unless there are cancellations among the $\mathcal{O}(N_c)$ baryon-meson scattering diagrams.

Let's consider the baryon-meson scattering amplitude at low energy. In the large N_c limit, the baryon-meson coupling can be studied in the rest frame of the baryon because of its static behavior compared to the meson. Since mesons are identified as the pseudo-scalar Goldstone bosons of Chiral symmetry breaking, they are derivatively coupled to the axial vector current of the baryons. In general, the baryon-meson coupling is written as the baryon axial vector current matrix element times the derivatively coupled meson field,

$$\frac{\partial_\mu \pi^a}{F_\pi} \langle B' | \bar{q} \gamma^\mu \gamma_5 T^a q | B \rangle. \quad (4.1)$$

where, a represents the flavor index of the meson and μ is the space-time index. Because, the baryon is infinitely heavy compared to the meson in the large N_c limit, the time component of the axial current between two baryons vanishes at rest. Thus, the baryon-meson coupling reduces to static-baryon coupling. The axial vector current matrix element simplifies to its space components

$$\langle B' | \bar{q} \gamma^\mu \gamma_5 T^a | B \rangle \rightarrow \langle B' | \bar{q} \gamma^i \gamma_5 T^a | B \rangle = g_A N_c \langle B' | X^{ia} | B \rangle \quad (4.2)$$

where the axial coupling constant g_A and the matrix element $\langle B' | X^{ia} | B \rangle$ are $\mathcal{O}(N_c^0)$. Therefore, the total amplitude for baryon-meson scattering process $B(p) + \pi^a(E, k) \rightarrow B'(p') + \pi^b(E, k')$ at fixed meson energy E is given by [50],

$$A = -i \frac{N_c^2 g_A}{F_\pi^2} \frac{k^i k'^j}{E} \langle B' | [X^{jb}, X^{ia}] | B \rangle \quad (4.3)$$

by considering the dominant baryon-meson scattering diagrams, shown in Fig. (4.1). The matrix element of the commutator $[X^{jb}, X^{ia}]$ appears in the above expression from the relative minus sign between those two diagrams in Fig. (4.1), because the intermediate baryon propagator in Fig. (4.1 (a)) is off-shell by energy E , whereas the intermediate baryon propagator in Fig. (4.1 (b)) is off-shell by energy $-E$. The product of the spin-flavor generators (X 's) sums over all possible baryon intermediate states. Since F_π is $\mathcal{O}(\sqrt{N_c})$ and the total scattering amplitude is $\mathcal{O}(1)$, the matrix element $\langle B' | [X^{jb}, X^{ia}] | B \rangle$ has to satisfy the condition:

$$[X^{jb}, X^{ia}] \leq \mathcal{O}(1/N_c) . \quad (4.4)$$

The spin-flavor generators X^{ia} of these baryon intermediate states can be expanded in powers of $1/N_c$.

$$X^{ia} = X_0^{ia} + \frac{1}{N_c} X_1^{ia} + \frac{1}{N_c^2} X_2^{ia} + \dots \quad (4.5)$$

Therefore in-order to satisfy unitarity, the baryon-meson couplings are constrained by the condition:

$$[X_0^{ia}, X_0^{jb}] = 0 , \quad (4.6)$$

[11–14], which is identified as the large N_c consistency condition at the leading order in the $1/N_c$ expansion. Thus in the large N_c limit, only the intermediate baryon states which are degenerate with initial and final baryons contribute to the scattering amplitude at leading order in $1/N_c$.

4.3 Contracted spin-flavor algebra

According to the leading order at large N_c , the consistency condition in Eq. (4.6), the generators X^{ia} of the baryon axial current matrix elements commute in the large N_c limit. Collectively, this consistency relation between the amplitudes X^{ia} with the algebra for spin operators S^i and flavor operators T^a lead to the contracted spin flavor algebra for large N_c baryons. Therefore in the $N_c \rightarrow \infty$ limit S^i , T^a and

X^{ia} generators form the contracted spin-flavor symmetry group $SU(2N_f)_c$ with N_f flavors [49, 50, 53].

$$\begin{aligned} [S^i, T^a] &= 0 & [T^a, T^b] &= if^{abc}T^c \\ [S^i, S^j] &= i\epsilon^{ijk}S^k & [T^a, X_0^{ib}] &= if^{abc}X_0^{ic} \\ [S^i, X_0^{ja}] &= i\epsilon^{ijk}X_0^{ka} & [X_0^{ia}, X_0^{jb}] &= 0 \end{aligned} \quad (4.7)$$

It's useful to compare the contracted spin-flavor $SU(2N_f)_c$ algebra with the ordinary spin-flavor $SU(2N_f)$ algebra, with N_f light quark flavors.

$$\begin{aligned} [S^i, T^a] &= 0 & [T^a, T^b] &= if^{abc}T^c \\ [S^i, S^j] &= i\epsilon^{ijk}S^k & [T^a, G^{ib}] &= if^{abc}G^{ic} \\ [S^i, G^{ja}] &= i\epsilon^{ijk}G^{ka} & [G^{ia}, G^{jb}] &= \frac{i}{4}\delta^{ij}f^{abc}T^c + \frac{i}{2N_f}\delta^{ab}\epsilon^{ijk}S^k + \frac{i}{2}\epsilon^{ijk}d^{abc}G^{kc} \end{aligned} \quad (4.8)$$

The link between the contracted and ordinary spin-flavor algebra for large N_c baryons is given by rescaling the G^{ia} and taking the limit,

$$X_0^{ia} = \lim_{N_c \rightarrow \infty} \frac{G^{ia}}{N_c} \quad (4.9)$$

which is considered as a Lie algebra contraction [48]. This contraction only affects the commutator $[G^{ia}, G^{jb}]$. Nevertheless, dividing $[G^{ia}, G^{jb}]$ by N_c^2 and taking the $N_c \rightarrow \infty$ limit reproduce the large N_c consistency condition. Therefore, one can work with the ordinary $SU(2N_f)$ algebra rather than the contracted spin-flavor algebra in the limit of large and finite N_c .

4.4 Large N_c baryon multiplets

The irreducible representations of the contracted spin-flavor $SU(2N_f)_c$ algebra contains the baryon representations of large N_c QCD. These irreducible representations were classified by Dashen et al. [49] using the theory of induced representations. Because, induced group representations provide a complete classification of all irreducible representations of a semi-direct product of a compact Lie group and an Abelian group, and those irreducible representations are induced by the irreducible

representations of the Abelian group. The contracted spin-flavor $SU(2N_f)$ algebra in the large N_c limit is a semi-direct product of an $SU(2)_{spin} \otimes SU(N_f)$ Lie algebra generated by S^i and T^a , and an Abelian algebra generated by X^{ia} from the large N_c consistency condition in Eq. (4.6). The eigenvalues of the generators X_0^{ia} can be used to label the states. Since the Abelian property, all states are obtained by applying spin and $SU(2N_f)$ transformations to the highest-weight state (reference state) of the corresponding irreducible representation.

The standard reference state for irreducible representations of large N_c baryons is,

$$X_0^{ia} = \delta^{ia} = \begin{pmatrix} 1 & 0 & 0 \\ 0 & 1 & 0 \\ 0 & 0 & 1 \end{pmatrix}, \quad (4.10)$$

where, $i = 1, 2, 3$ and $a = 1, 2, 3$ represent the rows and columns of the 3×3 matrix [53]. This reference state is invariant under transformations of a $SU(2)$ little group generated by the grand spin (\vec{K}),

$$\vec{K} = \vec{S} + \vec{I} \quad (4.11)$$

which specify the representation of the $SU(2)$ little group to label the states. Therefore, the irreducible representation can be completely specified by the states $|X^{ia}, K, k\rangle$, using the Abelian coordinate X^{ia} and representations $|K, k\rangle$ of the $SU(2)$ little group. The basis states $|X^{ia}, K, k\rangle$ diagonalize the baryon axial vector currents but are not eigenstates of definite spin and iso-spin. Thus, these states need to be projected on to states that diagonalize spin and iso-spin since baryon states have definite spin and iso-spin. The new basis states $|S, S_z, I, I_z; K\rangle$ do not diagonalize axial-vector currents, and leads to having off-diagonal matrix elements which connect baryons with different spin and iso-spin.

For a given value of K , one can consider all possible spin and iso-spin representations for large N_c baryons, as an infinite towers of (S, I) states. The baryon spin can vary from $1/2$ to $N_c/2$, where N_c is always an odd number. For example when $N_c = 3$, the possible baryon spins are $S = 1/2$ and $S = 3/2$.

- The irreducible representation with $K = 0$ that implies $S = I$ contains an infinite tower of state (S, I) .

$$\left(\frac{1}{2}, \frac{1}{2}\right), \left(\frac{3}{2}, \frac{3}{2}\right), \left(\frac{5}{2}, \frac{5}{2}\right), \dots \quad (4.12)$$

- The irreducible representation with $K = 1/2$ corresponds to an infinite tower of states (S, I) .

$$\left(\frac{1}{2}, 0\right), \left(\frac{1}{2}, 1\right), \left(\frac{3}{2}, 1\right), \left(\frac{3}{2}, 2\right), \left(\frac{5}{2}, 2\right), \left(\frac{5}{2}, 3\right), \dots \quad (4.13)$$

- The irreducible representation with $K = 1$ contains an infinite tower of states (S, I) .

$$\left(\frac{1}{2}, \frac{1}{2}\right), \left(\frac{1}{2}, \frac{3}{2}\right), \left(\frac{3}{2}, \frac{1}{2}\right), \left(\frac{3}{2}, \frac{3}{2}\right), \left(\frac{3}{2}, \frac{5}{2}\right), \left(\frac{5}{2}, \frac{3}{2}\right), \left(\frac{5}{2}, \frac{7}{2}\right), \dots \quad (4.14)$$

- The irreducible representation with $K = 3/2$ forms an infinite tower of states (S, I) .

$$\left(\frac{1}{2}, 1\right), \left(\frac{1}{2}, 2\right), \left(\frac{3}{2}, 0\right), \left(\frac{3}{2}, 1\right), \left(\frac{3}{2}, 2\right), \left(\frac{3}{2}, 3\right), \dots \quad (4.15)$$

For different K values, the spin and iso-spin quantum numbers of the baryon states can be identified with the physically known baryon octet with spin $S = 1/2$ and decuplet with spin $S = 3/2$ in QCD, if the quantum number K is related to the number of strange quarks N_s in baryons by, $K = N_s/2$. For example,

- $K = 0$ tower contains strangeness zero nucleon $(1/2, 1/2)$ and delta $(3/2, 3/2)$ states
- $K = 1/2$ tower contains strangeness $N_s = -1$ baryon states, $\Lambda(1/2, 0)$, $\Sigma(1/2, 1)$, and $\Sigma^*(3/2, 1)$
- $K = 1$ tower contains strangeness $N_s = -2$ baryon states, $\Xi(1/2, 1/2)$, $\Xi^*(3/2, 1/2)$
- $K = 3/2$ tower contains strangeness $N_s = -3$ baryon state, $\Omega(3/2, 0)$.

The other states correspond to baryons that exist for $N_c \rightarrow \infty$ but not for $N_c = 3$ [50, 53].

This observation of towers of possible (S, I) baryon states reveals the existence of an infinite number of intermediate baryon states as $N_c \rightarrow \infty$ which are degenerate with the initial and final baryon state as required by the large N_c consistency condition. These states reflect the cancellations between the dominant diagrams for the baryon-meson scattering as a requirement for the scattering amplitude to be unitary, according to the large N_c power counting by Witten.

4.5 $1/N_c$ corrections

$1/N_c$ corrections to $SU(2N_f)$ symmetry at finite N_c were studied by deriving the next to leading order large N_c consistency conditions in the $1/N_c$ expansion using the static baryon matrix elements [12, 14, 50], such as baryon masses and axial couplings.

4.5.1 $1/N_c$ corrections to axial currents

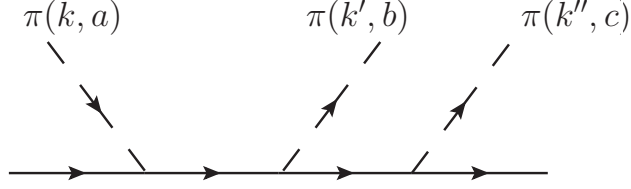


Figure 4.2. $B + \pi \rightarrow B + \pi + \pi$ scattering amplitude.

$1/N_c$ corrections to the axial couplings X^{ia} are determined through obtaining a consistency condition by considering the scattering process $B + \pi \rightarrow B + \pi + \pi$, as showed in Fig. (4.2). According to Witten's large N_c power counting each baryon-pion vertex is $\mathcal{O}(\sqrt{N_c})$ leads to each individual diagram to be $\mathcal{O}(N_c^{3/2})$. The scattering amplitude for this process is proportional to

$$N_c^{3/2}[X^{ia}, [X^{jb}, X^{kc}]] \quad (4.16)$$

times kinematic factors of $\mathcal{O}(1)$, which violates the unitarity. Since one can expect that the double commutator is of $\mathcal{O}(1/N_c^2)$, thus the total amplitude is at most $\mathcal{O}(1/\sqrt{N_c})$ [14, 48, 53] with summing over all possible tree level diagrams yields a constraint

$$N_c^{3/2}[X^{ia}, [X^{jb}, X^{kc}]] \leq \mathcal{O}(1/\sqrt{N_c}). \quad (4.17)$$

Using the consistency condition $[X^{ia}, X^{jb}] = 0$ and substituting the expanded form of the axial coupling X^{ia} in Eq. (4.5) in to the constraint give the large N_c consistency condition

$$[X_0^{ia}, [X_1^{jb}, X_0^{kc}]] + [X_0^{ia}, [X_0^{jb}, X_1^{kc}]] = 0 \quad (4.18)$$

for X_1^{ia} . The only solution to this consistency condition is $X_1^{ia} \propto X_0^{ia}$. This was verified by an explicit calculation of the matrix element of X^{ia} in Ref. [50]. Thus one

can re-write X^{ia} as

$$X^{ia} = X_0^{ia} + \frac{c}{N_c} X_0^{ia} + \mathcal{O}(1/N_c^2) + \dots, \quad (4.19)$$

where c is an unknown constant. This shows that $\mathcal{O}(1/N_c)$ corrections are proportional to the lowest order value X_0^{ia} , and the $1/N_c$ corrections to the axial coupling starts at $\mathcal{O}(1/N_c^2)$. The overall normalization factor $(1 + c/N_c)$ can be absorbed into g_A in Eq. (4.2) by rescaling $g_A \rightarrow g_A(1 + c/N_c)$, thus there are no parameters for the axial current at $\mathcal{O}(1/N_c)$. X^{ia} can be re-written as,

$$X^{ia} = X_0^{ia} + \mathcal{O}\left(\frac{1}{N_c^2}\right), \quad (4.20)$$

so that all baryon-pion couplings are determined up to $\mathcal{O}(1/N_c^2)$.

This result is valid for any baryon spin tower with fixed K , where the number of strange quarks in the baryon is given by $2K$. Therefore the pion couplings can be identified as the matrix elements of X_0^{ia} , and the expression for the axial current matrix elements in the large N_c limit is given by,

$$\begin{aligned} \langle S', S'_3; I', I'_3; K | A^{ia} | S, S_3; I, I_3; K \rangle &= N_c g(K) (-1)^{2S' + S - I' - K} \sqrt{(2S + 1)(2I + 1)} \\ &\times \begin{pmatrix} 1 & I & I' \\ K & S' & S \end{pmatrix} \begin{pmatrix} 1 & I & I' \\ I_3 & a & I'_3 \end{pmatrix} \begin{pmatrix} S & 1 & S' \\ S_3 & a & S'_3 \end{pmatrix} \end{aligned} \quad (4.21)$$

where $g(K)$ is an unknown coupling constant for a given K sector [50, 54]. $g(K)$ can be written as,

$$g(K) = g_0 + g_1 \frac{K}{N_c} + g_2 \frac{K^2}{N_c^2} + \dots \quad (4.22)$$

where g_i 's are K -independent coefficients. The first term is $\mathcal{O}(1)$ and it is K -independent, which implies $SU(3)$ flavor-symmetry of pion-baryon couplings at the leading order. The second term is of $\mathcal{O}(1/N_c)$ and linear in K , and the coefficient

g_1 is calculable in $SU(3)$ flavor-symmetry limit [50]. The ratios of pion-baryon couplings within a given K baryon tower has corrections of $\mathcal{O}(1/N_c^2)$, while the ratios of pion-baryon couplings between towers with two different K values can have $1/N_c$ corrections that are linear in K . Higher order corrections to baryon axial vector current can be calculated by considering the process $B + \pi \rightarrow B + n\pi$, where $n > 2$ [53]. All the above has been discussed only by analyzing tree level diagrams. The discussion including one-loop corrections is presented in chapter 10 in the case $N_f = 3$ the chiral corrections to the axial currents reveal that $SU(3)$ breaking effects are not suppressed by factors of $1/N_c$. Thus, the assertion above is only true in the strict $SU(3)$ symmetry case.

4.5.2 $1/N_c$ corrections to baryon masses

One can derive the large N_c consistency conditions for the baryon masses by considering the baryon mass splitting on the baryon-pion scattering amplitude [53]. The intermediate propagator for non-degenerate baryons can be written as $i/(kv - \Delta M)$, where k is the momentum of pion, v is the baryon velocity and ΔM is the baryon mass splitting. This propagator can be expanded in powers of $[\Delta M/(kv)]$ up to $\mathcal{O}(1/N_c)$ since the energy of the meson (kv) is $\mathcal{O}(1)$ and ΔM is $\mathcal{O}(1/N_c)$,

$$\frac{i}{kv - \Delta M} = \frac{1}{kv} + \frac{\Delta M}{(kv)^2} + \cdots. \quad (4.23)$$

Inserting this expanded version of the propagator with terms up to $\mathcal{O}(1/N_c)$ to the Eq. (4.3) of baryon-pion scattering amplitude, one can see that the first term of Eq. (4.23) reveal the leading order large N_c consistency condition in Eq. (4.6). The second term of Eq. (4.23) in the baryon-pion scattering amplitude yields the constraint

$$[X^{ia}, [X^{jb}, M_B]] \leq \mathcal{O}(1/N_c) \quad (4.24)$$

where M_B is the baryon mass which can be expanded as,

$$M_B = N_c M_0 + M_1 + \frac{1}{N_c} M_2 + \cdots . \quad (4.25)$$

Therefore the constraint in Eq. (4.24) implies that M_0 and M_1 terms have to satisfy,

$$[X^{ia}, [X^{jb}, M_0]] = 0 \quad \& \quad [X^{ia}, [X^{jb}, M_1]] = 0. \quad (4.26)$$

The only solutions for these large- N_c consistency conditions are $M_0 \propto M_1 \propto \mathcal{O}(1)$ [53]. Thus, one can see that the baryon tower is degenerate up to $\mathcal{O}(1/N_c)$ corrections and the baryon mass can be written in a simple form as,

$$M_B = N_c m_0 + \mathcal{O}(1/N_c) + \cdots , \quad (4.27)$$

in the $SU(3)$ symmetric limit. $1/N_c$ correction to the baryon mass can be obtained by the process $B + \pi \rightarrow B + \pi + \pi$, shown in Fig. (4.2). Also the constraint in Eq. (4.17) can be re-written as

$$[X^{ia}, [X^{jb}, [X^{kc}, M_B]]] \leq \mathcal{O}(1/N_c^2) \quad (4.28)$$

and it yields a large N_c consistency condition for $1/N_c$ correction to the baryon mass in Eq. (4.25).

$$[X_0^{ia}, [X_0^{jb}, [X_0^{kc}, M_2]]] = 0 \quad (4.29)$$

This consistency condition has solutions $M_2 = \vec{S}^2, \vec{I}^2$ and $X_0^{ia} X_0^{ia}$ [53]. Since $\vec{S}^2 = \vec{I}^2$ and $X_0^{ia} X_0^{ia} = 3$, then the only independent solution is $M_2 = \vec{S}^2$. Thus, the baryon mass can be given by,

$$M_B = m_0 N_c + m_2 \frac{\vec{S}^2}{N_c} + \mathcal{O}(1/N_c^2) + \cdots \quad (4.30)$$

including the $1/N_c$ correction. This implies that the leading order correction to the baryon mass is the hyperfine splitting.

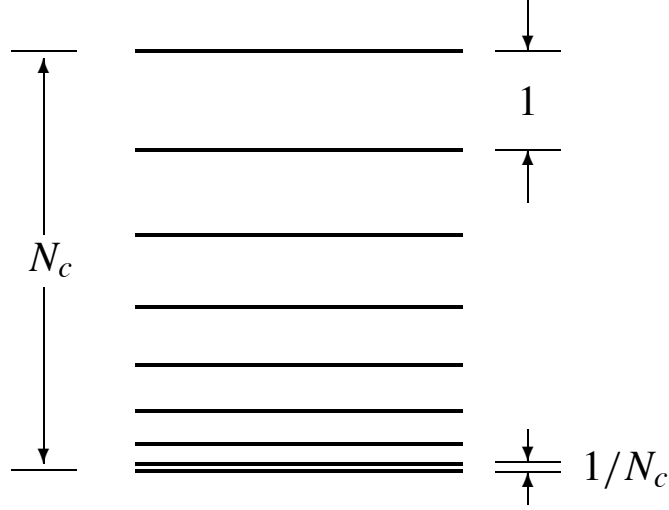


Figure 4.3. Hyperfine mass splitting of large N_c baryons.

For the baryons with spin $\mathcal{O}(1)$, the hyperfine mass splitting is $\mathcal{O}(1/N_c)$ and the baryons with spin of $\mathcal{O}(N_c)$ have hyperfine mass splitting of $\mathcal{O}(1)$. Also, the hyperfine splitting is $\mathcal{O}(N_c)$ between a baryon with spin of $\mathcal{O}(N_c)$ and a baryon with spin of $\mathcal{O}(1)$. Therefore, one can consider in general the baryon mass splitting as proportional to \vec{S}^2/N_c . This is shown explicitly in Fig. (4.3) which shows the baryon mass spectrum including the hyperfine \vec{S}^2/N_c mass splittings. These corrections are only small near the bottom of the baryon spectrum. Therefore, the $1/N_c$ expansion for baryons is well behaved for baryons with spin S held fixed as $N_c \rightarrow \infty$.

Studying the solution to the large N_c consistency conditions is essential for understanding the structure of large N_c baryons. One can directly write down the baryon operator in $1/N_c$ expansion. For example, any static baryon operator for the case of

two light quark flavors $N_f = 2$ can be written as,

$$N_c P \left(X_0, \frac{S}{N_c}, \frac{I}{N_c} \right) , \quad (4.31)$$

where P is a polynomial. The $1/N_c$ expansion can be extended to baryon towers with different K by including the K/N_c operator in the polynomial P , which provides the extension to study the $SU(3)$ flavor symmetry breaking.

CHAPTER 5

BARYON OPERATORS IN THE $1/N_c$ EXPANSION

5.1 Introduction

According to the previous chapter, the $1/N_c$ expansion of static baryon operators can be written in terms of operator products of the baryon spin-flavor generators. These operator products can be linearly independent or dependent. Redundant operators can be eliminated using operator identities. Each operator product appears with its order in $1/N_c$ and an unknown coefficient which contains the large N_c QCD dynamics. These unknown coefficients which correspond to static baryon observables can be extracted by fitting to the data from experiments. Since the number of operator products are finite at a given order in $1/N_c$, this framework can be used as a powerful predictive tool for baryons with finite spin and flavor.

The operator basis of the $1/N_c$ expansion can be constructed using two basic realizations of the baryon spin-flavor algebra in the large N_c limit. One is, the contracted spin-flavor $SU(2N_f)_c$ algebra with the generator X_0^{ia} , and the other one is the ordinary $SU(2N_f)$ algebra with the generator G^{ia} . These generators X_0^{ia} and G^{ia}/N_c differ at sub-leading order in $1/N_c$. The operator basis with X_0^{ia} is equivalent to the operator basis of large N_c Skyrme model, whereas the operator basis with G^{ia} is equivalent to the large N_c non-relativistic quark model. Since these operator bases parameterize the same large N_c physics, one can choose to work with either basis according to the convenience. Regardless of which basis is used, the operator products appear in $1/N_c$ expansion with unknown dynamical coefficients. Although, the coefficients of large N_c baryons are different from the coefficients of the large N_c Skyrme model and large N_c quark model, but the physics description will be equivalent up to higher order

corrections in $1/N_c$ than the leading order. The work by Dashen et al. [49], Luty et al. [55, 56], Goity et al. [21, 25, 44] and Carone et al. [57] are some examples of formulating large N_c operator products using baryon spin-flavor generators which are interpreted as quark operators.

The outline of this chapter is the following. The second section is on the baryon operator expansion with N_c power counting. Then the third section presents about the quark operator classification. The fourth section contains a discussion on operator identities derived in Dashen *et al.* [49]. In the last section, the $1/N_c$ expansion and operator identities are applied to the baryon mass operator.

5.2 Baryon operator expansion

The N_c dependence of the operator matrix elements of baryon states and their power counting can be obtained, using planar diagrams introduced by 'tHooft [10] and the power counting rules by Witten [15]. Let's consider the baryon matrix element of a single-quark operator. This is obtained by inserting the operator on any of the N_c quark lines as shown in Fig. 5.1(a). Since there are N_c possible insertions, one-quark QCD operator can have a matrix element of $\mathcal{O}(N_c)$ at most. It is not necessarily to be of $\mathcal{O}(N_c)$, since there may be possible cancellations among insertions on different quark lines. The single gluon exchange graphs as shown in Fig. 5.1(b) have an extra factor $1/N_c$ from the two gauge couplings at quark-gluon vertices. Also, diagrams with an additional non-planar gluon exchanges are suppressed by powers of $1/N_c$ as discussed in chapter 2. In general, QCD one-quark (or one-body) operator can be identified as $\mathcal{O}_{QCD}^{1\text{-body}} = \bar{q}\Gamma q$, where $\Gamma = \{\gamma_\mu, \gamma_\mu\gamma_5, T^a\gamma_\mu, T^a\gamma_\mu\gamma_5, \dots\}$.

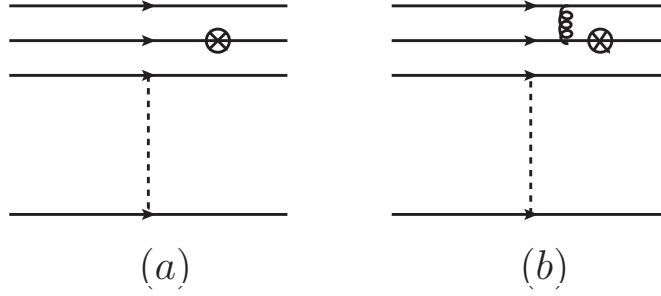


Figure 5.1. (a): single quark operator insertion. (b) : single quark operator insertion with a one-gluon-exchange.

At leading order in the $1/N_c$ expansion, the QCD 1-body operator which transforms according to $SU(2) \otimes SU(N_f)$ representation can be written [53] as a linear combination of n -body effective operators \mathcal{O}_n and c_n unknown coefficients.

$$\mathcal{O}_{QCD}^{1\text{-body}} = N_c \sum_n c_n \frac{1}{N_c^n} \mathcal{O}_n = \sum_n c_n \frac{1}{N_c^{n-1}} \mathcal{O}_n \quad (5.1)$$

For finite N_c , the degree n falls in the range $0 < n \leq N_c$. Every coefficient c_n has an expansion in $1/N_c$ and the leading term is $\mathcal{O}(1)$. \mathcal{O}_n is an n^{th} order operator product that consists of spin-flavor generators. Since each spin-flavor generator is accompanied by a factor of $1/N_c$, the operator product \mathcal{O}_n has a factor of $1/N_c^n$. There is another overall factor N_c that comes from all possible insertions of the 1-body operator among N_c quark lines in the baryon. Analogously, one can write down the general form of an m -body operator as,

$$\mathcal{O}_{QCD}^{m\text{-body}} = N_c^m \sum_n c_n \frac{1}{N_c^n} \mathcal{O}_n = \sum_n c_n \frac{1}{N_c^{n-m}} \mathcal{O}_n. \quad (5.2)$$

This N_c counting is also preserved under commutation [49]. For example, the commutator of an n -body and an m -body operator is an $(n+m-1)$ -body operator

$$[\mathcal{O}_n, \mathcal{O}_m] = \mathcal{O}_{n+m-1}, \quad (5.3)$$

accompanied by a factor $(1/N_c^{n-1})(1/N_c^{m-1}) = (1/N_c^{(n+m-1)-1})$. But, the anti-commutator of the same two operators is typically an $(n+m)$ -body operator. The commutativity requires one quark in \mathcal{O}_n to act on the same quark line as a quark in \mathcal{O}_m to produce non-zero commutator, because the quark operators acting on different quark lines commute with each other. Thus, it reduces the $(n+m)$ -body operator to an $(n+m-1)$ body operator.

One can construct the effective n -body operators \mathcal{O}_n using spin S^i , flavor T^a and spin-flavor G^{ia} generators of the $SU(2N_f)$ algebra [49], because the operator \mathcal{O}_n acts on the spin and flavor indices of n -quarks. Therefore \mathcal{O}_n has the generic form,

$$\mathcal{O}_n = \sum_{m,l} (S^i)^m (T^a)^l (G^{ia})^{n-m-l} , \quad (5.4)$$

and the QCD one-body operator becomes,

$$\mathcal{O}_{QCD}^{1\text{-body}} = \sum_{n,m,l} c_n \frac{1}{N_c^{n-1}} (S^i)^m (T^a)^l (G^{ia})^{n-m-l} . \quad (5.5)$$

The above form of the n -body operator \mathcal{O}_n is only applicable for ground state baryons. For orbitally excited baryons, one must include $SO(3)$ orbital angular momentum generators ℓ^i in the operator product [58, 59] in the Eq. (5.4).

There are two types of N_c dependences in QCD one-body operator. First one is an explicit N_c dependence by the factor $1/N_c^{n-1}$ accompanying the n -body operator \mathcal{O}_n , and the second one is an implicit N_c dependence from the matrix elements of \mathcal{O}_n . Since \mathcal{O}_n is a product of spin-flavor $SU(2N_f)$ generators, their matrix elements vary with the baryon states in different spin-flavor multiplets. For example, consider the baryon spin tower $S = \{1/2, 3/2, \dots, N_c/2\}$. The lower bottom of this tower contains baryons with spin of $\mathcal{O}(N_c^0)$, whereas, the top of the tower contains baryons

with spin of $\mathcal{O}(N_c)$. Since the matrix elements of S, I and G^{ia} of baryon states are $\leq \mathcal{O}(N_c)$, the n^{th} order operator \mathcal{O}_n has matrix elements $\leq \mathcal{O}(N_c^n)$. Consider a baryon with spin of $\mathcal{O}(N_c)$. It produces a factor N_c^n from the matrix elements of \mathcal{O}_n , which compensate with the explicit factor $1/N_c^n$. Thus, the $1/N_c$ expansion will not be a predictive tool for baryons with spin of $\mathcal{O}(N_c)$ since all the terms in the expansion are equally important. Baryons with spins of $\mathcal{O}(N_c^0)$ are systematically suppressed $1/N_c$, and the operator expansion can be truncated at any desired order in the $1/N_c$ expansion. Therefore, the $1/N_c$ expansion can be considered as a predictive tool for baryons with low-spin.

5.3 Quark operator classification

Let's consider the spin-flavor structure of ground-state baryons for large, odd and finite N_c . The completely symmetric spin-flavor representation of ground-state baryons can have spin $1/2, 3/2, \dots, N_c/2$. Also, spin-flavor $SU(2N_f)$ representation can be decomposed into a tower of $SU(2) \otimes SU(N_f)$ representations, as given in Eq. (3.33). For two quark flavors, the ground state baryon representation contains a tower of baryon states with $S = I$,

$$(S, I) = 1/2, 3/2, \dots, N_c/2 \quad (5.6)$$

which is finite dimensional unlike the infinite dimensional baryon tower (see Eq. (4.12)) of the contracted spin-flavor algebra. When $N_c = 3$, this reduces to N and Δ states. For three quark flavors, each baryon spin corresponds to a weight diagram (see Fig. (3.2) and Fig. (3.3)).

Quark representation of the spin-flavor symmetry of large N_c baryons manifests the non-relativistic quark model picture. However, this does not mean that the quarks in baryons are assumed to be non-relativistic. A detailed discussion of this approach are given in Refs. [55, 57]. Quark creation and annihilation operators q_f^\dagger and q_f are defined in the quark representation. The index f varies from 1 to $2N_f$, where $f = \{1, \dots, N_f\}$ represents the N_f quark flavors with spin up and $f = \{N_f+1, \dots, 2N_f\}$ represents the N_f quark flavors with spin down. Since baryons are fermions and the antisymmetry of the $SU(N_c)$ color symbol implies that the ground state baryons contain N_c quarks in the completely symmetric spin-flavor representation with N_c boxes (see Fig. (3.1)) according to Young Tableaux. Thus, one can consider them as bosonic objects by omitting the color quantum numbers of quark operators for the spin-flavor analysis, and the quark operators satisfy the bosonic commutation relation

$$[q^f, q_{f'}^\dagger] = \delta_f^{f'}. \quad (5.7)$$

An n -body operator can be written using quark creation and annihilation operators. These quark operators can be classified by considering the number of q^\dagger , q pairs in the operator.

- Zero-body operators :

A zero-body operator does not contain q or q^\dagger , and it is uniquely identified as the identity operator $\mathbb{1}$.

- One body operators :

A one-body operator acts on a single quark. It contains the quark number operator $q^\dagger q$:

$$q^\dagger q = \sum_{j=1}^{N_c} q_j^\dagger q_j = N_c \mathbb{1}, \quad (5.8)$$

and the spin-flavor adjoint $q^\dagger \Lambda^A q$, where Λ^A is spin-flavor generator with $A = \{1, \dots, (2N_f)^2 - 1\}$. It is convenient to decompose the $SU(2N_f)$ adjoint one-body operator $q^\dagger \Lambda^A q$ into $SU(2) \otimes SU(N_f)$:

$$\begin{aligned} S^i &= \sum_{j=1}^{N_c} q_j^\dagger (S^i \otimes \mathbb{1}) q_j & (1, 0) \\ T^a &= \sum_{j=1}^{N_c} q_j^\dagger (\mathbb{1} \otimes T^a) q_j & (0, adj) \\ G^{ia} &= \sum_{j=1}^{N_c} q_j^\dagger (S^i \otimes T^a) q_j & (1, adj) \end{aligned} \quad (5.9)$$

where S^i and T^a on the right-hand side are in the fundamental representations of $SU(2)$ and $SU(N_f)$ respectively. They are normalized as,

$$\begin{aligned} \text{Tr} \langle S^i S^j \rangle &= \frac{1}{2} \delta^{ij} \\ \text{Tr} \langle T^a T^b \rangle &= \frac{1}{2} \delta^{ab} \\ \text{Tr} \langle \Lambda^A \Lambda^B \rangle &= \frac{1}{2} \delta^{AB} \end{aligned} \quad (5.10)$$

where $i, j = \{1, 2, 3\}$, $a = \{1, \dots, 8\}$. When $N_c = 3$, S^i and T^a becomes σ^i and λ^a which represent Pauli and Gell-Mann matrices respectively. Also, the uppercase letters (A, B, \dots) denote indices transforming according to the adjoint representation of the $SU(2N_f)$ spin-flavor group, and the lowercase letters (a, b, \dots) denote indices transforming according to the adjoint representation of the $SU(N_f)$ flavor group. The brackets in the right hand side denote the dimension of the corresponding irreducible representation $SU(2) \otimes SU(N_f)$.

- Two-body operators : Two-body operators act on two quarks. It contains two creation and annihilation operators, q, q^\dagger . For example,

$$S^i T^a = \sum_{j, j'}^{N_c} \left(q_j^\dagger S^i q_j \right) \left(q_{j'}^\dagger T^a q_{j'} \right) \quad (5.11)$$

where each one-body operator acts on separate quark lines. When $j = j'$, two-body operator reduces to one-body operator. But for all the cases when $j \neq j'$, this operator is a pure two-body operator.

- In general, n -body operators : Considering the structure of two-body operators, one can generalize it into an n -body operator,

$$q^\dagger \cdots q^\dagger \mathcal{T} q \cdots q, \quad (5.12)$$

where \mathcal{T} is a traceless completely symmetric tensor. Because \mathcal{T} must be traceless in order to be a pure n -body operator, and symmetric as the spin-flavor part of the ground-state baryon wave function is symmetric.

5.4 Operator identities

In the previous section, the operator structures in the quark representation are discussed. In calculating matrix elements, it's easy to deal with lower-body operators than complex many-body operators. Therefore it's important if an n -body effective operator in the $1/N_c$ expansion can be reduced into linear combinations of lower-body operators. Operator identities play a key role in reduction of a many-body operator into linear combinations of lower-body operators by eliminating redundant operators. The operator reduction of 2-body operators was done by Dashen et al. [49], and their work is briefly summarized in this section.

The unique zero-body operator is the identity operator $\mathbb{1}$. One-body operators are the quark number operator : $q^\dagger q$ and spin-flavor generators : $q^\dagger \Lambda^A q$, where $\Lambda^A = \{S^i, T^a, G^{ia}\}$. The only operator reduction for a one-body operator is the reduction of quark number operator into the identity (see Eq.(5.8)). A two body operator

transforms as a singlet ($\mathbb{1}$), adjoint (T_β^α) and a completely symmetric traceless tensor ($\bar{s}s = T_{(\beta_1, \beta_2)}^{(\alpha_1, \alpha_2)}$) under $SU(2N_f)$.

$$\begin{aligned} \text{Two-body :} &= \mathbb{1} \oplus adj \oplus \bar{s}s \\ &= \mathbb{1} \oplus T_\beta^\alpha \oplus T_{(\beta_1, \beta_2)}^{(\alpha_1, \alpha_2)} \end{aligned} \quad (5.13)$$

Since the quark number operator can be eliminated by the identity in Eq. (5.8) one can only consider the adjoint bilinears $q^\dagger \Lambda^A q$ of $SU(2N_f)$. A product of two operators can be written in terms of its symmetric product (an anti-commutator) or/and anti-symmetric product (a commutator). The commutator can be reduced using the Lie algebra relations in Eq. (4.8), and the anti-commutator transform as the symmetric product of two adjoints:

$$\begin{aligned} (adj \otimes adj)_S &= \mathbb{1} \oplus adj \oplus \bar{a}a \oplus \bar{s}s \\ &= \mathbb{1} \oplus T_\beta^\alpha \oplus T_{[\beta_1 \beta_2]}^{[\alpha_1 \alpha_2]} \oplus T_{(\beta_1 \beta_2)}^{(\alpha_1 \alpha_2)}, \end{aligned} \quad (5.14)$$

where the traceless tensor ($\bar{a}a = T_{[\beta_1 \beta_2]}^{[\alpha_1 \alpha_2]}$) transforms as anti-symmetric in its upper and lower indices. One can directly notice that this $\bar{a}a$ does not appear in the representation of a two-body operator. Dashen et al [49] summarized the two-body identities into three different sets.

- The first identity (reduction to zero-body) : two-body operators contain a $SU(2N_f)$ singlet component which is a linear combination of a coefficient and the zero-body unit operator. The $SU(2N_f)$ singlet in $(adj \otimes adj)_S$ is the Casimir operator,

$$\{q^\dagger \Lambda^A q, q^\dagger \Lambda^A q\} = N_c(N_c + 2N_f) \left(1 - \frac{1}{N_f}\right) \mathbb{1}, \quad (5.15)$$

where the coefficient of $\mathbb{1}$ operator is the $SU(2N_f)$ Casimir invariant of $\mathcal{O}(N_c^2)$ for the completely symmetric baryon representation.

- The second identity (reduction to one-body) : two-body operators contain a $SU(2N_f)$ adjoint component which is a linear combination of a coefficient of $\mathcal{O}(N_c)$ times the one-body adjoint operator. This $SU(2N_f)$ adjoint in $(adj \otimes$

$adj)_S$ is obtained by a contraction of the anti-commutator with the $SU(2N_f)$ d symbol d^{ABC} ,

$$d^{ABC}\{q^\dagger\Lambda^B q, q^\dagger\Lambda^C q\} = 2(N_c + N_f)\left(1 - \frac{1}{N_f}\right)q^\dagger\Lambda^A q. \quad (5.16)$$

- The third identity (neglecting $\bar{a}a$ components) simply reveals that the $\bar{a}a$ representation in Eq.(5.14) must vanish by comparing the representations in Eq.(5.13) corresponding to the completely symmetric baryon representation.

In addition to the components of the two-body operator given in Eq.(5.13), a three-body operator has a traceless tensor:

$$\text{Three-body} := \mathbf{1} \oplus T_\beta^\alpha \oplus T_{(\beta_1\beta_2)}^{(\alpha_1\alpha_2)} \oplus T_{(\beta_1\beta_2\beta_3)}^{(\alpha_1\alpha_2\alpha_3)}. \quad (5.17)$$

This additional component $T_{(\beta_1\beta_2\beta_3)}^{(\alpha_1\alpha_2\alpha_3)}$ can be considered as a completely symmetric tri-linear products of adjoint one-body operators, since the products which are not completely symmetric can be reduced to two-body operators using the identities given in Eq.(4.8). Although there are ten irreducible $SU(2N_f)$ representations in $(adj \otimes adj \otimes adj)_S$ for the case of $N_f \geq 2$, but only four of them survive because the other six sets identically vanish according to the Eq.(5.17). Some of these three-body identities are products of two-body $\bar{a}a$ representation and one-body adjoint representation. By comparing all the representations of $(adj \otimes adj \otimes adj)_S$ and $\bar{a}a \otimes adj$ separately with the Eq.(5.17), and requiring that the adjoints in $(\bar{a}a \otimes adj)$ are completely symmetric; Dashen et al. [49] showed that the three-body identities are simply products of the one-body and two-body identities.

In summary, the allowed representations of $SU(2N_f)$ for n -body operators are $\mathbf{1} \oplus T_\beta^\alpha \oplus T_{(\beta_1\beta_2)}^{(\alpha_1\alpha_2)} \oplus \dots \oplus T_{(\beta_1\beta_2\dots\beta_n)}^{(\alpha_1\alpha_2\dots\alpha_n)}$. All the other representations can be ruled out

using the two-body $\bar{a}a$ operator identities, whereas the only “pure” n -body representation is $T_{(\beta_1\beta_2\cdots\beta_n)}^{(\alpha_1\alpha_2\cdots\alpha_n)}$. For an arbitrary light quark flavors N_f , two-body operator identities of $SU(2N_f)$ are given in the Table(5.1). The spin-flavor representation $(SU(2), SU(N_f))$ of each identity is given in the second column, and the entire table is divided into three separate horizontal sections. The first section contains the $SU(2N_f)$ Casimir identity. The second section contains the identities transforming the two-body operators into $SU(2N_f)$ adjoints. The third section contains the identities transforming two one-body adjoints into $\bar{a}a$ representation.

Table 5.1. $SU(2N_f)$ identities : Transformation properties of the identities under $SU(2) \times SU(N_f)$ are given in the second column [49].

$2\{S^i, S^i\} + N_f\{T^a, T^a\} + 4N_f\{G^{ia}, G^{ia}\} = N_c(N_c + 2N_f)(2N_f - 1)$	(0, 0)
$d^{abc}\{G^{ia}, G^{ib}\} + \frac{2}{N_f}\{J^i, G^{ic}\} + \frac{1}{4}d^{abc}\{T^a, T^b\} = (N_c + N_f)\left(1 - \frac{1}{N_f}\right)T^c$	(0, adj)
$\{T^a, G^{ia}\} = (N_c + N_f)\left(1 - \frac{1}{N_f}\right)S^i$	(1, 0)
$\frac{1}{N_f}\{S^k, T^c\} + d^{abc}\{T^a, G^{kb}\} - \epsilon^{ijk}f^{abc}\{G^{ia}, G^{jb}\} = 2(N_c + N_f)\left(1 - \frac{1}{N_f}\right)G^{kc}$	(1, adj)
$4N_f(2 - N_f)\{G^{ia}, G^{ia}\} + 3N_f^2\{T^a, T^a\} + 4(1 - N_f^2)\{S^i, S^i\} = 0$	(0, 0)
$(4 - N_f)\{G^{ia}, G^{ib}\} + 3N_f^2\{T^a, T^b\} - 2\left(N_f - \frac{4}{N_f}\right)\{J^i, G^{ia}\} = 0$	(0, adj)
$4\{G^{ia}, G^{ib}\} = -3\{T^a, T^b\}$	($\bar{a}a$) (0, $\bar{a}a$)
$4\{G^{ia}, G^{ib}\} = \{T^a, T^b\}$	($\bar{s}s$) (0, $\bar{s}s$)
$\epsilon^{ijk}\{S^i, G^{ic}\} = f^{abc}\{T^a, G^{kb}\}$	(1, adj)
$d^{abc}\{T^a, G^{kb}\} = \left(1 - \frac{2}{N_f}\right)(\{S^k, T^c\} - \epsilon^{ijk}f^{abc}\{G^{ia}, G^{jb}\})$	(1, adj)
$\epsilon^{ijk}\{G^{ia}, G^{jb}\} = f^{acg}d^{bch}\{T^g, G^{kh}\}$	($\bar{a}s + \bar{s}a$) (1, $\bar{a}s + \bar{s}a$)
$\{T^a, G^{ib}\} = 0$	($\bar{a}a$) (1, $\bar{a}a$)
$\{G^{ia}, G^{ja}\} = \frac{1}{2}\left(1 - \frac{1}{N_f}\right)\{S^i, S^j\}$	($S = 2$) (2, 0)
$d^{abc}\{G^{ia}, G^{jb}\} = \left(1 - \frac{2}{N_f}\right)\{S^i, G^{jc}\}$	($S = 2$) (2, adj)
$\{G^{ia}, G^{jb}\} = 0$	($S = 2, \bar{a}a$) (2, $\bar{a}a$)

5.5 An application : Baryon mass operator

The operator identities can be considered as valuable tool set in building and analyzing baryon operators such as baryon masses, magnetic moments, baryon axial currents etc,. As an example, one can illustrate the baryon mass operator for $N_f = 3$, in the $1/N_c$ expansion [47, 49]. For three light quark flavors, the baryon mass operator can be decoupled into two parts. The first part assumes the $SU(3)$ symmetric limit, *i.e.* up, down and strange quark masses are equal. The second part assumes the $SU(3)$ breaking limit with different quark masses.

5.5.1 Baryon masses in the $SU(3)$ symmetric limit

In the $SU(3)$ symmetric limit, the mass operator transforms as a spin-flavor singlet. Since the baryon mass operator is a QCD one-body operator, it has the same form as in Eq. (5.5),

$$M_B^{(1,1)} = \sum_{n,l} c_l^{(n)} \frac{1}{N_c^{n-1}} \mathcal{O}_l^{(n)}, \quad (5.18)$$

where $c_l^{(n)}$ are unknown dynamical coefficients. As a consequence of being the mass operator a spin-flavor singlet, the effective n -body operators $\mathcal{O}^{(n)}$ defined in Eq. (5.4) must be $SU(2) \times SU(3)$ scalars. To obtain a $SU(3)$ flavor singlet, all the flavor indices on T 's and G 's must be contracted using $SU(3)$ -invariant tensors δ^{ab} , d^{abc} , and f^{abc} . The latter operator products can be removed using the operator reduction rule.

The zero-body operator transforming as a singlet under $SU(2) \times SU(3)$ is the identity operator $\mathbb{1}$. Since the one-body operators do not transform as a singlet under $SU(2) \times SU(3)$, then there are no contributions from one-body operators to the baryon mass operator. There is only one two-body operator S^2 transforming as a singlet under $SU(2) \times SU(3)$, because the operator identities can be used to express T^2 and G^2 in terms of S^2 . Notice that the three-body operators and all other operators

with odd number of contributions can be removed by the operator reduction rule; and the only possible spin-flavor singlet operators are the identity $\mathbb{1}$ and even powers of S^2 . Therefore, the $SU(3)$ symmetric part of the baryon mass operator can be simply written as,

$$M_B^{(1,1)} = c_0 N_c \mathbb{1} + c_2 \frac{1}{N_c} S^2 + c_4 \frac{1}{N_c^3} S^4 + \cdots + c_{N_c-1} \frac{1}{N_c^{N_c-2}} S^{N_c-1} \quad (5.19)$$

5.5.2 Baryon masses in the $SU(3)$ breaking limit

The $SU(3)$ symmetry is not exact because the light quarks have different masses. The perturbation transforms as an octet $(1, 8)$ under $SU(2) \times SU(3)$. Therefore the $SU(3)$ breaking part of the baryon mass operator transforms as an octet [47],

$$M_B^{(1,8)} = \sum_{n=1}^{N_c} d_n \frac{1}{N_c^{n-1}} \mathcal{O}_n^a, \quad (5.20)$$

where d_n are unknown dynamical coefficients, and the effective operators \mathcal{O}_n^a are the products of $SU(3)$ generators with one free flavor index a . The operator reduction identities imply that, only the n -body operators with either one T^a or one G^{ia} need to be considered. There is only one independent one-body operator,

$$\mathcal{O}_1^a = T^a, \quad (5.21)$$

and only one two-body operator,

$$\mathcal{O}_2^a = \{S^i, G^{ia}\}, \quad (5.22)$$

are allowed after implementing the operator reduction [47]. Moreover, the operator reduction helps one to see that there is only one independent n -body for each n . All of these operators can be generated by recursively anti-commuting the 1-body and

2-body operators with S^2 [47, 49],

$$\mathcal{O}_{n+2}^a = \{S^2, \mathcal{O}_n^a\} . \quad (5.23)$$

Since S is of $\mathcal{O}(N_c^0)$, the operator \mathcal{O}_{n+2}^a is suppressed by $1/N_c^2$ relative to \mathcal{O}_n^a . It is valid to truncate the expansion in Eq. (5.20) for arbitrary a after the first two terms, up to corrections of relative order $1/N_c^2$ [47]. After the operator reduction, the three-body operator for an arbitrary a ,

$$\mathcal{O}_3^a = \{S^2, T^a\} , \quad (5.24)$$

which gives a reasonable estimation for truncation of the series in Eq. (5.20) at the $\mathcal{O}(\epsilon/N_c^2)$, where the explicit factor ϵ represents the order of the $SU(3)$ breaking ($\epsilon \sim 0.3$).

There are two one-body $\mathcal{O}_1^a = T^a$ operators which are relevant for the baryon mass splitting. One is T^8 : iso-spin symmetric ¹ operator, and the other one is T^3 : iso-spin breaking operator. The matrix elements of T^8 and T^3 are [47],

$$\begin{aligned} T^8 &= \frac{1}{2\sqrt{3}} (N_c - 3N_s) , \\ T^3 &= \frac{1}{2} (N_u - N_d) , \end{aligned} \quad (5.25)$$

where, $N_c = N_u + N_d + N_s$ represents the number of colors N_c in terms of the number of each quark-flavor u, d , and s (N_u, N_d, N_s) in the baryon.

¹The iso-spin symmetry implies that $m_u = m_d$.

Therefore the $SU(3)$ breaking part of the baryon mass operator in the $1/N_c$ expansion has the form,

$$M_B^{(1,8)} = \epsilon d_1 T^8 + \epsilon d_2 \frac{\{S^i, G^{i8}\}}{N_c} + \epsilon d_3 \frac{\{S^2, T^8\}}{N_c^2} + \mathcal{O}(\epsilon/N_c^3) . \quad (5.26)$$

CHAPTER 6

BARYON MASSES IN THE $1/N_C$ EXPANSION FRAMEWORK

6.1 Introduction

In this chapter, an analysis of a baryon masses using the $1/N_c$ expansion framework as presented in Ref. [27]. In the quark model picture, the two possible spins and N_f possible quark flavors of quarks lead to the idea of organizing the baryon states into irreducible representations of $SU(2N_f)$. Furthermore, one can consider the excited baryon states by considering the orbital excitations of quarks which can be identified with the orbital angular momentum quantum numbers. Therefore in general, baryon states can be organized into the irreducible representations or multiplets of $SU(2N_f) \times O(3)$, where $O(3)$ contains generators of the orbital angular momentum.

A key observation from the analysis carried out in Refs. [28, 29] is that, the source/sink operators which, in the continuum limit, are in irreducible representations of the spin-flavor and quark orbital angular momentum groups $SU(2N_f) \times O(3)$ are very close to being at the optimum for the selective overlap with the baryon states. This is a strong indication that the baryon mass eigenstates themselves must be approximately organized into multiplets of that group, a fact that is well-known to hold phenomenologically. This has been tested explicitly in the lattice QCD (LQCD) calculations by measuring the coupling strengths of sources in different representations to each of the baryon levels studied. The state admixture of different multiplets of $SU(2N_f) \times O(3)$ is known as the *configuration mixing*, cannot however be directly inferred from those strengths, as they depend on details of the operators.

One of the objectives in LQCD is the calculation of the light baryon spectrum, where in recent years substantive progress has been made. The implementation of optimized baryon source operators [28,29,60,61] has enabled improved signals for excited baryons, leading to remarkable progress in identifying states by their quantum numbers and in the determination of their masses. In calculations performed with quark masses corresponding to $390 \text{ MeV} \leq M_\pi \leq 702 \text{ MeV}$, the spectrum of non-strange baryons [28] and also of strange baryons [29] were obtained. The case of $M_\pi = 702 \text{ MeV}$ corresponds to the limit of exact $SU(3)$ flavor symmetry. These calculations were performed on anisotropic lattices $16^3 \times 128$ with a gluon Symanzik-improved action with tree-level tadpole-improved coefficients and an anisotropic clover fermion action as explained in Ref. [62]. Although other recent works on baryon LQCD spectroscopy have been carried out in Refs. [60,61,63–66], the present work will use the results obtained by the Jefferson Lab Lattice QCD Collaboration in Refs. [28,29]. The study can similarly be applied to other results, in particular those of the BGR Collaboration [63] where the masses of the states analyzed here have been calculated.

The existence of a spin-flavor symmetry in baryons can be rigorously justified in the large- N_c limit of QCD. The symmetry is the result of a consistency requirement imposed by unitarity on pion-baryon scattering in that limit [11–13], and spin-flavor symmetry is thus broken by corrections which can be organized in powers of $1/N_c$. Under the assumption that the real world with $N_c = 3$ baryons can be analyzed using a $1/N_c$ expansion, starting at the lowest order with an exact spin-flavor symmetry, many analyses of baryon masses and other properties have been carried out. In particular, excited baryon masses have been analyzed in numerous works for the cases considered in this work [21,23,25,44,46,58,59,67,68] as well as for other multiplets [69–72]. Although spin-flavor symmetry is justified in the large- N_c limit, the larger $SU(2N_f) \times O(3)$ is not. The latter can be broken due to spin-orbit effects at

$\mathcal{O}(N_c^0)$.

The states studied in this work are the ones corresponding to the $[\mathbf{56}, 0^+]$ or Roper multiplet, the $[\mathbf{56}, 2^+]$ and the $[\mathbf{70}, 1^-]$ of $SU(6) \times O(3)$ representation for three light quark flavors u, d , and s . These are of particular interest because they have been previously analyzed phenomenologically in the framework of the $1/N_c$ expansion employed here [73], where the assumption of no configuration mixing works very well up to the degree of accuracy that the input masses and other observables permit. For example, there are particular predictions that result when configuration mixings are disregarded. They have the form of parameter-independent mass relations which hold up to higher-order corrections in the $1/N_c$ or $SU(3)$ -breaking expansions. Among those relations are the well-known Gell-Mann-Okubo (GMO) and equal-spacing (EQS) relations, which are valid in general, and additional ones involving different spin-flavor states such as relations in the $\mathbf{56}$ -plets that follow from the Gürsey-Radicati (GR) mass formula, and other relations in the $\mathbf{70}$ -plet [21]. As it will be shown in the present analysis, LQCD baryon masses fulfill to the expected accuracy those relations.

The objective of this chapter is to analyze the baryon masses, both from the Particle Data Group (PDG) [74] and LQCD [28, 29], using the $1/N_c$ expansion to $\mathcal{O}(1/N_c)$ and to first order in $SU(3)$ symmetry breaking. For two flavors and the multiplets considered here all states are established, but for three flavors there is a significant number of missing strange baryon states. For example, in the $[\mathbf{70}, 1^-]$ multiplet there are 30 theoretical masses and only 17 are currently experimentally known. Although those 17 masses are sufficient for the purpose of the $1/N_c$ analysis, they are not sufficient for a thorough test of the mass relations. On the other hand, the LQCD results provide complete multiplets, enabling a complete test of mass re-

lations. In the particular case of the $[70, 1^-]$, the issue of state mixing can be sorted out in the phenomenological case thanks to the simultaneous analysis of partial decay widths and photo-couplings, as shown most recently in Ref. [68] for the non-strange baryons. These inputs are however not possible for the LQCD baryons, and therefore the state mixing relies very strongly on the criterion for identifying states. In this regard, level-crossing effects are possible as the quark masses are varied in the LQCD calculations [63, 65].

This chapter is outlined as follows. In section 6.2, a brief description of the $1/N_c$ expansion framework is given. Then from section 6.3 to section 6.5 contain the fit results to each baryon multiplet, an analysis of baryon mass relations and baryon mass predictions. Then the section 6.6 summarizes the fit results into three figures, each corresponds to a specific pion mass. The section 6.7 contains the conclusions and discussion.

6.2 Baryon mass operators for spin-flavor multiplets in the $1/N_c$ expansion

In the simplest non-relativistic quark shell model, the leading order baryon mass is governed by the constituent quark masses, which is of order N_c . Therefore, all the corrections to the masses are assumed to be added only by the interactions among N_c number of quarks, because in large N_c limit, baryons are static objects. Interactions can be represented by the n -body operators which are products of $SU(2N_f)$ generators, i.e, S^i, T^a, G^{ia} .

Since the quark spin and orbital angular momentum are in general weakly coupled, baryons have been lead to a phenomenologically successful scheme of organizing

the states in multiplets of $SU(2N_f) \times O(3)$. For finite N_c it is possible to work with the ordinary rather than the contracted spin-flavor group for the purposes of building the operator bases [49]. Any static baryon observable can be expressed by an effective operator which is decomposed in a basis of operators ordered in powers of $1/N_c$ and which can be expressed as appropriate tensor products of the symmetry generators. In the present case of baryon masses, the bases of operators are well-known. The details for obtaining those bases can be found in Refs. [21, 23, 25, 25, 44, 50, 58, 59].

The excited states considered here will be either in the totally symmetric (**56** multiplet) or in the mixed symmetric (**70** multiplet) irreducible representations of $SU(6)$. Because, in the spin-flavor $SU(6)$ representation, all the possible baryon multiplets are organized as, $\mathbf{6} \otimes \mathbf{6} \otimes \mathbf{6} = \mathbf{56}_S \oplus \mathbf{70}_{MS} \oplus \mathbf{70}_{MA} \oplus \mathbf{20}_A$, which can be decomposed into $SU(3) \times SU(2)$ irreducible representation:

$$\begin{aligned} \mathbf{56} &= \mathbf{10} \otimes \mathbf{4} \oplus \mathbf{8} \otimes \mathbf{2}, \\ \mathbf{70} &= \mathbf{10} \otimes \mathbf{2} \oplus \mathbf{8} \otimes \mathbf{4} \oplus \mathbf{8} \otimes \mathbf{2} \oplus \mathbf{1} \otimes \mathbf{2}, \\ \mathbf{20} &= \mathbf{8} \otimes \mathbf{2} \oplus \mathbf{1} \otimes \mathbf{4}. \end{aligned}$$

Following the large N_c Hartree picture of a baryon, without a loss of generality and for the purpose of dealing with the group theory of the spin-flavor and orbital degrees of freedom, one can describe a low excitation baryon as a spin-flavor symmetric core with $N_c - 1$ quarks and one excited quark. In this way it becomes straightforward to obtain the matrix elements of bases operators. The orbital excitations in the $O(3)$ representation with $\ell = \{0, 1, 2\}$ the parity can be defined as $P = (-1)^\ell$. The multiplets to be analyzed have the following state contents:

- $[\mathbf{56}, 0^+]$: one $SU(3)$ **8** with spin 1/2, and one **10** with spin 3/2,
- $[\mathbf{56}, 2^+]$: one $SU(3)$ **8** for each spin 1/2 and 5/2, and one **10** for each spin 1/2 though 7/2,

- $[70, 1^-]$: one **1** Λ baryon for each spin 1/2 and 3/2, two **8**'s for each spin 1/2 and 3/2, one **8** for spin 5/2, and one **10** for each spin 1/2 and 3/2 .

The mass operator bases are organized in powers of $1/N_c$ and involve $SU(3)$ singlet and octet operators, the latter for symmetry breaking by the parameter $\epsilon \equiv m_s - \hat{m}$, where $\hat{m} = (m_u + m_d)/2$. One may consider the expansion to $\mathcal{O}(\epsilon^0/N_c)$ and $\mathcal{O}(\epsilon)$. It turns out that contributions $\mathcal{O}(\epsilon/N_c)$ are almost insignificant in most cases as shown later. Therefore, using the large N_c power counting rules, we can write the baryon mass operator as an expansion in $1/N_c$. As we discussed earlier, any static baryon observable can be expressed by an effective operator which is decomposed in a basis of operators ordered in powers of $1/N_c$ and which can be expressed as appropriate tensor products of the symmetry generators. In general the baryon mass operator can be written as,

$$M_B = \sum_i c_i O_i + \sum_j b_j B_j , \quad (6.1)$$

where, first(second) summation represents the $SU(3)$ -symmetric ($SU(3)$ -breaking) linear combination of operators O_i (B_j) and their associated coefficients c_i (b_j).

The LQCD results used here are as follows: for non-strange baryons the results are those of Ref. [28], of which only the results for the negative parity baryon masses will be analyzed, and for the case of $SU(3)$ with three flavors the results of Ref. [29] are used. For two flavors the quark masses used correspond to $M_\pi = 396$ and 524 MeV, and for three flavors m_s has been kept fixed, and $M_\pi = 391, 524$ and 702 MeV, where the last one corresponds to exact $SU(3)$ symmetry. For each of the multiplets it is necessary to identify the states with the LQCD mass levels. This procedure is not unique and thus it requires some analysis. For instance, in lattice QCD results there are several possible states available for each spin. Therefore, there are many possible arrangements for the masses which can be considered for the fits. Most of

those possible arrangements do not satisfy well the mass relations and that model independent approach can filter out many arrangements. Only the arrangements are acceptable which satisfy the mass relations to a reasonable degree. Also, the arrangements that lead to un-natural values for the coefficients can be eliminated. Therefore, the most general acceptable mass arrangement can be selected using those criteria.

The notation used to designate the states will be as follows: B_S or B'_S for states with baryon spin S which belong predominantly in octets, and B''_S for baryons which belong predominantly in singlet or decuplet. For the case of the Δ and Ω baryons which can only belong in a decuplet, no primes are used, and the same for the $[\mathbf{56}, 0^+]$ baryons where $S = 1/2$ ($3/2$) states necessarily belong to $\mathbf{8}$ ($\mathbf{10}$).

6.3 $[\mathbf{56}, 0^+]$ multiplet : ground states and excited states

6.3.1 Introduction to $[\mathbf{56}, 0^+]$ multiplet

In the $SU(6)$ representation, $\mathbf{56}$ is the symmetric multiplet, and as default it is identified as the ground state baryons. But when there is no orbital excitations or $l = 0$, there is a possible radial excitation which produces the Roper states with same J^p quantum numbers, where J is the total angular momentum quantum number. This radially excited multiplet is identified as “*Roper*” because the p -wave nucleon Roper resonance belongs to this multiplet. The Roper resonance for the nucleon has a mass about $1440 \text{ MeV}/c^2$ and its Breit-Wigner width is about $\sim 300 \text{ MeV}/c^2$ [39]. Also according to the PDG the πN is the main decay channel of the Roper(1440) nucleon. Therefore, both ground state and excited Roper multiplets can be represented by $[\mathbf{56}, 0^+]$ in $SU(6) \times O(3)$ representation. As we discussed before, the $\mathbf{56}$ -plet can be decomposed in to the irreducible representation of $SU(3) \times SU(2)$ in flavor and spin.

In particular, we have one $SU(3)$ octet (**8**) with spin 1/2 and one $SU(3)$ decuplet (**10**) with spin 3/2. Therefore, in the iso-spin symmetric limit $N_{1/2}, \Lambda_{1/2}, \Sigma_{1/2}, \Xi_{1/2}$ masses belong to the octet and $\Delta_{3/2}, \Sigma_{3/2}, \Xi_{3/2}, \Omega_{3/2}$ masses belong to decuplet.

The analysis of LQCD ground-state baryon masses including higher-order terms in the $SU(3)$ breaking has been carried out in Ref. [75], for LQCD calculations other than the present ones. It is noted that the hyperfine (HF) mass splittings have the behavior observed also in other LQCD calculations, where it increases with M_π up to $M_\pi \sim 400$ MeV, and decreases for higher M_π (for a current summary see [76]). On the other hand for the excited baryons the HF splittings are almost always monotonously decreasing with increasing M_π .

6.3.2 Mass operators in $[56, 0^+]$ multiplet

In this case the mass operator is the famous Gürsey-Radicati (GR) mass formula [20], which, explicitly displaying the $1/N_c$ power counting, reads as follows:

$$\begin{aligned} M_{[56, 0^+]} &= c_1 N_c + \frac{c_2}{N_c} S(S+1) + b_1 N_s \\ &+ \frac{b_2}{2\sqrt{12} N_c} \left(3I(I+1) - S(S+1) - \frac{3}{4} N_s(N_s+2) \right) + \mathcal{O}(1/N_c^2), \end{aligned} \quad (6.2)$$

where S is the baryon spin operator, I the isospin, and N_s the number of strange quarks, and the c_i and b_i are coefficients determined by the QCD dynamics, which are obtained by fitting to the masses. The mass operators as defined is such that all coefficients are $\mathcal{O}(N_c^0)$. The $SU(3)$ breaking parameter ϵ is here included in the coefficients b_1 and b_2 . For all mass formulas, the quark mass dependencies are implicitly absorbed into the coefficients.

6.3.3 Mass relations for $[56, 0^+]$ multiplet

The input masses are given in the Table (6.1). Note that, for the physical Roper baryon states, only $N_{1/2}, \Lambda_{1/2}, \Sigma_{1/2}, \Delta_{3/2}$ data are available. Because of this limitation, it is difficult to check the mass relations for the physical case. In LQCD, all the ground-state and excited state baryon masses at three different pion masses are available. The checks with mass relations are given in Table (6.2) and Table (6.3) , which show that they are satisfied within errors for the LQCD results.

Table 6.1. Ground state (left), and $[56, 0^+]$ excited Roper (right) baryon masses in MeV. The inversion in the ordering of the masses of the $\Xi_{1/2}$ and the Δ masses at and above $M_\pi = 391$ MeV is similar to that observed in other LQCD calculations [60].

$M_\pi[\text{MeV}]$					$M_\pi[\text{MeV}]$				
Baryon	PDG	391	524	702	Baryon	PDG	391	524	702
$N_{1/2}$	938 ± 30	1202 ± 15	1309 ± 9	1473 ± 4	$N_{1/2}$	1450 ± 20	2221 ± 52	2300 ± 30	2339 ± 21
$\Lambda_{1/2}$	1116 ± 30	1279 ± 20	1371 ± 7	1473 ± 4	$\Lambda_{1/2}$	1630 ± 70	2189 ± 44	2330 ± 26	2339 ± 21
$\Sigma_{1/2}$	1189 ± 30	1309 ± 13	1375 ± 6	1473 ± 4	$\Sigma_{1/2}$	1660 ± 30	2252 ± 46	2357 ± 52	2339 ± 21
$\Xi_{1/2}$	1315 ± 30	1351 ± 15	1420 ± 9	1473 ± 4	$\Xi_{1/2}$	\cdots	2278 ± 22	2321 ± 54	2339 ± 21
$\Delta_{3/2}$	1228 ± 30	1518 ± 20	1582 ± 9	1673 ± 6	$\Delta_{3/2}$	1625 ± 75	2356 ± 33	2450 ± 17	2454 ± 55
$\Sigma_{3/2}$	1383 ± 30	1582 ± 15	1622 ± 6	1673 ± 6	$\Sigma_{3/2}$	\cdots	2369 ± 31	2423 ± 19	2454 ± 55
$\Xi_{3/2}$	1532 ± 30	1636 ± 11	1655 ± 11	1673 ± 6	$\Xi_{3/2}$	\cdots	2453 ± 26	2463 ± 45	2454 ± 55
$\Omega_{3/2}$	1672 ± 30	1691 ± 13	1694 ± 9	1673 ± 6	$\Omega_{3/2}$	\cdots	2501 ± 33	2504 ± 35	2454 ± 55

Table 6.2. Mass relations for the ground state octet and decuplet. The relations are valid up to corrections $\mathcal{O}(\epsilon^2/N_c)$ in the case of the GMO and EQS relations, and up to $\mathcal{O}(\epsilon/N_c^2)$ for the rest.

Relation	$M_\pi[\text{MeV}]$		
	PDG	391	524
$2(N + \Xi) - (3\Lambda + \Sigma) = 0$	30.2 ± 0.4	38 ± 75	32 ± 32
$\Sigma'' - \Delta = \Xi'' - \Sigma'' = \Omega'' - \Xi''$	155 ± 2	64 ± 25	40 ± 11
	149.0 ± 0.5	55 ± 19	33 ± 13
	140.7 ± 0.5	54 ± 17	40 ± 14
$\frac{1}{3}(\Sigma + 2\Sigma'') - \Lambda - (\frac{2}{3}(\Delta - N)) = 0$	9 ± 1	1 ± 28	14 ± 12
$\Sigma'' - \Sigma - (\Xi'' - \Xi) = 0$	23.5 ± 0.5	12 ± 25	12 ± 15
$3\Lambda + \Sigma - 2(N + \Xi) + (\Omega - \Xi'' - \Sigma'' + \Delta) = 0$	16 ± 2	29 ± 81	32 ± 36
$\Sigma'' - \Delta + \Omega - \Xi'' - 2(\Xi'' - \Sigma'') = 0$	2.5 ± 2.4	8 ± 51	14 ± 37

Table 6.3. Mass relations for the Roper multiplet. The relations hold at the same orders as in the case of the ground state baryons.

Relation	$M_\pi[\text{MeV}]$	
	391	524
$2(N + \Xi) - (3\Lambda + \Sigma) = 0$	179 ± 180	106 ± 155
$\Sigma'' - \Delta = \Xi'' - \Sigma'' = \Omega'' - \Xi''$	13 ± 45	-27 ± 26
	84 ± 40	41 ± 49
	48 ± 42	41 ± 57
$\frac{1}{3}(\Sigma + 2\Sigma'') - \Lambda - (\frac{2}{3}(\Delta - N)) = 0$	51 ± 65	29 ± 41
$\Sigma'' - \Sigma - (\Xi'' - \Xi) = 0$	58 ± 63	77 ± 80
$3\Lambda + \Sigma - 2(N + \Xi) + (\Omega'' - \Xi'' - \Sigma'' + \Delta) = 0$	144 ± 189	174 ± 170
$\Sigma'' - \Delta + \Omega'' - \Xi'' - 2(\Xi'' - \Sigma'') = 0$	107 ± 110	67 ± 147

6.3.4 Fit results for $[56, 0^+]$ multiplet masses to data

Using the GR mass formula Eq. (6.2) the ground-state and excited $[56, 0^+]$ Roper baryon masses are fitted to the data . The input masses from Particle Data Group and from the LQCD are summarized in Table (6.1). In all **56**-plet masses the flavor singlet breaking of $SU(6) \times O(3)$ is $\mathcal{O}(1/N_c)$ and it is governed by the hyperfine interaction. The $SU(3)$ -breaking effects on the hyperfine interaction is controlled by the coefficient b_2 .

In the Roper baryons, the identification of the $\mathbf{8}_{1/2}$ is obvious, being the lightest positive parity excited states above the ground state, but for the $\mathbf{10}_{3/2}$ one needs to distinguish between two possible excited multiplets, one which will be a Roper and one which be in the $[56, 2^+]$. One of the choices, namely that in which the Roper $\mathbf{10}_{3/2}$ is the lightest one, does not seem to be consistent with the magnitude of the HF splittings observed throughout the spectrum. Therefore, $\mathbf{10}_{3/2}$ belonging to the $[56, 0^+]$ are the second from the lowest ones. i.e, the $\mathbf{10}_{3/2}$ belonging to the $[56, 2^+]$ are the lowest-lying excitations, followed by the Roper ones.

Table (6.4) gives the results of the fits for the ground-state baryons, and Table (6.5) for the Roper baryons.

Table 6.4. Coefficients of the GR mass formula for the ground state baryons. The case $M_\pi = 702$ MeV corresponds to exact $SU(3)$ symmetry. χ^2_{dof} is the χ^2 per degree of freedom.

Coefficients [MeV]	$M_\pi[\text{MeV}]$			
	PDG	391	524	702
c_1	293 ± 6	377 ± 3	420 ± 2	474 ± 1
c_2	247 ± 12	296 ± 5	251 ± 3	200 ± 2
b_1	189 ± 12	75 ± 6	45 ± 3	0
b_2	94 ± 26	43 ± 11	14 ± 7	0
χ^2_{dof}	0.19	0.15	1.43	0

Table 6.5. Fit to the $[56, 0^+]$ excited Roper baryons. It is found that the $SU(3)$ breaking effects on the HF interactions can be neglected, thus $b_2 = 0$ throughout.

Coefficients [MeV]	$M_\pi[\text{MeV}]$			
	PDG	391	524	702
c_1	469 ± 8	714 ± 6	760 ± 5	770 ± 3
c_2	175 ± 44	165 ± 12	124 ± 9	115 ± 20
b_1	204 ± 18	48 ± 12	15 ± 12	0
χ^2_{dof}	0.16	0.53	0.76	0

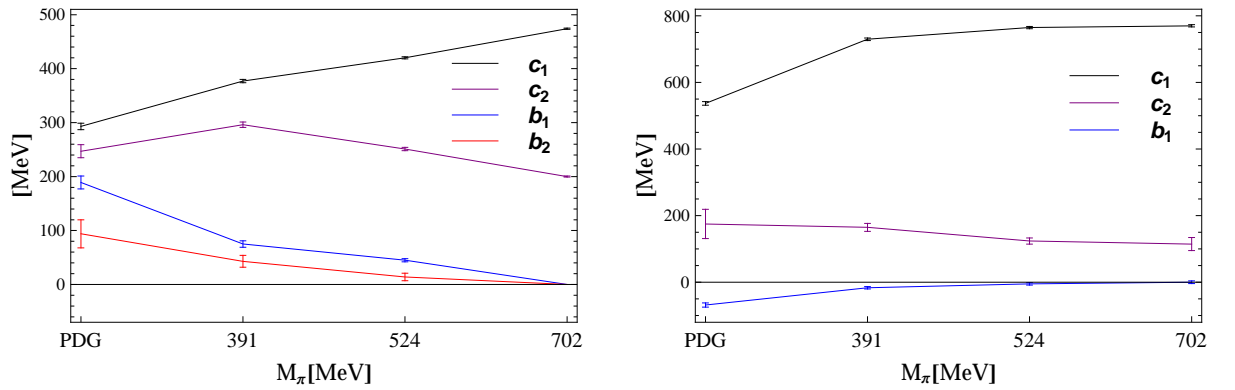


Figure 6.1. Evolution of the coefficients with M_π for the ground state baryons (left panel) and the Roper baryons (right panel).

In Fig. (6.1) the dependencies on M_π of the coefficients are displayed. The well-known dramatic downturn with decreasing M_π of the Roper baryon masses is clearly driven by the spin-flavor singlet component of the masses, given by the coefficient c_1 . The HF effects determined by c_2 have a smooth behavior in M_π but significantly different strength in the GS than in the Roper states, being reduced in the latter. Unlike the GS baryons, no significant $SU(3)$ breaking in the HF interaction is observed in the Roper baryons, so the coefficient b_2 is consistent with zero for the LQCD masses.

The mass relations are given in Tables (6.2) and (6.3), which show that they are satisfied within errors for the LQCD results. In the physical case, the knowledge of the Roper states is rather incomplete. Based on the mass relations the predictions shown in Table (6.6) are made. As shown below, the listed PDG candidate states may also match predictions from the $[56, 2^+]$ multiplet, as discussed in section 6.4.

Table 6.6. Predictions of physically unknown states in the Roper multiplet. These predictions agree with the ones in Ref. [77].

Baryon	Predicted mass [MeV]	Fitted Mass [MeV]	PDG candidate and mass [MeV]
$\Sigma''_{3/2}$	1790 ± 131	1800	$\Sigma(1840)(3/2^+)^*$ with mass ~ 1840
$\Xi_{1/2}$	1825 ± 108	1815	...
$\Xi''_{3/2}$	1955 ± 171	1975	$\Xi(1950)(?)^{***}$ with mass $\sim 1950 \pm 15$
$\Omega_{3/2}$	2120 ± 219	2150	...

6.4 $[56, 2^+]$ excited states

6.4.1 Introduction to $[56, 2^+]$ multiplet

The $[56, 2^+]$ multiplet has $\ell = 2$ with the $S = 1/2$ octet and $S = 3/2$ decuplet. Because of $\vec{J} = \vec{S} + \vec{L}$, it gives two $SU(3)$ octets with total angular momentum $J = 3/2$ and $5/2$, and four decuplets with $J = 1/2, 3/2, 5/2$ and $7/2$.

There is mixing between states in the octet and decuplet, namely the Σ and the Ξ pairs of states with $S = 3/2$ and with $S = 5/2$, namely $(\Sigma_S^{(8)}, \Sigma_S^{(10)})$ and $(\Xi_S^{(8)}, \Xi_S^{(10)})$. These mixings obviously result from $SU(3)$ breaking, and the physical states are defined as follows:

$$\begin{pmatrix} \Sigma_S \\ \Sigma'_S \end{pmatrix} = \begin{pmatrix} \cos \theta_{\Sigma_S} & \sin \theta_{\Sigma_S} \\ -\sin \theta_{\Sigma_S} & \cos \theta_{\Sigma_S} \end{pmatrix} \begin{pmatrix} \Sigma_S^{(8)} \\ \Sigma_S^{(10)} \end{pmatrix}, \quad \begin{pmatrix} \Xi_S \\ \Xi'_S \end{pmatrix} = \begin{pmatrix} \cos \theta_{\Xi_S} & \sin \theta_{\Xi_S} \\ -\sin \theta_{\Xi_S} & \cos \theta_{\Xi_S} \end{pmatrix} \begin{pmatrix} \Xi_S^{(8)} \\ \Xi_S^{(10)} \end{pmatrix} \quad (6.3)$$

6.4.2 Mass operators in $[56, 2^+]$ multiplet

The mass operator for this multiplet contains three $SU(3)$ -symmetric and three $SU(3)$ -breaking operators.

$$M_{[56, 2^+]} = \sum_{i=1}^3 c_i O_i + \sum_{i=1}^3 b_i \bar{B}_i, \quad (6.4)$$

The basis of operators along with the matrix elements are given in Table (6.7),

Table 6.7. Matrix elements of $SU(3)$ singlet operators (top) and $SU(3)$ breaking operators (bottom). Here, $a_S = 1, -2/3$ for $S = 3/2, 5/2$, respectively and $b_S = 1, 2/3, 1/9, -2/3$ for $S = 1/2, 3/2, 5/2, 7/2$, respectively.

	O_1 $N_c \mathbf{1}$	O_2 $\frac{1}{N_c} \ell_i s_i$	O_3 $\frac{1}{N_c} S_i S_i$
$8_{3/2}$	N_c	$-\frac{3}{2N_c}$	$\frac{3}{4N_c}$
$8_{5/2}$	N_c	$\frac{1}{N_c}$	$\frac{3}{4N_c}$
$10_{1/2}$	N_c	$-\frac{9}{2N_c}$	$\frac{15}{4N_c}$
$10_{3/2}$	N_c	$-\frac{3}{N_c}$	$\frac{15}{4N_c}$
$10_{5/2}$	N_c	$-\frac{1}{2N_c}$	$\frac{15}{4N_c}$
$10_{7/2}$	N_c	$\frac{3}{N_c}$	$\frac{15}{4N_c}$
	\bar{B}_1 N_s	\bar{B}_2 $\frac{1}{N_c} \ell_i G_{i8} - \frac{1}{2\sqrt{3}} O_2$	\bar{B}_3 $\frac{1}{N_c} S_i G_{i8} - \frac{1}{2\sqrt{3}} O_3$
N_S	0	0	0
Λ_S	1	$\frac{3\sqrt{3} a_S}{4N_c}$	$-\frac{3\sqrt{3}}{8N_c}$
Σ_S	1	$-\frac{\sqrt{3} a_S}{4N_c}$	$\frac{\sqrt{3}}{8N_c}$
Ξ_S	2	$\frac{\sqrt{3} a_S}{N_c}$	$-\frac{\sqrt{3}}{2N_c}$
Δ_S	0	0	0
Σ''_S	1	$\frac{3\sqrt{3} b_S}{4N_c}$	$-\frac{5\sqrt{3}}{8N_c}$
Ξ''_S	2	$\frac{3\sqrt{3} b_S}{2N_c}$	$-\frac{5\sqrt{3}}{4N_c}$
Ω_S	3	$\frac{9\sqrt{3} b_S}{4N_c}$	$-\frac{15\sqrt{3}}{8N_c}$
$\Sigma_{3/2} - \Sigma''_{3/2}$	0	$\frac{\sqrt{3}}{2N_c}$	0
$\Sigma_{5/2} - \Sigma''_{5/2}$	0	$\frac{\sqrt{3}}{2N_c}$	0
$\Xi_{3/2} - \Xi''_{3/2}$	0	$\frac{\sqrt{42}}{6N_c}$	0
$\Xi_{5/2} - \Xi''_{5/2}$	0	$\frac{\sqrt{42}}{6N_c}$	0

6.4.3 Mass relations for $[56, 2^+]$ multiplet

The input masses are given in Table (6.8). The mass relations for the $[56, 2^+]$ multiplet are depicted in [25] were checked with the baryon masses and the results are given in Table (6.9). In addition to GMO and EQS relations, there are several relations which relate $SU(3)$ mass splittings in multiplets with different baryon spin, as well as relations among the masses of baryons with the same strangeness but dif-

ferent baryon spin. Almost all the mass relations are satisfied by the LQCD results, with some exceptions of the results at $M_\pi = 702$ MeV. Those exceptional deviations are corresponding to the relations among different spin-candidates, and their sizes are expected to be included in the higher order corrections.

Table 6.8. The input baryon masses (physical and LQCD [28, 29]) corresponding to the $[56, 2^+]$ multiplet. The experimental values are those for baryons with a three star or higher rating by the PDG.

$M_\pi[\text{MeV}]$					$M_\pi[\text{MeV}]$				
Baryon	PDG	391	524	702	Baryon	PDG	391	524	702
$N_{3/2}$	1700 ± 50	2148 ± 33	2178 ± 61	2314 ± 17	$\Delta_{3/2}$	1935 ± 35	2270 ± 37	2344 ± 17	2387 ± 19
$\Lambda_{3/2}$	1800 ± 30	2225 ± 28	2227 ± 39	2314 ± 17	$\Sigma''_{3/2}$	\cdots	2318 ± 26	2379 ± 15	2387 ± 19
$\Sigma_{3/2}$	\cdots	2243 ± 24	2238 ± 26	2314 ± 17	$\Xi''_{3/2}$	\cdots	2374 ± 13	2409 ± 6	2387 ± 19
$\Xi_{3/2}$	\cdots	2263 ± 31	2305 ± 15	2314 ± 17	$\Omega_{3/2}$	\cdots	2420 ± 28	2450 ± 13	2387 ± 19
$N_{5/2}$	1683 ± 8	2140 ± 31	2198 ± 17	2271 ± 13	$\Delta_{5/2}$	1895 ± 25	2333 ± 35	2359 ± 17	2388 ± 17
$\Lambda_{5/2}$	1820 ± 5	2228 ± 20	2249 ± 15	2271 ± 13	$\Sigma''_{5/2}$	\cdots	2368 ± 20	2392 ± 19	2388 ± 17
$\Sigma_{5/2}$	1918 ± 18	2229 ± 22	2253 ± 17	2271 ± 13	$\Xi''_{5/2}$	\cdots	2430 ± 24	2418 ± 13	2388 ± 17
$\Xi_{5/2}$	\cdots	2296 ± 22	2275 ± 13	2271 ± 13	$\Omega_{5/2}$	\cdots	2487 ± 24	2470 ± 13	2388 ± 17
$\Delta_{1/2}$	1895 ± 25	2284 ± 107	2312 ± 28	2398 ± 32	$\Delta_{7/2}$	1950 ± 10	2390 ± 31	2384 ± 19	2403 ± 21
$\Sigma''_{1/2}$	\cdots	2270 ± 26	2348 ± 17	2398 ± 32	$\Sigma''_{7/2}$	2033 ± 8	2428 ± 22	2418 ± 15	2403 ± 21
$\Xi''_{1/2}$	\cdots	2293 ± 35	2391 ± 13	2398 ± 32	$\Xi''_{7/2}$	\cdots	2494 ± 22	2455 ± 13	2403 ± 21
$\Omega_{1/2}$	\cdots	2378 ± 42	2426 ± 13	2398 ± 32	$\Omega_{7/2}$	\cdots	2553 ± 22	2477 ± 13	2403 ± 21

Table 6.9. Mass relations for the $[56, 2^+]$ multiplet. The relations hold at the same orders as in the case of the ground state baryons.

Relation	$M_\pi[\text{MeV}]$		
	391	524	702
$2(N_{3/2} + \Xi_{3/2}) - (3\Lambda_{3/2} + \Sigma_{3/2}) = 0$	98 ± 126	49 ± 173	0
$2(N_{5/2} + \Xi_{5/2}) - (3\Lambda_{5/2} + \Sigma_{5/2}) = 0$	40 ± 98	55 ± 65	0
$\Sigma''_{1/2} - \Delta_{1/2} = \Xi''_{1/2} - \Sigma''_{1/2} = \Omega_{1/2} - \Xi''_{1/2}$	-13 ± 110	36 ± 33	0
	23 ± 44	43 ± 22	0
	85 ± 54	35 ± 19	0
$\Sigma''_{3/2} - \Delta_{3/2} = \Xi''_{3/2} - \Sigma''_{3/2} = \Omega_{3/2} - \Xi''_{3/2}$	48 ± 46	36 ± 23	0
	56 ± 29	30 ± 16	0
	45 ± 31	41 ± 15	0
$\Sigma''_{5/2} - \Delta_{5/2} = \Xi''_{5/2} - \Sigma''_{5/2} = \Omega_{5/2} - \Xi''_{5/2}$	35 ± 40	34 ± 26	0
	62 ± 31	26 ± 23	0
	57 ± 34	52 ± 18	0
$\Sigma''_{7/2} - \Delta_{7/2} = \Xi''_{7/2} - \Sigma''_{7/2} = \Omega_{7/2} - \Xi''_{7/2}$	38 ± 38	35 ± 25	0
	67 ± 31	36 ± 20	0
	59 ± 31	22 ± 18	0
$\Delta_{5/2} - \Delta_{3/2} - (N_{5/2} - N_{3/2}) = 0$	70 ± 68	4 ± 68	44 ± 33
$(\Delta_{7/2} - \Delta_{5/2}) - \frac{7}{5}(N_{5/2} - N_{3/2}) = 0$	68 ± 78	2.5 ± 92	75 ± 41
$\Delta_{7/2} - \Delta_{1/2} - 3(N_{5/2} - N_{3/2}) = 0$	129 ± 175	13 ± 192	133 ± 74
$\frac{8}{15}(\Lambda_{3/2} - N_{3/2}) + \frac{22}{15}(\Lambda_{5/2} - N_{5/2})$			
$-(\Sigma_{5/2} - \Lambda_{5/2}) - 2(\Sigma''_{7/2} - \Delta_{7/2}) = 0$	91 ± 100	29 ± 75	0
$\Lambda_{5/2} - \Lambda_{3/2} + 3(\Sigma_{5/2} - \Sigma_{3/2}) - 4(N_{5/2} - N_{3/2}) = 0$	10 ± 207	10 ± 272	0
$\Lambda_{5/2} - \Lambda_{3/2} + \Sigma_{5/2} - \Sigma_{3/2} - 2(\Sigma''_{5/2} - \Sigma''_{3/2}) = 0$	111 ± 81	12 ± 72	87 ± 59
$7(\Sigma''_{3/2} - \Sigma''_{7/2}) - 12(\Sigma''_{5/2} - \Sigma''_{7/2}) = 0$	44 ± 319	39 ± 268	67 ± 266
$4(\Sigma''_{1/2} - \Sigma''_{7/2}) - 5(\Sigma''_{3/2} - \Sigma''_{7/2}) = 0$	83 ± 170	87 ± 104	58 ± 161

6.4.4 Fit results for $[56, 2^+]$ multiplet masses to data

The first step is the identification of the states in LQCD results. With the exception of the $\mathbf{10}_{3/2}$, all the states are in spin-flavor states which appear for the first time, and thus the lightest states with given spin and flavor are the ones of interest. In the case of the $\mathbf{10}_{3/2}$, as discussed earlier, there are two possible excited levels to consider, one of which will belong to the excited $[56, 0^+]$, where the arguments for the identification were already given. Which is, the $\mathbf{10}_{3/2}$ belonging to the $[56, 2^+]$ are the lowest lying excitations, followed by the Roper ones. For Σ and Ξ baryons, the LQCD analysis [29] has assigned the dominant $SU(3)$ multiplet to which they belong, $\mathbf{8}$ or $\mathbf{10}$. Therefore, there is no ambiguity about the identification of states in the present multiplet.

Two different fits are carried out, one includes all the $SU(3)$ breaking operators, and a second one only including the one-body operator giving the spin independent breaking effects. Since the symmetry breaking by the operator B_1 does not produce mixing between $\mathbf{8}$ and $\mathbf{10}$, the mixing angles are actually $\propto \epsilon/N_c$, and thus naturally very small. The results are shown in Table (6.10). It is checked that the present fit fully agrees with a previous one for the physical case [25]. One important observation is that based on the quality of the fits the mixings cannot be definitely established for the LQCD results.

Table 6.10. Two fits, with (second column) and without (third column) the operators B_2 and B_3 (see Table (6.7)). The second fit does not describe well the physical baryons.

M_π [MeV] Coefficients	PDG	391	524	702	391	524	702
c_1	540 ± 11	704 ± 2	718 ± 1	754 ± 1	710 ± 2	724 ± 1	753 ± 1
c_2	18 ± 5	48 ± 6	28 ± 3	-6 ± 5	59 ± 6	21 ± 3	0
c_3	244 ± 4	169 ± 5	166 ± 3	104 ± 4	151 ± 5	148 ± 3	106 ± 4
b_1	217 ± 4	75 ± 3	54 ± 1	0	56 ± 3	36 ± 1	0
b_2	95 ± 14	-23 ± 11	13 ± 5	0	0	0	0
b_3	268 ± 16	59 ± 9	55 ± 4	0	0	0	0
Mixing angles [Rad]							
$\theta_{\Sigma_{3/2}}$	-0.16 ± 0.02	0.06 ± 0.03	-0.03 ± 0.01	0	0	0	0
$\theta_{\Xi_{3/2}}$	-0.26 ± 0.04	0.07 ± 0.03	-0.03 ± 0.01	0	0	0	0
$\theta_{\Sigma_{5/2}}$	-0.22 ± 0.03	0.05 ± 0.03	-0.03 ± 0.01	0	0	0	0
$\theta_{\Xi_{5/2}}$	-0.20 ± 0.02	0.08 ± 0.04	-0.03 ± 0.01	0	0	0	0
χ^2_{dof}	0.84	0.60	0.47	0.92	0.63	0.53	0.80

The evolution with M_π of the coefficients is shown in Fig. (6.2). It is interesting to notice that the coefficient c_1 has qualitatively similar but less dramatic behavior than in the case of the Roper baryons, which must be an indication of a similar mechanism as the one which drives down the Roper masses with decreasing M_π . The HF interaction given by c_3 behaves smoothly with M_π , decreasing slowly as M_π increases, and it has similar strength as in the Roper baryons. Although the operators B_2 and B_3 are significant in the physical case, their contributions are negligible in the LCQD cases, as shown by the second fit in Table (6.10). The latter observation tells that the mixing between octet and decuplet states, which are driven by those operators, are very small as confirmed by the small mixing angles in the first fit in Table (6.10).

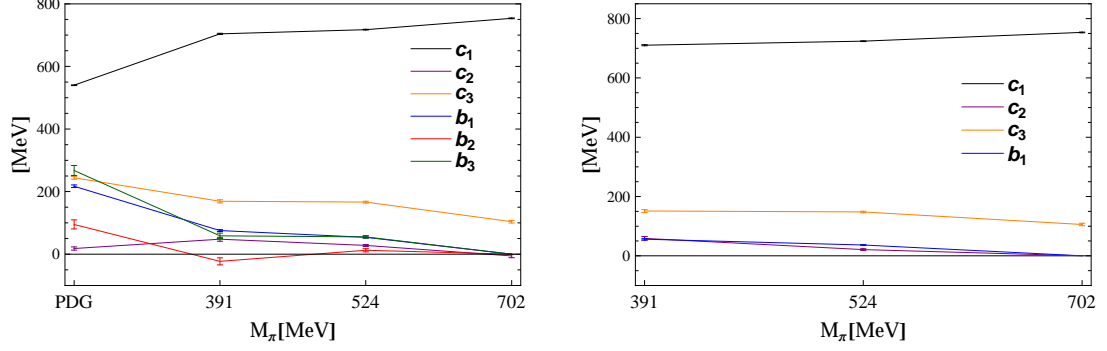


Figure 6.2. Evolution of the operator coefficients with M_π for the two fits of the $[56, 2^+]$ masses.

6.4.5 Mass predictions

The fit and the mass relations predictions for the experimentally unknown or poorly known states are shown in Table (6.11). The PDG candidate state $\Sigma(1840)(3/2^+)^*$ could be identified with the $\Sigma_{3/2}(1889)$ state in Table (6.11), but as discussed earlier it can also be identified with the Roper $\Sigma_{3/2}$. The PDG candidate state $\Xi(2120)^*(?)$ is consistent with both $\Xi_{3/2}$ and $\Xi_{7/2}''$ in Table (6.11), so its parity could be predicted as positive.

Table 6.11. Predictions of physically unknown states in the $[56, 2^+]$ multiplet, and suggested identifications with PDG listed states. The first two GMO relations and the 12th equation in Table (6.9), which is a large N_c parameter independent mass relation, were used to predict the above masses.

Missing states	Fitted mass [MeV]	Mass listed in PDG [MeV]	Mass from mass relations [MeV]
$\Sigma_{3/2}$	1889	$\Sigma(1840)(3/2^+)^*$ with mass ~ 1840	1920 ± 70
$\Xi_{3/2}$	2074	$\Xi(2120)^*(?)$: 2130 ± 7	2080 ± 75
$\Xi_{5/2}$	2000	$\Xi(2030)^{***}(S \geq 5/2^+)$ with 2025 ± 5	2006 ± 14
$\Sigma''_{1/2}$	2059.5	...	2127 ± 120
$\Xi''_{1/2}$	2221	$\Xi(2250)^{**}(?)$: 2214 ± 5	...
$\Omega_{1/2}$	2382
$\Sigma''_{3/2}$	2059.35	$\Sigma(2080)^{**}(3/2^+)$: 2120 ± 40	2109 ± 96
$\Xi''_{3/2}$	2211.8
$\Omega_{3/2}$	2350
$\Sigma''_{5/2}$	2053	$\Sigma(2070)^*(5/2^+)$: 2070 ± 10	2077 ± 56
$\Xi''_{5/2}$	2178
$\Omega_{5/2}$	2297
$\Xi''_{7/2}$	2129	$\Xi(2120)^*(?)$: 2130 ± 7	...
$\Omega_{7/2}$	2222

6.5 $[70, 1^-]$ excited states

6.5.1 Introduction to $[70, 1^-]$ multiplet

In the $SU(6)$ representation, the **70**-plet contains one $SU(3)$ decuplet with spin $3/2$, two octets with spin $1/2$ and one singlet with spin $1/2$ in the irreducible representation of $SU(3) \times SU(2)$. The two octets differ in their total quark spins which are $1/2$ and $3/2$. In the notation of $(2s + 1)$, they are **2** and **4** respectively, where s

is the quark spin. The following notation is used to represent the states correspond to this multiplet : B_S or B'_S for states with baryon spin S which belong to octets, and B''_S for baryons which belong to singlet or decuplet. In this $[70, 1^-]$ multiplet, $\ell = 1$ and it will couple with the spins and produce one $SU(3)$ **1** (singlet) Λ baryon for each $S = 1/2$ and $3/2$, two **8'** for each $S = 1/2$ and $3/2$, one **8** for each $S = 5/2$ and one **10** for each $S = 1/2$ and $3/2$.

In the case of two flavors, the baryon states are belong to $[20', 1^-]$ multiplet in $SU(4) \times O(3)$ representation. There are two mixing angles for the pairs of nucleon states with $S = 1/2$ and $S = 3/2$. Denoting by $^{(2s+1)}N_S$, the physical states are given by:

$$\begin{pmatrix} N_S \\ N'_S \end{pmatrix} = \begin{pmatrix} \cos \theta_{2S} & \sin \theta_{2S} \\ -\sin \theta_{2S} & \cos \theta_{2S} \end{pmatrix} \begin{pmatrix} {}^2N_S \\ {}^4N_S \end{pmatrix}. \quad (6.5)$$

Understanding these mixings is very important, as the decays and photo-couplings are sensitive to them. These mixings are predicted at the leading level of breaking of spin-flavor symmetry [67]. Indeed, if the $\mathcal{O}(N_c^0)$ spin-orbit operators $O_{2,3,4}$ would have contributions of natural size, the mixing angles would be $\theta_1 = \cos^{-1}(-\sqrt{2/3}) = 2.526$ radians and $\theta_3 = \cos^{-1}(-\sqrt{5/6}) = 2.721$ radians up to $1/N_c$ corrections. However, it is known phenomenologically that the contributions from those operators are weak, and thus the mixing angles are significantly affected by the sub-leading in $1/N_c$ operators, in particular the hyperfine operator O_6 . The determination of the mixing angles requires in principle more information than just masses, as there are seven masses, and nine mass operators up to the order $1/N_c$, which means that the angles cannot be predicted. A biased prediction is obtained by neglecting the 3-body operators, which gives one angle as a function of the other one according the the relation [68]:

$$3 \left(M_{N_{\frac{1}{2}}} + M_{N'_{\frac{1}{2}}} - 4M_{N_{\frac{3}{2}}} - 4M_{N'_{\frac{3}{2}}} + 6M_{N_{\frac{5}{2}}} + 8M_{\Delta_{\frac{1}{2}}} - 8M_{\Delta_{\frac{3}{2}}} \right) = \quad (6.6)$$

$$\left(13 \cos 2\theta_1 + \sqrt{32} \sin 2\theta_1 \right) \left(M_{N'_{\frac{1}{2}}} - M_{N_{\frac{1}{2}}} \right) - 4 \left(\cos 2\theta_3 - \sqrt{20} \sin 2\theta_3 \right) \left(M_{N'_{\frac{3}{2}}} - M_{N_{\frac{3}{2}}} \right).$$

However a determination of the angles in a more rigorous way requires the input of additional observables, namely the partial decay widths and/or photo-couplings. The details of that analysis are provided in Ref. [68].

In the case of three flavors there are two-state and also three-state mixings. For the nucleons one has the same case as for two flavors, while for Σ , Λ and Ξ baryons there is three-state mixings. The physical states are given in terms of the quark spin and $SU(3)$ eigenstates by:

$$\begin{pmatrix} \mathbf{10_S} \text{ or } \mathbf{1_S} \\ \mathbf{8_S} \\ \mathbf{8'_S} \end{pmatrix} = \Theta \begin{pmatrix} \mathbf{^210_S} \text{ or } \mathbf{^21_S} \\ \mathbf{^28_S} \\ \mathbf{^48_S} \end{pmatrix}, \quad (6.7)$$

where the physical states are indicated by the dominant $SU(3)$ content, and the Euler mixing matrix is given by:

$$\Theta = \begin{pmatrix} c\phi c\psi - c\theta s\phi s\psi & c\psi s\phi + c\theta c\phi s\psi & s\theta s\psi \\ -c\theta c\psi s\phi - c\phi s\psi & c\theta c\phi c\psi - s\phi s\psi & c\psi s\theta \\ s\theta s\phi & -c\phi s\theta & c\theta \end{pmatrix}, \quad c\theta \equiv \cos \theta, \quad s\theta \equiv \sin \theta, \quad \text{etc.} \quad (6.8)$$

The angles θ can always be taken in the interval $[0, \pi)$. The mixing angles ϕ and ψ vanish in the limit of exact $SU(3)$ symmetry, and are thus proportional to the parameter ϵ . The $SU(3)$ symmetric limit becomes similar to the non-strange case except that there are two additional masses, namely the ones of the singlet Λ

baryons. The determination of the mixing angles would be similar to the non-strange case. In the absence of additional information to that of the masses, the angles can be determined only through exclusion of some operators. For instance, one strategy would be to exclude the 3-body operators, which seem in general to have particularly weak contributions to masses.

For the states which are subjected to mixing it is necessary to make the identification of the physical states. As mentioned in the introduction, for the physical case the identification has been clear for a long time, thanks to the simultaneous use of strong decay partial widths and helicity amplitudes [21, 68, 78, 79], but that information is not available for the LQCD baryons. The identifications of the LQCD states were analyzed separately (a total of 256 possibilities). It turns out that most assignments pass the tests of χ^2 , mass relations and naturalness of the coefficients. Thus on a general rigorous ground the problem of state assignment is not completely resolved. However, if one requires that the coefficients flow reasonably smoothly towards the physical ones which are known, then only one assignment becomes possible, namely the one discussed here.

6.5.2 Mass operators in $[70, 1^-]$ multiplet

In the case of non-strange baryons, where the states belong to a **20** plet of $SU(4)$ the mass formula reads [58]:

$$M_{[70, 1^-]} = \sum_{i=1}^8 c_i O_i, \quad (6.9)$$

Where the eight basis operators up to and including $\mathcal{O}(1/N_c)$ are given in Table (6.12).

Table 6.12. Mass operator basis and matrix elements for the $[20, 1^-]$ multiplet.

	O_1	O_2	O_3	O_4
	$N_c \mathbf{1}$	$\ell_i s_i$	$\frac{3}{N_c} \ell_{ij}^{(2)} g_{ia} G_{ja}^c$	$\ell_i s_i + \frac{4}{N_c+1} \ell_i t_a G_{ja}^c$
$N_{1/2}$	N_c	$-\frac{(2N_c-3)}{3N_c}$	0	$\frac{2}{N_c+1}$
$N'_{1/2}$	N_c	$-\frac{5}{6}$	$-\frac{5(N_c+1)}{48N_c}$	0
$N'_{1/2} - N_{1/2}$	0	$-\frac{1}{3} \sqrt{\frac{N_c+3}{2N_c}}$	$-\frac{5}{48N_c} \sqrt{\frac{(N_c+3)(2N_c-1)^2}{2N_c}}$	$-\sqrt{\frac{N_c+3}{2N_c(N_c+1)^2}}$
$N_{3/2}$	N_c	$\frac{(2N_c-3)}{6N_c}$	0	$-\frac{1}{N_c+1}$
$N'_{3/2}$	N_c	$-\frac{1}{3}$	$\frac{1}{12N_c} (N_c+1)$	0
$N'_{3/2} - N_{3/2}$	0	$-\frac{1}{6} \sqrt{\frac{5(N_c+3)}{N_c}}$	$\frac{1}{96N_c} \sqrt{\frac{5(N_c+3)(2N_c-1)^2}{N_c}}$	$-\sqrt{\frac{5(N_c+3)}{4N_c(N_c+1)^2}}$
$N'_{5/2}$	N_c	$+\frac{1}{2}$	$-\frac{1}{48N_c} (N_c+1)$	0
$\Delta_{1/2}$	N_c	$+\frac{1}{3}$	0	0
$\Delta_{3/2}$	N_c	$-\frac{1}{6}$	0	0
	O_5	O_6	O_7	O_8
	$\frac{1}{N_c} \ell_i S_i^c$	$\frac{1}{N_c} S_i^c S_i^c$	$\frac{1}{N_c} s_i S_i^c$	$\frac{2}{N_c} \ell_{ij}^{(2)} s_i S_j^c$
$N_{1/2}$	$-\frac{(N_c+3)}{3N_c^2}$	$\frac{(N_c+3)}{2N_c^2}$	$-\frac{(N_c+3)}{4N_c^2}$	0
$N'_{1/2}$	$-\frac{5}{3N_c}$	$\frac{2}{N_c}$	$\frac{1}{2N_c}$	$\frac{5}{6N_c}$
$N'_{1/2} - N_{1/2}$	$\sqrt{\frac{N_c+3}{18N_c^2}}$	0	0	$\frac{5}{12N_c} \sqrt{\frac{N_c+3}{2N_c}}$
$N_{3/2}$	$\frac{(N_c+3)}{6N_c^2}$	$\frac{(N_c+3)}{2N_c^2}$	$-\frac{(N_c+3)}{4N_c^2}$	0
$N'_{3/2}$	$-\frac{2}{3N_c}$	$\frac{2}{N_c}$	$\frac{1}{2N_c}$	$-\frac{2}{3N_c}$
$N'_{3/2} - N_{3/2}$	$\sqrt{\frac{5(N_c+3)}{36N_c^3}}$	0	0	$-\frac{1}{24} \sqrt{\frac{5(N_c+3)}{N_c^3}}$
$N'_{5/2}$	$\frac{1}{N_c}$	$\frac{2}{N_c}$	$\frac{1}{2N_c}$	$\frac{1}{6N_c}$
$\Delta_{1/2}$	$-\frac{4}{3N_c}$	$\frac{2}{N_c}$	$-\frac{1}{N_c}$	0
$\Delta_{3/2}$	$\frac{2}{3N_c}$	$\frac{2}{N_c}$	$-\frac{1}{N_c}$	0

For three flavors, the mass formula reads [21, 23]:

$$M_{[\mathbf{70}, 1^-]} = \sum_{i=1}^{11} c_i O_i + \sum_{i=1}^4 b_i \bar{B}_i, \quad (6.10)$$

where the basis operators up to and including $\mathcal{O}(1/N_c)$ or $\mathcal{O}(\epsilon)$ are given in Table (6.13) and Table (6.14). In order that the $SU(3)$ breaking operators do not contribute to the non-strange baryon masses, they have been redefined according to:

$$\bar{B}_1 = t_8 - \frac{1}{2\sqrt{3}N_c} O_1, \quad \bar{B}_2 = T_8^c - \frac{N_c-1}{2\sqrt{3}N_c} O_1, \quad \bar{B}_3 = \frac{10}{N_c} d_{8ab} g_{ia} G_{ib}^c + \frac{5(N_c^2-9)}{8\sqrt{3}N_c^2(N_c-1)} O_1 + \frac{5}{2\sqrt{3}(N_c-1)} O_6 + \frac{5}{6\sqrt{3}} O_7, \quad \bar{B}_4 = 3\ell_i g_{i8} - \frac{\sqrt{3}}{2} O_2.$$

Table 6.13. $SU(3)$ singlet basis of operators for the $[\mathbf{70}, 1^-]$ masses.

	O_1	O_2	O_3	O_4	O_5	O_6
	$N_c 1$	$\ell_i s_i$	$\frac{3}{N_c} \ell_{ij}^{(2)} g_{ia} G_{ja}^c$	$\frac{4}{N_c+1} \ell_i t_a G_{ja}^c$	$\frac{1}{N_c} \ell_i S_i^c$	$\frac{1}{N_c} S_i^c S_i^c$
$^2 8_{1/2}$	N_c	$\frac{3-2N_c}{3N_c}$	0	$\frac{2(N_c+3)(3N_c-2)}{9N_c(N_c+1)}$	$-\frac{N_c+3}{3N_c^2}$	$\frac{N_c+3}{2N_c^2}$
$^4 8_{1/2}$	N_c	$-\frac{5}{6}$	$-\frac{5(3N_c+1)}{48N_c}$	$\frac{5(3N_c+1)}{18(N_c+1)}$	$-\frac{5}{3N_c}$	$\frac{2}{N_c}$
$^2 8_{1/2} - ^4 8_{1/2}$	0	$-\sqrt{\frac{(N_c+3)}{18N_c}}$	$-\frac{5}{24} \sqrt{\frac{(N_c+3)(3N_c-2)^2}{2N_c^3}}$	$-\frac{(5-3N_c)}{9(N_c+1)} \sqrt{\frac{N_c+3}{2N_c}}$	$\sqrt{\frac{N_c+3}{18N_c^3}}$	0
$^2 1_{1/2}$	N_c	-1	0	0	0	0
$^2 10_{1/2}$	N_c	$\frac{1}{3}$	0	$-\frac{(3N_c+7)}{9(N_c+1)}$	$-\frac{4}{3N_c}$	$\frac{2}{N_c}$
$^2 8_{3/2}$	N_c	$\frac{2N_c-3}{6N_c}$	0	$-\frac{(N_c+3)(3N_c-2)}{9N_c(N_c+1)}$	$\frac{N_c+3}{6N_c^2}$	$\frac{N_c+3}{2N_c^2}$
$^4 8_{3/2}$	N_c	$-\frac{1}{3}$	$\frac{3N_c+1}{12N_c}$	$\frac{3N_c+1}{9(N_c+1)}$	$-\frac{2}{3N_c}$	$\frac{2}{N_c}$
$^2 8_{3/2} - ^4 8_{3/2}$	0	$-\sqrt{\frac{5(N_c+3)}{36N_c}}$	$-\frac{1}{48} \sqrt{\frac{5(N_c+3)(2-3N_c)^2}{N_c^3}}$	$-\sqrt{\frac{5(N_c+3)(5-3N_c)^2}{324N_c(N_c+1)^2}}$	$\sqrt{\frac{5(N_c+3)}{36N_c^3}}$	0
$^2 1_{3/2}$	N_c	$\frac{1}{2}$	0	0	0	0
$^2 10_{3/2}$	N_c	$-\frac{1}{6}$	0	$\frac{3N_c+7}{18(N_c+1)}$	$\frac{2}{3N_c}$	$\frac{2}{N_c}$
$^4 8_{5/2}$	N_c	$\frac{1}{2}$	$-\frac{3N_c+1}{48N_c}$	$-\frac{3N_c+1}{6(N_c+1)}$	$\frac{1}{N_c}$	$\frac{2}{N_c}$
	O_7	O_8	O_9	O_{10}	O_{11}	
	$\frac{1}{N_c} s_i S_i^c$	$\frac{2}{N_c} \ell_{ij}^{(2)} s_i S_j^c$	$\frac{3}{N_c^2} \ell_i g_{ja} \{S_j^c, G_{ja}^c\}$	$\frac{2}{N_c^2} t_a \{S_i^c, G_{ja}^c\}$	$\frac{3}{N_c^2} \ell_i g_{ia} \{S_j^c, G_{ja}^c\}$	
$^2 8_{1/2}$	$-\frac{N_c+3}{4N_c^2}$	0	$\frac{(N_c+3)(7-15N_c)}{24N_c^3}$	$-\frac{(N_c+3)(3N_c+1)}{12N_c^3}$	$-\frac{(N_c+3)(3N_c+1)}{24N_c^3}$	
$^4 8_{1/2}$	$\frac{1}{2N_c}$	$\frac{5}{3N_c}$	$\frac{5(3N_c+1)}{24N_c^2}$	$-\frac{(3N_c+1)}{3N_c^2}$	$\frac{5(3N_c+1)}{12N_c^2}$	
$^2 8_{1/2} - ^4 8_{1/2}$	0	$\sqrt{\frac{25(N_c+3)}{72N_c^3}}$	$\sqrt{\frac{(N_c+3)(3N_c-2)^2}{288N_c^3}}$	0	$\sqrt{\frac{(N_c+3)(3N_c+1)^2}{72N_c^3}}$	
$^2 1_{1/2}$	0	0	0	0	0	
$^2 10_{1/2}$	$-\frac{1}{N_c}$	0	$\frac{(3N_c+7)}{6N_c^2}$	$\frac{(3N_c+7)}{6N_c^2}$	$\frac{(3N_c+7)}{12N_c^2}$	
$^2 8_{3/2}$	$-\frac{N_c+3}{4N_c^2}$	0	$\frac{(N_c+3)(15N_c-7)}{48N_c^3}$	$-\frac{(N_c+3)(3N_c+1)}{12N_c^3}$	$\frac{(N_c+3)(3N_c+1)}{48N_c^3}$	
$^4 8_{3/2}$	$\frac{1}{2N_c}$	$-\frac{4}{3N_c}$	$\frac{(3N_c+1)}{12N_c^2}$	$-\frac{(3N_c+1)}{3N_c^2}$	$\frac{(3N_c+1)}{6N_c^2}$	
$^2 8_{3/2} - ^4 8_{3/2}$	0	$-\sqrt{\frac{5(N_c+3)}{144N_c^3}}$	$\sqrt{\frac{5(N_c+3)(3N_c-2)^2}{576N_c^3}}$	0	$\sqrt{\frac{5(N_c+3)(3N_c+1)^2}{144N_c^3}}$	
$^2 1_{3/2}$	0	0	0	0	0	
$^2 10_{3/2}$	$-\frac{1}{N_c}$	0	$-\frac{(3N_c+7)}{12N_c^2}$	$\frac{(3N_c+7)}{6N_c^2}$	$-\frac{(3N_c+7)}{24N_c^2}$	
$^4 8_{5/2}$	$\frac{1}{2N_c}$	$\frac{1}{3N_c}$	$-\frac{(3N_c+1)}{8N_c^2}$	$-\frac{(3N_c+1)}{3N_c^2}$	$-\frac{(3N_c+1)}{4N_c^2}$	

Table 6.14. $SU(3)$ octet basis of operators for the $[\mathbf{70}, 1^-]$ masses.

	B_1 t_8	B_2 T_8^c
${}^2\mathbf{8}_{1/2}, {}^2\mathbf{8}_{3/2}$	$\frac{N_c^3 - (7N_s - 8I^2)N_c^2 + 3(4N_s - 8I^2 + 1)N_c - 9N_s}{2\sqrt{3}N_c(N_c - 1)(N_c + 3)}$	$\frac{N_c^4 - (3N_s - 1)N_c^3 + (N_s - 8I^2 - 3)N_c^2 - 3(N_s - 8I^2 + 1)N_c + 9N_s}{2\sqrt{3}N_c(N_c - 1)(N_c + 3)}$
${}^4\mathbf{8}_{1/2}, {}^4\mathbf{8}_{3/2}, {}^4\mathbf{8}_{5/2}$	$\frac{N_c - N_s - 4I^2}{2\sqrt{3}(N_c - 1)}$	$\frac{N_c^2 - (3N_s + 2)N_c + 4(I^2 + N_s)}{2\sqrt{3}(N_c - 1)}$
${}^2\mathbf{8}_{1/2} - {}^4\mathbf{8}_{1/2}, {}^2\mathbf{8}_{3/2} - {}^4\mathbf{8}_{3/2}$	0	0
${}^2\mathbf{1}_{1/2}, {}^2\mathbf{1}_{3/2}$	$\frac{(3 - N_c)}{\sqrt{3}(N_c + 3)}$	$\frac{(N_c + 5)(N_c - 3)}{2\sqrt{3}(N_c + 3)}$
${}^2\mathbf{8}_{1/2} - {}^2\mathbf{1}_{1/2}, {}^2\mathbf{8}_{3/2} - {}^2\mathbf{1}_{3/2}$	$-\frac{3(N_c - 1)}{2\sqrt{N_c}(N_c + 3)}$	$-\frac{3(N_c - 1)}{2\sqrt{N_c}(N_c + 3)}$
${}^4\mathbf{8}_{1/2} - {}^2\mathbf{1}_{1/2}, {}^4\mathbf{8}_{3/2} - {}^2\mathbf{1}_{3/2}$	0	0
$\mathbf{10}_{1/2}, \mathbf{10}_{3/2}$	$\frac{N_c - 8N_s + 5}{2\sqrt{3}(N_c + 5)}$	$\frac{N_c^2 - (3N_s - 4)N_c - 7N_s - 5}{2\sqrt{3}(N_c + 5)}$
${}^2\mathbf{8}_{1/2} - {}^2\mathbf{10}_{1/2}, {}^2\mathbf{8}_{3/2} - {}^2\mathbf{10}_{3/2}$	$-\sqrt{\frac{2}{3}} \frac{N_c + 3}{N_c(N_c - 1)(N_c + 5)}$	$\sqrt{\frac{2}{3}} \frac{N_c + 3}{N_c(N_c - 1)(N_c + 5)}$
${}^4\mathbf{8}_{1/2} - {}^2\mathbf{10}_{1/2}, {}^4\mathbf{8}_{3/2} - {}^2\mathbf{10}_{3/2}$	0	0
B_3 $\frac{10}{N_c} d_{8ab} g_{ia} G_{ib}^c$		
${}^2\mathbf{8}_{1/2}, {}^2\mathbf{8}_{3/2}$		$\frac{3N_c^3 - (13N_s - 8I^2 + 3)N_c^2 + (31N_s - 44I^2 - 12)N_c - 6(N_s - 14I^2)}{-\frac{24}{5}\sqrt{3}N_c^2(N_c - 1)}$
${}^4\mathbf{8}_{1/2}, {}^4\mathbf{8}_{3/2}, {}^4\mathbf{8}_{5/2}$		$\frac{3N_c^2 - (7N_s + 4I^2 - 3)N_c + (N_s - 20I^2)}{-\frac{24}{5}\sqrt{3}N_c(N_c - 1)}$
${}^2\mathbf{8}_{1/2} - {}^4\mathbf{8}_{1/2}, {}^2\mathbf{8}_{3/2} - {}^4\mathbf{8}_{3/2}$		0
${}^2\mathbf{1}_{1/2}, {}^2\mathbf{1}_{3/2}$		0
${}^2\mathbf{8}_{1/2} - {}^2\mathbf{1}_{1/2}, {}^2\mathbf{8}_{3/2} - {}^2\mathbf{1}_{3/2}$		$\frac{5(3N_c + 1)}{16N_c\sqrt{N_c}}$
${}^4\mathbf{8}_{1/2} - {}^2\mathbf{1}_{1/2}, {}^4\mathbf{8}_{3/2} - {}^2\mathbf{1}_{3/2}$		0
$\mathbf{10}_{1/2}, \mathbf{10}_{3/2}$		$-\frac{3N_c^2 - 14(N_s - 1)N_c - 22N_s - 5}{\frac{24}{5}\sqrt{3}N_c(N_c + 5)}$
${}^2\mathbf{8}_{1/2} - {}^2\mathbf{10}_{1/2}, {}^2\mathbf{8}_{3/2} - {}^2\mathbf{10}_{3/2}$		$\frac{5(N_c + 2)}{6\sqrt{6}N_c} \sqrt{\frac{N_c + 3}{N_c(N_c - 1)(N_c + 5)}}$
${}^4\mathbf{8}_{1/2} - {}^2\mathbf{10}_{1/2}, {}^4\mathbf{8}_{3/2} - {}^2\mathbf{10}_{3/2}$		0
B_4 $3\ell_i g_{i8}$		
${}^2\mathbf{8}_{1/2}$		$-\frac{N_c^3 - (10N_s - 14I^2 + 3)N_c^2 + 3(7N_s - 8I^2)N_c - 9(N_s - 2I^2)}{\sqrt{3}N_c(N_c - 1)(N_c + 3)}$
${}^4\mathbf{8}_{1/2}$		$-\frac{5(N_c - N_s - 4I^2)}{4\sqrt{3}(N_c - 1)}$
${}^2\mathbf{8}_{1/2} - {}^4\mathbf{8}_{1/2}$		$-\frac{N_c - N_s - 4I^2}{2\sqrt{6}(N_c - 1)} \sqrt{1 + \frac{3}{N_c}}$
${}^2\mathbf{1}_{1/2}$		$\frac{\sqrt{3}(N_c - 3)}{(N_c + 3)}$
${}^2\mathbf{8}_{1/2} - {}^2\mathbf{1}_{1/2}$		$\frac{9(N_c - 1)}{2(N_c + 3)\sqrt{N_c}}$
${}^4\mathbf{8}_{1/2} - {}^2\mathbf{1}_{1/2}$		0
${}^2\mathbf{10}_{1/2}$		$\frac{N_c - 8N_s + 5}{2\sqrt{3}(N_c + 5)}$
${}^2\mathbf{8}_{1/2} - {}^2\mathbf{10}_{1/2}$		$-\sqrt{\frac{2}{3}} \sqrt{\frac{N_c + 3}{N_c(N_c - 1)(N_c + 5)}}$
${}^4\mathbf{8}_{1/2} - {}^2\mathbf{10}_{1/2}$		$\frac{4}{\sqrt{3}} \sqrt{\frac{1}{(N_c - 1)(N_c + 5)}}$
${}^2\mathbf{8}_{3/2}$		$\frac{N_c^3 - (10N_s - 14I^2 + 3)N_c^2 + 3(7N_s - 8I^2)N_c - 9(N_s - 2I^2)}{2\sqrt{3}N_c(N_c - 1)(N_c + 3)}$
${}^4\mathbf{8}_{3/2}$		$-\frac{N_c - N_s - 4I^2}{2\sqrt{3}(N_c - 1)}$
${}^2\mathbf{8}_{3/2} - {}^4\mathbf{8}_{3/2}$		$-\sqrt{\frac{5}{3}} \frac{N_c - N_s - 4I^2}{4(N_c - 1)} \sqrt{1 + \frac{3}{N_c}}$
${}^2\mathbf{1}_{3/2}$		$-\frac{\sqrt{3}(N_c - 3)}{2(N_c + 3)}$
${}^2\mathbf{8}_{3/2} - {}^2\mathbf{1}_{3/2}$		$-\frac{9(N_c - 1)}{4(N_c + 3)\sqrt{N_c}}$
${}^4\mathbf{8}_{3/2} - {}^2\mathbf{1}_{3/2}$		0
${}^2\mathbf{10}_{3/2}$		$-\frac{N_c - 8N_s + 5}{4\sqrt{3}(N_c + 5)}$
${}^2\mathbf{8}_{3/2} - {}^2\mathbf{10}_{3/2}$		$\sqrt{\frac{N_c + 3}{6N_c(N_c - 1)(N_c + 5)}}$
${}^4\mathbf{8}_{3/2} - {}^2\mathbf{10}_{3/2}$		$\frac{2\sqrt{10}}{\sqrt{3(N_c - 1)(N_c + 5)}}$
${}^4\mathbf{8}_{5/2}$		$\frac{\sqrt{3}(N_c - N_s - 4I^2)}{4(N_c - 1)}$

6.5.3 Mass relations for $[70, 1^-]$ multiplet

Theoretically, there are 30 baryon masses in the $[70, 1^-]$ multiplet, but only 17 masses are identified experimentally with a three-star or higher rating by the PDG. In LQCD, all the baryon masses are available for each respective pion mass with an ambiguity of identification of the mass levels corresponding to each baryon spin. Therefore, all the possibilities have to be taken into account to find the most general assignments of masses. One can realize that there are 256 possibilities in total referring to the Fig (11) of Ref. [29]. The criteria for the identification of most general assignment includes a test of χ^2 , mass relations and the naturalness of the fitted coefficients. Also, one required that the coefficients flow reasonably smooth towards the physical ones which are known, then only one assignment becomes possible, namely the one selected here. All the input masses after identification of states are given in Table (6.15).

GMO and ES relations are tested with the LQCD input masses and results are given in Table (6.16), but cannot be tested for the physical case due to insufficient number of experimentally known states. The parameter independent mass relations are written with a different notation where, S_B is the mass splitting between the state B and the non-strange states in the $SU(3)$ multiplet to which it belongs. The results for the parameter independent mass relations with the input masses are given in Table (6.17).

Table 6.15. $[\mathbf{70}, 1^-]$ masses. The experimental values are those for baryons with a three star or higher rating by the PDG.

Baryon	PDG	$M_\pi[\text{MeV}]$			Baryon	PDG	$M_\pi[\text{MeV}]$		
		391	524	702			391	524	702
$N_{1/2}$	1538 \pm 18	1681 \pm 51	1797 \pm 32	1968 \pm 8	$N_{5/2}$	1678 \pm 8	2012 \pm 26	2033 \pm 20	2109 \pm 11
$\Lambda_{1/2}$	1670 \pm 10	1777 \pm 32	1852 \pm 27	1968 \pm 8	$\Lambda_{5/2}$	1820 \pm 10	2057 \pm 19	2068 \pm 12	2109 \pm 11
$\Sigma_{1/2}$	\cdots	1783 \pm 25	1852 \pm 27	1968 \pm 8	$\Sigma_{5/2}$	1775 \pm 5	2059 \pm 21	2066 \pm 15	2109 \pm 11
$\Xi_{1/2}$	\cdots	1846 \pm 32	1899 \pm 32	1968 \pm 8	$\Xi_{5/2}$	\cdots	2127 \pm 21	2105 \pm 15	2109 \pm 11
$N_{3/2}$	1523 \pm 8	1820 \pm 40	1896 \pm 17	2000 \pm 8	$\Delta_{1/2}$	1645 \pm 30	1885 \pm 40	1964 \pm 42	2023 \pm 60
$\Lambda_{3/2}$	1690 \pm 5	1904 \pm 25	1939 \pm 17	2000 \pm 8	$\Sigma''_{1/2}$	\cdots	1952 \pm 25	1998 \pm 37	2023 \pm 60
$\Sigma_{3/2}$	1675 \pm 10	1905 \pm 23	1940 \pm 20	2000 \pm 8	$\Xi''_{1/2}$	\cdots	1987 \pm 27	2038 \pm 17	2023 \pm 60
$\Xi_{3/2}$	1823 \pm 5	1974 \pm 25	1976 \pm 17	2000 \pm 8	$\Omega_{1/2}$	\cdots	2011 \pm 41	2060 \pm 20	2023 \pm 60
$N'_{1/2}$	1660 \pm 20	1892 \pm 35	1928 \pm 37	2045 \pm 11	$\Delta_{3/2}$	1720 \pm 50	1955 \pm 32	2033 \pm 17	2098 \pm 11
$\Lambda'_{1/2}$	1785 \pm 65	1849 \pm 36	1944 \pm 37	2045 \pm 11	$\Sigma''_{3/2}$	\cdots	1958 \pm 36	2071 \pm 15	2098 \pm 11
$\Sigma'_{1/2}$	1765 \pm 35	1840 \pm 36	1941 \pm 37	2045 \pm 11	$\Xi''_{3/2}$	\cdots	2040 \pm 31	2108 \pm 15	2098 \pm 11
$\Xi'_{1/2}$	\cdots	1876 \pm 27	2001 \pm 22	2045 \pm 11	$\Omega_{3/2}$	\cdots	2101 \pm 30	2139 \pm 15	2098 \pm 11
$N'_{3/2}$	1700 \pm 50	1895 \pm 29	1935 \pm 37	2077 \pm 10	$\Lambda''_{1/2}$	1407 \pm 4	1710 \pm 32	1796 \pm 20	1922 \pm 11
$\Lambda'_{3/2}$	\cdots	1936 \pm 30	1981 \pm 27	2077 \pm 10	$\Lambda''_{3/2}$	1520 \pm 1	1817 \pm 21	1816 \pm 40	1903 \pm 11
$\Sigma'_{3/2}$	\cdots	1951 \pm 27	1977 \pm 25	2077 \pm 10					
$\Xi'_{3/2}$	\cdots	1998 \pm 31	2030 \pm 27	2077 \pm 10					

Table 6.16. GMO and ES relations for the $[\mathbf{70}, 1^-]$ multiplet. Due to the insufficient number of physically known states with three or more stars, the mass relations for physical states cannot be checked for the physical case.

Relation	M_π [MeV]		
	PDG	391	524
$2(N_{1/2} + \Xi_{1/2}) - (3\Lambda_{1/2} + \Sigma_{1/2}) = 0$...	59 ± 156	17 ± 125
$2(N_{3/2} + \Xi_{3/2}) - (3\Lambda_{3/2} + \Sigma_{3/2}) = 0$...	31 ± 121	13 ± 74
$2(N_{5/2} + \Xi_{5/2}) - (3\Lambda_{5/2} + \Sigma_{5/2}) = 0$...	46 ± 91	6 ± 64
$\Sigma''_{1/2} - \Delta_{1/2} = \Xi''_{1/2} - \Sigma''_{1/2} = \Omega_{1/2} - \Xi''_{1/2}$...	67 ± 47	35 ± 56
	...	34 ± 36	40 ± 41
	...	24 ± 49	22 ± 26
$\Sigma''_{3/2} - \Delta_{3/2} = \Xi''_{3/2} - \Sigma''_{3/2} = \Omega_{3/2} - \Xi''_{3/2}$...	2 ± 49	39 ± 23
	...	82 ± 47	37 ± 21
	...	61 ± 43	31 ± 21

Table 6.17. Octet-Decuplet mass relations for the $[\mathbf{70}, 1^-]$ multiplet. S_B is the mass splitting between the state B and the non-strange states in the $SU(3)$ multiplet to which it belongs. The results shown correspond to the relation divided by the sum of the positive coefficients in the relation (e.g., 163 for the first relation).

Relation	M_π [MeV]	
	391	524
$14(S_{\Lambda_{3/2}} + S_{\Lambda'_{3/2}}) + 63S_{\Lambda_{5/2}} + 36(S_{\Sigma_{1/2}} + S_{\Sigma'_{1/2}})$		
$-68(S_{\Lambda_{1/2}} + S_{\Lambda'_{1/2}}) - 27S_{\Sigma_{5/2}} = 0$	9.4 ± 40	0.96 ± 34
$14(S_{\Sigma_{3/2}} + S_{\Sigma'_{3/2}}) + 21S_{\Lambda_{5/2}} - 9S_{\Sigma_{5/2}}$		
$-18(S_{\Lambda_{1/2}} + S_{\Lambda'_{1/2}}) - 2(S_{\Sigma_{1/2}} + S_{\Sigma'_{1/2}}) = 0$	37 ± 45	5.4 ± 38
$14S_{\Sigma''_{1/2}} + 49S_{\Lambda_{5/2}} + 23(S_{\Sigma_{1/2}} + S_{\Sigma'_{1/2}})$		
$-45(S_{\Lambda_{1/2}} + S_{\Lambda'_{1/2}}) - 19S_{\Sigma_{5/2}} = 0$	9.4 ± 40	0.7 ± 34
$14S_{\Sigma''_{3/2}} + 28S_{\Lambda_{5/2}} + 11(S_{\Sigma_{1/2}} + S_{\Sigma'_{1/2}})$		
$-27(S_{\Lambda_{1/2}} + S_{\Lambda'_{1/2}}) - 10S_{\Sigma_{5/2}} = 0$	0.8 ± 40	0.1 ± 33

6.5.4 Fit results for $[70, 1^-]$ multiplet masses to data

The fits can be done separately for the $[20', 1^-]$ multiplet which corresponds to two flavors, and $[70, 1^-]$ multiplet which corresponds to three flavors. The fit results for the non-strange (case of two flavors) baryons are given in Table (6.18)¹. The physical case is in good agreement with previous works [58, 59]. If one considers only the seven known masses as inputs to the fit, one operator must be eliminated: the operator O_8 is thus dismissed as it always results virtually irrelevant. A second fit where only the three dominant operators are kept turns out to be consistent for the lattice QCD results, but gives a poor fit to the physical case. In that case, the M_π evolution of the coefficients is shown in Fig. (6.3).

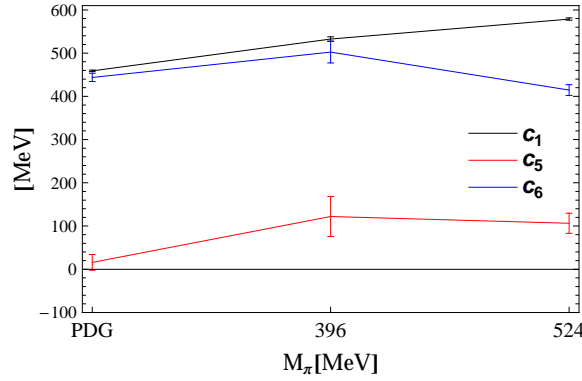


Figure 6.3. Evolution of the minimum set of operator coefficients with M_π in $SU(4) \times O(3)$.

A comparison of the physical case shows that it is consistent with earlier work [58, 59], but differs significantly for the coefficients c_3 and c_6 with respect to the recent global analysis carried out in Ref. [68]. Since all those fits are consistent in terms of the χ^2 , it is an indication of the ambiguity that results when only the masses are fitted. This means that also for the LQCD results one should expect several con-

¹In order to compare with the coefficients C_i obtained in the global analysis [68], where the operators are given in spherical basis and with different normalizations than here, the correspondence is: $C_1 = c_1$, $C_2 = -\frac{5}{6}c_2$, $C_3 = -\frac{75}{144}c_3$, $C_4 = \frac{3}{2}c_4$, $C_5 = -\frac{5}{3}c_5$, $C_6 = 2c_6$, $C_7 = -c_7$, and $C_8 = \frac{5}{3}c_8$.

sistent fits in terms of the value of the χ^2 , which will have some of the parameters significantly different.

Table 6.18. Fits to the non-strange $[20, 1^-]$ baryon masses. Unless the mixing angles are inputs to the fit, the operator O_8 is not necessary due to linear dependence as there are only seven mass inputs to fit. For the physical case with seven parameter fit (second column), the mixing angles from the global analysis ($\theta_{N_{1/2}}=0.49\pm0.29$, $\theta_{N_{3/2}}=3.01\pm0.17$) were used as inputs. For the minimal fit (third column) with c_1, c_5, c_6 , the mixing angles in the physical case are not inputs.

M_π [MeV] Coefficients	PDG	396	524	PDG	396	524
c_1	463 \pm 2	543 \pm 5	598 \pm 3	459 \pm 2	533 \pm 5	579 \pm 3
c_2	-36 \pm 12	39 \pm 35	13 \pm 14	0	0	0
c_3	313 \pm 69	-83 \pm 215	-96 \pm 74	0	0	0
c_4	65 \pm 31	-70 \pm 71	-95 \pm 30	0	0	0
c_5	71 \pm 18	99 \pm 48	107 \pm 24	16 \pm 18	122 \pm 46	106 \pm 23
c_6	443 \pm 10	446 \pm 25	307 \pm 13	443 \pm 10	502 \pm 25	414 \pm 13
c_7	-20 \pm 31	-0.37 \pm 62.89	-66 \pm 34	0	0	0
$\theta_{N_{1/2}}$ [Rad]	0.52 \pm 0.13	2.94 \pm 0.21	2.76 \pm 0.06	3.13 \pm 0.01	3.04 \pm 0.05	3.03 \pm 0.03
$\theta_{N_{3/2}}$ [Rad]	3.02 \pm 0.09	2.88 \pm 0.42	2.38 \pm 0.11	3.12 \pm 0.02	2.98 \pm 0.08	2.97 \pm 0.05
χ^2_{dof}	0.05	0	0	0.68	0.52	1.0

For two flavors, and following the global analysis of Ref. [68], the two mixing angles are given as input, and in this way it is possible to fit with the complete basis of operators up to 2-body. If the additional information provided by partial decay widths and/or photocouplings is not available, as it is the case for the LQCD results, one possibility is to neglect some of the basis operators, which allows one to predict the mixing angles solely using the masses. A guidance on what operator(s) to exclude is given by the rather clear hierarchy in the importance the different operators have, as measured by the magnitude of their coefficients. In fact, it becomes clear that the

mixing angles are mostly controlled by the operators O_2 , O_6 and to a lesser extend O_4 and O_5 .

In the case of three flavors the number of masses is much larger than the number of basis operators, and thus in principle the mixing angles can be determined with the information on the masses, of course after the above mentioned identification of states has been performed. Such identification is clearly displayed in Table (6.15). For the sake of brevity, only those operators which have effects of any significance have been included here: after an initial analysis, several operators whose coefficients resulted consistent with zero have been eliminated. The fits for three flavors are given in Tables (6.19) and (6.20) for the corresponding subsets of operators. Because of the different definitions of the basis operators for the different multiplets, in order to compare contributions which are of common nature across mutliplets such as the spin-flavor singlet contributions, the HF and the $SU(3)$ breaking, the following identification of coefficients should be done: $c_{1_{\mathbf{56}}} \leftrightarrow (c_1 + (b_1 + b_2)/\sqrt{3})_{\mathbf{70}}$, $c_{2_{[\mathbf{56},0+]}} \leftrightarrow c_{3_{[\mathbf{56},2+]}} \leftrightarrow \frac{1}{3}c_{6_{\mathbf{70}}}$, $b_{1_{\mathbf{56}}} \leftrightarrow -((b_1 + b_2)\sqrt{3}/2)_{\mathbf{70}}$. The mixing angles are given in Table (6.21).

Table 6.19. Fit to the $[\mathbf{70}, 1^-]$ masses using a subset of operators chosen as a minimal subset such the χ^2_{dof} is acceptable for all input sets. For the physical case the mixing angles from the global analysis [68] ($\theta_{N_{1/2}}=0.49\pm0.29$, $\theta_{N_{3/2}}=3.01\pm0.17$) were used as inputs.

Coefficients		$M_\pi[\text{MeV}]$			
[MeV]	PDG	391	524	702	
c_1	444.3 ± 0.3	572 ± 2	585 ± 1	636 ± 1	
c_2	84 ± 2	68 ± 12	-7 ± 6	-16 ± 4	
c_3	117 ± 13	59 ± 22	-40 ± 18	2 ± 8	
c_4	115 ± 5	-12 ± 12	-28 ± 9	-13 ± 4	
c_5	84 ± 10	134 ± 17	132 ± 14	84 ± 7	
c_6	538 ± 5	327 ± 10	350 ± 6	262 ± 4	
c_7	-159 ± 13	49 ± 27	-59 ± 17	13 ± 11	
b_1	-214 ± 5	-100 ± 13	-43 ± 9	0	
b_2	-188 ± 2	-62 ± 6	-46 ± 4	0	
b_3	-92 ± 2	-41 ± 10	-6 ± 7	0	
χ^2_{dof}	0.74	0.65	0.14	0.09	

Table 6.20. Fit results with minimal set of mass operators for the $[\mathbf{70}, 1^-]$. Only masses are used as inputs.

Coefficients		$M_\pi[\text{MeV}]$			
[MeV]	PDG	391	524	702	
c_1	462 ± 0.3	582 ± 2	587 ± 1	637 ± 1	
c_2	83 ± 2	92 ± 10	13 ± 8	-11 ± 4	
c_5	-67 ± 11	136 ± 17	127 ± 13	96 ± 7	
c_6	420 ± 4	270 ± 9	344 ± 6	257 ± 4	
c_7	-78 ± 14	4 ± 31	-47 ± 16	21 ± 11	
b_1	-92 ± 4	-53 ± 13	-34 ± 9	0	
b_2	-179 ± 2	-58 ± 6	-48 ± 4	0	
$\theta_{N_{1/2}}$	0.33 ± 0.02	0.79 ± 0.21	2.95 ± 0.05	2.94 ± 0.02	
$\theta_{N_{3/2}}$	0.45 ± 0.02	0.79 ± 0.13	2.86 ± 0.07	2.84 ± 0.03	
χ^2_{dof}	6.7	0.86	0.46	0.13	

Table 6.21. Mixing angles in the $[\mathbf{70}, 1^-]$ predicted from the fit to the masses.

Mixing angles [Rad]	M_π [MeV]			
	PDG	391	524	702
$\theta_{N_{1/2}}$	0.76 ± 0.03	0.61 ± 0.12	2.77 ± 0.06	2.98 ± 0.05
$\theta_{N_{3/2}}$	3.09 ± 0.40	0.10 ± 0.81	2.70 ± 0.10	2.84 ± 0.03
$\phi_{\Lambda_{1/2}}$	-0.15 ± 0.01	-0.15 ± 0.01	-0.14 ± 0.01	0
$\theta_{\Lambda_{1/2}}$	0.83 ± 0.01	0.70 ± 0.01	2.76 ± 0.01	2.98 ± 0.05
$\psi_{\Lambda_{1/2}}$	0.05 ± 0.01	0.11 ± 0.01	-0.18 ± 0.02	0
$\phi_{\Lambda_{3/2}}$	-0.21 ± 0.03	-0.16 ± 0.04	-0.12 ± 0.02	0
$\theta_{\Lambda_{3/2}}$	3.08 ± 0.01	0.13 ± 0.01	2.69 ± 0.02	2.84 ± 0.03
$\psi_{\Lambda_{3/2}}$	-0.18 ± 0.01	0.07 ± 0.03	-0.03 ± 0.01	0
$\phi_{\Sigma_{1/2}}$	-0.25 ± 0.02	0.03 ± 0.01	-0.05 ± 0.04	0
$\theta_{\Sigma_{1/2}}$	1.01 ± 0.01	0.75 ± 0.01	2.75 ± 0.01	2.98 ± 0.05
$\psi_{\Sigma_{1/2}}$	-0.10 ± 0.01	0.01 ± 0.07	0.03 ± 0.04	0
$\phi_{\Sigma_{3/2}}$	-0.08 ± 0.06	0.06 ± 0.04	-0.02 ± 0.04	0
$\theta_{\Sigma_{3/2}}$	3.05 ± 0.01	0.16 ± 0.02	2.66 ± 0.01	2.84 ± 0.03
$\psi_{\Sigma_{3/2}}$	0.04 ± 0.02	0.03 ± 0.02	0.005 ± 0.001	0
$\phi_{\Xi_{1/2}}$	-0.30 ± 0.03	0.03 ± 0.01	-0.05 ± 0.06	0
$\theta_{\Xi_{1/2}}$	0.94 ± 0.01	0.78 ± 0.01	2.77 ± 0.04	2.98 ± 0.05
$\psi_{\Xi_{1/2}}$	-0.14 ± 0.02	0.01 ± 0.07	0.03 ± 0.06	0
$\phi_{\Xi_{3/2}}$	-0.09 ± 0.07	0.05 ± 0.03	-0.02 ± 0.04	0
$\theta_{\Xi_{3/2}}$	3.07 ± 0.01	0.19 ± 0.03	2.69 ± 0.02	2.84 ± 0.03
$\psi_{\Xi_{3/2}}$	0.05 ± 0.03	0.02 ± 0.01	0.006 ± 0.001	0

The fits in the physical case are checked to be consistent with previous analysis [21, 23]. It is interesting to observe the evolution of the mixing angles θ with M_π , as they can give a clue on the possible level crossing as M_π evolves. As it is the case in the non-strange case discussed above, in the $S = 3/2$ baryons these angles remain continuous from the physical case to $M_\pi = 702$ MeV, while in the case of the $S = 1/2$

baryons there is a change by more than $\pi/2$, indicating a level crossing along the way. This qualitatively agrees with the LQCD results in Refs. [63, 65]. It is interesting to observe that for $M_\pi = 702$ MeV all baryons are stable, and almost all are still stable for $M_\pi = 524$ MeV, while below $M_\pi = 391$ MeV they are unstable. Since the $S = 1/2$ baryons have S-wave decays, they are the ones to be sensitive to the opening of the decay. These observations suggest a synchronization between the mixing angle and the stability of the baryon. In fact, the change in θ_1 shown in Table (6.21) in going from $M_\pi = 391$ to 524 MeV is approximately $\pi/2$, as expect for a level crossing. Is this an explanation for the observed level crossings?. Perhaps, but it is not clear at this point, and it deserves further study.

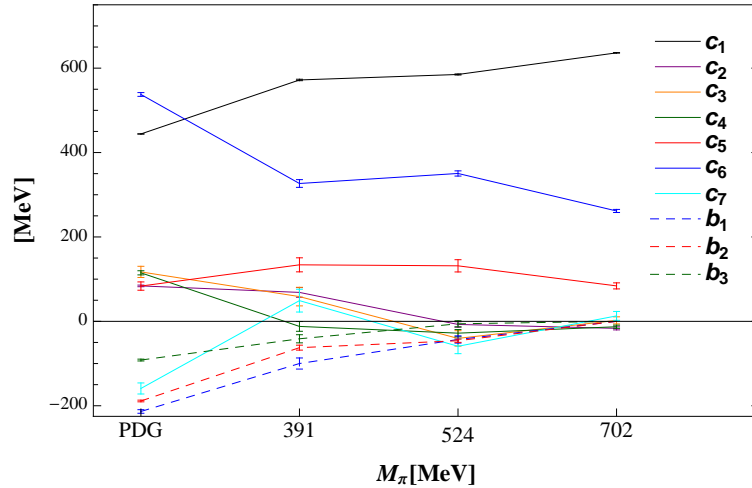


Figure 6.4. Evolution with respect to M_π of the coefficients of the basis operators used to fit both the physical and the LQCD [70, 1⁻] masses.

Consistent fits to only LQCD results can be achieved by a minimal set of significant operators. It is found that the relevant $SU(3)$ singlet operators are the spin-flavor singlet O_1 , the HF O_6 and the two spin-orbit ones O_2 and O_5 and the first two $SU(3)$ breaking operators. These results are illustrated in Fig. (6.5). Note that all the $SU(3)$ breaking operators are relevant for fitting the physical case. The operator O_3 is found to be important for the physical masses, but irrelevant for the LQCD masses, where

the operator O_5 is instead significant. It is interesting to observe that in models with pion exchange between quarks, such as certain versions of the chiral quark model, O_3 is naturally important, and should fade as the M_π increases.

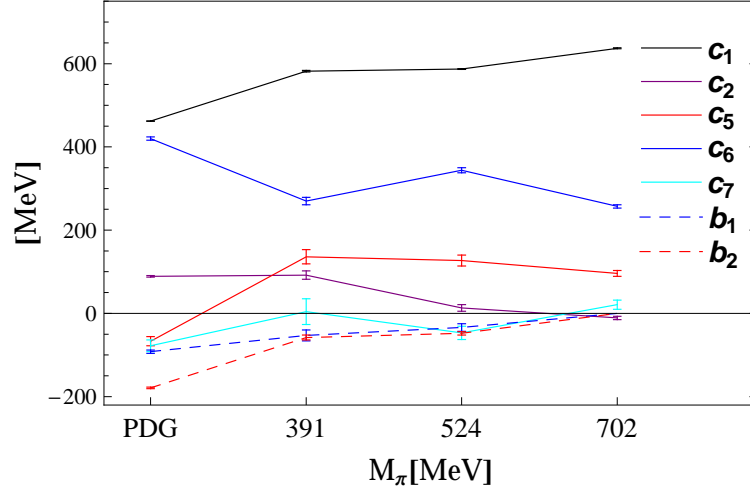


Figure 6.5. Evolution with respect to M_π of the coefficients in Table (6.20). .

The mass relations are depicted in Tables 6.16 and 6.17. All are well satisfied, except for the EQS relation for $M_\pi = 391$ MeV involving $\Sigma''_{3/2}$. A shift of its mass by $\sim +30$ MeV leads to consistency. The mass predictions are given in Table (6.22). Since, the PDG candidate state $\Xi(1950)^{***}(?)$ is consistent with $\Xi'_{3/2}, \Xi_{5/2}$ and $\Xi''_{1/2}$ in Table (6.22), its parity could be predicted as negative.

Table 6.22. Predictions of physically unknown states in the $[70, 1^-]$ multiplet from the fit in Table (6.19).

Missing State	Fitted mass with union set of operators [MeV]	PDG [MeV]
$\Sigma_{1/2}$	1644.72	$\Sigma(1620)1/2^{-**}=1620\pm10$
$\Xi_{1/2}$	1800.93	...
$\Xi'_{1/2}$	1930.24	...
$\Lambda'_{3/2}$	1824.59	...
$\Sigma'_{3/2}$	1780.37	...
$\Xi'_{3/2}$	1943.64	$\Xi(1950)(?)^{***}=1950\pm15$
$\Xi_{5/2}$	1938.95	$\Xi(1950)(?)^{***}=1950\pm15$
$\Sigma''_{1/2}$	1827.51	...
$\Xi''_{1/2}$	1968.76	$\Xi(1950)(?)^{***}=1950\pm15$
$\Omega_{1/2}$	2107.31	...
$\Sigma''_{3/2}$	1916.21	$\Sigma(1940)3/2^{-***}=1950\pm30$
$\Xi''_{3/2}$	2057.24	...
$\Omega_{3/2}$	2197.75	...

6.6 Summary of the fits to baryon masses

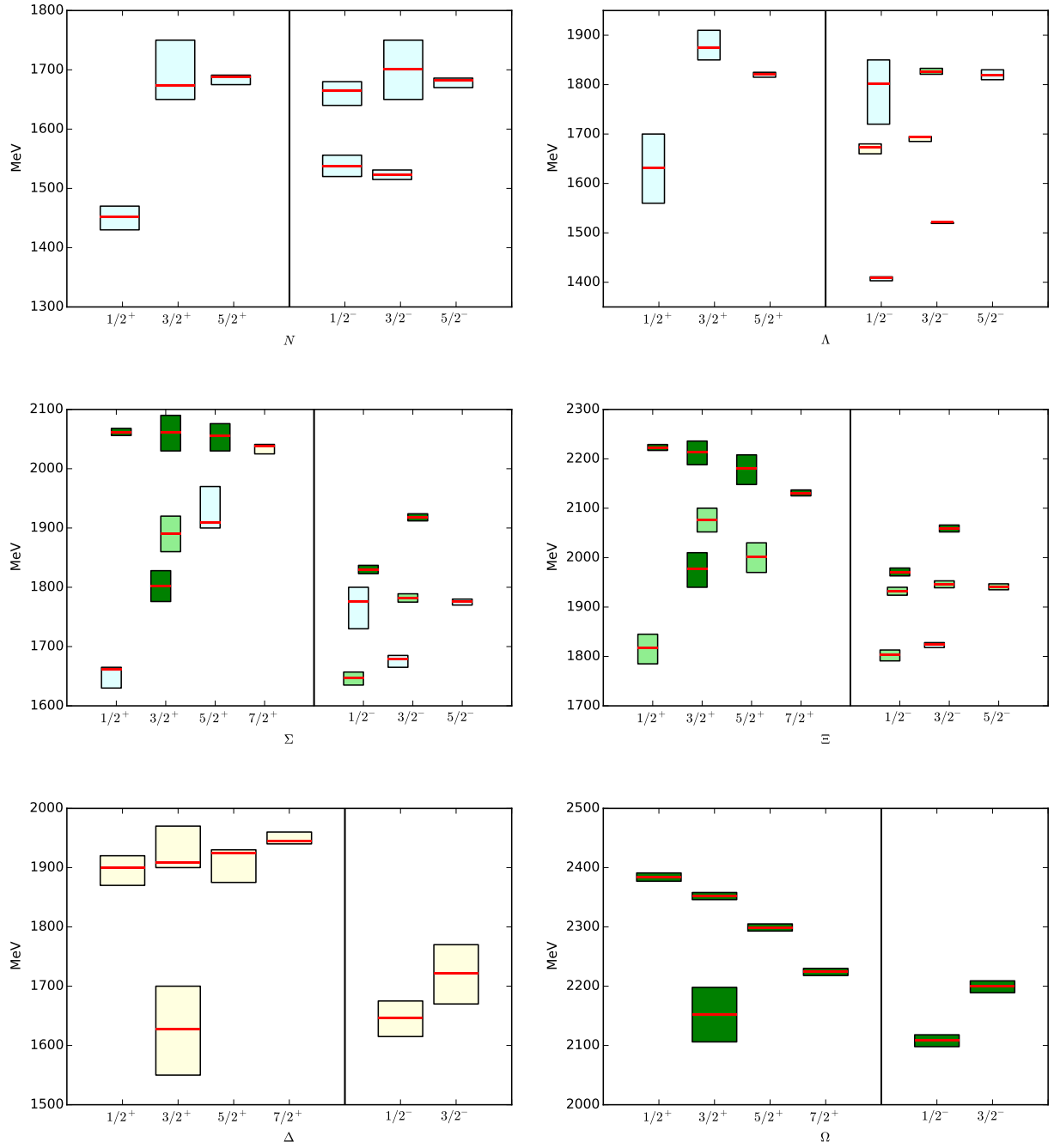


Figure 6.6. At $M_\pi=139$ MeV (physical) : green colored boxes represent the physically unidentified states which were calculated using the mass relations and, the red colored line represents the corresponding baryon mass from the fit. Light-blue color represents the octets and light-yellow color represents a singlet (for the case of Λ) or decuplet (for the cases of Σ, Ξ).

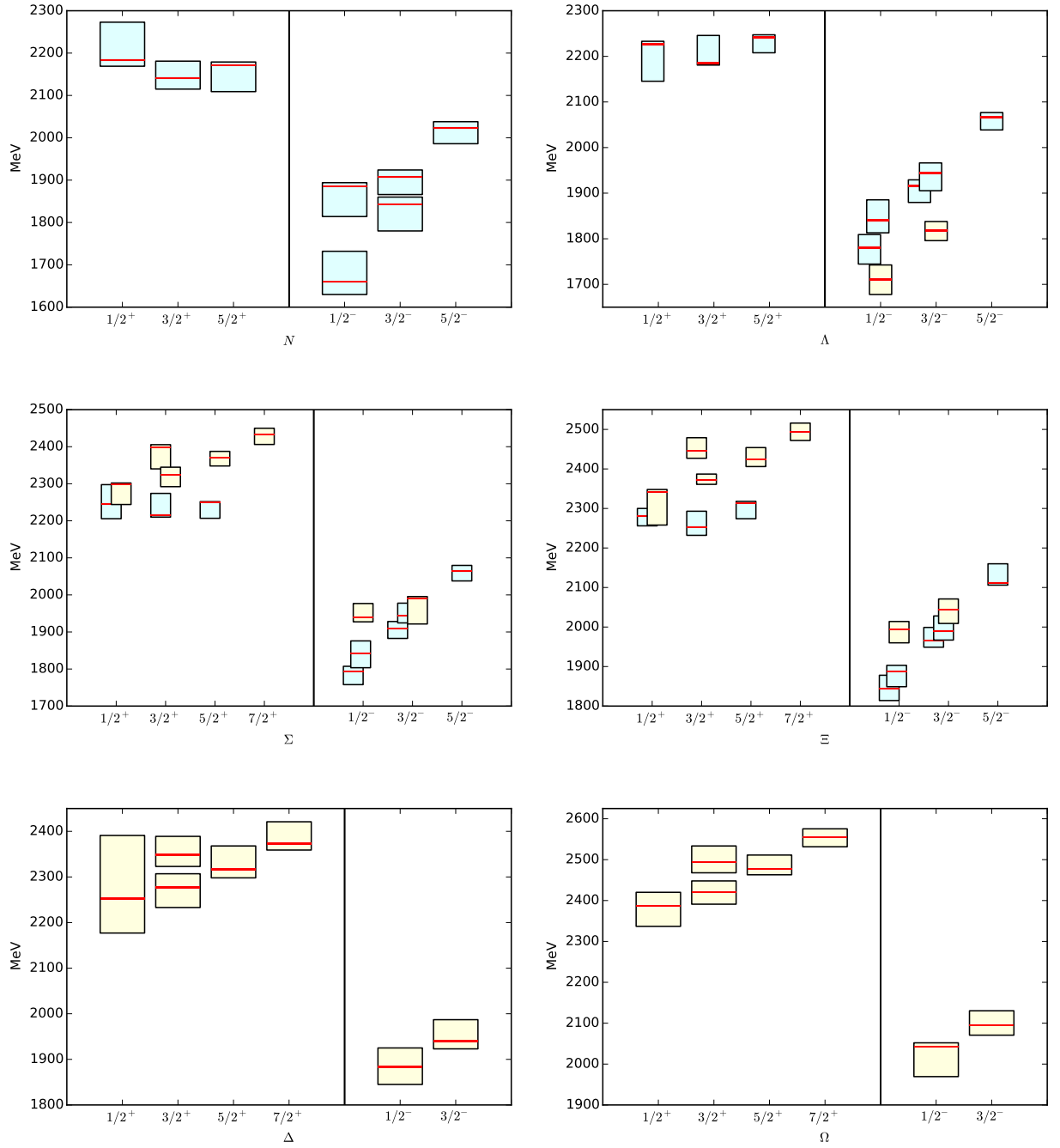


Figure 6.7. Baryon spectrum for $M_\pi=391$ MeV with LQCD input from Edwards *et al.* [29] and the fits from $1/N_c$ expansion framework. Light-blue color represents the octets and light-yellow color represents a singlet (for the case of Λ) or decuplet (for the cases of Σ, Ξ).

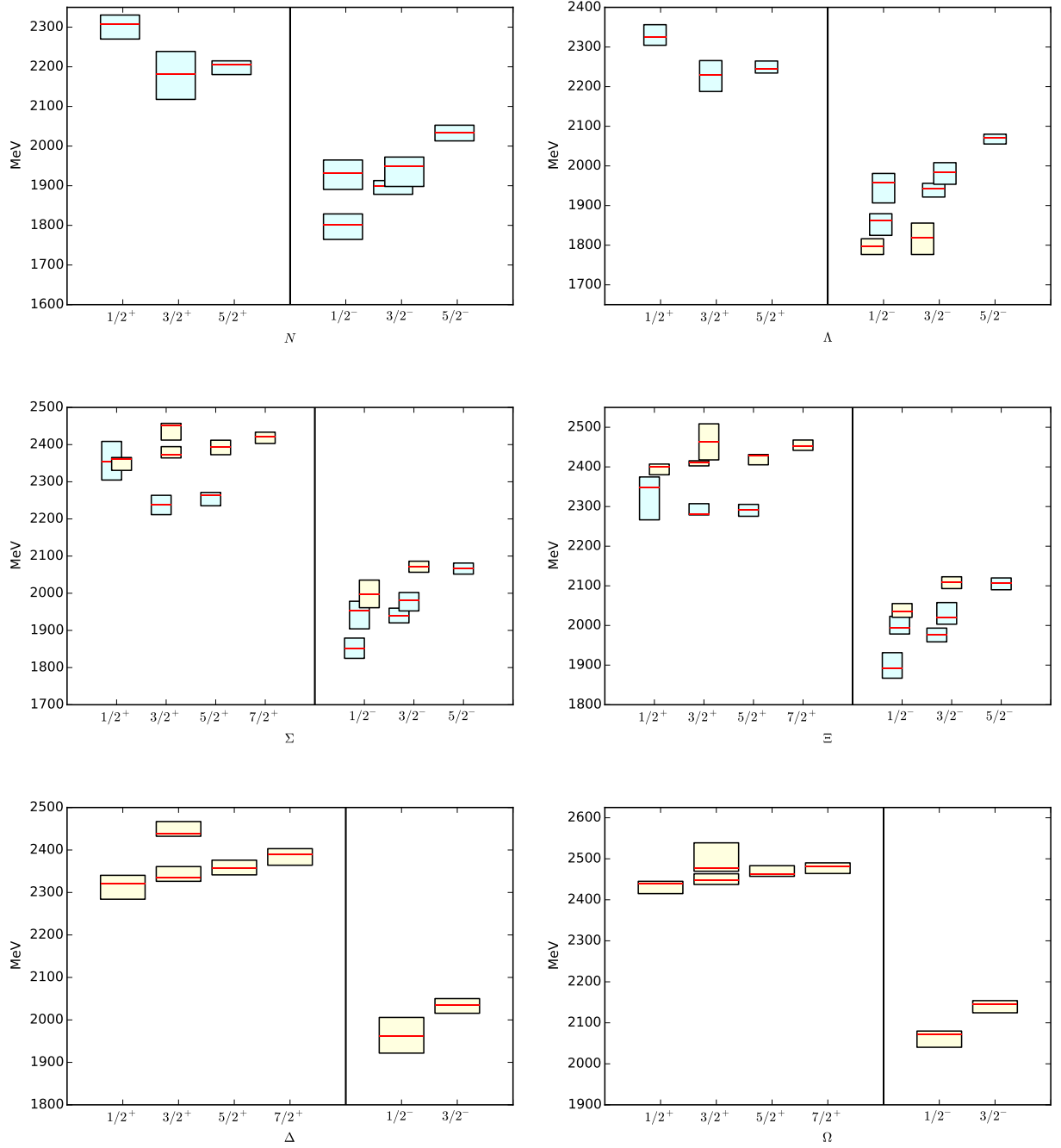


Figure 6.8. Baryon spectrum for $M_\pi=524$ MeV with LQCD input from Edwards *et al.* [29] and the fits from $1/N_c$ expansion framework. Light-blue color represents the octets and light-yellow color represents a singlet (for the case of Λ) or decuplet (for the cases of Σ, Ξ).

6.7 Conclusions and discussion

From the study presented here of recent LQCD results for the low-lying baryon excitations, it can be concluded that a picture of the spin-flavor composition of excited baryons is derived from their masses calculated in LQCD and the $1/N_c$ expansion. The results obtained entirely support the picture seen from the lattice QCD analysis of the mass eigenstate couplings to source/sink operators. A similar, and even simpler picture than the physical case emerges at increasing quark masses, where with very few dominant operators the LQCD masses can be described. The expected narrowness of the states analyzed for the quark masses in the LQCD results suggests that those results are very realistic. For higher excited baryons, which will be broader, the present LQCD results may be a poorer approximation. Nonetheless, they should be interesting to study.

A strong conclusion is that the baryon masses calculated in LQCD are even closer to an approximate $SU(6) \times O(3)$ symmetry limit than the physical ones. This is most likely due to the fact that the composition of baryons becomes increasingly closer to a constituent quark model picture as the quark masses increase, emphasizing the mass operators which are naturally large in those models and suppressing the rest.

For the quark masses employed in the LQCD calculations used here, the dramatic downturn in c_1 for the Roper baryons is not manifest. This is an effect where probably chiral symmetry plays an important role as it becomes restored towards lighter M_π . In recent LQCD work on nucleon resonances [63, 65] a first evidence of that downturn is observed. It remains to be determined what precise mechanism drives that effect, and perhaps some clever strategy in LQCD calculations could be used for that purpose. While in the Roper multiplet the c_1 coefficient should have a large negative curvature as a function of M_π to match the physical masses, it lies along

an almost perfect straight line for the ground-state baryons, and it has a moderate negative curvature in the other cases.

Identifying the HF coefficients as mentioned earlier, one finds that for the LQCD results the strength of the HF in the ground-state baryons is almost twice as large as in the excited baryons, which is significantly different from the physical case, where it is only about 25 % larger. One should point out that in a picture of large N_c baryons with very heavy quark masses the hyperfine interaction will scale as $m_q = N_c$, implying that in LQCD calculations at even larger quark masses than the ones used so far the hyperfine interaction coefficient should eventually scale approximately as m_q .

The spin-orbit contributions are all smaller than the natural size. In the $[56, 2^+]$ it is an effect $\mathcal{O}(1/N_c)$, and the coefficient slowly decreases with increasing M_π . In the $[70, 1^-]$ the $\mathcal{O}(N_c^0)$ contribution is determined by c_2 which decreases with increasing M_π , and the $\mathcal{O}(1/N_c)$ contribution is determined by c_3 remains roughly independent of M_π .

An interesting open problem is how to relate the $SU(6) \times O(3)$ decomposition of the physical baryons determined via the $1/N_c$ expansion as presented here, with the information on the coupling strengths of the mass eigenstates to the different source/sink operators obtained in the LQCD calculations.

Part II

COMBINED EFT APPROACH: ChPT AND THE $1/N_c$ EXPANSION

CHAPTER 7

CHIRAL PERTURBATION THEORY AS AN EFT IN QCD

7.1 Introduction

An effective field theory (EFT) is a theory (or Lagrangian) which includes all the relevant physics at some specific length scale, as the relevant degrees of freedom to the problem. Also one can identify a small parameter which allows one to perform perturbative power counting, and systematically work to any desired level of precision. The foundation of EFT comes from the ideas by Ken Wilson, Steven Weinberg, etc [9, 80, 81]. The EFT approach has become a very strong mathematical tool in particle physics, especially when dealing with the nontrivial phenomenology of producing the hadron spectrum (mesons and baryons) from quarks and gluons as the fundamental degrees of freedom in QCD. Since the perturbative expansion in terms of the gauge coupling is only possible at high energies, the low energy phenomenology needs a reformulation of the QCD Lagrangian in terms of “hadron” degrees of freedom with some small parameters in order to perform perturbative expansion to describe the physical observables.

This chapter is organized as follows; The next section contains a brief overview of the symmetries of the QCD Lagrangian, including a discussion on symmetry breaking due to quark mass and QCD in the presence of external fields. The third section explains a flavor of the effective field theory approach. Then the fourth and fifth sections summarize the chiral effective theory for mesons and baryons with applications. The last section is devoted to the heavy baryon approach.

7.2 Symmetries of \mathcal{L}_{QCD}

The QCD Lagrangian \mathcal{L}_{QCD} respects the Poincaré symmetry, local color gauge invariance, flavor symmetry and discrete symmetries such as parity and charge conjugation. In addition to those symmetries, there are more symmetries emerge according to the Noether's theorem i.e., any continuous symmetry transformation (local or global) which preserves the invariance of the action implies the existence of a conserved current associated with the symmetry, and the corresponding charge is a constant of motion.

7.2.1 Global $U(1)_V$ symmetry

This is identified as the $U(1)$ “vector symmetry” with the subscript V , and the transformations associated with the $U(1)_V$ symmetry can be defined as,

$$\psi(x) \rightarrow \psi'(x) = e^{i\theta}\psi. \quad (7.1)$$

where θ is a constant. One can directly see that the QCD Lagrangian is invariant under these transformations and the associated conserved current is:

$$J_V^\mu(x) = \bar{\psi}(x)\gamma^\mu\psi(x), \quad \partial_\mu J_V^\mu(x) = 0 \quad (7.2)$$

and the conserved charge is identified as the “*baryon number*”:

$$\mathcal{B} = \int d^3x \psi^\dagger(x)\psi(x) \quad (7.3)$$

7.2.2 Global $U(1)_A$ symmetry

This is identified as the $U(1)$ "axial-vector symmetry" with the subscript A , and the transformations associated with the $U(1)_A$ symmetry,

$$\psi(x) \rightarrow \psi'(x) = e^{i\theta\gamma_5}\psi. \quad (7.4)$$

yields the axial-vector current,

$$J_A^\mu(x) = \bar{\psi}(x)\gamma^\mu\gamma_5\psi(x), \quad (7.5)$$

which is not conserved,

$$\partial_\mu J_A^\mu(x) = 2im\bar{\psi}\gamma_5\psi \quad (7.6)$$

due to the quark mass. Therefore the $U(1)_A$ is a symmetry for the quark fields in the limit of zero quark mass, which is identified as the "Chiral limit", where γ_5 is identified as the "Chirality matrix".

7.2.3 Isospin $SU(2)_f$ symmetry

In the case of two light quark flavors ($N_f = 2$), the quark fields can be identified as an "*isospin doublet*" : $\psi(x) = \begin{pmatrix} u(x) \\ d(x) \end{pmatrix}$, and in the symmetry limit one assumes $m_u = m_d$. The $SU(2)_f$ symmetry transformations can be defined as,

$$\psi(x) \rightarrow \psi'(x) = e^{i\theta_i \frac{\tau_a}{2}} \psi \quad (7.7)$$

where θ_a is the a^{th} group parameter associated with $SU(2)$ generator τ_a (Pauli matrices with $a = \{1, 2, 3\}$). Since the QCD Lagrangian is invariant under $SU(2)_f$

transformations, the associated conserved current can be defined as,

$$J_a^\mu(x) = \bar{\psi}(x) \gamma^\mu \frac{\tau_a}{2} \psi(x) \quad (7.8)$$

and the time-independence of the conserved isospin charge,

$$Q_a = \int d^3x J_a^0(x) = \int d^3x \psi^\dagger(x) \frac{\tau_a}{2} \psi(x) \quad (7.9)$$

implies that it commutes $[H, Q_a] = 0$ with the QCD Hamiltonian.

7.2.4 $SU(3)_f$ symmetry

For three light quark flavors ($N_f = 3$), one can consider $\psi(x) = \begin{pmatrix} u(x) \\ d(x) \\ s(x) \end{pmatrix}$, with $m_u = m_d = m_s$ approximation. Therefore the QCD Lagrangian is invariant under $SU(3)_f$ transformations,

$$\psi(x) \rightarrow \psi'(x) = e^{i\theta_a \frac{\lambda_a}{2}} \psi \quad ; \quad (a = \{1, 2, 3, \dots, 8\}) \quad (7.10)$$

where λ_a are 3×3 Gell-Mann matrices with $a = \{1, \dots, 8\}$, and the invariance under $SU(3)_f$ transformations introduces the conserved current:

$$J_a^\mu(x) = \bar{\psi}(x) \gamma^\mu \frac{\lambda_a}{2} \psi(x) \quad (7.11)$$

and the conserved charge:

$$Q_a = \int d^3x \psi^\dagger(x) \frac{\lambda_a}{2} \psi(x) \quad (7.12)$$

7.2.5 Chiral symmetry

“*Chirality*” is defined as the *helicity* (spin projection on the momentum direction) of a particle in the massless limit. Only two types of chirality or helicity are possible along the axis of propagation: left-handed and right-handed. This allows one to decompose the quark fields as,

$$\psi = \psi_R + \psi_L \quad (7.13)$$

with,

$$\psi_R = \underbrace{\frac{1}{2}(1 + \gamma_5)}_{P_R} \psi \quad , \quad \psi_L = \underbrace{\frac{1}{2}(1 - \gamma_5)}_{P_L} \psi \quad , \quad \bar{\psi}_{R/L} = \underbrace{\frac{1}{2}(1 \mp \gamma_5)}_{P_{L/R}} \bar{\psi} \quad (7.14)$$

where the “*chirality matrix*” γ_5 is defined as,

$$\gamma_5 = \gamma^5 = i\gamma^0\gamma^1\gamma^2\gamma^3 = \begin{pmatrix} 0 & \mathbb{1} \\ \mathbb{1} & 0 \end{pmatrix} , \quad \{\gamma^\mu, \gamma_5\} = 0 , \quad \gamma_5^2 = \begin{pmatrix} \mathbb{1} & 0 \\ 0 & \mathbb{1} \end{pmatrix} \quad \text{with} \quad \mathbb{1} = \begin{pmatrix} 1 & 0 \\ 0 & 1 \end{pmatrix} , \quad (7.15)$$

in the Dirac representation [82]. P_R and P_L are identified as projection operators which project the quark fields to their chiral components ψ_R and ψ_L . The chirality projection operators also satisfy the following properties:

$$\begin{aligned} P_R + P_L &= 1 & : & \text{“completeness relation”} \\ P_R^2 = P_R, \quad P_L^2 = P_L & & : & \text{“idempotent”} \\ P_R P_L = P_L P_R &= 0 & : & \text{“orthogonal”} . \end{aligned} \quad (7.16)$$

The Chiral symmetry (or left-right handed symmetry) in \mathcal{L}_{QCD} emerges in the massless limit of $SU(3)_f$ symmetry. In other words, QCD in the $\{m_u, m_d, m_s\} \rightarrow 0$ limit, is called the “*chiral*” limit. Also, this approximation is reasonable since we can argue that the real world is not so different from this theoretical limit. Therefore,

one can re-write the QCD Lagrangian,

$$\mathcal{L}_{\text{QCD}} = \underbrace{\bar{\psi}(x)i\gamma^\mu D_\mu\psi(x) - \frac{1}{4}\mathcal{G}_{\mu\nu}(x)^a\mathcal{G}_a^{\mu\nu}(x)}_{\mathcal{L}_{\text{QCD}}^0} - \underbrace{\bar{\psi}(x)m_f\psi(x)}_{\mathcal{L}_M} \quad (7.17)$$

by separating the mass term \mathcal{L}_M .

In the goal of analyzing the symmetry of \mathcal{L}_{QCD} under the independent global transformations of left- and right-handed fields, there are 16 quadratic forms of quark bilinears [82]:

$$\bar{\psi}\Gamma_i\psi = \begin{cases} \psi_R\bar{\Gamma}_1\psi_R + \psi_L\bar{\Gamma}_1\psi_L & \text{for } \Gamma_1 \in \{\gamma^\mu, \gamma^\mu\gamma_5\} \\ \psi_R\bar{\Gamma}_2\psi_L + \psi_L\bar{\Gamma}_2\psi_R & \text{for } \Gamma_2 \in \{1, \gamma_5, \sigma^{\mu\nu}\} \end{cases} . \quad (7.18)$$

Also note that, $\{\Gamma_1, \gamma_5\} = 0$ and $[\Gamma_2, \gamma_5] = 0$ combined with the orthogonality of P_R and P_L give,

$$P_R\Gamma_1P_R = P_L\Gamma_1P_L = \Gamma_1P_LP_R = P_R\Gamma_2P_L = P_L\Gamma_2P_R = 0 . \quad (7.19)$$

Applying these properties in the QCD Lagrangian in the *chiral limit*, one can separate the quark field term in $\mathcal{L}_{\text{QCD}}^0$ into its left- and right-handed components,

$$\mathcal{L}_{\text{QCD}}^0 = \bar{\psi}_R(x)i\gamma^\mu D_\mu\psi_R(x) + \bar{\psi}_L(x)i\gamma^\mu D_\mu\psi_L(x) - \frac{1}{4}\mathcal{G}_{\mu\nu}(x)^a\mathcal{G}_a^{\mu\nu}(x). \quad (7.20)$$

Since the covariant derivative is flavor-independent, $\mathcal{L}_{\text{QCD}}^0$ is invariant under the transformations [82] ,

$$\psi_{R,L} = U_{R,L} \psi_{R,L} \quad (7.21)$$

where,

$$\underbrace{U_{R,L}}_{U(3)_{R,L}} = \underbrace{\exp \left(-i \sum_{a=1}^8 \Theta_a^{R,L} \frac{\lambda_a}{2} \right)}_{SU(3)_{R,L}} \underbrace{e^{-i\Theta^{R,L}}}_{U(1)_{R,L}} \quad (7.22)$$

for the case of three flavors $N_f = 3$ with Gell-Mann Matrices λ_a . Therefore $\mathcal{L}_{\text{QCD}}^0$ is considered to have $U(3)_R \otimes U(3)_L$ Chiral symmetry, and the invariance of $\mathcal{L}_{\text{QCD}}^0$ under this symmetry produces $2 \times (8 + 1) = 18$ total conserved currents (associated with left- and right-handed transformations),

$$L^{\mu,a} = \bar{\psi}_L \gamma^\mu \frac{\lambda_a}{2} \psi_L, \quad \partial_\mu L^{\mu,a} = 0, \quad R^{\mu,a} = \bar{\psi}_R \gamma^\mu \frac{\lambda_a}{2} \psi_R, \quad \partial_\mu R^{\mu,a} = 0, \quad (7.23)$$

where $L^{\mu,a}$ and $R^{\mu,a}$ are left and right-handed currents which can be derived by considering the variation [83] of $\mathcal{L}_{\text{QCD}}^0$ under the infinitesimal transformations.

$$\delta \mathcal{L}_{\text{QCD}}^0 = \bar{\psi}_{R,L} \left(\sum_{a=1}^8 \partial_\mu \Theta_a^{R,L} \frac{\lambda_a}{2} + \partial_\mu \Theta^{R,L} \right) \psi_{R,L} \quad (7.24)$$

These chiral current densities $L^{\mu,a}$ and $R^{\mu,a}$ separately transform under $SU(3)_L \otimes SU(3)_R$ as a singlet and octet which we can denote as $(1,8)$ multiplet. The vector and axial-vector current densities are defined as linear combinations of these chiral current densities as follows,

“*octet*” current densities:

$$\begin{aligned} V^{\mu,a} &= R^{\mu,a} + L^{\mu,a} = \bar{\psi} \gamma^\mu \frac{\lambda_a}{2} \psi \\ A^{\mu,a} &= R^{\mu,a} - L^{\mu,a} = \bar{\psi} \gamma^\mu \gamma_5 \frac{\lambda_a}{2} \psi \end{aligned} \quad (7.25)$$

“*singlet*” current densities:

$$\begin{aligned} V^\mu &= \bar{\psi}_R \gamma^\mu \psi_R + \bar{\psi}_L \gamma^\mu \psi_L = \bar{\psi} \gamma^\mu P_R \psi + \bar{\psi} \gamma^\mu P_L \psi = \bar{\psi} \gamma^\mu \psi \\ A^\mu &= R^\mu - L^\mu = \bar{\psi} \gamma^\mu P_R \psi + \bar{\psi} \gamma^\mu P_L \psi = \bar{\psi} \gamma^\mu \gamma_5 \psi \end{aligned} \quad (7.26)$$

One can also obtain the conserved singlet vector current by transforming left- and right-handed quark fields by a “same” phase, whereas the singlet axial-vector currents can be obtained by transforming the left- and right-handed quark fields with “opposite” phase. However, this singlet axial-vector current is only conserved in classical level, but there will be extra terms (anomalies) in the quantum level which are of pure quantum origin and explicitly break the classical $U(1)$ axial symmetry [82]. It can be identified as,

$$\partial^\mu A_\mu = \frac{N_f g^2}{32\pi^2 N_c} \epsilon_{\mu\nu\rho\sigma} \mathcal{G}_a^{\mu\nu} \mathcal{G}_{\rho\sigma}^a \quad (7.27)$$

where, one can see that it is conserved at large N_c limit when the $g \rightarrow g/\sqrt{N_c}$ rescaling [10] is applied.

7.2.6 Symmetry breaking due to quark mass

The discussion above described that the QCD has $SU(3)_L \otimes SU(3)_R \otimes U(1)_V$ symmetry at the limit of zero quark mass. The breaking of the symmetry can be studied by investigating the effect of the quark mass matrix. Let's consider the \mathcal{L}_M piece in the Eq. (7.17).

$$\mathcal{L}_M = \sum_f \bar{\psi} m_f \psi = \bar{\psi} \mathcal{M} \psi \quad (7.28)$$

where \mathcal{M} is the diagonal quark mass matrix. In the case of two light-flavors,

$$\mathcal{M} = \text{diag}(m_u, m_d) = \left(\frac{m_u + m_d}{2} \right) \mathbb{1} + (m_u - m_d) \frac{\lambda_3}{2} \quad (7.29)$$

and in the case of three light-flavors,

$$\mathcal{M} = \text{diag}(m_u, m_d, m_s) = \left(\frac{m_u + m_d + m_s}{3} \right) \mathbb{1} + (m_u - m_d) \frac{\lambda_3}{2} + \left(\frac{m_u + m_d - 2m_s}{\sqrt{3}} \right) \frac{\lambda_8}{2}. \quad (7.30)$$

Applying the left- and right-handed transformations in Eq. (7.13) to the quark fields using the properties in Eq. (7.18), one can clearly see that the quark mass term mixes the left and right-handed fields.

$$\mathcal{L}_M = -\bar{\psi}\mathcal{M}\psi = -(\bar{\psi}_R\mathcal{M}\psi_L + \bar{\psi}_L\mathcal{M}\psi_R) \quad (7.31)$$

The variation $\delta\mathcal{L}_M$ under the chiral transformations in Eq. (7.22),

$$\begin{aligned} \delta\mathcal{L}_M = & - \left[\sum_{a=1}^8 \Theta_a^R \left(\bar{\psi}_R \frac{\lambda_a}{2} \mathcal{M} \psi_L - \bar{\psi}_L \mathcal{M} \frac{\lambda_a}{2} \psi_R \right) + \Theta^R (\bar{\psi}_R \mathcal{M} \psi_L - \bar{\psi}_L \mathcal{M} \psi_R) \right. \\ & \left. + \sum_{a=1}^8 \Theta_a^L \left(\bar{\psi}_L \frac{\lambda_a}{2} \mathcal{M} \psi_R - \bar{\psi}_R \mathcal{M} \frac{\lambda_a}{2} \psi_L \right) + \Theta^L (\bar{\psi}_L \mathcal{M} \psi_R - \bar{\psi}_R \mathcal{M} \psi_L) \right] , \end{aligned} \quad (7.32)$$

can be combined with the $\delta\mathcal{L}_{\text{QCD}}$ to obtain the corresponding vector and axial-vector current densities for the full QCD Lagrangian for the case of $N_f = 3$:

$$\begin{aligned} \partial_\mu V^{\mu,a} &= i\bar{\psi} \left[\mathcal{M}, \frac{\lambda_a}{2} \right] \psi , \\ \partial_\mu A^{\mu,a} &= i\bar{\psi} \left\{ \frac{\lambda_a}{2}, \mathcal{M} \right\} \psi , \\ \partial_\mu V^\mu &= 0 , \\ \partial_\mu A^{\mu a} &= 2i\bar{\psi} \mathcal{M} \gamma_5 \psi + \frac{3g^2}{32\pi^2} \epsilon_{\mu\nu\rho\sigma} \mathcal{G}_a^{\mu\nu} \mathcal{G}_{\rho\sigma}^a , \quad \epsilon_{0123} = 1 . \end{aligned} \quad (7.33)$$

These current densities associated with the symmetries and their deviations can be summarized as follows [82].

- In the limit of massless quarks, the octet current densities $V^{\mu,a}, A^{\mu,a}$ and the vector current density V^μ are conserved, whereas the singlet axial-vector current A^μ has an anomaly.
- All the axial currents are also not conserved when quark masses are non-zero.
- When the quark masses are equal ($m_u = m_d = m_s$), the eight vector currents $V^{\mu,a}$ are conserved since $[\lambda_a, 1] = 0$ according to the Eq. (7.33). This reflects to

origin of the $SU(3)$ symmetry originally proposed by Gell-Mann and Ne'eman [82].

- It is important to notice that the $SU(3)_f$ symmetry is a global symmetry of \mathcal{L}_{QCD} for both cases: with massless ($m_q = 0$), and massive ($\{m_u = m_d = m_s\} > 0$) quarks.
- For the quark masses with any value, each individual flavor's vector current density ($\bar{u}\gamma^\mu u, \bar{d}\gamma^\mu d, \bar{s}\gamma^\mu s, \dots$), and their sum are conserved. This reflects the flavor independence of strong interactions.

7.2.7 QCD in the presence of external fields and PCAC

In the presence of external fields the QCD Lagrangian can be re-written by adding $\mathcal{L}_{\text{external}}$ into the $\mathcal{L}_{\text{QCD}}^0$,

$$\begin{aligned}\mathcal{L}_{\text{QCD}} &= \mathcal{L}_{\text{QCD}}^0 + \mathcal{L}_{\text{external}} \\ &= \mathcal{L}_{\text{QCD}}^0 + \bar{\psi}\gamma_\mu(v^\mu + \gamma_5 a^\mu)\psi - \bar{\psi}(s - i\gamma_5 p)\psi ,\end{aligned}\tag{7.34}$$

by following the Gasser and Leutwyler's procedure [84, 85], where v^μ, a^μ, s, p respectively represents the vector, axial-vector, scalar and pseudo-scalar currents which are hermitian, color neutral, 3×3 matrices in the flavor space:

$$v^\mu = \frac{\lambda^a}{2}v_a^\mu, \quad a^\mu = \frac{\lambda^a}{2}a_a^\mu, \quad s = \lambda^a s_a, \quad p = \lambda^a p_a \quad (\text{for } a = 1, \dots, 8).\tag{7.35}$$

Since QCD Lagrangian is invariant under Parity (P), Charge-conjugation (C) and Time-reversal (T) transformations the external fields also follow the same invariance. One can summarize the transformation properties as follows,

- Parity :
– quark fields :

$$\psi_f(\vec{x}, t) \xrightarrow{P} \gamma^0 \psi_f(-\vec{x}, t) ,\tag{7.36}$$

– external fields :

$$\begin{aligned} v^\mu(\vec{x}, t) &\xrightarrow{P} v^\mu(-\vec{x}, t) , & a^\mu(\vec{x}, t) &\xrightarrow{P} -a^\mu(-\vec{x}, t) , \\ s^\mu(\vec{x}, t) &\xrightarrow{P} s^\mu(-\vec{x}, t) , & p^\mu(\vec{x}, t) &\xrightarrow{P} -p^\mu(-\vec{x}, t) \end{aligned} \quad (7.37)$$

• Charge-conjugation :

– quark fields :

$$\psi_{\alpha,f}(\vec{x}, t) \xrightarrow{C} C_{\alpha\beta} \bar{\psi}_{\beta,f}(-\vec{x}, t) , \quad \psi_{\alpha,f}(\vec{x}, t) \xrightarrow{C} \bar{\psi}_{\beta,f}(-\vec{x}, t) C_{\beta\alpha}^{-1} , \quad (7.38)$$

where, α, β are Dirac spinor indices, and $C = i\gamma^2\gamma^0 = -C^{-1}$

– external fields :

$$v^\mu \xrightarrow{C} -v_\mu^T , \quad a^\mu \xrightarrow{C} a_\mu^T , \quad s \xrightarrow{C} s^T , \quad p \xrightarrow{C} p^T \quad (7.39)$$

where the transposition apply in the flavor space, and the arguments change from (\vec{x}, t) to $(-\vec{x}, t)$.

In order to see the behavior of the external fields under local $SU(3)_L \otimes SU(3)_R \otimes U(1)_V$ transformations, let's define

$$v_\mu = \frac{1}{2}(r_\mu + l_\mu) , \quad a_\mu = \frac{1}{2}(r_\mu - l_\mu) \quad (7.40)$$

and apply to the $\mathcal{L}_{\text{external}}$ in the Eq. (7.34). Therefore one obtains,

$$\bar{\psi}\gamma^\mu (v_\mu + \gamma_5 a_\mu) \psi = \bar{\psi}_R \gamma^\mu r_\mu \psi_R + \bar{\psi}_L \gamma^\mu l_\mu \psi_L \quad (7.41)$$

for the first term in $\mathcal{L}_{\text{external}}$, and

$$\bar{\psi}\gamma^\mu (s - i\gamma_5 a_\mu) \psi = \bar{\psi}_L \gamma^\mu (s - ip) \psi_R + \bar{\psi}_R \gamma^\mu (s + ip) \psi_L \quad (7.42)$$

for the second term; with the aid of some auxiliary properties,

$$\begin{aligned}\gamma_5 P_R &= P_R \gamma_5 = P_R, & \gamma_5 P_L &= P_L \gamma_5 = -P_L \\ \gamma^\mu P_R &= P_L \gamma^\mu, & \gamma^\mu P_L &= P_R \gamma^\mu\end{aligned}\tag{7.43}$$

which are associated with the chiral transformations of quark-fields. Therefore, the QCD Lagrangian can be re-written as,

$$\mathcal{L}_{\text{QCD}} = \mathcal{L}_{\text{QCD}}^0 + \bar{\psi}_R \gamma^\mu r_\mu \psi_R + \bar{\psi}_L \gamma^\mu l_\mu \psi_L - \bar{\psi}_L \gamma^\mu (s - ip) \psi_R - \bar{\psi}_R \gamma^\mu (s + ip) \psi_L, \tag{7.44}$$

which remains invariant under local transformations,

$$\begin{aligned}\psi_R &= \exp\left(-\frac{\theta(x)}{3}\right) U_R(x) \psi_R \\ \psi_L &= \exp\left(-\frac{\theta(x)}{3}\right) U_L(x) \psi_L\end{aligned}\tag{7.45}$$

where, $U(x)_{L,R}$ are independent space-time dependent $SU(3)$ matrices which transforms the external fields with the following properties [82]:

$$\begin{aligned}r_\mu &\rightarrow U_R r_\mu U_R^\dagger + i U_R \partial_\mu U_R^\dagger, \\ l_\mu &\rightarrow U_L r_\mu U_L^\dagger + i U_L \partial_\mu U_L^\dagger, \\ s + ip &\rightarrow U_R (s + ip) U_L^\dagger, \\ s - ip &\rightarrow U_L (s - ip) U_R^\dagger.\end{aligned}\tag{7.46}$$

7.3 Construction of effective field theories

The construction of the effective Lagrangian is directly based on the known symmetries of the parent theory (which is QCD, in our case). Comparing the quark masses with the non-perturbative scale Λ_χ of dynamical chiral symmetry breaking ~ 1 GeV [86] the quarks can be separated into “*light*” and “*heavy*” sectors:

$$\underbrace{m_u, m_d, m_s}_{\text{light quarks}} \ll \Lambda_\chi (\sim 1 \text{ GeV}) \leq \underbrace{m_c, m_t, m_b}_{\text{heavy quarks}}. \tag{7.47}$$

As discussed in the introduction of Chapter 2, the quark masses are not determined directly by experiment; their values are determined with the help of theory and some assumptions. The heavy quark masses are to a first approximation determined from the heavy meson masses (eg: J/ψ , B-meson, etc.), and the light quark masses require many theoretical twists for the estimations. Only lattice QCD calculations are able to provide a determination of quark masses, but this is still not very precise.

This work is focused on the hadron states which belong to light quarks. Therefore, the heavy particles can be integrated out from the generating functional of the theory, such that only the light degrees of freedom are left behind with an effective Lagrangian. If Φ_l are the light fields and Φ_h are the heavy fields, then it is possible to define effective vertices (or couplings) by summing all the contributions of the intermediate states of the Φ_h in the elements of the S-matrix. Thus the effective Lagrangian can be introduced :

$$e^{i \int d^4x \mathcal{L}_{\text{eff}}(\Phi_l)} = \int \mathcal{D}\Phi e^{i \int d^4x \mathcal{L}(\Phi_l, \Phi_h)} , \quad (7.48)$$

where the S-matrix elements calculated from \mathcal{L}_{eff} are equivalent to those from the original one for all energies smaller than Λ_χ , because the contribution of the heavy field intermediate states is suppressed for $E \ll \Lambda_\chi$. Therefore an expansion of the effective couplings in terms of momenta would converge for $E \ll \Lambda_\chi$, in other words the \mathcal{L}_{eff} can be ordered as a momentum (or derivative) expansion with a cut-off Λ_χ .

The construction of effective field theories require an essential prerequisite to be satisfied, called “Weinberg’s theorem” [9]. It states that, “if one writes down the most general possible Lagrangian, including all terms consistent with assumed symmetry principles, and then calculates matrix elements with this Lagrangian to any given

order of perturbation theory, the result will simply be the most general possible S-matrix consistent with analyticity, perturbative unitarity, cluster decomposition and the assumed symmetry principles ". Although there are infinite number of possible terms with their free parameters in the effective Lagrangian, one has to have a proper criterion to select the appropriate number of terms to turn Weinberg's theorem into a practical mode. Therefore, a proper scheme, and a systematic method of assessing the importance of diagrams (generated by the couplings) allows us to organize all the terms in the Lagrangian. This is identified as the Weinberg's power counting scheme, and will be discussed with mesons in the next section.

7.4 Meson Chiral Perturbation Theory

The spontaneous breaking of chiral $SU(3)_L \times SU(3)_R$ symmetry into $SU(3)_V$ generates the members of the pseudo-scalar meson octet (pion (π), kaon (K), eta (η)) which are identified as the Goldstone bosons. Although the Goldstone bosons are theoretically massless, in the real world they acquire a mass due to the explicit symmetry breaking of the light quark masses. It is interesting to emphasize that, it is not fully understood theoretically yet why QCD should exhibit this spontaneous symmetry breaking phenomenon [82]. On the other hand, the experimental observation of the hadron spectrum accompanied by the non-vanishing singlet scalar quark condensate account for the spontaneous symmetry breaking in QCD.

As described in the previous chapter, QCD exhibits the $SU(3)_L \times SU(3)_R \times U(1)_V$ symmetry in the chiral limit. $U(1)_V$ symmetry reflects to the baryon number conservation and the classification of hadrons into baryons and mesons. The linear combinations $Q_V^a = Q_R^a + Q_L^a$ and $Q_A^a = Q_R^a - Q_L^a$ commute with the chirally symmetric part of the QCD Hamiltonian (H_{QCD}^0). If the symmetries of H_{QCD}^0 would also be symmetries of the vacuum state, there should be degenerate parity doublets. How-

ever the low energy baryon spectrum does not contain degenerate baryon octet with negative parity. For example, there is no evidence of the existence of two degenerate states for the nucleon with same spin but opposite parity. This observation leads to the assumption that the Q_A^a generator does not annihilate the QCD ground state, and the Q_V^a does. Therefore the two empirical facts,

- There is no left-right symmetry observed in the hadron spectrum. $SU(3)$ is the approximately realized symmetry of the hadrons,
- The masses of the pseudo-scalar mesons are small compare to the scale of the theory (eg : masses of vector mesons),

suggest that the spontaneous symmetry breaking happens in the chiral limit of QCD. It was shown in Witten *et al.* [87] that, the ground state is invariant under $SU(3)_V \times U(1)_V$. Also, Q_V^a satisfy the commutation relations in $SU(3)$ Lie algebra. Therefore the eight vector charge (octet) Q_V^a as well as the baryon number operator $Q_V/3$ (singlet) annihilate the QCD ground state

$$Q_V^a|0\rangle = Q_V|0\rangle = 0, \quad [Q_V^a, Q_V^b] = if^{abc}Q_V^c, \quad (7.49)$$

where as,

$$[Q_A^a, Q_A^b] = if^{abc}Q_V^c, \quad [Q_V^a, Q_A^b] = if^{abc}Q_A^c, \quad (7.50)$$

shows that Q_A^a operators do not form a closed algebra. Also it is very important to emphasize that the reason why one can assume Q_A^a do not annihilate the ground state,

$$Q_A^a|0\rangle \neq 0, \quad (7.51)$$

is because the parity-doubling is not observed for the lower lying baryon states in experiments. In other words, the QCD ground state is not invariant under “axial” transformations. For each generator Q_A^a , there exist an associated massless spin 0

Goldstone boson field $\phi^a(x)$ which transforms under parity,

$$\phi^a(\vec{x}, t) \xrightarrow{P} -\phi^a(-\vec{x}, t) \quad (7.52)$$

as pseudo-scalars, and leaves the vacuum invariant from the transformations under the sub group $SU(3)_V$

$$[Q_V^a, \phi^b(x)] = if^{abc} \phi^c(x) . \quad (7.53)$$

On the other hand, it is interesting to note the scalar and pseudo-scalar quark densities

$$\begin{aligned} S_a(x) &= \bar{\psi}(x) \lambda_a \psi(x) , \\ P_a(x) &= i \bar{\psi} \gamma_5 \lambda_a \psi(x) , \end{aligned} \quad (7.54)$$

have important commutation properties with the vector charge (octet) at equal-time,

$$Q_V^a(t) = \int d^3x \psi^\dagger(\vec{x}, t) \frac{\lambda_a}{2} \psi(\vec{x}, t) \quad (7.55)$$

namely [82],

$$[Q_V^a(t), A_0(x)] = 0 , \quad a = \{1, \dots, 8\} \quad (7.56)$$

and,

$$[Q_V^a(t), A_b(x)] = i \sum_{c=1}^8 f_{abc} A_c(x) , \quad a, b = \{1, \dots, 8\} \quad (7.57)$$

where $A_0 = \{S_0, P_0\}$ and $A_a = \{S_a, P_a\}$ with $a = \{1, \dots, 8\}$. Here, one has to use the properties $[\frac{\lambda_a}{2}, \gamma_0 \lambda_0] = 0$ and $[\frac{\lambda_a}{2}, \gamma_0 \lambda_b] = \gamma_0 i f_{abc} \lambda_c$. Therefore, one can re-write the octet components of scalar and pseudo-scalar quantities,

$$A_a(x) = -\frac{i}{3} \sum_{b,c=1}^8 f_{abc} [Q_V^b(t), A_c(x)] , \quad (7.58)$$

to observe that it has vanishing matrix elements with the ground state, in the chiral limit. Because in the chiral limit, the ground state is invariant under $SU(3)_V$

transformations, i.e $Q_V^a|0\rangle = 0$ leads to the condition,

$$\langle 0|A_a(x)|0\rangle \xrightarrow{\text{translation invariance}} \langle 0|A_a(0)|0\rangle \equiv \langle A_a\rangle = 0, \quad a = \{1, \dots, 8\}. \quad (7.59)$$

which leads one to obtain that the octet scalar quark condensate must vanish,

$$\begin{aligned} a = 3 & \rightarrow \langle \bar{u}u \rangle - \langle \bar{d}d \rangle = 0, \\ a = 8 & \rightarrow \langle \bar{u}u \rangle + \langle \bar{d}d \rangle - 2\langle \bar{s}s \rangle = 0, \end{aligned} \quad (7.60)$$

i.e. $\langle \bar{u}u \rangle = \langle \bar{d}d \rangle = \langle \bar{s}s \rangle$. But according to Eq. (7.56), the singlet scalar quark condensate is assumed to be non-vanishing.

$$\langle \bar{\psi}\psi \rangle = \langle \bar{u}u + \bar{d}d + \bar{s}s \rangle = 3\langle \bar{u}u \rangle = 3\langle \bar{d}d \rangle = 3\langle \bar{s}s \rangle \neq 0. \quad (7.61)$$

Therefore using the property $(i)^2 [\gamma_5 \frac{\lambda_a}{2}, \gamma_0 \gamma_5 \lambda_a] = \lambda_a^2 \gamma_0$, one can obtain,

$$i[Q_A^a(t), P_a(x)] = \begin{cases} \bar{u}u + \bar{d}d, & a = 1, 2, 3 \\ \bar{u}u + \bar{s}s, & a = 4, 5 \\ \bar{d}d + \bar{s}s, & a = 6, 7 \\ \frac{1}{3} (\bar{u}u + \bar{d}d + \bar{s}s), & a = 8 \end{cases}. \quad (7.62)$$

Applying the Eq. (7.62) for the ground state which is invariant under $SU(3)_V$ with including the assumption of non-vanishing singlet scalar quark condensate, one obtains

$$\langle 0|i[Q_A^a(t), P_a(x)]|0\rangle = \frac{2}{3}\langle \bar{\psi}\psi \rangle \quad a = \{1, \dots, 8\} \quad (7.63)$$

with the use of translational invariance property. Inserting a complete set of states into the Eq. (7.63) yields that both pseudo-scalar density $P_a(x)$ and axial charge operator Q_A^a have non-vanishing matrix elements between vacuum and massless one particle states [82]. Because of the Lorentz covariance, the matrix element of Q_A^a between the vacuum and the massless Goldstone boson states can be written as,

$$\langle 0|A_\mu^a(0)|\phi^b\rangle = ip_\mu F_0 \delta^{ab} \quad (7.64)$$

where F_0 ($\approx 93\text{MeV}$) is the “*decay constant*” of Goldstone bosons in the chiral limit with momentum p_μ . The assumption $Q_A^a|0\rangle$ requires a non-zero value for F_0 is necessary and sufficient condition for spontaneous symmetry breaking.

7.4.1 Construction of the effective Lagrangian

The standard application of effective field theory procedure to QCD which leads to Chiral perturbation theory (ChPT) is to start with the generating functional of vector currents, axial vector currents, scalar and pseudoscalar densities in the form [84, 88]

$$e^{i\mathcal{Z}[v,a,s,p,\theta]} = \langle 0_{out}|0_{in}\rangle = \int \mathcal{D}\Phi \, e^{i \int d^4x \, \mathcal{L}[v,a,s,p,\theta]} . \quad (7.65)$$

The Lagrangian in the presence of external fields reads:

$$\mathcal{L}[v, a, s, p, \theta] = \mathcal{L}_{\text{QCD}}^0 + \bar{\psi}\gamma_\mu(v^\mu + \gamma_5 a^\mu)\psi - \bar{\psi}(s - i\gamma_5 p)\psi - \frac{1}{16\pi^2}\theta\mathcal{G}_{\mu,\nu}^a\mathcal{G}_a^{\mu,\nu} ,$$

where, $s = \mathcal{M}$ quark mass matrix from Eq.(7.30). Note that, in the absence of anomalies (or $\theta = 0$), the Ward identities satisfied by the Green functions are equivalent to an invariance of the generating functional under a local transformation of external fields [89]. Thus the last term in the Lagrangian is neglected (or $\theta = 0$) through-out this work.

The reconstruction of the effective version of this generating functional in Eq. (7.65) requires the transformation properties of the Goldstone bosons, which will replace the quarks and gluons as the low-energy degrees of freedom. Conventionally, these Goldstone bosons are uniquely identified by 3×3 , unitary and uni-modular matrix-valued field,

$$U(x) = \exp\left(\frac{i}{F_0}\phi^a(x)\lambda_a\right) , \quad U(x)U(x)^\dagger = \mathbb{1} , \quad \det U(x) = 1 \quad (7.66)$$

which transforms non-linearly under chiral transformations;

$$U(x) \rightarrow RU(x)L^\dagger, \quad (7.67)$$

where ϕ^a are Goldstone boson fields, F_0 is a free parameter in the theory (related to meson-decay constant), and λ_a are Gell-Mann matrices. Because the chiral $SU(N_f)_L \times SU(N_f)_R$ symmetry is spontaneously broken by the emergence of massless Goldstone bosons, the Lagrangian has to be written in terms of the generators of the broken $SU(N_f)_L \times SU(N_f)_R$ symmetry [80, 81]. For the case of $N_f = 2$, the generators are Pauli matrices and for the case of $N_f = 3$ they are Gell-Mann matrices. Therefore, the Goldstone boson fields can be written as a matrix valued function ϕ which is a product of generators and combinations of coefficients which can be identified with the physical mesons,

$$\phi = \phi^a(x)\lambda_a = \sqrt{2} \begin{pmatrix} \frac{1}{\sqrt{2}}\pi^0 + \frac{1}{\sqrt{6}}\eta & \pi^+ & K^+ \\ \pi^- & -\frac{1}{\sqrt{2}}\pi^0 + \frac{1}{\sqrt{6}}\eta & K^0 \\ K^- & \bar{K}^0 & -\frac{2}{\sqrt{6}}\eta \end{pmatrix}. \quad (7.68)$$

Also, the covariant derivative was introduced,

$$D_\mu U = \partial_\mu U - i[v_\mu, U] - i\{a_\mu, U\} \quad (7.69)$$

because the chiral invariance only permits the occurrence of vector and axial vector sources in the covariant derivatives and field strength tensors in order to preserve the correct transformation properties of the effective Lagrangian under the chiral symmetry group (here, U represents the $U(x)$). Therefore, the most general “*chiral*” effective Lagrangian can be written as [90],

$$\mathcal{L}_{\text{eff}} = \mathcal{L}_{\text{eff}}(U, \partial U, \partial^2 U, \dots) \quad (7.70)$$

in terms of the Goldstone boson fields. The most important fact is, this effective Lagrangian has the same symmetries as in QCD : C, P, T , Lorentz invariance and chiral $SU(3)_L \times SU(3)_R$ symmetry. This chiral Lagrangian can be expanded in “*chiral powers*” (number of derivatives acting on Goldstone boson fields), and the chiral power counting of the Lagrangian,

$$\mathcal{L}_{\text{eff}} = \mathcal{L}_{\text{eff}}^{(0)} + \mathcal{L}_{\text{eff}}^{(2)} + \mathcal{L}_{\text{eff}}^{(4)} + \cdots \quad (7.71)$$

contains only “*even*” powers, because the Lorentz invariance permits terms with only even number of derivatives.

7.4.2 The lowest-order effective Lagrangian

At *zeroth* chiral order the chiral $SU(3)_L \times SU(3)_R$ invariance implies that, $\mathcal{L}_{\text{eff}}^{(0)}$ can only be a function of $UU^\dagger = \mathbb{1}$, contributing to a constant term in the effective Lagrangian which can be dropped.

At second order, there are two possible chiral invariant terms with two derivatives; $\langle \partial_\mu U^\dagger \partial^\mu U \rangle$ and $\langle U^\dagger \partial^\mu \partial_\mu U \rangle$, where $\langle \cdots \rangle$ is the trace in flavor space. These can be reduced to a single term because [82],

$$\langle U^\dagger \partial^\mu \partial_\mu U \rangle = \partial^\mu \langle \partial_\mu U^\dagger U \rangle - \langle \partial_\mu U^\dagger \partial^\mu U \rangle, \quad \langle \partial_\mu U^\dagger U \rangle = 0. \quad (7.72)$$

Therefore $\mathcal{L}_{\text{eff}}^{(2)}$ is,

$$\mathcal{L}_{\text{eff}}^{(2)} = c_1 \langle \partial_\mu U^\dagger \partial^\mu U \rangle \quad (7.73)$$

where the coupling constant c_1 is identified as a Low Energy Constant (LEC). It can be fixed to $F_0^2/4$ by expanding the Goldstone boson fields U ,

$$U = 1 + \frac{i}{F_0}\phi - \frac{1}{2F_0^2}\phi^2 + \mathcal{O}(\phi^3) , \quad (7.74)$$

with the trace property $\langle \lambda_a \lambda_b \rangle = 2\delta_{ab}$. This results in the standard kinetic term of the Lagrangian,

$$\mathcal{L}_{\text{eff}}^{(2)} = \frac{1}{2}\partial_\mu \phi^a \partial^\mu \phi^a + \mathcal{O}(\phi^4) . \quad (7.75)$$

Because the terms of zeroth chiral order have been dropped, the second chiral order is effectively the leading (lowest) order (LO) Lagrangian,

$$\mathcal{L}_{\text{eff}}^{(2)} = \frac{F_0^2}{4} \langle \partial_\mu U^\dagger \partial^\mu U \rangle . \quad (7.76)$$

Therefore at the leading-chiral-order, F_0 is the only LEC appears in $\mathcal{L}_{\text{eff}}^{(2)}$ (in the chiral limit). The interpretation of this F_0 can be directly visualized by considering the Noether axial current ($J_A^{\mu,a}$) of chiral symmetry for $\mathcal{L}_{\text{eff}}^{(2)}$. One can obtain the $J_L^{\mu,a}$ and $J_R^{\mu,a}$ by using the variation $\delta\mathcal{L}_{\text{eff}}^{(2)}$ under the chiral $SU(3)_L \times SU(3)_R$ transformations,

$$L = \exp\left(-i\Theta_L^a \frac{\lambda_a}{2}\right) , \quad R = \exp\left(-i\Theta_R^a \frac{\lambda_a}{2}\right) , \quad (7.77)$$

by using the property,

$$J_{L/R}^{\mu,a} = \frac{\partial\left(\delta\mathcal{L}_{\text{eff}}^{(2)}\right)}{\partial\partial_\mu\Theta_{L/R}^a} . \quad (7.78)$$

Then, the linear combinations of $J_L^{\mu,a}$ and $J_R^{\mu,a}$ yield [82],

$$J_V^{\mu,a} = J_R^{\mu,a} + J_L^{\mu,a} = -i\frac{F_0^2}{4}\langle \lambda_a [U, \partial^\mu U^\dagger] \rangle , \quad (7.79)$$

$$J_A^{\mu,a} = J_R^{\mu,a} - J_L^{\mu,a} = -i\frac{F_0^2}{4}\langle \lambda_a \{U, \partial^\mu U^\dagger\} \rangle . \quad (7.80)$$

Applying the expanded form of U matrices gives,

$$J_A^{\mu,a} = -i \frac{F_0^2}{4} \left\langle \lambda_a \left\{ 1 + \dots, -i \frac{\lambda_b \partial^\mu \phi_b}{F_0} + \dots \right\} \right\rangle = -F_0 \partial^\mu \phi_a \quad (7.81)$$

which reveals that the non-vanishing matrix element when $J_A^{\mu,a}(x)$ between the vacuum and a Goldstone boson state,

$$\begin{aligned} \langle 0 | J_A^{\mu,a}(x) | \phi_b(p) \rangle &= \langle 0 | -F_0 \partial^\mu \phi_a(x) | \phi_b(p) \rangle = -F_0 \partial^\mu e^{-ip \cdot x} \delta_{ab} \\ &= ip^\mu F_0 e^{-ip \cdot x} \delta_{ab} \end{aligned} \quad (7.82)$$

leads to interpret F_0 as the Goldstone boson decay constant in the chiral limit.

7.4.3 Explicit symmetry breaking due to quark mass

The discussion up to this point assumed the chiral limit ($m_u = m_d = m_s = 0$) where the chiral symmetry is exact, therefore $\mathcal{L}_{\text{eff}}^{(2)}$ doesn't contain a mass term, and describes the dynamics of the massless Goldstone bosons. In nature, the quark masses are non-zero (but small), which leads to an explicit chiral symmetry breaking. Therefore, one has to introduce a symmetry breaking term to the existing $\mathcal{L}_{\text{eff}}^{(2)}$ in order to account for the explicit symmetry breaking. Consider the mass term \mathcal{L}_M (see Eq. (7.31)) in the QCD Lagrangian, which breaks the chiral symmetry,

$$\mathcal{L}_M = -\bar{\psi} \mathcal{M} \psi = -(\bar{\psi}_R \mathcal{M} \psi_L + \bar{\psi}_L \mathcal{M}^\dagger \psi_R) . \quad (7.83)$$

It is important to notice that the \mathcal{M} transform as,

$$\mathcal{M} \rightarrow \mathcal{M}' = L \mathcal{M} R^\dagger \quad (7.84)$$

under the chiral transformations and leaves \mathcal{L}_M invariant. Therefore, one can introduce an external scalar field (s) in the effective Lagrangian $\mathcal{L}_{\text{eff}}^{(2)}$ which transforms as,

$$s \rightarrow LsR^\dagger \quad (7.85)$$

under chiral transformations which leave the $\mathcal{L}_{\text{eff}}^{(2)}$ invariant. Therefore at leading chiral order ($\mathcal{O}(p^2)$) the $\mathcal{L}_{\text{eff}}^{(2)}$ gets the form,

$$\begin{aligned} \mathcal{L}_{\text{eff}}^{(2)} &= \frac{F_0^2}{4} \langle \partial_\mu U^\dagger \partial^\mu U \rangle + \frac{F_0^2}{2} B_0 \langle sU^\dagger + s^\dagger U \rangle \\ &= \frac{F_0^2}{4} \langle \partial_\mu U^\dagger \partial^\mu U \rangle + \frac{F_0^2}{2} B_0 \langle \mathcal{M} (U^\dagger + U) \rangle \end{aligned} \quad (7.86)$$

where, $s = \mathcal{M} = \mathcal{M}^\dagger$, and B_0 is an additional constant associated with the explicit chiral symmetry breaking. Let's consider expanding the second term of $\mathcal{L}_{\text{eff}}^{(2)}$ in Eq. (7.86), which can be labeled as $\mathcal{L}_{\text{eff-sb}}^{(2)}$ (sb - symmetry breaking),

$$\mathcal{L}_{\text{eff-sb}}^{(2)} = \frac{F_0^2}{2} B_0 \langle \mathcal{M} (U^\dagger + U) \rangle = B_0 F_0^2 (m_u + m_d + m_s) - \frac{1}{2} B_0 \langle \mathcal{M} \phi^2 \rangle + \mathcal{O}(\phi^4) .$$

The first term of $\mathcal{L}_{\text{eff-sb}}^{(2)}$ is related to the vacuum expectation values of the scalar quark densities [90],

$$\langle 0 | \bar{q}q | 0 \rangle = \langle 0 | \frac{\partial \mathcal{H}_{\text{QCD}}}{\partial m_q} | 0 \rangle = - \langle 0 | \frac{\partial \mathcal{L}_{\text{eff}}^{(2)}}{\partial m_q} | 0 \rangle = -B_0 F_0^2 + \mathcal{O}(m_q) , \quad (7.87)$$

which yields,

$$\langle 0 | \bar{u}u | 0 \rangle = \langle 0 | \bar{d}d | 0 \rangle = \langle 0 | \bar{s}s | 0 \rangle = -B_0 F_0^2 \quad (7.88)$$

at the leading order, where the quark condensates are degenerate in the chiral limit.

The second term of $\mathcal{L}_{\text{eff-sb}}^{(2)}$ can be expanded using Eq. (7.68),

$$\begin{aligned}
-\frac{B_0}{2}\langle\mathcal{M}\phi^2\rangle &= -B_0(m_u+m_d)\pi^+\pi^- - B_0(m_u+m_s)K^+K^- - B_0(m_d+m_s)K^0\bar{K}^0 \\
&\quad -\frac{B_0}{2}(m_u+m_d)\pi^0\pi^0 - \frac{B_0}{\sqrt{3}}(m_u-m_d)\pi^0\eta - \frac{B}{2}\left(\frac{m_u+m_d+m_s}{3}\right)\eta^2,
\end{aligned} \tag{7.89}$$

therefore one can write down the expression for the Goldstone bosons, to the lowest order in the quark masses,

$$\begin{aligned}
M_\pi^2 &= 2B_0\hat{m} \\
M_K^2 &= B_0(\hat{m}+m_s) \\
M_\eta^2 &= \frac{2}{3}B_0(\hat{m}+2m_s)
\end{aligned} \tag{7.90}$$

where $\hat{m} = (\frac{m_u+m_d}{2})$, and neglecting the π^0 - η mixing since it has smaller effects which will vanish in the iso-spin limit ($m_u = m_d$). These expressions for the Goldstone boson (GB) masses in Eq. (7.90) comparing with the Gell-Mann-Oakes-Renner relation [91],

$$M_\pi^2 = (m_u+m_d)\left|\frac{\langle 0|\bar{u}u|0\rangle}{F_0^2}\right| + \mathcal{O}(\hat{m}^2) \tag{7.91}$$

infer that the $s = \mathcal{O}(p^2)$ since the mass of Goldstone boson $\approx B_0 m_q$. Moreover, the Eq. (7.90) can be used to deduce the Gell-Mann-Okubo mass formula for mesons,

$$3M_\eta^2 = 4M_K^2 - M_\pi^2 \tag{7.92}$$

in the iso-spin limit. Another important thing to notice is that the absolute values of the quark masses cannot be extracted since they depend on the QCD renormalization scale, but the quark mass ratios are independent of the scale. Therefore, extracting the light quark mass ratios from phenomenology is one important goal of chiral perturbation theory,

$$\begin{aligned}
\frac{M_K^2}{M_\pi^2} &= \frac{\hat{m} + m_s}{2\hat{m}} \\
\frac{M_\eta^2}{M_\pi^2} &= \frac{\hat{m} + 2m_s}{3\hat{m}}
\end{aligned} \tag{7.93}$$

Following the convention introduced by Gasser and Leutwyler, scalar and pseudo-scalar (see Eq. (7.35)) are combined linearly to define,

$$\chi = 2B_0 (s + ip) , \tag{7.94}$$

where, B_0 is the QCD order parameter in Eq. (7.88), and χ is of $\mathcal{O}(p^2)$. Although, in principle $\langle \chi U^\dagger \pm U \chi^\dagger \rangle$ provide Lorentz invariant quantities, but the term with minus sign has the wrong behavior under parity. Therefore, the most general, locally invariant lowest order “*chiral*” effective Lagrangian reads [82]:

$$\mathcal{L}_{\text{eff}}^{(2)} = \frac{F_0^2}{4} \langle \partial_\mu U^\dagger \partial^\mu U \rangle + \frac{F_0^2}{4} \langle \chi U^\dagger + U \chi^\dagger \rangle . \tag{7.95}$$

7.4.4 Higher order effective Lagrangians

So far, the construction of the leading/lowest order $\mathcal{O}(p^2)$ chiral Lagrangian $\mathcal{L}_{\text{eff}}^{(2)}$ has been outlined. The importance of higher order terms $\mathcal{L}_{\text{eff}}^{(4)}, \mathcal{L}_{\text{eff}}^{(6)}, \dots$ comes into account in order to make higher precision predictions in the perturbative chiral expansion. Note that the Goldstone boson momenta (associated with the derivative terms of Goldstone boson fields) are of $\mathcal{O}(p)$, and quark masses are of $\mathcal{O}(p^2)$ establish the chiral power counting of tree level interaction terms at each chiral order. In addition to the tree-level power counting, one needs a proper power counting scheme for loop diagrams when the calculation incorporates with higher chiral orders. For example, at next-to-leading-order (NLO) in chiral expansion, in addition to the tree level terms of $\mathcal{L}_{\text{eff}}^{(4)}$, one needs the tree level terms from $\mathcal{L}_{\text{eff}}^{(2)}$ and the loop diagrams

with the vertices from $\mathcal{L}_{\text{eff}}^{(2)}$.

Weinberg introduced a scheme¹ [9] to determine the chiral dimension D in order to facilitate the power counting of diagrams. If N_L is the number of loops, and N_n is the number of vertices formed from interactions with n derivatives, then

$$D = 2 + 2N_L + \sum_n N_n(n - 2) \quad (7.96)$$

represents the correlation between D , N_L and N_n , where $n = \{2, 4, 6, \dots(\text{even numbers})\}$ (more details on the derivation of this formula can be found in references [9, 82]). Let's consider $\pi\pi$ scattering process to understand the behavior of this formula in Eq. (7.96).

- At lowest chiral order $\mathcal{O}(p^2)$: $D = 2 \rightarrow N_n = 0 \rightarrow$ only tree level graphs contribute.
- At $\mathcal{O}(p^4)$ there are two possibilities with $D = 4 \rightarrow N_L + N_4 = 1$:
 - (i) One-loop graphs composed only of lowest-order $\mathcal{L}_{\text{eff}}^{(2)}$ vertices ($N_4 = 0$, $N_L = 1$)
 - (ii) Tree-graphs with only $\mathcal{L}_{\text{eff}}^{(4)}$ vertices ($N_4 = 1$, $N_L = 0$)
- At $\mathcal{O}(p^6)$ there are four possibilities with $D = 6 \rightarrow N_L + N_4 + 2N_6 = 2$:
 - (i) Tree-graphs with only $\mathcal{L}_{\text{eff}}^{(6)}$ vertices ($N_L = 0$, $N_4 = 0$, $N_6 = 1$)
 - (ii) Tree-graphs with two $\mathcal{L}_{\text{eff}}^{(4)}$ vertices ($N_L = 0$, $N_4 = 2$, $N_6 = 0$)
 - (iii) Graphs composed of one tree-level $\mathcal{L}_{\text{eff}}^{(4)}$ vertex with one-loop with $\mathcal{L}_{\text{eff}}^{(2)}$ vertices ($N_L = 1$, $N_4 = 1$, $N_6 = 0$)
 - (iv) Graphs composed of two-loops with $\mathcal{L}_{\text{eff}}^{(2)}$ vertices ($N_L = 2$, $N_4 = 0$, $N_6 = 0$)

¹A linear rescaling of external momenta and quadratic rescaling of quark masses.

7.4.5 The chiral effective Lagrangian at order $\mathcal{O}(p^4)$

The most general chiral Lagrangian at $\mathcal{O}(p^4)$ has been constructed by Gasser and Leutwyler in [88] by considering the procedure of respecting the relevant symmetries of QCD, and letting the one-loop divergence to be absorbed into the low energy constants (LECs) by an appropriate renormalization. The result is,

$$\begin{aligned}
\mathcal{L}_{\text{eff}}^{(4)} = & L_1 \langle D_\mu U^\dagger D^\mu U \rangle^2 + L_2 \langle D_\mu U^\dagger D_\nu U \rangle \langle D^\mu U^\dagger D^\nu U \rangle + L_3 \langle D_\mu U^\dagger D^\mu U D_\nu U^\dagger D^\nu U \rangle \\
& + L_4 \langle D_\mu U^\dagger D^\mu U \rangle \langle \chi U^\dagger + U \chi^\dagger \rangle + L_5 \langle D_\mu U^\dagger D^\mu U (\chi^\dagger U + U^\dagger \chi) \rangle \\
& + L_6 \langle \chi U^\dagger + U \chi^\dagger \rangle^2 + L_7 \langle \chi U^\dagger - U \chi^\dagger \rangle^2 + L_8 \langle \chi U^\dagger \chi U^\dagger + U \chi^\dagger U \chi^\dagger \rangle \\
& - i L_9 \langle F_{\mu\nu}^R D_\mu U^\dagger D_\nu U + F_{\mu\nu}^L D_\mu U D_\nu U^\dagger \rangle + L_{10} \langle U^\dagger F_{\mu\nu}^R U F_L^{\mu\nu} \rangle \\
& + H_1 \langle F_{\mu\nu}^R F_R^{\mu\nu} + F_{\mu\nu}^L F_L^{\mu\nu} \rangle + H_2 \langle \chi^\dagger \chi \rangle
\end{aligned} \tag{7.97}$$

with the renormalized LECs L_i^r and H_i^r defined as,

$$L_i = L_i^r + \Gamma_i R, \quad i = 1, \dots, 10, \tag{7.98}$$

$$H_i = H_i^r + \Delta_i R, \quad i = 1, 2 \tag{7.99}$$

$$R = \frac{\mu^{d-4}}{(4\pi)^2} \left\{ \frac{1}{d-4} - \frac{1}{2} (\ln(4\pi) + \gamma_E + 1) \right\} \tag{7.100}$$

where the renormalized LECs L_i^r (empirical values) at the scale $\mu = m_\rho$, and Γ_i values are given in the Table (7.1).

Table 7.1. Renormalized LECs L_i^r (empirical values) at the scale $\mu = m_\rho$ [82].

i	Empirical value (L_i^r)	Γ_i
1	0.4 ± 0.3	$\frac{3}{32}$
2	1.35 ± 0.3	$\frac{3}{16}$
3	-3.5 ± 1.1	0
4	-0.3 ± 0.5	$\frac{1}{8}$
5	1.4 ± 0.5	$\frac{3}{8}$
6	-0.2 ± 0.3	$\frac{11}{144}$
7	-0.4 ± 0.2	0
8	0.9 ± 0.3	$\frac{5}{48}$
9	6.9 ± 0.7	$\frac{1}{4}$
10	-5.5 ± 0.7	$-\frac{1}{4}$

In Eq. (7.97) the term $\chi = 2B_0(s + ip)$ contains the scalar and pseudo-scalar sources, whereas the vector and axial-vector currents enter through,

$$\begin{aligned} F_R^{\mu\nu} &= \partial^\mu r^\nu - \partial^\nu r^\mu - i[r^\mu, r^\nu] \\ F_L^{\mu\nu} &= \partial^\mu l^\nu - \partial^\nu l^\mu - i[l^\mu, l^\nu] \end{aligned} \quad (7.101)$$

where $r_\mu = v_\mu + a_\mu$ and $l_\mu = v_\mu - a_\mu$. Considering the individual terms of $\mathcal{L}_{\text{eff}}^{(4)}$ in Eq. (7.97) one can identify their interaction structure. For example, L_{1-3} terms contain four derivatives, $L_{4,5}$ contain two derivatives and one quark mass term, L_{6-8} contain squared quark mass terms, and $L_{9,10}$ contribute to observables with external vector and axial vector sources.

7.4.6 Application : Goldstone boson masses to $\mathcal{O}(p^4)$

As an example for a higher order calculation, one can consider calculating the meson mass at $\mathcal{O}(p^4)$. At this order, the loop diagrams with $\mathcal{L}_{\text{eff}}^{(2)}$ vertices, and contact diagrams with $\mathcal{L}_{\text{eff}}^{(4)}$ contribute to so called “self-energy”. The necessary diagrams are

shown in Fig. (7.1) (free propagator, tad-pole, tree level $\mathcal{O}(p^4)$). Therefore, expanding the U fields in $\mathcal{L}_{\text{eff}}^{(2)}$ yields,

$$\begin{aligned}\mathcal{L}_{\text{eff}}^{(2)} &= \frac{F_0^2}{4} \langle \partial_\mu U^\dagger \partial^\mu U \rangle + \frac{F_0^2}{2} B_0 \langle \mathcal{M} (U^\dagger + U) \rangle \\ &= \frac{1}{4} \langle \partial_\mu \phi \partial^\mu \phi \rangle - \frac{B_0}{2} \langle \mathcal{M} \phi^2 \rangle + \frac{1}{48 F_0^2} \langle [\partial_\mu \phi, \phi] [\partial^\mu \phi, \phi] \rangle + \frac{B_0}{24 F_0^2} \langle \mathcal{M} \phi^4 \rangle + \dots\end{aligned}\quad (7.102)$$

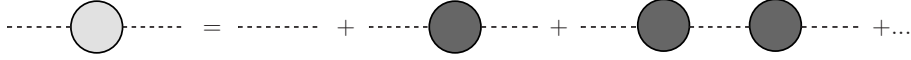


Figure 7.1. Unrenormalized meson propagator (light-gray color) as a sum of irreducible self-energy diagrams (dark-gray color).

The 3rd term of Eq. (7.102) result in either p^2 or M_{GB}^2 depending on whether the ϕ or the $\partial_\mu \phi$ are contracted, and the 4th term does not generate a momentum dependence.

In order to determine the masses, one needs to calculate the self-energies $\Sigma(p^2)$ of the Goldstone bosons. The propagator of a scalar/ pseudo-scalar fields is defined as,

$$\begin{aligned}i\Delta(p) &= \int d^4x e^{-ip \cdot x} \langle 0 | T[\phi_0(x) \phi_0(0)] | 0 \rangle \\ &= \frac{i}{p^2 - M_0^2 + i\epsilon},\end{aligned}\quad (7.103)$$

where ϕ_0 are un-renormalized bare Goldstone boson fields, and M_0 (lowest order masses) are given in Eq. (7.90) with assuming iso-spin symmetry $m_u = m_d = m$,

$$\begin{aligned}M_{\pi,0}^2 &= 2B_0 m, \\ M_{K,0}^2 &= B_0(m + m_s), \\ M_{\eta,0}^2 &= \frac{2}{3}B_0(m + 2m_s).\end{aligned}\quad (7.104)$$

The loop diagrams with $\mathcal{L}_{\text{eff}}^{(2)}$ and the contact diagrams with $\mathcal{L}_{\text{eff}}^{(4)}$ result in so called proper self-energy insertions $-i\Sigma(p^2)$ [82], which may represent a sum of a series of diagrams as in Fig. (7.1). Thus the propagator becomes,

$$\begin{aligned}
i\Delta(p) &= \frac{i}{p^2 - M_0^2 + i\epsilon} + \frac{i}{p^2 - M_0^2 + i\epsilon} [-\Sigma(p^2)] \frac{i}{p^2 - M_0^2 + i\epsilon} + \dots \\
&= \frac{i}{p^2 - M_0^2 - \Sigma(p^2) + i\epsilon} .
\end{aligned} \tag{7.105}$$

Assuming that the $\Sigma(p^2)$ is expanded around $p^2 = \lambda^2$,

$$\Sigma(p^2) = \Sigma(\lambda^2) + (p^2 - \lambda^2)\Sigma'(\lambda^2) + \tilde{\Sigma}(p^2) , \tag{7.106}$$

then at $\lambda^2 = M^2$ the propagator can be re-written as,

$$i\Delta(p) = \frac{iZ_\phi}{p^2 - M^2 - Z_\phi\tilde{\Sigma}(p^2) + i\epsilon} \tag{7.107}$$

where,

$$Z_\phi = \frac{1}{1 - \Sigma'(M^2)} \tag{7.108}$$

is the wave function renormalization constant. With the renormalized fields $\phi_R = \phi_0/\sqrt{Z_\phi}$, the physical mass M can be identified as the pole position of the renormalized propagator,

$$M^2 = M_0^2 + \Sigma(M^2) . \tag{7.109}$$

The calculation of the one-loop (tad-pole) diagram involves the loop-integration,

$$I(M^2, \mu) = \mu^{4-d} \int \frac{d^d k}{(2\pi)^d} \frac{i}{k^2 - M^2 + i\epsilon} . \tag{7.110}$$

This loop integral is quadratically ultraviolet divergent. Therefore, a regularization scheme is necessary which maintains the symmetries of the theory, in particular chiral symmetry. “Dimensional regularization” provides a convenient mass-independent regularization scheme, which also preserves the symmetries. Therefore according the dimensional regularization method, the integration yields,

$$\begin{aligned}
I(M^2, \mu) &= \mu^{4-d} \int \frac{d^d k}{(2\pi)^d} \frac{i}{k^2 - M^2 + i\epsilon} \\
&= \frac{M^2}{(4\pi)^{d/2}} \left(\frac{M}{\mu} \right)^{d-4} \Gamma \left(1 - \frac{d}{2} \right)
\end{aligned} \tag{7.111}$$

for arbitrary space-time dimension d . Expanding this result in $4 - d$ gives,

$$I(M^2, \mu) = M^2 \left\{ 2R + \frac{1}{(4\pi)^2} \ln \left(\frac{M^2}{\mu^2} \right) \right\} + \mathcal{O}(d - 4) , \tag{7.112}$$

where R absorbs the ultraviolet divergence and the scale dependence in order to renormalize the LECs of $\mathcal{L}_{\text{eff}}^{(4)}$, as given in Eq. (7.98). The LECs L_9, L_{10}, H_1 , and H_2 does not contribute since this calculation is done assuming there are no external fields. Also, L_1, L_2, L_3 does not contribute since they are of $\mathcal{O}(\phi^4)$. Therefore, only the L_4, L_5, L_6 , and L_8 terms contribute. Therefore the tree level contributions with either two derivatives or no derivatives can be generalized as [82],

$$\begin{aligned}
\mathcal{L}_{\text{eff}(2\phi)}^{(4)} &= \frac{1}{2} (a_\pi \partial_\mu \pi^0 \partial^\mu \pi^0 - b_\pi \pi^0 \pi^0) + a_\pi \partial_\mu \pi^+ \partial^\mu \pi^- - b_\pi \pi^+ \pi^- + a_K \partial_\mu K^+ \partial^\mu K^- \\
&\quad - b_K K^+ K^- + a_K \partial_\mu K^0 \partial^\mu \bar{K}^0 - b_K K^0 \bar{K}^0 + \frac{1}{2} (a_\eta \partial_\mu \eta \partial^\mu \eta - b_\eta \eta \eta)
\end{aligned} \tag{7.113}$$

where, the constants a_ϕ and b_ϕ ($\phi = \{\pi, K, \eta\}$) can be given by,

$$\begin{aligned}
a_\pi &= \frac{16B_0}{F_0^2} [(2m + m_s)L_4 + mL_5] , \\
b_\pi &= \frac{64B_0^2}{F_0^2} [(2m + m_s)mL_6 + m^2L_8] , \\
a_K &= \frac{16B_0}{F_0^2} \left[(2m + m_s)L_4 + \frac{1}{2}(m + m_s)L_5 \right] , \\
b_K &= \frac{32B_0^2}{F_0^2} \left[(2m + m_s)(m + m_s)L_6 + \frac{1}{2}(m + m_s)^2 L_8 \right] , \\
a_\eta &= \frac{16B_0}{F_0^2} \left[(2m + m_s)L_4 + \frac{1}{3}(m + 2m_s)L_5 \right] , \\
b_\eta &= \frac{64B_0^2}{3F_0^2} [(2m + m_s)(m + 2m_s)L_6 + 2(m - m_s)^2 L_7 + (m^2 + 2m_s^2)L_8] .
\end{aligned} \tag{7.114}$$

At $\mathcal{O}(p^4)$ the self-energy for a given Goldstone boson has the form,

$$\Sigma_\phi(p^2) = A_\phi p^2 + B_\phi . \quad (7.115)$$

where, the constants A_ϕ, B_ϕ contains the tree-level contribution from $\mathcal{L}_{\text{eff}}^{(4)}$ and one-loop (tad pole) contribution with a vertex from $\mathcal{L}_{\text{eff}}^{(2)}$ (see Figure Kubis fig 5). In addition to the loop integral in Eq. (7.111), one needs

$$\mu^{4-d} i \int \frac{d^d k}{(2\pi)^d} \frac{k^2}{k^2 - M^2 + i\epsilon} = M^2 I(M^2, \mu) \quad (7.116)$$

because of there are vertex contributions from of $\mathcal{L}_{\text{eff}}^{(2)}$ proportional to two derivatives. It is equal to $M^2 I(M^2, \mu)$ since $\mu^{4-d} \int \frac{d^d k}{(2\pi)^d} = 0$ in dimensional regularization.

After analyzing all possible loop contributions for the case of $SU(3)_{\text{flavor}}$, the constants A_ϕ and B_ϕ can be given in terms of the LECs of $\mathcal{L}_{\text{eff}}^{(2)}$ and $\mathcal{L}_{\text{eff}}^{(4)}$ as in Ref. [82],

$$\begin{aligned} A_\pi &= \frac{1}{3F_0^2} \left\{ 2 I(M_\pi^2, \mu) + I(M_K^2, \mu) - 48B_0 [(2m + m_s)L_4 + mL_5] \right\} , \\ B_\pi &= \frac{M_\pi^2}{F_0^2} \left\{ -\frac{1}{6} I(M_\pi^2, \mu) - \frac{1}{6} I(M_\eta^2, \mu) - \frac{1}{3} I(M_K^2, \mu) \right\} , \\ A_K &= \frac{1}{4F_0^2} \left\{ I(M_\pi^2, \mu) + I(M_\eta^2, \mu) - 2 I(M_K^2, \mu) \right. \\ &\quad \left. - 64B_0 \left[(2m + m_s)L_4 + \frac{1}{2}(m + m_s)L_5 \right] \right\} , \\ B_K &= \frac{M_\pi^2}{F_0^2} \left\{ \frac{1}{12} I(M_\eta^2, \mu) - \frac{1}{4} I(M_\pi^2, \mu) - \frac{1}{2} I(M_K^2, \mu) \right. \\ &\quad \left. + 32B_0 \left[(2m + m_s)L_6 + \frac{1}{2}(m + m_s)L_8 \right] \right\} , \\ A_\eta &= \frac{1}{F_0^2} \left\{ I(M_K^2, \mu) - 8B_0 [2(2m + m_s)L_4 + M_\eta^2 L_5] \right\} , \\ B_\eta &= \frac{1}{6F_0^2} \left\{ (M_\pi^2 - 4M_\eta^2) I(M_\eta^2, \mu) + M_\pi^2 (2 I(M_K^2, \mu) - 3 I(M_\pi^2, \mu)) \right. \\ &\quad \left. + \frac{8M_\eta^2}{3} (M_\eta^2 L_8 + 2(2m + m_s)B_0 L_6) + \frac{64}{27} B_0^2 (m - m_s)^2 (3L_7 + L_8) \right\} , \end{aligned} \quad (7.117)$$

Since the integrals $I(M_\phi^2, \mu)$ as well as the bare LECs contain $1/(d-4)$ poles (divergent when $d \rightarrow 4$), then the cancellations between those ultraviolet divergences (infinities) result in leaving only the finite pieces with the renormalized LECs. According to the equations Eq. (7.109) & Eq. (7.115), the masses of a Goldstone boson at $\mathcal{O}(p^4)$ can be written as,

$$\begin{aligned} M_\phi^2 &= M_{\phi,0}^2 + A_\phi M_\phi^2 + B_\phi \\ &= \frac{M_{\phi,0}^2 + B_\phi}{1 - A_\phi} = M_{\phi,0}^2(1 + A_\phi) + B_\phi + \mathcal{O}(p^6) \end{aligned} \quad (7.118)$$

where $M_{\phi,0}^2$ denotes the lowest order squared mass of Goldstone boson $\phi = \{\pi, K, \eta\}$ given in Eq. (7.104), and note that $A_\phi = \mathcal{O}(p^4)$ and $\{B_\phi, M_{\phi,0}^2\} = \mathcal{O}(p^2)$.

Therefore the finite Goldstone masses at $\mathcal{O}(p^4)$ can be written as in Ref. [82],

$$\begin{aligned} M_{\pi,4}^2 &= M_{\pi,2}^2 \left\{ 1 + \frac{M_{\pi,2}^2}{32\pi^2 F_0^2} \ln \left(\frac{M_{\pi,2}^2}{\mu^2} \right) - \frac{M_{\eta,2}^2}{96\pi^2 F_0^2} \ln \left(\frac{M_{\eta,2}^2}{\mu^2} \right) \right. \\ &\quad \left. \frac{16}{F_0^2} [(2m + m_s)B_0(2L_6^r - L_4^r) + mB_0(2L_8^r - L_5^r)] \right\}, \\ M_{K,4}^2 &= M_{K,2}^2 \left\{ 1 + \frac{M_{\eta,2}^2}{48\pi^2 F_0^2} \ln \left(\frac{M_{\eta,2}^2}{\mu^2} \right) \right. \\ &\quad \left. \frac{16}{F_0^2} \left[(2m + m_s)B_0(2L_6^r - L_4^r) + \frac{1}{2}(m + m_s)B_0(2L_8^r - L_5^r) \right] \right\}, \\ M_{\eta,4}^2 &= M_{\eta,2}^2 \left\{ 1 + \frac{M_{K,2}^2}{16\pi^2 F_0^2} \ln \left(\frac{M_{K,2}^2}{\mu^2} \right) - \frac{M_{\eta,2}^2}{24\pi^2 F_0^2} \ln \left(\frac{M_{\eta,2}^2}{\mu^2} \right) \right. \\ &\quad \left. \frac{8}{F_0^2} [2(2m + m_s)B_0(2L_6^r - L_4^r) + M_{\eta,2}^2(2L_8^r - L_5^r)] \right\} \\ &\quad + M_{\pi,2}^2 \left\{ \frac{M_{\eta,2}^2}{96\pi^2 F_0^2} \ln \left(\frac{M_{\eta,2}^2}{\mu^2} \right) + \frac{M_{K,2}^2}{48\pi^2 F_0^2} \ln \left(\frac{M_{K,2}^2}{\mu^2} \right) - \frac{M_{\pi,2}^2}{32\pi^2 F_0^2} \ln \left(\frac{M_{\pi,2}^2}{\mu^2} \right) \right\} \\ &\quad + \frac{128}{9F_0^2} B_0^2 (m - m_s)^2 (3L_7^r - L_8^r), \end{aligned} \quad (7.119)$$

where the subscript 2 and 4 of $M_{\phi,2}^2$ and $M_{\phi,4}^2$ respectively indicate their chiral order. Notice that the $\mathcal{O}(p^4)$ Goldstone masses vanish in the chiral limit, which was also

expected from QCD in the chiral limit. Also note that the finite pieces of $M_{\phi,4}^2$ contain terms which are,

- analytic in quark masses ($\sim m_q^2 L_i^r$) which are proportional to L_i^r ,
- non-analytic in quark masses ($\sim m_q^2 \ln(m_q^2)$), which are so called “chiral logarithms”.

Moreover, one can deduce that the scale dependence of the LECs and the finite part of the loop integrals compensate each other, such that the squared Goldstone boson masses are scale independent.

7.5 Baryon Chiral Perturbation Theory

The previous sub-section was dedicated to the meson sector involving the interactions of Goldstone bosons. Therefore, this sub-section basically concentrates on the interactions of baryons with each other and with Goldstone bosons and other external fields. In particular, the interest is calculating matrix elements associated with a single baryon in the initial and final states, which can be used to describe static properties of baryons such as masses, magnetic moments, form-factors, and also low energy processes such as pion-nucleon scattering, Compton scattering, etc.

The time ordered baryon matrix elements of the quark currents are generated by the baryon-to-baryon transition amplitude in the presence of external fields [82, 85, 92],

$$\mathcal{F}(\vec{\mathbf{p}}', \vec{\mathbf{p}}, v, a, s, p) = \langle \vec{\mathbf{p}}'_{\text{out}} | \vec{\mathbf{p}}_{\text{in}} \rangle_{a,v,s,p}^{\text{connected}} \quad \vec{\mathbf{p}}' \neq \vec{\mathbf{p}} \quad (7.120)$$

determined by the Lagrangian of Eq. (7.66),

$$\mathcal{L}[v, a, s, p] = \mathcal{L}_{\text{QCD}}^0 + \bar{\psi} \gamma_\mu (v^\mu + \gamma_5 a^\mu) \psi - \bar{\psi} (s - i \gamma_5 p) \psi \quad (7.121)$$

in the presence of external fields, and in the absence of anomalies. The states $|\vec{\mathbf{p}}_{\text{in}}\rangle$ ($|\vec{\mathbf{p}}'_{\text{outn}}\rangle$) specify the incoming (outgoing) baryon state with momentum \mathbf{p} (\mathbf{p}'). The functional \mathcal{F} contains only the connected diagrams. The first step is constructing an effective Lagrangian for the interacting fields by specifying its transformation properties. In the case of meson-baryon interactions, one can directly recall the transformation properties of the Goldstone bosons fields U which were discussed in the previous subsection. It turns out it is more convenient to consider the square root of U -fields by defining,

$$u^2(x) = U(x) . \quad (7.122)$$

Since in general, U -field transforms under $SU(N_f)_R \times SU(N_f)_L$ as $U \rightarrow LUR^\dagger$, thus the u -field has to transform as,

$$u \rightarrow u' = \sqrt{LUR^\dagger} \equiv L u h^{-1}(L, R, U) = h(L, R, U) u L^{-1} \quad (7.123)$$

where, $h(L, R, U) \in SU(N_f)$ is the so-called compensator field which depends in a non-trivial way on L, R , and U ,

$$h(L, R, U) = u'^{-1} L u = \sqrt{LUR^\dagger}^{-1} L \sqrt{U} . \quad (7.124)$$

Since a general feature of transformation behavior under the sub-group $SU(N_f)_V$ leaves the ground state invariant, and independent of U , leads to have $L = R = V$, such that $u' = V u V^\dagger$. Therefore one can observe,

$$h^{-1}(V, V, U) = V^\dagger \quad \text{or} \quad h(V, V, U) = V . \quad (7.125)$$

This linear transformation property under the sub-group $SU(N_f)_V$ of $SU(N_f)_L \times SU(N_f)_R$ can be directly used for the baryon fields.

Therefore, for the particular case $N_f = 3$, let's consider a matrix valued field \mathcal{B} which contains the ground state octet baryons where each element is associated with a space-time (x) dependent, complex, four-component Dirac field:

$$\mathcal{B} = \sum_{a=1}^8 \lambda_a B_a = \begin{pmatrix} \frac{1}{\sqrt{2}}\Sigma^0 + \frac{1}{\sqrt{6}}\Lambda & \Sigma^+ & P \\ \Sigma^- & -\frac{1}{\sqrt{2}}\Sigma^0 + \frac{1}{\sqrt{6}}\Lambda & N \\ \Xi^- & \Xi^0 & -\frac{2}{\sqrt{6}}\Lambda \end{pmatrix}. \quad (7.126)$$

where the matrix \mathcal{B} is traceless but not real (Hermitian), i.e., $\mathcal{B} \neq \mathcal{B}^\dagger$, and transforms non-linearly under $SU(3)_L \times SU(3)_R$ as,

$$\mathcal{B} \rightarrow \mathcal{B}' = h(L, R, U)\mathcal{B} h^{-1}(L, R, U). \quad (7.127)$$

Since the chiral symmetry constrains the baryon Green functions generated by the functional in Eq. (7.120) to satisfy the chiral ward identities, then the corresponding most general Lagrangian has to preserve the invariance under local chiral transformations, in the presence of external fields. Therefore, the covariant derivative has to be introduced in order to preserve the local $SU(3)_L \times SU(3)_R \times U(1)_V$ symmetry,

$$D_\mu = \partial_\mu + \Gamma_\mu \quad (7.128)$$

with the chiral connection Γ_μ (transforms as a 4-vector under parity),

$$\Gamma_\mu = \frac{1}{2} \left[u^\dagger (\partial_\mu - ir_\mu) u + u (\partial_\mu - il_\mu) u^\dagger \right], \quad (7.129)$$

which transforms as,

$$\Gamma_\mu \rightarrow \Gamma'_\mu = h\Gamma_\mu h^\dagger - (\partial_\mu h) h^\dagger, \quad (7.130)$$

such that the covariant derivative satisfies the expected transformation behavior:

$$D_\mu \mathcal{B}(x) \rightarrow h D_\mu \mathcal{B}. \quad (7.131)$$

The other building block is called the “chiral vielbein” u_μ (transforms as an axial-vector under parity), which is Hermitian ,

$$u_\mu = i \left[u^\dagger (\partial_\mu - i r_\mu) u - u (\partial_\mu - i l_\mu) u^\dagger \right] , \quad (7.132)$$

and transforms as $u_\mu \rightarrow h u_\mu h^\dagger$ under chiral transformations. Then, the scalar, pseudo-scalar sources can be introduced by χ_\pm using the χ defined in Eq. (7.94),

$$\chi_\pm = u^\dagger \chi u^\dagger \pm u \chi^\dagger u , \quad (7.133)$$

which has $\chi_\pm \rightarrow h \chi_\pm h^\dagger$ transformation behavior under the $SU(3)_L \times SU(3)_R \times U(1)_V$ symmetry.

7.5.1 The leading order meson-baryon chiral Lagrangian

In the meson ChPT, meson-chiral Lagrangians contain even powers of momenta due to the Lorentz invariance. Also the power counting of the covariant derivative and external fields acting on meson fields remains the same as in meson ChPT. Therefore, starting with the baryon fields consist of two light quark flavors, one can notice that the nucleon mass does not vanish in the chiral limit, also the partial derivative ∂_μ acting on nucleon fields produce “large” momentum for the time-component and a “small” quantity $\sim \mathcal{O}(M_\pi)$ for the spatial component (3-momentum). This requires the chiral power counting for the baryonic sector has to be specified carefully.

In order to summarize the chiral counting scheme, one can simply consider the counting of bilinears $\bar{\Psi} \Gamma \Psi$, where Ψ denotes the nucleon state. Considering the

positive energy solution to the Dirac equation [82],

$$\Psi^{(+)}(\vec{x}, t) = e^{-ip_N^\mu x_\mu} \sqrt{E_N + m_N} \begin{pmatrix} \chi^* \\ \frac{\vec{\sigma} \cdot \vec{p}_N}{E_N + m_N} \chi^* \end{pmatrix} \quad (7.134)$$

where χ^* is the two-component Pauli spinor and $p_N^\mu = (E_N, \vec{p}_N)$ with $E_N = \sqrt{\vec{p}_N^2 + m_N^2}$, allows at the low-energy limit $\left(\frac{\vec{\sigma} \cdot \vec{p}_N}{E_N + m_N} \rightarrow \frac{|\vec{p}_N|}{m_N}\right)$ to distinguish the matrix elements of bilinears $\Gamma = \{\gamma_5, \gamma_5 \gamma_0, \gamma_i, \sigma_{i0}\}$ which couples large and small components in the nucleon state Ψ . Therefore, ∂_μ acting on Ψ produces,

$$p_N^\mu = \begin{pmatrix} (m_N, \vec{0}) \sim \mathcal{O}(p^0) \\ (E_N - m_N, \vec{p}_N) \sim \mathcal{O}(p) \end{pmatrix}. \quad (7.135)$$

With this observation for the case of $SU(2)_{\text{flavor}}$, one can summarize the chiral power counting for baryon ChPT (BChPT) for $SU(3)_{\text{flavor}}$ [92] by considering the minimum possible chiral order of the elements:

$$\begin{aligned} \mathcal{B}, \bar{\mathcal{B}} &= \mathcal{O}(p^0), & D_\mu \mathcal{B} &= \mathcal{O}(p^0), & (i\gamma^\mu D_\mu - \dot{m}_{\mathcal{B}}) \mathcal{B} &= \mathcal{O}(p) \\ \{\mathbb{1}, \gamma_\mu, \gamma\gamma_\mu, \sigma_{\mu\nu}\} &= \mathcal{O}(p^0), & \gamma_5 &= \mathcal{O}(p) \end{aligned}, \quad (7.136)$$

where $\dot{m}_{\mathcal{B}}$ denotes the mass of the octet baryon in the chiral limit. Note that, due to the spin (Dirac structures) odd powers in momentum are possible in BChPT.

Therefore, using the building blocks discussed above, one can construct the lowest order ($\mathcal{O}(p)$) $SU(3)_L \times SU(3)_R$ meson-baryon chiral Lagrangian [82],

$$\mathcal{L}_{MB}^{(1)} = \langle \bar{\mathcal{B}} (i\gamma^\mu D_\mu - \dot{m}_{\mathcal{B}}) \mathcal{B} \rangle - \frac{D}{2} \langle \mathcal{B} \gamma^\mu \gamma_5 \{u_\mu, \mathcal{B}\} \rangle - \frac{F}{2} \langle \mathcal{B} \gamma^\mu \gamma_5 [u_\mu, \mathcal{B}] \rangle \quad (7.137)$$

where D and F are two axial-vector coupling constants which can be determined by fitting the semi-leptonic decays of baryons $B \rightarrow B' + e^- + \bar{\nu}_e$ at tree level. The $\dot{m}_{\mathcal{B}}$ denotes the baryon mass in the chiral limit. Also, the covariant derivative of \mathcal{B} is

defined using the chiral connection Γ_μ given in Eq. (7.129) as,

$$D_\mu \mathcal{B} = \partial_\mu \mathcal{B} + [\Gamma_\mu, \mathcal{B}] . \quad (7.138)$$

For the case of $N_f = 2$, this Lagrangian in Eq. (7.137) becomes,

$$\mathcal{L}_{\pi N}^{(1)} = \Psi \left(i\gamma^\mu D_\mu - \mathring{m}_N + \frac{\mathring{g}_A}{2} \gamma^\mu \gamma_5 u_\mu \right) \Psi , \quad (7.139)$$

where \mathring{g}_A is the axial-vector coupling.

7.5.2 An application at tree level : Goldberger-Treiman relation

The nucleon matrix element of the pseudo-scalar density is given in Ref. [82] as,

$$m_q \langle N(p') | P_i(0) | N(p) \rangle = \frac{M_\pi^2 F_\pi}{M_\pi^2 - t} G_{\pi N}(t) i \bar{u}(p') \gamma_5 \tau_i u(p) \quad (7.140)$$

where $t = (p' - p)^2$ and $G_{\pi N}(t)$ is referred to the pion-nucleon form factor. Also the pion-nucleon coupling $g_{\pi N}$ is defined as,

$$g_{\pi N} = G_{\pi N}(t)|_{t=M_\pi^2} . \quad (7.141)$$

Since the Lagrangian $\mathcal{L}_{\pi N}^{(1)}$ in Eq. (7.139) does not contain a direct coupling of pseudo-scalar field $P_i(x)$ to nucleon (i.e., does not contain terms with χ or χ^\dagger), the matrix element of the pseudo-scalar density is therefore given by Fig. (7.2), at lowest order in chiral expansion.

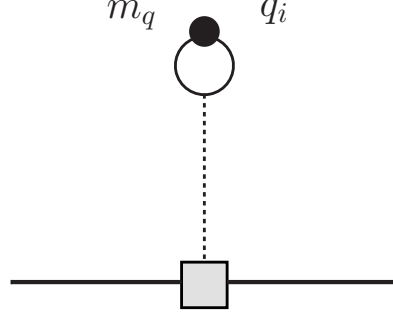


Figure 7.2. Lowest-order contribution to the single-nucleon matrix element of the pseudoscalar density.

Analogous to the scalar coupling discussed in Eq. (7.86), one can write down the coupling of pseudo-scalar field to a pion as,

$$\mathcal{L}_{\text{ext}} = i \frac{F_0^2 B_0}{2} \langle p U^\dagger - U p \rangle = 2 B_0 F_0 q_i \phi_i + \dots \quad (7.142)$$

where q_i is the four-momentum of the pion. Also, one needs the interaction term of a nucleon with a single pion. Expanding the vielbein of Eq. (7.132) in the absence of external fields, and inserting it to the $\mathcal{L}_{\pi N}^{(1)}$ in Eq. (7.139) gives,

$$\mathcal{L}_{\text{int}} = -\frac{\dot{g}_A}{2F_0} \Psi \gamma^\mu \gamma_5 \vec{\tau} \cdot \partial_\mu \vec{\phi} \Psi. \quad (7.143)$$

Therefore, the Feynman rule for the pion-nucleon $V_{\pi NN}$ vertex becomes,

$$V_{\pi NN} = -\frac{\dot{g}_A}{2F_0} \gamma^\mu q_\mu \gamma_5 \vec{\tau}. \quad (7.144)$$

Using the components $\mathcal{L}_{\text{ext}}, V_{\pi NN}$ the expression for the diagram in Fig. (7.2) reads:

$$2B_0 F_0 m_q \left(\frac{i}{t - M_\pi^2} \right) \bar{u}(p') \left(-\frac{\dot{g}_A}{2F_0} \gamma^\mu q_\mu \gamma_5 \vec{\tau} \right) u(p) = \frac{M_\pi^2 F_0}{M_\pi^2 - t} \frac{\dot{g}_A \dot{m}_N}{F_0} \bar{u}(p') \gamma_5 i \tau_i u(p),$$

with the aid of $M_\pi^2 = 2B_0 m_q$, $\bar{u}\gamma^\mu q_\mu \gamma_5 u = 2\mathring{m}_N \bar{u}\gamma_5 u$, and $F_\pi = F_0$ at $\mathcal{O}(p^2)$. Comparing Eq. (7.140) and Eq. (7.145),

$$G_{\pi N}(t) = \frac{\mathring{m}_N}{F_0} \mathring{g}_A \quad (7.145)$$

which yields the “Goldberger-Treiman (GT) relation”,

$$g_{\pi N} = \frac{\mathring{m}_N}{F_0} \mathring{g}_A \quad (7.146)$$

at the leading order in chiral expansion when $t = M_\pi^2$.

7.6 Heavy Baryon Approach

In the heavy baryon chiral perturbation theory (HBChPT), the baryons are considered as heavy static fermions [31, 93]. The velocity of the baryon is nearly unchanged or effectively conserved when it exchanges a small momentum with a meson. Therefore the baryon four-momentum can be decomposed into a large component $m_B v$ and a small residual momentum component k_μ ,

$$p_\mu = m_B v_\mu + k_\mu, \quad v^\mu v_\mu = 1, \quad v \cdot k \ll m_B. \quad (7.147)$$

7.6.1 Power counting scheme in HBChPT

In the HBChPT, the derivative expansion for both mesons and baryons becomes an expansion in powers of (k/Λ_χ) , where k is a momentum of the order of the meson mass and Λ_χ is the chiral symmetry breaking scale. Therefore, the higher derivative terms in the effective theory are suppressed by powers of (k/Λ_χ) . The baryon propagator can be revised into

$$\frac{1}{p^2 - m_B^2} \rightarrow \frac{1}{2m_B} \frac{1}{(v \cdot k)} + \mathcal{O}(1/m_B^2), \quad (7.148)$$

a version where the mass dependence can be resided in the vertices which can be ordered according to their power in $1/m_{\mathcal{B}}$. The chiral dimension D for a given Feynman diagram is given by [82],

$$D_{\text{dim}} = 4N_L - 2I_M - I_{\mathcal{B}} + \sum_{n=1}^{\infty} 2n N_{2n}^M + \sum_{n=1}^{\infty} n N_n^{\mathcal{B}}, \quad (7.149)$$

where, N_L is the number of loops, I_M is the number of internal meson lines, N_{2n}^M is the number of meson vertices from \mathcal{L}_{2n} , $N_n^{\mathcal{B}}$ is the number of baryon vertices from $\mathcal{L}_{M\mathcal{B}}^{(n)}$, and $I_{\mathcal{B}}$ is the number of internal baryon lines. For the processes which have single baryon in the initial and final states, the Eq. (7.149) becomes,

$$D_{\text{dim}} = 2N_L + 1 + \sum_{n=1}^{\infty} 2(n-1) N_{2n}^M + \sum_{n=1}^{\infty} (n-1) N_n^{\mathcal{B}}, \quad (7.150)$$

because the total number of mesonic vertices N_M can be related to I_M by $N_L = I_M + I_{\mathcal{B}} - N_M - N_{\mathcal{B}} + 1$, and the total number of baryonic vertices can be written as,

$$N_{\mathcal{B}} = \sum_{n=1}^{\infty} N_n^{\mathcal{B}} = I_{\mathcal{B}} + 1. \quad (7.151)$$

Note that the loop contribution starts from $D_{\text{dim}} \geq 3$.

7.6.2 Octet baryons in HBChPT

The effective baryon fields \mathcal{B}_v with definite velocity v_{μ} can be related to the original baryon fields \mathcal{B} by ,

$$\mathcal{B}_v(x) = e^{im_{\mathcal{B}} \not{v} x^{\mu}} \mathcal{B}(x), \quad (7.152)$$

satisfying a modified Dirac equation [31],

$$i \not{\partial} \mathcal{B}_v(x) = 0. \quad (7.153)$$

which no longer contains the baryon mass term. Derivatives on \mathcal{B}_v fields produce powers of k rather than p , thus higher derivative terms in the effective theory are suppressed by powers of k/Λ_χ rather than p/Λ_χ , where Λ_χ is the chiral symmetry breaking scale. Therefore, it leads to a consistent derivative expansion.

On the other hand, the Dirac structure of the effective theory simplifies in the heavy baryon limit. The B_v is a two component spinor which contain the particle (positive-energy) solution and the anti-particle (negative energy) solution. This can be projected into the particle solution, using the velocity projection operator

$$P_v = \left(\frac{1 + \not{v}}{2} \right) , \quad B_v = P_v B_v \quad (7.154)$$

whereas, anti-baryon solutions are suppressed by $1/m_B$. Also, it is important to introduce a special spin operators S_v^μ called the ‘‘Pauli-Lubanski spin vector’’ which satisfies the properties

$$\begin{aligned} v \cdot S_v &= 0 , & S_v^2 B_v &= -\frac{3}{4} B_v , & \{S_v^\lambda, S_v^\sigma\} &= \frac{1}{2} (v^\lambda v^\sigma - g^{\lambda\sigma}) , \\ [S_v^\lambda, S_v^\sigma] &= i\epsilon^{\lambda\sigma\alpha\beta} v_\alpha S_{v\beta} \end{aligned} \quad (7.155)$$

where, $\epsilon_{0123} = +1$. These spin operators are valid in an arbitrary Lorentz frame, and can be reduced to usual spin operators (written in terms of Pauli-matrices) for non-relativistic spin 1/2 particles in the rest frame, $v_\mu = (1, 0, 0, 0)$. Using the properties of Eq. (7.155) one can obtain the identities given by Jenkins and Manohar in Ref. [31] to systematically replace the Dirac structures by S_v and v_μ :

$$\begin{aligned} \bar{\mathcal{B}}_v \gamma_5 \mathcal{B}_v &= 0 , & \bar{\mathcal{B}}_v \gamma^\mu \mathcal{B}_v &= v^\mu \bar{\mathcal{B}}_v \mathcal{B}_v , & \bar{\mathcal{B}}_v \gamma^\mu \gamma_5 \mathcal{B}_v &= 2 \bar{\mathcal{B}}_v S_v^\mu \mathcal{B}_v \\ \bar{\mathcal{B}}_v \sigma^{\mu\nu} \mathcal{B}_v &= 2\epsilon^{\mu\nu\alpha\beta} v_\alpha \bar{\mathcal{B}}_v S_{v\beta} \mathcal{B}_v , & \bar{\mathcal{B}}_v \sigma^{\mu\nu} \gamma_5 \mathcal{B}_v &= 2i (v^\mu \bar{\mathcal{B}}_v S_v^\nu \mathcal{B}_v - v^\nu \bar{\mathcal{B}}_v S_v^\mu \mathcal{B}_v) , \end{aligned} \quad (7.156)$$

where the B_v is represents the octet baryon multiplet,

$$\mathcal{B}_v = \begin{pmatrix} \frac{1}{\sqrt{2}}\Sigma_v^0 + \frac{1}{\sqrt{6}}\Lambda_v & \Sigma_v^+ & P_v \\ \Sigma_v^- & -\frac{1}{\sqrt{2}}\Sigma_v^0 + \frac{1}{\sqrt{6}}\Lambda_v & N_v \\ \Xi_v^- & \Xi_v^0 & -\frac{2}{\sqrt{6}}\Lambda_v \end{pmatrix}. \quad (7.157)$$

Let's recall the meson fields U and u defined in Eq. (7.122) with the use of Eq. (7.68),

$$U = u^2 = \exp\left(i\frac{2\phi^a T^a}{F_0}\right). \quad (7.158)$$

where,

$$\phi = 2\phi^a T^a = \sqrt{2} \begin{pmatrix} \frac{1}{\sqrt{2}}\pi^0 + \frac{1}{\sqrt{6}}\eta & \pi^+ & K^+ \\ \pi^- & -\frac{1}{\sqrt{2}}\pi^0 + \frac{1}{\sqrt{6}}\eta & K^0 \\ K^- & \bar{K}^0 & -\frac{2}{\sqrt{6}}\eta \end{pmatrix}. \quad (7.159)$$

Under a $SU(3)_L \times SU(3)_R$ transformation, these \mathcal{B}_v, u, U fields transform as,

$$\begin{aligned} U &\rightarrow LUR^\dagger, & \mathcal{B}_v &\rightarrow h(L, R, U)\mathcal{B}_v h^\dagger(L, R, U), \\ u &\rightarrow Lu h^\dagger(L, R, U) = h(L, R, U)uR^\dagger \end{aligned} \quad (7.160)$$

where, $h(L, R, U)$ is recalled from the section (7.5). The most general lowest order chiral Lagrangian for octet-baryon is [31],

$$\begin{aligned} \mathcal{L}_{v,8} &= i\langle \bar{\mathcal{B}}_v(v.\mathcal{D})\mathcal{B}_v \rangle + 2D\langle \bar{\mathcal{B}}_v S_v^\mu(v.\mathcal{D})\{A_\mu, \mathcal{B}_v\} \rangle + 2F\langle \bar{\mathcal{B}}_v S_v^\mu(v.\mathcal{D})[A_\mu, \mathcal{B}_v] \rangle \\ &\quad + \frac{F_0^2}{4}\langle \partial_\mu U \partial^\mu U^\dagger \rangle + a\langle \mathcal{M}(U + U^\dagger) \rangle, \end{aligned} \quad (7.161)$$

where,

$$\mathcal{D}^\mu \mathcal{B}_v = \partial^\mu \mathcal{B}_v + [V^\mu, \mathcal{B}_v], \quad (7.162)$$

$$V^\mu = \frac{1}{2}(u\partial u^\dagger + u^\dagger\partial^\mu u), \quad A^\mu = \frac{i}{2}(u\partial u^\dagger - u^\dagger\partial^\mu u), \quad (7.163)$$

$$\mathcal{M} = \text{diag}(m, m_d, m_s). \quad (7.164)$$

Note, the mass term $m_B \bar{\mathcal{B}}_v \mathcal{B}_v$ is absent in the Lagrangian because of the redefinition in Eq. (7.152).

7.6.3 Decuplet baryons in HBChPT

The motivation for including the decuplet baryons in the effective chiral Lagrangian reflects to the pioneering work done on “chiral corrections to the baryon axial currents” by Jenkins and Manohar in Ref. [32]. It has been shown that, the explicit inclusion of the decuplet degree of freedom plays an important role in the convergence of effective theories such as combined ChPT and $1/N_c$ expansion [36]. Therefore, in the main focus of this thesis work on one-loop corrections to baryon masses and currents in $SU(3)$ using the combined framework containing the explicit inclusion of decuplet degrees of freedom. Analogous to the spin 1/2 baryon octet fields, the decuplet fields are also treated as heavy fermion fields in the effective chiral Lagrangian. In order to include the spin 3/2 decuplet, it is necessary to introduce a field called, Rarita-Schwinger field \mathcal{T}_{abc}^μ which contains both spin 3/2 and spin 1/2 contributions. The spin 1/2 pieces are projected out using the constraint $\gamma^\mu \mathcal{T}_\mu = 0$ in the rest frame, which implies :

$$v^\mu \mathcal{T}_\mu = 0. \quad (7.165)$$

\mathcal{T}_{abc}^μ is a completely symmetric $SU(3)$ tensor in the flavor indices “ a, b, c ”, and also a color singlet. Under $SU(3)_L \times SU(3)_R$ \mathcal{T}_{abc}^μ transform as,

$$\mathcal{T}_{abc}^\mu \rightarrow h_a^d h_b^e h_c^f \mathcal{T}_{def}^\mu, \quad (7.166)$$

where h is the same as for octet baryons. The velocity dependent fields also can be defined analogous to the Eq.(7.152) as,

$$\mathcal{T}_v^\mu(x) = e^{im\tau \not{v} x^\mu} \mathcal{T}^\mu(x). \quad (7.167)$$

The spin algebra for \mathcal{T}_v^μ can be simply obtained by replacing B_v by \mathcal{T}_v^μ in Eq. (7.155). The total angular momentum operator J_v^μ of spin 3/2 baryon is defined as [32],

$$(J_v^\nu \mathcal{T}_\nu)^\mu = S_v^\nu \mathcal{T}_\nu^\mu + i\epsilon^{\mu\nu\alpha\beta} v_\alpha \mathcal{T}_{v\beta}^\mu, \quad J_v^2 \mathcal{T}_v^\mu = -\frac{15}{4} \mathcal{T}_v^\mu. \quad (7.168)$$

The propagator for the Rarita-Schwinger field for a decuplet baryon contains an additional term namely, the polarization projector $P_v^{\mu\nu}$. The decuplet propagator is then given by $iP_v^{\mu\nu}/(v.k)$, where $P_v^{\mu\nu}$ projects out the positive energy solutions to the equation of motion \mathcal{U}_i^μ . The polarization sum can be written as [32],

$$P_v^{\mu\nu} = \sum_{i=1}^4 \mathcal{U}_i^\mu \bar{\mathcal{U}}_i^\nu = (v^\mu v^\nu - g^{\mu\nu}) - \frac{4}{3} S_v^\mu S_v^\nu \quad (7.169)$$

and, also the identities,

$$\begin{aligned} v \cdot S_v &= 0, & P_v^{\mu\nu} P_{v\nu}^\lambda &= -P_v^{\mu\lambda}, \\ P_v^{\mu\nu} P_{v\nu}^\lambda &= 0, & P_v^{\mu\nu} v_\nu &= P_v^{\mu\nu} v_\mu = 0, & P_v^{\mu\nu} g_{\mu\nu} &= -2, \\ P_v^{\mu\nu} S_{v\nu} &= S_{v\mu} P_v^{\mu\nu} = 0, & P_v^{\mu\nu} S_{v\mu} &= -\frac{4}{3} S_v^\nu, & S_{v\nu} P_v^{\mu\nu} &= -\frac{4}{3} S_v^\mu \end{aligned} \quad (7.170)$$

are useful when computing the Feynman diagrams. The most general lowest order chiral Lagrangian for decuplet-baryon is [32, 33],

$$\mathcal{L}_{v,10} = -i\langle \bar{\mathcal{T}}_v^\mu \mathcal{D} \mathcal{T}_{v\mu} \rangle + \Delta m \langle \bar{\mathcal{T}}_v^\mu \mathcal{T}_{v\mu} \rangle + \mathcal{C} \langle \bar{\mathcal{T}}_v^\mu A_\mu \mathcal{B}_v + \bar{\mathcal{B}}_v A_\mu \mathcal{T}_v^\mu \rangle + 2\mathcal{H} \langle \bar{\mathcal{T}}_v^\mu S_{v\nu} A^\nu \mathcal{T}_{v\mu} \rangle. \quad (7.171)$$

There are couple of important things to notice in this Lagrangian :

- The kinetic term has the opposite sign from that for the octet, because the spinor solutions \mathcal{U}^μ are space-like ($\mathcal{U}^2 < 0$).
- Because of the redefinition of \mathcal{T}_v^μ in Eq. (7.152), there will be no factors of $\exp(i(m_{\mathcal{T}-\mathcal{B}})\not{v}_\mu x^\mu)$ from the terms which contain both decuplet and octet fields.

- The decuplet-octet mass splitting $\Delta m = m_{\mathcal{T}-\mathcal{B}}$ has a magnitude approximately of the order of small momentum ($\sim \mathcal{O}(\text{meson mass})$). Therefore it enters to the theory through the decuplet propagator,

$$\frac{i\mathcal{P}_v^{\mu\nu}}{(k.v - \Delta m)} . \quad (7.172)$$

7.6.4 Most general Lagrangian at lowest order

The most general Lagrangian in HBChPT consist of two main contributions namely, the octet baryon contribution and the decuplet baryon contribution,

$$\begin{aligned} \mathcal{L}_v^{(0)} &= \mathcal{L}_{v,8}^{(0)} + \mathcal{L}_{v,10}^{(0)} \\ &= i\langle \bar{\mathcal{B}}_v(v.\mathcal{D})\mathcal{B}_v \rangle + 2D\langle \bar{\mathcal{B}}_v S_v^\mu(v.\mathcal{D})\{A_\mu, \mathcal{B}_v\} \rangle + 2F\langle \bar{\mathcal{B}}_v S_v^\mu(v.\mathcal{D})[A_\mu, \mathcal{B}_v] \rangle \\ &\quad - i\langle \bar{\mathcal{T}}_v^\mu \mathcal{D}\mathcal{T}_{v\mu} \rangle + \Delta m\langle \bar{\mathcal{T}}_v^\mu \mathcal{T}_{v\mu} \rangle + \mathcal{C}\langle \bar{\mathcal{T}}_v^\mu A_\mu \mathcal{B}_v + \bar{\mathcal{B}}_v A_\mu \mathcal{T}_v^\mu \rangle + 2\mathcal{H}\langle \bar{\mathcal{T}}_v^\mu S_{v\nu} A^\nu \mathcal{T}_{v\mu} \rangle \\ &\quad + \frac{F_0^2}{4}\langle \partial_\mu U \partial^\mu U^\dagger \rangle \end{aligned} \quad (7.173)$$

where the superscript (0) of $\mathcal{L}_v^{(0)}$ indicates the chiral limit ($m_q \rightarrow 0$).

CHAPTER 8

COMBINED EFFECTIVE THEORY OF THE $1/N_c$ AND CHIRAL EXPANSIONS

8.1 Introduction

This chapter focuses on combining the $1/N_c$ expansion and the Chiral expansion in baryons with three light quark flavors. The early version of baryon ChPT by H. Pagels [94] has evolved into several EFT's based on different versions effective Chiral Lagrangians [80, 81, 95] discussed in chapter 7. One is the relativistic version namely, Baryon ChPT (BChPT) [85, 96] followed by the non-relativistic version based in an expansion in the inverse baryon mass [31, 96] or Heavy Baryon ChPT (HBChPT). And other versions are Lorentz covariant versions based on the IR regularization scheme [97–99]. All these versions of baryon effective theories are associated with its own low energy expansion. But the convergence of all these low energy expansions became an important issue. This convergence problem arises with the loop contributions of $\mathcal{O}(p^2)$ and $\mathcal{O}(p^3)$ to the physical observables. It is natural to expect a slower convergence of an expansion that progresses in steps of $\mathcal{O}(p)$ as is the case for the baryon sector, compared to the expansion that progresses in steps of $\mathcal{O}(p^2)$ in the Goldstone boson sector. Jenkins and Manohar [32] realized that the closeness of mass between octet and decuplet has a key impact to the convergence. Therefore an explicit inclusion of decuplet degrees of freedom in the theory plays an important role of ameliorating the convergence of the one-loop contributions to certain observables such as the $\pi - N$ scattering amplitude and the axial currents and magnetic moments. There have been since then numerous works [100–108] including spin 3/2 baryons. The key enlightenment resulted from the study of baryons in the large N_c limit of QCD [10]. It was shown in the previous chapters that in the large N_c limit baryons be-

have differently than mesons [15], in particular because their masses scale like $\mathcal{O}(N_c)$ and the π -baryon couplings are $\mathcal{O}(\sqrt{N_c})$. These properties were shown to require for consistency, that at large N_c baryons must respect a dynamical contracted spin-flavor symmetry $SU(2N_f)$, where N_f being the number of light flavors [11–14], broken by effects ordered in powers of $1/N_c$ and in the quark mass differences. The inclusion of these large N_c consistency requirements into the effective theory can be naturally implemented through a combination of the $1/N_c$ expansion and HBChPT [109], which is the framework followed in chapters 9 and 10. The study of one-loop corrections in that framework was first carried out in Refs. [34,35,109]. In the combined theory, one has to deal with the fact that the $1/N_c$ and Chiral expansions do not commute [30]. The physics behind this non-commutativity is the role of Δ resonance which introduces the small mass scale $m_\Delta - m_N$ mass difference of $\mathcal{O}(1/N_c)$. Therefore, it is necessary to define the order of this mass splitting with respect to the low energy expansion. A specific linking between $1/N_c$ and Chiral expansions has been implemented when the baryon mass splitting of $\mathcal{O}(1/N_c)$ is considered to be $\mathcal{O}(p)$ in the Chiral expansion, which is called the ξ -expansion : $\mathcal{O}(p) = 1/N_c = \mathcal{O}(\xi)$. Following the work by Cordon et. al. and [34,35,109], the theoretical framework is discussed in detail, in particular the power counting, the renormalization, and the linked $1/N_c$ and low energy expansions, along with observations that further clarify the significance of the framework.

The determination of the quark mass dependence of the various low energy observables, such as masses, axial couplings, magnetic moments, electromagnetic polarizabilities, etc., are of key importance as a significant test of the effective theory, in particular its range of validity in quark masses, as well as for the determination of its low energy constants (LECs). Lattice QCD (LQCD) has made a significant progress in the calculations [110–112] of baryon observables, which open new opportunities

for further understanding the low energy effective theory of baryons. This in turn can give insights on LQCD results, in particular an understanding on the role and relevance of including the spin $3/2$ baryons consistently with large N_c requirements.

This chapter is organized as follows. In the section 8.2, the foundation of the effective Lagrangian with its properties are described along with the building blocks of the combined chiral and $1/N_c$ expansion approach. Then section 8.3 describes the interactions between the fields associated with the baryon effective Lagrangians up to $\mathcal{O}(\xi^3)$. The ξ -power counting is illustrated in the section 8.4. The section 8.5 is dedicated to the calculation of one-loop correction to the self-energy, and the last section discusses the one-loop corrections to the baryon currents.

8.2 Foundation of the Effective Lagrangian

The symmetries that the effective Lagrangian must respect in the chiral and large N_c limits are Chiral $SU_L(N_f) \otimes SU_R(N_f)$ and contracted dynamical spin-flavor symmetry $SU(2N_f)$ [11–14], where N_f is the number of light quark flavors, which is considered to be three in this work. For the case of $N_f = 2$ was successfully done in Cordon et. al [36]. In the limit $N_c \rightarrow \infty$ the spin-flavor symmetry with two (three) quark flavors requires baryons to belong into degenerate multiplets of $SU(4)$ ($SU(6)$). At finite N_c the spin-flavor symmetry is broken by effects suppressed by powers of $1/N_c$, and the mass splittings in the GS multiplet between the states with spin $S + 1$ and spin S are proportional to $(S + 1)/N_c$. The effects of finite N_c are then implemented as an expansion in $1/N_c$ at the level of the effective Lagrangian. Because baryon masses scale as proportional to N_c , it becomes natural to use the framework of HBChPT [31, 32], where the expansion in inverse powers of the baryon mass becomes part of the $1/N_c$ expansion. The framework presented next follows

that of Refs. [34, 109].

As discussed in chapter 4, baryons in the large N_c limit must appear in multiplets of spin-flavor $SU(2N_f)$, where $N_f = 3$ is the number of light flavors. A dynamical contracted $SU(2N_f)$ symmetry results from the requirement of large N_c consistency of baryon observables [11–14]. There are 35 generators of $SU(6)$ and their commutation relations can be recalled from Eq. (4.8),

$$\begin{aligned} [S^i, T^a] &= 0 & [T^a, T^b] &= if^{abc}T^c \\ [S^i, S^j] &= i\epsilon^{ijk}S^k & [T^a, G^{ib}] &= if^{abc}G^{ic} \\ [S^i, G^{ja}] &= i\epsilon^{ijk}G^{ka} & [G^{ia}, G^{jb}] &= \frac{i}{4}\delta^{ij}f^{abc}T^c + \frac{i}{6}\delta^{ab}\epsilon^{ijk}S^k + \frac{i}{2}\epsilon^{ijk}d^{abc}G^{kc}. \end{aligned} \quad (8.1)$$

The ground state baryons belong to the totally symmetric spin-flavor irreducible representation with N_c Young boxes (see Fig (3.1)) which consist of states with spin $S = 1/2, \dots, N_c/2$. The dimension of the $SU(3)$ multiplet can be written as $(p, q) = (2S, \frac{1}{2}(N_c - 2S))$, for a given spin S .

8.2.1 Building blocks of the effective Lagrangian

In HBChPT, the baryon field in general can be denoted by \mathbf{B} with its well defined spin which defines its irreducible representation in $SU(3)$. The Goldstone bosons are represented by u fields :

$$u = \exp^{i\phi^a T^a / F_\pi} \quad (8.2)$$

which is already defined in the chapter 7 with its non-linear transformation,

$$R u h^\dagger(L, R, u) = h(L, R, u) u L^\dagger \quad (8.3)$$

where $L(R)$ transforms in $SU(3)_L(SU(3)_R)$, and “ h ” handles the $SU(3)$ flavor transformations. The Chiral transformations on baryon fields B can be defined as,

$$(L, R) : \mathbf{B} = h(L, R, u) \mathbf{B} . \quad (8.4)$$

Although Chiral transformations do not commute with $SU(6)$ group, but they leave the commutation relations unchanged. The covariant derivative is defined,

$$D_\mu \mathbf{B} = \partial_\mu \mathbf{B} - i\Gamma_\mu \mathbf{B} \quad (8.5)$$

with,

$$\Gamma_\mu = \frac{1}{2} \left(u^\dagger (i\partial_\mu + r_\mu) u + u (i\partial_\mu + l_\mu) u^\dagger \right) , \quad u_\mu = u^\dagger (i\partial_\mu + r_\mu) u - u (i\partial_\mu + l_\mu) u^\dagger , \quad (8.6)$$

where, $l_\mu = v_\mu - a_\mu$ and $r_\mu = v_\mu + a_\mu$ are gauge sources, and u_μ is the “chiral vielbein”. The transformation properties of all these building blocks of the covariant derivative under chiral transformation are,

$$\Gamma_\mu \rightarrow \Gamma'_\mu = h\Gamma_\mu h^\dagger - (\partial_\mu h)h^\dagger , \quad u_\mu \rightarrow u'_\mu = hu_\mu h^\dagger . \quad (8.7)$$

The scalar (s) and pseudo-scalar (p) sources can be collected by recalling the definitions of χ_\pm from Eq. (7.133), and χ from Eq. (7.94),

$$\begin{aligned} \chi &= 2B_0(s + ip) , \\ \chi_\pm &= u^\dagger \chi u^\dagger \pm u \chi^\dagger u , \\ \chi_\pm^0 &= \langle \chi_\pm \rangle , \\ \tilde{\chi}_\pm &\equiv \chi_\pm^a T^a , \quad \text{where } \chi_\pm^a \equiv \frac{1}{2} \langle \lambda^a \chi_\pm \rangle , \end{aligned} \quad (8.8)$$

where χ_\pm transforms as $\chi_\pm \rightarrow h\chi_\pm h^\dagger$ under the $SU(3)_L \times SU(3)_R \times U(1)_V$ symmetry.

Also, the field-strength associated with the gauge sources can be collected as,

$$\begin{aligned} F_L^{\mu\nu} &= \partial^\mu \ell^\nu - \partial^\nu \ell^\mu - i[\ell^\mu, \ell^\nu] , \quad F_R^{\mu\nu} = \partial^\mu r^\nu - \partial^\nu r^\mu - i[r^\mu, r^\nu] , \\ F_{X\pm}^{\mu\nu} &= u^\dagger F_X^{\mu\nu} u^\dagger \pm u F_X^{\mu\nu\dagger} u . \end{aligned} \quad (8.9)$$

Also in general, if A is an $SU(3)$ octet operator which can be defined as $A = A^a T^a$ where, in the fundamental irrep, one denotes:

$$A^a = \frac{1}{2} \langle \lambda^a A \rangle . \quad (8.10)$$

8.2.2 Properties of the effective Lagrangian

The effective Lagrangian should contain contracted symmetry in the $N_c \rightarrow \infty$ limit. In particular, the couplings of Goldstone Bosons to baryons will violate the symmetry at sub-leading order in $1/N_c$. The Goldstone Boson fields transform as singlets under the spin-generators, octets under both $SU(3)$ and X^{ia} generators; which are the generators of the contracted $SU(6)_c$ group.

The effective Lagrangian can be systematically written as a power series in the low energy expansion or Chiral expansion, and simultaneously in $1/N_c$. It is most convenient to write the Lagrangian to be chiral invariant as this is a Noether symmetry of QCD. This means that each term will, through the unitary parametrization of the Goldstone Boson fields, show different orders in $1/N_c$ through the powers of $1/F_\pi$. In addition, the low energy constants (LECs) will themselves admit an expansion in powers of $1/N_c$. For the HBChPT expansion the large mass of the expansion is taken to be the spin-flavor singlet component of the baryon masses in the chiral limit, $M_0 = N_c m_0$ (m_0 can be considered here to be a LEC defined in the chiral limit and which will have itself an expansion in $1/N_c$).

In the following the effective HB chiral Lagrangian is implemented. It is constructed in terms of tensors involving the Goldstone Boson operators and the external sources, and spin-flavor tensors built with products of the $SU(6)$ generators that have been already discussed. A scale “ Λ ” is introduced in order to render most of

the LECs dimensionless. In the calculations $\Lambda = m_\rho$ will be conveniently chosen as the QCD scale. In order to ensure the validity of the OZI rule for the quark mass dependency of baryon masses, the following combination of the source χ_+ is defined:

$$\hat{\chi}_+ \equiv \tilde{\chi}_+ + N_c \chi_+^0, \quad (8.11)$$

where, $\hat{\chi}_+$ is of $\mathcal{O}(N_c)$, such that the non-strange baryon mass dependence on m_s is $\mathcal{O}(N_c^0)$. Requiring the Lagrangian to satisfy the QCD symmetries, and implementing the dynamical symmetry constraints as discussed before, one can systematically build the Lagrangian order by order in the chiral and $1/N_c$ expansions.

8.3 Interactions from the effective Lagrangians

The fields which are associated with the phenomenology are Goldstone boson fields, Baryon fields and external sources. Therefore the complete theory consist of two main pieces of Lagrangians: the meson Lagrangian and baryon Lagrangian. The amplitudes of interactions between these degrees of freedom are identified as *interaction vertices*, and those can be obtained up to a desired order by expanding the Lagrangians using the tools mentioned in the section 8.2.1.

8.3.1 Meson Lagrangian

The meson fields are described using the meson Lagrangian given in Eq. (7.95) as follows:

$$\mathcal{L}_\pi = \frac{F_\pi^2}{4} \langle \partial_\mu U^\dagger \partial^\mu U \rangle + \frac{F_\pi^2}{4} \langle \chi U^\dagger + U \chi^\dagger \rangle. \quad (8.12)$$

This Lagrangian can be expanded using the definitions of Goldstone boson fields given in Eq. (8.2), and then one can obtain the interaction vertices for vector and axial vector currents in terms of momentum, as given in the third column of Table (8.1).

8.3.2 Baryon effective Lagrangians of $\mathcal{O}(\xi)$, $\mathcal{O}(\xi^2)$ and $\mathcal{O}(\xi^3)$

The lowest order Lagrangian is $\mathcal{O}(\xi)$ and, reads [109]:

$$\mathcal{L}_{\mathbf{B}}^{(1)} = \mathbf{B}^\dagger \left(iD_0 + \mathring{g}_A u^{ia} G^{ia} - \frac{C_{HF}}{N_c} \hat{S}^2 + \frac{c_1}{\Lambda} \hat{\chi}_+ \right) \mathbf{B}, \quad (8.13)$$

where \mathring{g}_A is the axial coupling in the chiral and large N_c limits (it has to be rescaled by a factor 5/6 to coincide with the usual axial coupling as defined for the nucleon, i.e., $g_A = \frac{5}{6} \mathring{g}_A$). Here one notes an important point which will be present in other instances as well: the baryon mass dependence on the current quark mass behaves at $\mathcal{O}(N_c m_q)$ (c_1 is of zeroth order in N_c), and this indicates that in a strict large N_c limit the expansion in the quark masses of certain quantities such as the baryon masses cannot be defined due to divergent coefficients of $\mathcal{O}(N_c)$. This in particular impacts the σ terms discussed later. In the present case those terms are spin-flavor singlet.

The Lagrangian is manifestly invariant under chiral transformations, translations and rotations (the latter also involving obviously the action of the S^i generators of $SU(6)$). It is not invariant under the contracted $SU(6)$ transformations generated by the X^{ia} generators. At large N_c such transformations affect the leading GB-baryon interaction contained in the covariant derivative term D_0 (the Weinberg-Tomozawa type interaction) by terms of the same order, i.e., $\mathcal{O}(1/N_c)$, but since those terms are also $\mathcal{O}(p)$, they are $\mathcal{O}(\xi^2)$; the effect on the GB-baryon couplings proportional to \mathring{g}_A is $\mathcal{O}(1/N_c)$ with respect to the term itself; the effect on the hyperfine term proportional to C_{HF} is of the same order as the term itself, and finally the term pro-

portional to c_1 is obviously invariant. The construction of higher order Lagrangians can be accomplished making use of the tools provided in Appendix B.

The interaction vertices can be obtained using the later mentioned tools, up to any desired order in ξ . Since the focus of this work is to calculate one-loop corrections to the masses and currents, one only needs the interaction vertices from the lowest order Lagrangian. These interaction vertex types are : Derivative interactions, vector currents and axial-vector currents. The Feynman diagrams and corresponding expressions for each vertex is given in Table (8.1).

The $\mathcal{O}(\xi^2)$ Lagrangian is given by:

$$\begin{aligned}
\mathcal{L}_{\mathbf{B}}^{(2)} = & \mathbf{B}^\dagger \left(\left(\frac{z_1}{N_c} + \frac{z_2}{N_c} \hat{S}^2 + \frac{z_3}{\Lambda^2} N_c \chi_+^0 \right) i\tilde{D}_0 + \left(-\frac{1}{2N_c m_0} + \frac{w_1}{\Lambda} \right) \vec{D}^2 \right. \\
& + \left(\frac{1}{2N_c m_0} - \frac{w_2}{\Lambda} \right) \tilde{D}^2 + \frac{c_2}{\Lambda} \chi_+^0 \frac{C_1^A}{N_c} u^{ia} S^i T^a + \frac{C_2^A}{N_c} \epsilon^{ijk} u^{ia} \{S^j, G^{ka}\} \\
& + \kappa_0 \epsilon^{ijk} F_{+ij}^0 S^k + \kappa_1 \epsilon^{ijk} F_{+ij}^a G^{ka} + \rho_0 F_{-0i}^0 S^i + \rho_1 F_{-0i}^a G^{ia} \\
& \left. + \frac{\tau_1}{N_c} u_0^a G^{ia} D_i + \frac{\tau_2}{N_c^2} u_0^a S^i T^a D_i + \frac{\tau_3}{N_c} \nabla_i u_0^a S^i T^a + \tau_4 \nabla_i u_0^a G^{ia} + \dots \right) \mathbf{B}.
\end{aligned} \tag{8.14}$$

The terms involving \tilde{D}_0 contribute to the wave function renormalization factors at this order. Note that there are also $\mathcal{O}(\xi^2)$ terms stemming from the $1/N_c$ suppressed terms in the LECs of the lower order Lagrangian. Similar comments apply to the higher order Lagrangians. Such terms require knowledge of the physics at $N_c > 3$ to be determined, which can be studied using LQCD, see for instance [76, 113].

For the $\mathcal{O}(\xi^3)$ Lagrangian, where only those terms that contribute to baryon masses, wave function renormalization and vector and axial currents are explicitly displayed in Eq. (8.15).

$$\begin{aligned}
\mathcal{L}_{\mathbf{B}}^{(3)} = & \mathbf{B}^\dagger \left(\frac{z_4}{\Lambda^2} \tilde{\chi}_+ i\tilde{D}_0 + \frac{z_5}{\Lambda^2} [i\tilde{D}_0, \tilde{\chi}_+] + \frac{c_3}{N_c \Lambda^3} \hat{\chi}_+^2 \frac{h_1}{N_c^3} \hat{S}^4 + \frac{h_2}{N_c^2 \Lambda} \hat{\chi}_+ \hat{S}^2 \right. \\
& + \frac{h_3}{N_c \Lambda} \chi_+^0 \hat{S}^2 + \frac{h_4}{N_c \Lambda} \chi_+^a \{S^i, G^{ia}\} + \frac{C_3^A}{N_c^2} u^{ia} \{\hat{S}^2, G^{ia}\} + \frac{C_4^A}{N_c^2} u^{ia} S^i S^j G^{ja} \\
& + \frac{D_1^A}{\Lambda^2} \chi_+^0 u^{ia} G^{ia} + \frac{D_2^A}{\Lambda^2} \chi_+^a u^{ia} S^i + \frac{D_3^A(d)}{\Lambda^2} d^{abc} \chi_+^a u^{ib} G^{ic} + \frac{D_3^A(f)}{\Lambda^2} f^{abc} \chi_+^a u^{ib} G^{ic} \\
& \left. + g_E [D_i, F_{+i0}] + \alpha_1 \frac{i}{N_c} \epsilon^{ijk} F_{+0i}^a G^{ia} D_k + \beta_1 \frac{i}{N_c} F_{-ij}^a G^{ia} D_j + \dots \right) \mathbf{B} \quad (8.15)
\end{aligned}$$

As it will be shown later, the components of the LECs needed to subtract the UV divergencies do consistently satisfy these constraints.

Some terms $\mathcal{O}(\xi^4)$ are needed for subtracting UV divergencies, but they are beyond the order of the present calculations and can therefore systematically and consistently be eliminated. For instance, one needs terms such as:

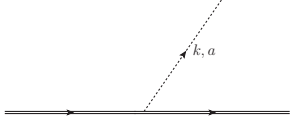
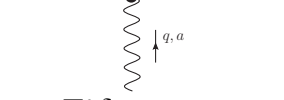
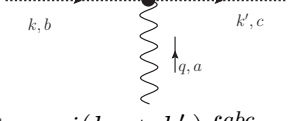
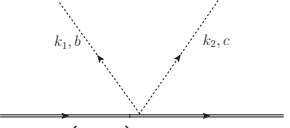
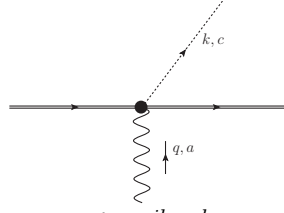

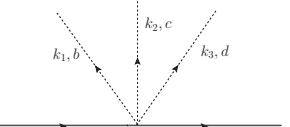
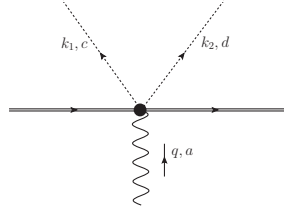
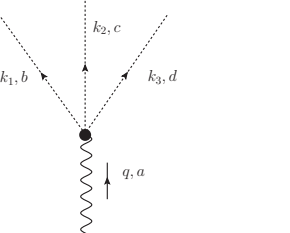
$$\mathcal{L}_{\mathbf{B}}^{(4)} = \mathbf{B}^\dagger \left(\left(\frac{z_6}{N_c^3} \hat{S}^4 + \frac{z_7}{N_c \Lambda^2} \chi_+^0 \hat{S}^2 + \frac{z_8}{N_c \Lambda^2} \chi_+^a \{S^i, G^{ia}\} \right) i\tilde{D}_0 + \dots \right) \mathbf{B}. \quad (8.16)$$

Through the calculation of the one loop corrections to the self-energies and the vector and axial vector currents the β functions associated with several of the terms will be determined. The β functions are defined such that the LECs are renormalized:

$$X = X(\mu) + \frac{1}{(4\pi)^2} \beta_X \lambda_\epsilon, \quad (8.17)$$

where $X(\mu)$ are the LECs and μ is the renormalization scale.

Table 8.1. Vertices from the lowest order effective Lagrangians.

Baryons	Baryon	Meson
Derivative Interactions	Currents	Currents
<p>(a)</p>  <p>$(i) \left(\frac{-g_A}{F_\pi} \right) (ik_i) G^{ia}$</p>	<p>(d)</p>  <p>vector : $T^a \delta_{\mu 0}$ axial-vector : $g_A G^{ia} \delta_{\mu i}$</p>	<p>(g)</p>  <p>vector : $i(k_\mu + k'_\mu) f^{abc}$</p>
<p>(b)</p>  <p>$(-i) \left(\frac{1}{2F_\pi^2} \right) (ik_{2,0} - ik_{1,0}) f^{abc} T^a$</p>	<p>(e)</p>  <p>vector : $\frac{g_A}{F_\pi} G^{ib} f^{abc} \delta_{\mu i}$ axial-vector : $\frac{1}{F_\pi} f^{abc} T^b \delta_{\mu 0}$</p>	<p>(h)</p>  <p>axial-vector : $(-i) F_\pi q_\mu \delta^{ab}$</p>
<p>(c)</p>  <p>$(i) \left(\frac{g_A}{6F_\pi^3} \right) (ik_{2,i}) f^{cde} f^{abe} G^{ia}$</p>	<p>(f)</p>  <p>vector : $\left(-\frac{1}{2F_\pi^2} \right) T^b f^{ade} f^{ebc} \delta_{\mu 0}$ axial-vector : $\left(-\frac{g_A}{2F_\pi^2} \right) G^{ib} f^{ade} f^{ebc} \delta_{\mu i}$</p>	<p>(i)</p>  <p>$(-i) \frac{2}{3F_\pi} f^{abe} f^{cde} k_{3,\mu}$</p>

8.4 ξ power counting

The spin-flavor operators appearing in the effective Lagrangians will be scaled by the appropriate powers of $1/N_c$ in such a way that all LECs are of zeroth order in N_c . Therefore, the $1/N_c$ power of a Lagrangian term with n_π pion fields is given by [49]:

$$n - 1 - \kappa + \frac{n_\pi}{2}, \quad (8.18)$$

where the spin-flavor operator is n -body (n is the number of factors of $SU(6)$ generators appearing in the operator), and κ is basically the number of factors of the coherent generators G^{ia} remaining after reducing the operator using commutators. The last term, $n_\pi/2$, stems from the factor $(1/F_\pi)^{n_\pi}$ carried by any term with n_π pion fields. It is opportune to point out that commutators of spin-flavor generators will always reduce the n -bodiness of the product of operators: e.g., let \mathcal{G} be any generator of $SU(6)$, and consider the commutator $[\mathcal{G}, \vec{S}^2] = \{S^i, [\mathcal{G}, S^i]\}$. In principle this looks like a three-body operator, but because $[\mathcal{G}, S^i]$ is a 1-body operator, $[\mathcal{G}, \vec{S}^2]$ is actually a 2-body operator.

The terms in the effective Lagrangian are constrained in their N_c dependence by the requirement of the consistency of QCD at large N_c . This constraint is in the form of an upper bound in the power in $1/N_c$ for each term one could write down in the Lagrangian. This leads to constraints on the N_c dependencies of the ultra-violet (UV) divergencies, which have to be subtracted by the corresponding counter-terms in the Lagrangian. One very important point to mention is that the UV divergencies are necessarily polynomials in low momenta p (derivatives), in M_π^2 and in $1/N_c$ (modulo factors of $1/\sqrt{N_c}$ due to $1/F_\pi$ factors in terms where pions are attached). Therefore, the structure of counter-terms is independent of any linking between the $1/N_c$ and chiral expansions. For this reason, one can simply take the large N_c and low energy

limits independently in order to determine the UV divergencies. For a connected diagram with n_B external baryon legs, n_π external pion legs, n_i vertices of type i which has n_{B_i} baryon legs and n_{π_i} pion legs, and L loops, the following topological relations hold [114, 115],

$$L = 1 + I_\pi + I_B - \sum n_i, \quad 2I_B + n_B = \sum n_i n_{B_i}, \quad 2I_\pi + n_\pi = \sum n_i n_{\pi_i}, \quad (8.19)$$

where I_π is the number of pion propagators and I_B the number of baryon propagators. The chiral or low energy order of a diagram, where ν_{p_i} is the chiral power of the vertex of type i , is then given by [115]:

$$\nu_p = 2 - \frac{n_B}{2} + 2L + \sum_i n_i \left(\nu_{p_i} + \frac{n_{B_i}}{2} - 2 \right), \quad (8.20)$$

Note that n_{B_i} is equal to 0 or 2 in the single baryon sector.

On the other hand, the $1/N_c$ power of a connected diagram is determined by looking only at the vertices: the order in $1/N_c$ of a vertex of type i is given according to Eq. (8.18) by: $\nu_{O_i} + \frac{n_{\pi_i}}{2}$, where ν_{O_i} is the order of the spin-flavor operator. Thus, the $1/N_c$ power of a diagram, upon use of the third Eq. (8.19), is given by:

$$\nu_{1/N_c} = \frac{n_\pi}{2} + I_\pi + \sum n_i \nu_{O_i}, \quad (8.21)$$

where n_π is the number of external pions, and ν_{O_i} the $1/N_c$ order of the spin-flavor operator of the vertex of type i . Since ν_{O_i} can be negative (due to factors of G^{ia} in vertices), one can think of individual diagrams with ν_{1/N_c} negative and violating large N_c consistency, requiring cancellation with other diagrams. Such a sum will have to respect the mentioned upper bound on the $1/N_c$ power corresponding to the sum of such diagrams. The explicit example of such cancellation in the axial currents

at one-loop which is given later.

One can determine now the nominal counting of the one-loop contributions to the baryon masses and axial currents. The LO baryon masses are $\mathcal{O}(N_c)$. The one loop correction shown in Fig. (8.1) has: ($L = 1$, $n_B = 2$, $n_\pi = 0$, $n_1 = 2$, $\nu_{O_1} = -1$, $n_{B_1} = 2$, $\nu_{p_1} = 1$) giving $\nu_p = 3$ as it is well known, and $\nu_{1/N_c} = -1$. Since there is only one possible diagram, this must be consistent by contributing $\mathcal{O}(N_c)$ to the spin-flavor singlet component of the masses, which is the case as shown in the section (8.5). The diagrams for vector and the axial currents are given in Tables (8.5), (8.6), and (8.7). The current at tree level is $\mathcal{O}(N_c)$, and the sum of the diagrams cannot scale like a higher power of N_c . Performing the counting for the individual diagrams one obtains: $\nu_p(j) = 2$ for $j = 1, \dots, 4$, and $\nu_{1/N_c}(j) = -2$, $j = 1, 2, 3$ and $\nu_{1/N_c}(4) = 0$. Thus a cancellation must occur of the $\mathcal{O}(N_c^2)$ terms when the contributions to the axial currents by the set of diagrams are added. Since the acceptable bound is that the sum be $\mathcal{O}(N_c)$, one concludes that the axial current has, at one-loop, corrections $\mathcal{O}(p^2 N_c)$ or higher.

One can consider the case of two-loop diagrams, in particular diagrams where the same meson-baryon vertex Eq.(8.13) appears four times. For the masses one has $\nu_p(j) = 5$, and individual diagrams give $\nu_{1/N_c} = -2$. A cancellation must occur to restore the bound on the N_c counting for the masses, i.e., $\mathcal{O}(N_c)$. Thus, at two-loops the UV divergencies of the masses must be $\mathcal{O}(p^5 N_c)$ or higher. For the axial currents a similar discussion requires that counter-terms to the axial currents must be $\mathcal{O}(p^4 N_c)$ or higher.

Defining the linked power counting ξ by: $\mathcal{O}(1/N_c) = \mathcal{O}(p) = \mathcal{O}(\xi)$, the ξ order of a given Feynman diagram will be simply equal to $\nu_p + \nu_{1/N_c}$ as given by Eqs.(8.20)

and (8.21), which upon use of the topological formulas Eq. (8.19) leads to:

$$\nu_\xi = 1 + 3L + \frac{n_\pi}{2} + \sum_i n_i (\nu_{O_i} + \nu_{p_i} - 1). \quad (8.22)$$

The ξ -power counting of the UV divergences is obvious from the earlier discussion. At one-loop one finds that the masses have $\mathcal{O}(\xi^2)$ and $\mathcal{O}(\xi^3)$ counter-terms, while the axial currents will have $\mathcal{O}(\xi)$ and $\mathcal{O}(\xi^2)$ counter-terms. To two loops one expects $\mathcal{O}(\xi^4)$ and $\mathcal{O}(\xi^5)$, and $\mathcal{O}(\xi^3)$ and $\mathcal{O}(\xi^4)$ counter-terms for masses and axial currents respectively. The non-commutativity of limits is manifested in the finite terms where M_π and or momenta and $\delta\hat{m}$ appear combined in non-analytic terms, and are therefore sensitive to the linking of the two expansions.

8.5 One-loop correction to the baryon self-energy

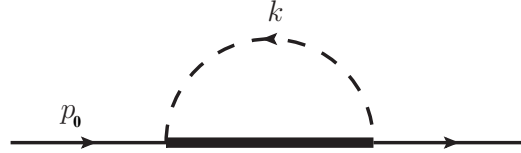


Figure 8.1. One-loop contribution to the self-energy of a baryon field.

The self-interaction of baryon fields governed by emission and absorption of Goldstone bosons gives rise to contributions to the baryon masses and also contribute to their wave function renormalization. The lowest order contribution of this type of interaction can be represented by the one-loop diagram, as shown in Fig. (8.1). The interaction has two contributions which are symmetric by each vertex, because we only focus on the processes which involve the same incoming and outgoing baryon. Therefore the two interaction vertices can be seen as, the incoming (outgoing) baryon field couples to an intermediate baryon propagator (thick line) and a Goldstone boson propagator (dashed line). The intermediate baryon can be either a member of baryon octet or decuplet. Therefore, the contributions from the baryon octet and decuplet

are taken into the account systematically, in the effective theory.

The p_0 is the energy of the external baryon which can be defined as,

$$p_0 = \delta m_{in} + \mathbf{p}^0 \quad (8.23)$$

where \mathbf{p}^0 is the kinetic energy $\mathcal{O}(p^2/N_c)$, and $\delta m_{in} = \delta m_{out}$. In the heavy baryon formalism, the velocity dependent baryon propagator contains a residual mass, while the (heavy) baryon mass is absorbed into the interaction vertex for the renormalization. For convenience, one can define

$$\begin{aligned} \delta \hat{m} &\equiv \frac{C_{HF}}{N_c} \vec{S}^2 - \frac{c_1}{\Lambda} \hat{\chi}_+ , \\ i\tilde{D}_0 &\equiv iD_0 - \delta \hat{m} . \end{aligned} \quad (8.24)$$

where $\delta \hat{m}$ gives rise to mass splittings between baryons, which are of $\mathcal{O}(1/N_c)$ or $\mathcal{O}(p^2)$. Therefore, the residual mass of a baryon propagator evaluated for state x can be written as $\delta \hat{m}_x$, which leads to the baryon mass shift,

$$\delta m_n = \delta \hat{m}_n - \delta \hat{m}_{in} . \quad (8.25)$$

The first term in $\delta \hat{m}$ is the hyper-fine interaction and the second term corresponds to the $SU(3)$ breaking effects. In the ξ expansion $SU(3)$ breaking effects do not show in δm_n as they are $\mathcal{O}(\xi^2)$. Thus, one can reasonably neglect the $SU(3)$ breaking effects in the baryon propagator in the loop by assuming that the residual mass is $SU(3)$ symmetric, i.e. $\delta \hat{m} \rightarrow \frac{C_{HF}}{N_c} \hat{S}^2$.

Combining all the propagators and the vertices the expression for the one-loop correction to the self-energy can be written as,

$$\delta\Sigma_{1-loop} = \frac{\dot{g}_A^2}{F_\pi^2} \sum_{a=1}^8 \sum_n G^{ia} \mathcal{P}_n G^{ja} \mu^{(4-d)} \int \frac{d^d k}{(2\pi)^d} \frac{k_i k_j}{(k^2 - M_a^2 + i\epsilon)(p_0 - k_0 - \delta m_n + i\epsilon)}$$

where, \mathcal{P}_n is the projector which projects the intermediate baryon labeled by n , and M_a is the corresponding Goldstone boson mass with the $SU(3)$ flavor index a . The final expression for $\delta\Sigma_{1-loop}$ can be obtained using the Feynman parameterization with *dimensional regularization* method, and all the necessary tools are given in Appendix C. The expression for the loop integral $\mathbf{H}_{ij}(M_\pi, \delta m_n, p_0)$ can be simplified as,

$$\begin{aligned} \mathbf{H}_{ij}(M_\pi, \delta m_n, p_0) &= \mu^{(4-d)} \int \frac{d^d k}{(2\pi)^d} \frac{k_i k_j}{(k^2 - M_a^2 + i\epsilon)(p_0 - k_0 - \delta m_n + i\epsilon)} \\ &= \frac{\delta_{ij}}{d-1} \left(2i\mu^{(4-d)} \left(\frac{d-1}{d} \right) \left(\frac{d}{2(4\pi)^{d/2}} \frac{\Gamma(1-\frac{d}{2})}{\Gamma(2)} \right) J((M_a^2 - Q^2), 1, Q, d, 1) \right) \end{aligned} \quad (8.26)$$

where, $Q = (p_0 - \delta m_n)$ and the Appendix C provides the definition of the J function and it's properties. Also this expression for the loop integral in Eq. (8.26) agrees with the result given for the integral in Eq. (15) of [116].

The ultraviolet divergent pieces of the self-energy can be brought to a compact form:

$$\begin{aligned} \delta\Sigma_{1-loop}^{UV} &= \frac{\lambda_\epsilon}{(4\pi)^2} \left(\frac{\dot{g}_A}{F_\pi} \right)^2 \left(\mathbf{p}^0 M_a^2 G^{ia} G^{ia} + \frac{1}{2} M_a^2 [[\delta\hat{m}, G^{ia}], G^{ia}] - \frac{2}{3} \mathbf{p}^{03} \right. \\ &\quad \left. - \mathbf{p}^{02} [[\delta\hat{m}, G^{ia}], G^{ia}] - \mathbf{p}^0 [[\delta\hat{m}, [\delta\hat{m}, G^{ia}]], G^{ia}] - \frac{1}{3} [[\delta\hat{m}, [\delta\hat{m}, [\delta\hat{m}, G^{ia}]]], G^{ia}] \right), \end{aligned} \quad (8.27)$$

where $\lambda_\epsilon \equiv 1/\epsilon - \gamma + \log 4\pi$. Using the $SU(3)$ singlet and octet components of the quark masses, m^0 and m^a , one can write the meson mass squared matrix:

$$M^{2ab} = 4B_0(\delta^{ab}m^0 + d^{abc}m^c), \quad (8.28)$$

and therefore,

$$M_a^2 W^{aa} = M^{2ab} W^{ab}, \quad (8.29)$$

for any symmetric 8×8 tensor W . In terms of M_π and M_K one has: $m^0 = \frac{1}{3}(2\hat{m} + m_s) = \frac{2M_K^2 + M_\pi^2}{12B_0}$ and $m^a = \frac{1}{\sqrt{3}}(\hat{m} - m_s) = \delta^{8a} \frac{(-M_K^2 + M_\pi^2)}{2\sqrt{3}B_0}$.

In order to obtain from Eq. (8.28) the counterterms necessary to renormalize the mass and wave function, one uses the results in Appendix D. The explicit UV divergent and polynomial (in $1/N_c$, m^0 , m^a and \mathbf{p}^0) terms of the self-energy are

$$\begin{aligned} \delta\Sigma^{\text{Poly}} = & -\frac{1}{(4\pi)^2} \left(\frac{g_A}{F_\pi} \right)^2 \left\{ \frac{B_0 C_{HF}}{6N_c} \left(\frac{7}{3} + \lambda_\epsilon \right) \left(m^0(9N_c(N_c + 6) - 84\hat{S}^2) - 24m^a(2\{S^i, G^{ia}\} \right. \right. \\ & - \left. \frac{3}{4}(N_c + 3)T^a) \right) + \frac{C_{HF}^3}{N_c^2} \left(\frac{8}{3} + \lambda_\epsilon \right) \left(-(N_c + 6) + \frac{36 - 5N_c(N_c + 6)}{3N_c} \hat{S}^2 + \frac{4}{N_c} \hat{S}^4 \right) \\ & - \mathbf{p}^0 \left((1 + \lambda_\epsilon)12B_0 \left(m^0 \left(\frac{1}{4}N_c(N_c + 6) + \frac{5}{9}\hat{S}^2 \right) + m^a \left(\frac{7}{12}\{S^i, G^{ia}\} - \frac{1}{2}(N_c + 3)T^a \right) \right. \right. \\ & \left. \left. + \frac{C_{HF}^2}{N_c^2} (2 + \lambda_\epsilon) \left(\frac{3}{2}N_c(N_c + 6) + (-18 + N_c(N_c + 6))\hat{S}^2 - 4\hat{S}^4 \right) \right) \right\}, \quad (8.30) \end{aligned}$$

where terms of higher powers in \mathbf{p}^0 have been disregarded. There are few observations on $\delta\Sigma^{\text{Poly}}$ which can be summarized as follows.

- The contributions to the spin-flavor singlet component of the masses is $\mathcal{O}(p^2 N_c^0)$, the spin symmetry breaking is $\mathcal{O}(1/N_c^2)$, and the $SU(3)$ breaking is $\mathcal{O}(p^2/N_c)$.
- The UV divergencies in the mass are produced by the contribution of the partner baryon and is determined by the mass splitting, i.e., by C_{HF} .
- The contributions to δZ are suppressed by powers of $1/N_c$, but with two exceptions, namely, there is a spin-flavor singlet contribution proportional to m^0 which is $\mathcal{O}(N_c)$ and a term proportional to m^a which is $\mathcal{O}(N_c^0)$.

The term $\mathcal{O}(N_c)$ in δZ is of key importance for the mechanism of cancellations of $1/N_c$ power counting violating terms, as it is shown later in the analysis of the

one-loop contributions to the currents.

The counterterms for renormalizing the masses and wave functions are $\mathcal{O}(\xi^2)$ and $\mathcal{O}(\xi^3)$ (all contributions $\mathcal{O}(\xi^4)$ are consistently dropped) and involve terms that appear in $\mathcal{L}_{\mathbf{B}}^{(1)}$ with LECs of higher order in $1/N_c$, and terms in $\mathcal{L}_{\mathbf{B}}^{(2,3)}$. To renormalize, the LECs are written as in terms of the β functions defined in Eq.(8.17), and the beta-functions β_X are given in Table(8.2).

Table 8.2. β functions for mass renormalization.

LEC	$\beta/[g_A^2/F_\pi^2]$
m_0	$-\frac{N_c+6}{N_c^3}C_{HF}^3$
C_{HF}	$\frac{36-5N_c(N_c+6)}{3N_c^2}C_{HF}^3$
c_1	$\frac{3}{4}\frac{N_c+3}{N_c}\Lambda C_{HF}$
c_2	$\frac{3}{16}N_c\Lambda C_{HF}$
c_3	0
h_1	$-12C_{HF}^3$
h_2	0
h_3	$\frac{7}{4}\Lambda C_{HF}$
h_4	$\frac{1}{2}\Lambda C_{HF}$

Finally the non-analytic contributions to $\delta\Sigma_{1\text{-loop}}$ are:

$$\begin{aligned}
\delta\Sigma^{\text{NA}} &= -\frac{1}{(4\pi)^2} \left(\frac{\dot{g}_A}{F_\pi}\right)^2 \sum_{a=1}^8 \sum_n G^{ia} \mathcal{P}_n G^{ia} \\
&\times \left\{ (p_0 - \delta m_n) \left(M_a^2 - \frac{2}{3}(p_0 - \delta m_n)^2 \right) \log \frac{M_a^2}{\mu^2} \right. \\
&+ \left. \frac{2}{3} (M_a^2 - (p_0 - \delta m_n)^2)^{\frac{3}{2}} (\pi + 2 \arctan \left(\frac{p_0 - \delta m_n}{\sqrt{M_a^2 - (p_0 - \delta m_n)^2}} \right)) \right\}, \tag{8.31}
\end{aligned}$$

where, the total non-analytic contribution to the one-loop can be obtained by summing over all the possible intermediate states, which can be identified as *partial contributions*. Each partial contribution is associated with set of matrix elements of two-body, three-body, many-body operators, etc. which has to be projected to the corresponding combination of intermediate state and Goldstone boson state. Table (8.3) gives the reduction procedure of a product of two vectors, and the Table (8.4) gives the reduction of the $SU(3)$ $\mathbf{8} \otimes \mathbf{8}$ product of operators. Note that the tensors in the last column of Table (8.4) are indeed projectors, i.e., idempotent.

Table 8.3. Projection operators for operator products of irreps of $SU(2)$.

irrep ℓ	component	projection tensor \mathcal{P}_ℓ
0	$P^i Q^i$	$\frac{1}{3} \delta^{ij} \delta^{i'j'}$
1	$i \epsilon^{ijk} P^j Q^k$	$\frac{1}{2} \epsilon^{ijk} \epsilon^{ki'j'}$
2	$\frac{1}{2} (P^i Q^j + P^j Q^i) - \frac{1}{3} \delta^{ij} P^k Q^k$	$\frac{1}{2} (\delta^{ii'} \delta^{jj'} + \delta^{ij'} \delta^{ji'}) - \frac{1}{3} \delta^{ij} \delta^{i'j'}$

Table 8.4. Projection tensors for the operator products of irreps. of $SU(3)$.

irrep R	component	projection tensor \mathcal{P}_R
1	$P^a Q^a$	$\frac{1}{8} \delta^{ab} \delta^{cd}$
8	$i f^{abc} P^b Q^c$	$\frac{1}{3} f^{abe} f^{ecd}$
8'	$d^{abc} P^b Q^c$	$\frac{3}{5} d^{abe} d^{ecd}$
$10 + \overline{10}$	$(\frac{1}{2} (\delta^{ac} \delta^{bd} - \delta^{ad} \delta^{bc}) - \frac{1}{3} f^{abe} f^{ecd}) P^c Q^d$	$\frac{1}{2} (\delta^{ac} \delta^{bd} - \delta^{ad} \delta^{bc}) - \frac{1}{3} f^{abe} f^{ecd}$
27	$\frac{1}{2} (P^a Q^b + P^b Q^a) - \frac{1}{8} \delta^{ab} P^c Q^c - \frac{3}{5} d^{abc} d^{cde} P^d Q^e$	$\frac{1}{2} (\delta^{ac} \delta^{bd} + \delta^{ad} \delta^{bc}) - \frac{1}{8} \delta^{ab} \delta^{cd} - \frac{3}{5} d^{abe} d^{ecd}$

The typical reductions associated with the operator products in the one-loop integrals has the general form:

$$P^a Q^b L^{ab} = \sum_{R=1,8,8',10+\overline{10},27} (PQ)_R L_R \quad (8.32)$$

where L is the loop integral and:

$$(PQ)_R^{ab} = \mathcal{P}_{Rcd}^{ab} P^c Q^d \quad L_R^{ab} = \mathcal{P}_{Rcd}^{ab} L^{cd}. \quad (8.33)$$

By observing the terms in the $\delta\Sigma_{1-loop}^{UV}$ in Eq.(8.28) and the $\delta\Sigma^{\text{NA}}$ in Eq.(8.31), one can directly visualize the structures of operator products which are needed to calculate the matrix elements between baryon states. The reductions of those multi-body spin-flavor operators which appear in the polynomial contributions of the one-loop corrections to the self-energy and the currents require some lengthy calculations using identities, such as DJM relations given in Table (5.1), etc. These reductions are only valid for matrix elements between states in the totally symmetric irrep of $SU(6)$.

$$\begin{aligned} [[\delta\hat{m}, G^{ia}], G^{ia}] &= \frac{C_{HF}}{N_c} \left(\frac{7}{2} \hat{S}^2 - \frac{3}{8} N_c(N_c + 6) \right) \\ [[\delta\hat{m}, [\delta\hat{m}, G^{ia}]], G^{ia}] &= \left(\frac{C_{HF}}{N_c} \right)^2 (4\hat{S}^4 - (N_c(N_c + 6) - 18)\hat{S}^2 - \frac{3}{2} N_c(N_c + 6)) \\ [[\delta\hat{m}, [\delta\hat{m}, [\delta\hat{m}, G^{ia}]]], G^{ia}] &= \left(\frac{C_{HF}}{N_c} \right)^3 (36\hat{S}^4 - (5N_c(N_c + 6) - 36)\hat{S}^2 - 3N_c(N_c + 6)) \\ M_a^2 G^{ia} G^{ia} &= 2B_0 \left(m^0 \hat{G}^2 + m^a \left(-\frac{7}{24} \{S^i, G^{ia}\} + \frac{3}{16} (N_c + 3) T^a \right) \right) \\ M_a^2 [[\delta\hat{m}, G^{ia}], G^{ia}] &= 4 \frac{C_{HF}}{N_c} B_0 \left(\frac{8}{3} m^0 \hat{S}^2 + \frac{5}{12} m^a \{S^i, G^{ia}\} \right) - 4M_a^2 G^{ia} G^{ia} \end{aligned} \quad (8.34)$$

where, $\delta\hat{m} = \frac{C_{HF}}{N_c} \hat{S}^2$. Appendix A contains more details on spin-flavor operator bases, matrix elements of spin-flavor operators, and the operator identities respectively. A direct application : self-energy correction to the baryon mass is discussed in the chapter 9 in detail.

8.6 One-loop corrections to the baryon currents

Similarly, the one-loop corrections to baryon vector and axial-vector currents can be calculated using the combined effective framework. The corresponding one-loop

diagrams for the vector currents are summarized in Table (8.5) and for the axial vector currents are summarized in Table (8.6) and Table (8.7). For the simplicity of expression, the definition of $\mathbf{H}_{ij}(M_a, \delta m_n, p_0)$ is used to some loop integrals:

$$\mathbf{H}_{ij}(M_a, \delta m_n, p_0) = \mu^{(4-d)} \int \frac{d^d k}{(2\pi)^d} \frac{k_i k_j}{(k^2 - M_a^2 + i\epsilon)(p_0 - k_0 - \delta m_n + i\epsilon)}. \quad (8.35)$$

Note that, the diagrams for the vector currents are associated with two types of loop-integrals: self-energy diagram and triangle diagram. Except the triangle diagram, the expressions for the other diagrams can be written in terms of the self-energy integral. The one-loop integrals for the axial vector currents in Table (8.6) are analogous to the loop-integrals corresponding to the vector diagrams in Table (8.5). The loop-integrals for axial-vector currents in Table (8.7) involve the Goldstone boson propagator and can be evaluated using the standard integrals given in [117]. Each loop-integral is accompanied by matrix elements of operator products of $SU(2) \times SU(3)$ irreps., and one can build a set of relations between those operator products to perform operator reduction. A detailed calculation of these diagrams in order to obtain the vector charges and axial couplings are given in the last chapter along with the fit results to the LQCD calculations.

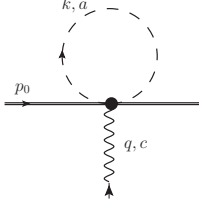
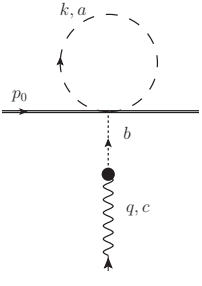
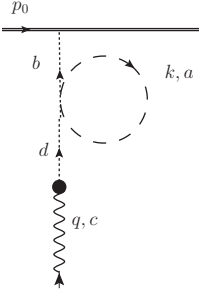
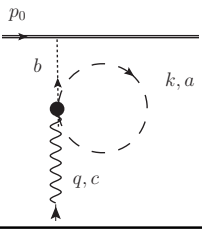
Table 8.5. One loop diagrams for the vector currents. The subscript of δm refers to either the intermediate baryon propagator δm_n or the incoming/outgoing $\delta m_{in/out}$ baryon propagator with respect to the current-vertex.

Vector current diagram	Expression
	$i\delta_{\mu 0} \left(\frac{g_A}{F_\pi} \right)^2 \frac{(\mathbf{H}_{ij}(M_a, \delta m_n, p_0))}{(p_0 - \delta m_{in} + i\epsilon)} \langle T_c G^{ia} G^{ja} \rangle$
	$i\delta_{\mu 0} \left(\frac{g_A}{F_\pi} \right)^2 \frac{(\mathbf{H}_{ij}(M_a, \delta m_n, p_0 + q_0))}{(p_0 + q_0 - \delta m_{out} + i\epsilon)} \langle G^{ia} G^{ja} T_c \rangle$
	$i\delta_{\mu 0} \left(\frac{g_A}{F_\pi} \right)^2 \left(\frac{\langle G^{ia} T_c G^{ja} \rangle}{\delta m_{in} - \delta m_{out} + q_0} \right) (\mathbf{H}_{ij}(M_a, \delta m_{in}, p_0) - \mathbf{H}_{ij}(M_a, \delta m_{out}, p_0 + q_0))$
	$\left(\frac{g_A}{F_\pi} \right)^2 G^{ia} f^{abc} G^{jb} \mu^{(4-d)} \int \frac{d^d k}{(2\pi)^d} \frac{(k_i + q_i)(2k_\mu + q_\mu)(k_j)}{((k+q)^2 - M_b^2 + i\epsilon)(p_0 - k_0 - \delta m_1 + i\epsilon)(k^2 - M_a^2 + i\epsilon)}$
	$-i \left(\frac{f^{abc} f^{abd}}{2F_\pi^2} T^d \right) \mu^{(4-d)} \int \frac{d^d k}{(2\pi)^d} \frac{(2k_0 + q_0)(2k_\mu + q_\mu)}{((k+q)^2 - M_b^2 + i\epsilon)(k^2 - M_a^2 + i\epsilon)}$
	$-i\delta_{\mu 0} \frac{1}{2F_\pi^2} f^{cae} f^{eda} T^d \mu^{(4-d)} \int \frac{d^d k}{(2\pi)^d} \frac{1}{(k^2 - M_a^2 + i\epsilon)}$

Table 8.6. Axial-Vector Currents (I).

Axial-vector current diagram	Expression
	$i \left(\frac{g_A^3}{F_\pi^2} \right) \frac{G^{\mu c} G^{ia} G^{ja}}{(p_0 - \delta m_{in} + i\epsilon)} \mathbf{H}_{ij}(M_a, \delta m_n, p_0)$
	$(-i) \left(\frac{g_A^3}{F_\pi^2} \right) \frac{G^{lb} G^{ia} G^{ja} \delta^{bc} q_\mu q_l}{(q^2 - M_b^2 + i\epsilon)(p_0 - \delta m_{in} + i\epsilon)} \mathbf{H}_{ij}(M_a, \delta m_n, p_0)$
	$i \left(\frac{g_A^3}{F_\pi^2} \right) \frac{G^{ia} G^{ja} G^{\mu c}}{(p_0 + q_0 - \delta m_{out} + i\epsilon)} \mathbf{H}_{ij}(M_a, \delta m_n, p_0 + q_0)$
	$(-i) \left(\frac{g_A^3}{F_\pi^2} \right) \frac{G^{ia} G^{ja} G^{lb} \delta^{bc} q_l q_\mu}{(p_0 + q_0 - \delta m_{out} + i\epsilon)(q^2 - M_b^2 + i\epsilon)} \mathbf{H}_{ij}(M_a, \delta m_n, p_0 + q_0)$
	$i \delta_{\mu 0} \left(\frac{g_A^3}{F_\pi^2} \right) \left(\frac{\langle G^{ia} G^{\mu c} G^{ja} \rangle}{\delta m_{in} - \delta m_{out} + q_0} \right) (\mathbf{H}_{ij}(M_a, \delta m_{in}, p_0) - \mathbf{H}_{ij}(M_a, \delta m_{out}, p_0 + q_0))$
	$(-i) \left(\frac{g_A^3}{F_\pi^2} \right) \frac{G^{ia} G^{lb} G^{ja} \delta^{bc}}{(q^2 - M_b^2 + i\epsilon)(\delta m_{in} - \delta m_{out} + q_0)} q_l q_\mu \times$
	$\times (\mathbf{H}_{ij}(M_a, \delta m_{in}, p_0) - \mathbf{H}_{ij}(M_a, \delta m_{out}, p_0 + q_0))$

Table 8.7. Axial-Vector Currents (II).

Axial-vector current diagram	Expression
	$-i \left(\frac{g_A}{2F_\pi^2} \right) \delta_{\mu i} f^{cae} f^{eda} G^{id} \mu^{(4-d)} \int \frac{d^d k}{(2\pi)^d} \frac{1}{k^2 - M_a^2 + i\epsilon}$
	$i \left(\frac{g_A}{2F_\pi^2} \right) f^{bae} f^{dae} (q_i q_\mu) G^{id} \mu^{(4-d)} \int \frac{d^d k}{(2\pi)^d} \frac{1}{(k^2 - M_a^2 + i\epsilon)(q^2 - M_b^2 + i\epsilon)}$
	$-i \frac{g_A}{3F_\pi^2} \frac{q_\mu q_i}{q^2 - M_c^2} G^{ib} f^{cae} f^{bae} \mu^{4-d} \int \frac{d^d k}{(2\pi)^d} \frac{1}{k^2 - M_a^2 + i\epsilon}$
	$-i \frac{2g_A}{3F_\pi^2} \frac{q_\mu q_i}{q^2 - M_b^2 + i\epsilon} G^{id} f^{cae} f^{bae} \left(\mu^{4-d} \int \frac{d^d k}{(2\pi)^d} \frac{1}{k^2 - M_a^2 + i\epsilon} \right)$

CHAPTER 9

GROUND STATE BARYON MASSES FROM THE COMBINED FRAMEWORK

9.1 Introduction

The effective Lagrangian is manifestly chiral invariant, and can be systematically written as a power series in the low energy expansion or in the chiral expansion, and simultaneously in $1/N_c$. In the HBChPT formalism, the larger contribution to the baryon mass is governed by the spin-flavor singlet component, whereas the leading order splitting between baryon masses is due to the hyperfine interaction which is considered to be a *small* energy scale for the theory. The size of the hyperfine splitting in the low energy expansion plays an important role since it combines with the Goldstone boson masses to appear as powers in the contributions from the loop diagrams. This implies that the low energy expansion and $1/N_c$ expansion does not commute [30, 118]. As discussed in the chapter 8, the emphasis of the framework goes to the linking between two expansions : $\mathcal{O}(p) = 1/N_c = \mathcal{O}(\xi)$.

The application of this combined framework to the baryon masses for the case of $SU(2)_{\text{flavor}}$ was successfully done by Cordon and Goity [36]. It is important to notice that the combined approach allows one to study the convergence the low energy expansion, with the availability of LQCD baryon masses. It has been clearly shown that, the decuplet contribution as intermediate states for the loop play an important role in the convergence, with increasing quark mass (see Fig.(4) of Ref. [36]). In average, it is believed that the consistent range of quark mass for the ξ -expansion is $M_{\pi}^{\text{Physical}} \leq M_{\pi} \lesssim 300\text{MeV}$, which is also considered in this work. One loop-correction to the non-strange baryon masses involves N , Δ baryons and π meson. In the case of

$SU(3)_{\text{flavor}}$, this becomes a bit complicated since one has to consider octet baryons, decuplet baryons as well as the π, K, η mesons, as well as the matrix elements associated with each loop integral. Especially, obtaining these matrix elements as well as the expressions for octet and decuplet baryon masses for any generic N_c is a remarkable achievement in this work.

This chapter is organized as follows. In the section 9.2, the leading order (LO) baryon mass is introduced which is of $\mathcal{O}(\xi)$. The section 9.3 contains a detailed discussion on the one-loop correction to the baryon mass in ξ -expansion for the case of $SU(3)$. The section 9.4 is dedicated to an analysis of mass relations such as Gell-Mann-Okubo (GMO), Equal Spacing (ES), Gürsey Radicati (GR) mass relations. The fit results to the available data for baryon masses from the experiments as well as from the LQCD are discussed in section 9.5 along with an analysis on mass relations. The section 9.6 is focused on an application of baryon masses from the combined formalism to extract the baryon σ -terms. In the last section some observations, conclusions and prospective applications are discussed.

9.2 Baryon mass at leading order

Considering the leading order Lagrangian, the baryon mass at $\mathcal{O}(\xi)$ can be written as [12, 14],

$$m_{\mathbf{B}}(S, Y, I) = N_c m_0 + \frac{C_{HF}}{N_c} S(S+1) - \frac{c_1}{\Lambda} \hat{\chi}_+ \quad (9.1)$$

where, m_0 , C_{HF} and c_1 are LECs to be determined by fitting to the baryon masses. m_0 is the spin-flavor singlet contribution to the baryon mass and it is correlated with the quark mass contribution which is coupled by the LEC, c_1 . C_{HF} is the hyper-fine interaction and it is equal to $M_{\Delta} - M_N$ for $N_c = 3$ at $\mathcal{O}(1/N_c)$.

9.3 One-loop correction to the baryon mass

A propagating baryon can self interact by emitting and absorbing a Goldstone boson. This is parameterized by the terms represent the baryon-meson interaction in the effective Lagrangian. This contribution to the baryon propagator is called the self-energy correction, in which the lowest order contribution is diagrammatically represented by one-loop diagram is depicted in Fig. (8.1).

The expression for the one-loop diagram $\delta\Sigma_{1-loop}$ contains the vertices from $\mathcal{L}_{\mathbf{B}}^{(1)}$, external (incoming/out-going) baryon propagator, intermediate baryon propagator as well as a projector \mathcal{P}_n which projects the incoming baryon to the intermediate baryon labeled by n , and the loop integral J :

$$\delta\Sigma_{1-loop} = i \frac{g_A^2}{F_\pi^2} \sum_{a=1}^8 \sum_n G^{ia} \mathcal{P}_n G^{ia} \frac{\Gamma(1 - \frac{d}{2})}{(4\pi)^{\frac{d}{2}}} J((M_a^2 - (p_0 - \delta m_n)^2), 1, (p_0 - \delta m_n), d, 1) , \quad (9.2)$$

where, the explicit evaluation of the loop integral J is given in the Appendix C.

The non-commutativity of the $1/N_c$ and chiral expansions of course resides in the non-analytic terms of the loop integral through their dependence on the ratios of the small scales $\delta m_n/M_a$. Notice that when the one loop integrals are written in terms of the residual momentum \mathbf{p}^0 , they do not depend on the spin-flavor singlet piece of $\delta\hat{m}$. \mathbf{p}^0 is naturally associated with $i\tilde{D}^0$. The one-loop contribution to the wave function renormalization constant is given by:

$$\delta Z_{1-loop} = \left. \frac{\partial}{\partial \mathbf{p}^0} \delta\Sigma_{1-loop} \right|_{\mathbf{p}^0 \rightarrow 0} . \quad (9.3)$$

An important fact which has to be considered throughout the one-loop diagram calculation for self-energy is that, the initial and final baryon has to be the same.

The selection rules corresponding to the quantum numbers : Spin S , Hyper-charge Y , Iso-spin I which can determine the possible channels associated with different combinations of intermediate baryon and corresponding meson states. Therefore, for a given baryon, the total contribution will be the sum of each individual channel, which is represented by the two summations in Eq. (9.2). Each combination of intermediate baryon + meson, can be identified as a “partial contribution” to a given baryon mass. Therefore, if the baryon state is defined as,

$$|\mathbf{B}\rangle = \left| \begin{array}{cc} S & S_z \\ R & YII_z \end{array} \right\rangle, \quad (9.4)$$

then matrix element of a partial contribution can be simply represented by,

$$\langle \mathbf{B} | G^{ia} \mathcal{P}_n G^{ia} | \mathbf{B} \rangle = \left\langle \begin{array}{cc} S & S_z \\ R & YII_z \end{array} \left| G^{ia} \mathcal{P}_n G^{ia} \right| \begin{array}{cc} S & S_z \\ R & YII_z \end{array} \right\rangle, \quad (9.5)$$

where, the explicit expression for the projection operator is,

$$\mathcal{P}_n = \sum_n \left| \begin{array}{cc} S_n & S_{n_z} \\ R_n & Y_n I_n I_{n_z} \end{array} \right\rangle \left\langle \begin{array}{cc} S_n & S_{n_z} \\ R_n & Y_n I_n I_{n_z} \end{array} \right|. \quad (9.6)$$

Appendix A provides all the necessary elements for the evaluation of the spin-flavor matrix elements in the $\delta\Sigma_{1-loop}$ in Eq. (9.2). The explicit final expressions for the self-energy are not given here because they are too lengthy, but with those elements they can be easily calculated. One loop corrections to baryon masses start at $\mathcal{O}(\xi^2)$. Because the ξ -power counting $M_\pi \rightarrow \xi M_\pi$ and $F_\pi \rightarrow \sqrt{\frac{N_c}{3}} F_\pi$ with $N_c \rightarrow N_c/\xi$, the ξ -order of one-loop integral is $\mathcal{O}(\xi^4)$. But, the matrix elements can be of $\mathcal{O}(1/\xi)$ or $\mathcal{O}(1/\xi^2)$ suppress the ξ power of the loop-integral corresponding to each partial contribution. Therefore the loops contain terms of $\mathcal{O}(\xi^2)$ and $\mathcal{O}(\xi^3)$.

Table 9.1. Partial contributions to the one-loop correction of the self-energy.

N	Λ	Σ	Ξ
$N \rightarrow N + \pi$	$\Lambda \rightarrow N + K$	$\Sigma \rightarrow \Sigma + \pi$	$\Xi \rightarrow \Xi + \pi$
$N \rightarrow N + \eta$	$\Lambda \rightarrow \Lambda + \eta$	$\Sigma \rightarrow \Sigma + \eta$	$\Xi \rightarrow \Xi + \eta$
$N \rightarrow \Sigma + K$	$\Lambda \rightarrow \Sigma + \pi$	$\Sigma \rightarrow N + K$	$\Xi \rightarrow \Sigma + K$
$N \rightarrow \Lambda + K$	$\Lambda \rightarrow \Xi + K$	$\Sigma \rightarrow \Lambda + \pi$	$\Xi \rightarrow \Lambda + K$
$N \rightarrow \Delta + \pi$	$\Lambda \rightarrow \Sigma^* + \pi$	$\Sigma \rightarrow \Xi + K$	$\Xi \rightarrow \Xi^* + \pi$
$N \rightarrow \Sigma^* + K$	$\Lambda \rightarrow \Xi^* + K$	$\Sigma \rightarrow \Delta + K$	$\Xi \rightarrow \Xi^* + \eta$
		$\Sigma \rightarrow \Sigma^* + \pi$	$\Xi \rightarrow \Sigma^* + K$
		$\Sigma \rightarrow \Sigma^* + \eta$	$\Xi \rightarrow \Omega + \pi$
		$\Sigma \rightarrow \Xi^* + K$	
Δ	Σ^*	Ξ^*	Ω
$\Delta \rightarrow N + \pi$	$\Sigma^* \rightarrow \Sigma + \pi$	$\Xi^* \rightarrow \Xi + \pi$	$\Omega \rightarrow \Omega + \pi$
$\Delta \rightarrow \Sigma + K$	$\Sigma^* \rightarrow \Sigma + \eta$	$\Xi^* \rightarrow \Xi + \eta$	$\Omega \rightarrow \Xi + K$
$\Delta \rightarrow \Delta + \eta$	$\Sigma^* \rightarrow N + K$	$\Xi^* \rightarrow \Sigma + K$	$\Omega \rightarrow \Xi^* + K$
$\Delta \rightarrow \Delta + \pi$	$\Sigma^* \rightarrow \Lambda + \pi$	$\Xi^* \rightarrow \Lambda + K$	
$\Delta \rightarrow \Sigma^* + K$	$\Sigma^* \rightarrow \Xi + K$	$\Xi^* \rightarrow \Xi^* + \pi$	
	$\Sigma^* \rightarrow \Delta + K$	$\Xi^* \rightarrow \Xi^* + \eta$	
	$\Sigma^* \rightarrow \Sigma^* + \pi$	$\Xi^* \rightarrow \Sigma^* + K$	
	$\Sigma^* \rightarrow \Sigma^* + \eta$	$\Xi^* \rightarrow \Omega + K$	
	$\Sigma^* \rightarrow \Xi^* + K$		

The one-loop corrections to the baryon mass is given by setting $\mathbf{p}^0 = 0$ in the self-energy contributions. Thus, the mass of the baryon state $|S, YI\rangle$ then reads:

$$m_{\mathbf{B}}(S, Y, I) = N_c m_0 + \frac{C_{HF}}{N_c} S(S+1) - \frac{c_1}{\Lambda} \hat{\chi}_+ + \delta m_{\mathbf{B}}^{1-loop+CT}(S, Y, I), \quad (9.7)$$

where $\delta m_{\mathbf{B}}^{1-loop+CT}(S, Y, I)$ involves contributions from the one-loop diagram in Fig. (8.1), and CT denotes counter-term contributions. From both types of contributions, there are $\mathcal{O}(\xi^2)$ and $\mathcal{O}(\xi^3)$ terms from the Lagrangians $\mathcal{L}_{\mathbf{B}}^{(2)}$ and $\mathcal{L}_{\mathbf{B}}^{(3)}$ respectively. The calculation is exact to the latter order, as can be deduced from the previous discussion on power counting. The notation for the $\mathcal{O}(\xi)$ mass shift is used: $\delta m_n \equiv \frac{C_{HF}}{N_c} S_n(S_n + 1) - \frac{c_1}{\Lambda} \hat{\chi}_+$. Note that C_{HF} is equal to the LO term in $M_{\Delta} - M_N$ in the real world $N_c = 3$.

9.4 Corrections to baryon mass relations

Mass relations among baryon states are a direct consequence of its symmetry structure. One can check those relations with the experimentally measured baryon masses. In nature, these mass relations are violated by small amounts. The sensitivity to the deviations from this relations is a good measure of the precision/validity of the symmetry behind the theory. In other words, the size of the violations to these mass relations indicate the predictive power of the theory. Three main mass relations namely, Gell-Mann-Okubo (GMO), Equal spacing (ES) and Gürsey-Radicati (GR) relations are analyzed to $\mathcal{O}(\xi^3)$. The relations are exact at tree level except the GR relation. The deviations to these relations are basically given by the non-analytic terms in the self-energy which will be briefly discussed under the analysis of each relation. It is very important to highlight that the violations to these mass relations are obtained explicitly in terms of N_c . This allows one to study the spin-flavor symmetry breaking of the mass relations at finite N_c .

9.4.1 Gell-Mann-Okubo (GMO) relation

The GMO relation and its violation can be defined as,

$$2(m_N + m_{\Xi}) = (3m_{\Lambda} + m_{\Sigma}) , \quad \Delta_{GMO} = 2(m_N + m_{\Xi}) - (3m_{\Lambda} + m_{\Sigma}) . \quad (9.8)$$

The combined effective theory exactly satisfies the GMO relation at tree level for any arbitrary N_c . It's very impressive to observe that the deviation to the GMO relation is calculable and the LECs it depends on is the C_{HF}, g_A , and F_{π} , where at leading order $C_{HF} = m_{\Delta} - m_N$. The experimentally observed baryon masses produce a deviation $\Delta_{GMO}^{\text{exp}} = 30 \pm 10$ whereas, the theoretical calculation from the fit to physical mass yields $\Delta_{GMO}^{\text{th}} = 44 \pm 5$, where for the theoretical evaluation $\dot{g}_A = \frac{6}{5} \times 1.27$ and $F_{\pi} = 93$ MeV.

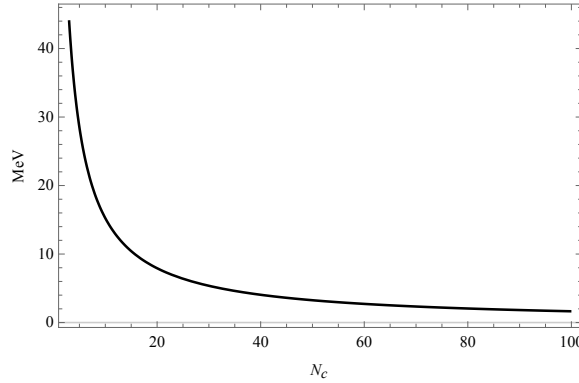


Figure 9.1. The deviation of GMO relation with N_c .

Another very important observation is that the Δ_{GMO}^{th} behaves like $1/N_c$ as depicted in Fig. (9.1), so that the GMO relation is exact at the large N_c limit. Since the complete expression for Δ_{GMO}^{th} is a lengthy expression, one can see the above observation by expanding it in the large N_c limit,

$$\begin{aligned} \Delta_{GMO} = & - \left(\frac{\dot{g}_A}{4\pi F_{\pi}} \right)^2 \left(\frac{2\pi}{3} (M_K^3 - \frac{1}{4} M_{\pi}^3 - \frac{2}{\sqrt{3}} (M_K^2 - \frac{1}{4} M_{\pi}^2)^{\frac{3}{2}}) \right. \\ & + \frac{2C_{HF}}{N_c} \left(-M_K^2 \log M_K^2 + \frac{1}{4} M_{\pi}^2 \log M_{\pi}^2 + (M_K^2 - \frac{1}{4} M_{\pi}^2) \log(\frac{4}{3} M_K^2 - \frac{1}{3} M_{\pi}^2) \right) \\ & + \mathcal{O}(1/N_c^3) . \end{aligned} \quad (9.9)$$

For the physical M_K and M_π one can check that the shown expansion is within 30% of the exact result, and the expansion seems to converge for $N_c > 5$. The explicit expression for Δ_{GMO} at $N_c = 3$ is,

$$\begin{aligned}
\Delta_{GMO} = & \frac{\dot{g}_A^2}{288F_\pi^2\pi} \left((4M_K^3 - M_\pi^3 - 3M_\eta^3) + 8(M_K^2 - C_{HF}^2)^{3/2} - 6(M_\eta^2 - C_{HF}^2)^{3/2} \right. \\
& - 2(M_\pi^2 - C_{HF}^2)^{3/2} \Big) + \frac{\dot{g}_A^2}{F_\pi^2\pi^2} \left(\frac{(C_{HF}^2 - M_K^2)^{3/2}}{18} \text{Tanh}^{-1} \left[\sqrt{\frac{C_{HF}^2}{C_{HF}^2 - M_K^2}} \right] \right. \\
& - \frac{(C_{HF}^2 - M_\eta^2)^{3/2}}{24} \text{Tanh}^{-1} \left[\sqrt{\frac{C_{HF}^2}{C_{HF}^2 - M_\eta^2}} \right] - \frac{(C_{HF}^2 - M_\pi^2)^{3/2}}{72} \text{Tanh}^{-1} \left[\sqrt{\frac{C_{HF}^2}{C_{HF}^2 - M_\pi^2}} \right] \Big) \\
& + \frac{\dot{g}_A^2}{F_\pi^2\pi^2} \left(-\frac{C_{HF}}{96} (4M_K^2 \text{Log}[M_K^2] - 3M_\eta^2 \text{Log}[M_\eta^2] - M_\pi^2 \text{Log}[M_\pi^2]) \right. \\
& \left. \frac{C_{HF}^3}{144} (4\text{Log}[M_K^2] - 3\text{Log}[M_\eta^2] - \text{Log}[M_\pi^2]) + \left(\frac{C_{HF}}{288} (4M_K^2 - M_\pi^2 - 3M_\eta^2) \right) (3\text{Log}[\mu^2] + 7) \right) ,
\end{aligned} \tag{9.10}$$

where, one can clearly see that the scale μ dependence vanishes in Eq. (9.10) when the GMO relation for mesons,

$$M_\eta^2 = \frac{(4M_K^2 - M_\pi^2)}{3} \tag{9.11}$$

is exact. Also note that, according to the expression in Eq. (9.10), Δ_{GMO} is exact (when $M_\eta = M_K = M_\pi$) in the $SU(3)$ symmetric limit.

9.4.2 Equal Spacing (ES) relation

ES relation involves three difference. Therefore, the violations can be studied by defining two differences Δ_{ES1} , Δ_{ES2} ,

$$\begin{aligned}
m_{\Sigma^*} - m_\Delta &= m_{\Xi^*} - m_{\Sigma^*} = m_\Omega - m_{\Xi^*} , \\
\Delta_{ES1} &= m_{\Xi^*} - 2m_{\Sigma^*} + m_\Delta , \quad \Delta_{ES2} = m_{\Omega^-} - 2m_{\Xi^*} + m_{\Sigma^*} .
\end{aligned} \tag{9.12}$$

With experimentally measured masses, Δ_{ES1} gives -6 ± 7 MeV and Δ_{ES2} gives -9 ± 7 MeV, whereas theoretically both of them are -14 ± 5 MeV. The behavior

of Δ_{ES1} and Δ_{ES2} with N_c are identical, and its expression can be expanded in $1/N_c$ gives,

$$\Delta_{\text{ES1}} = \Delta_{\text{ES2}} = \frac{\hat{g}_A^2}{N_c F_\pi^2} \left(\frac{4M_K^3 - M_\pi^3 - M_\eta^3}{64\pi} \right) + \mathcal{O}\left(\frac{1}{N_c^2}\right). \quad (9.13)$$

Since Δ_{ES1} and Δ_{ES2} have exactly the same behavior in N_c , then one can observe that the both deviations are identically vanish in the large N_c limit, as shown in Fig. (9.2).

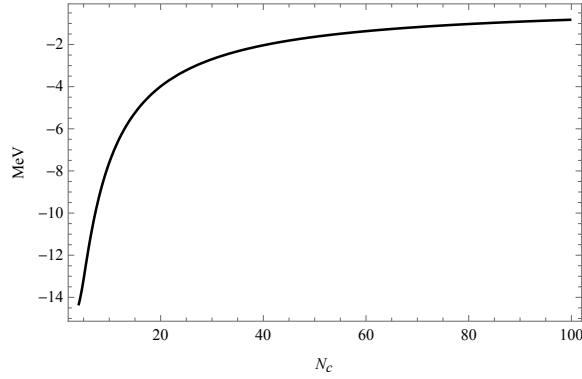


Figure 9.2. The deviation of ES1 and ES2 relation with N_c .

9.4.3 Gürsey-Radicati (GR) relation

In contrast to the GMO relation (or the ES relation) containing only the octet (decuplet) baryon masses, the Gürsey-Radicati (GR) mass relation connects both octet and decuplet masses. It relates $SU(3)$ breaking in the octet and decuplet, and which generalizes to arbitrary N_c . If one disregards the term proportional to h_2 in the $\mathcal{L}_{\mathbf{B}}^{(3)}$ in Eq. (8.15) which gives $SU(3)$ breaking in the hyperfine splittings, one obtains one additional relation first found by Gürsey and Radicati [20], namely:

$$m_{\Xi^*} - m_{\Xi} = m_{\Sigma^*} - m_{\Sigma}, \quad \Delta_{GR} = (m_{\Xi^*} - m_{\Xi}) - (m_{\Sigma^*} - m_{\Sigma}), \quad (9.14)$$

where, Δ_{GR} denotes the violation to the relation, which is 21 ± 7 MeV for the physical ground state baryon masses. The deviation of the relation (9.14) is due to $SU(3)$ breaking effects in the hyperfine interaction (C_{HF}) that splits **8** and **10** baryons, and

such a deviation starts with the term proportional to h_2 which is $\mathcal{O}(p^2/N_c)$ or $\mathcal{O}(\xi^3)$.

The one-loop contributions to GR relation are free of UV divergences, and the complete expression for the Δ_{GR} can be written as,

$$\begin{aligned}
\Delta_{GR} &= \frac{h_2}{\Lambda} \frac{12}{N_c} M_K^2 + \left(\frac{\dot{g}_A}{4\pi F_\pi} \right)^2 \left(\frac{2\pi}{9} M_K^3 + \frac{(9N_c - 43)\pi}{72} \left(M_K^2 - \left(\frac{3C_{HF}}{N_c} \right)^2 \right)^{\frac{3}{2}} \right. \\
&\quad - \frac{N_c - 3}{24} \left[3 \left(M_K^2 - \left(\frac{5C_{HF}}{N_c} \right)^2 \right)^{\frac{3}{2}} \left(\pi - 2 \arctan \frac{5C_{HF}}{N_c \sqrt{M_K^2 - \left(\frac{5C_{HF}}{N_c} \right)^2}} \right) \right. \\
&\quad \left. \left. + 10 \left(M_K^2 - \left(\frac{3C_{HF}}{N_c} \right)^2 \right)^{\frac{3}{2}} \arctan \frac{3C_{HF}}{N_c \sqrt{M_K^2 - \left(\frac{3C_{HF}}{N_c} \right)^2}} + \frac{240}{N_c^3} C_{HF}^3 \log M_K^2 \right] \right) \\
&\quad - (M_K \rightarrow M_\pi) , \\
&= \frac{h_2}{\Lambda} \frac{12}{N_c} (M_K^2 - M_\pi^2) + \frac{3\pi}{N_c} \left(\frac{\dot{g}_A C_{HF}}{4\pi F_\pi} \right)^2 (M_K - M_\pi) + \mathcal{O} \left(\frac{\log(M_K/M_\pi)}{N_c^3} \right) ,
\end{aligned} \tag{9.15}$$

where the last line corresponds to expanding in the large N_c limit. For the case with keeping $h_2 = 0$, the behavior of the Δ_{GR} with N_c is the same as for Δ_{GMO} , as depicted in Fig. (9.3).

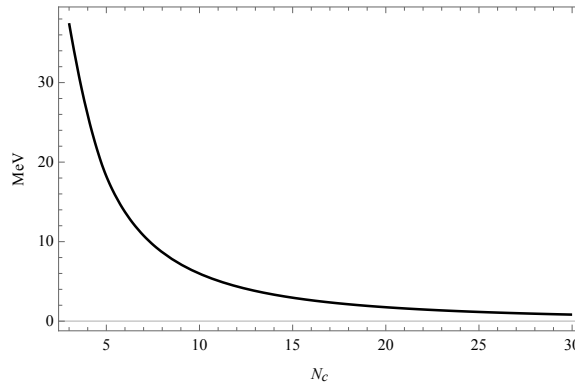


Figure 9.3. The deviation of Gürsey-Radicati (GR) relation with N_c .

9.5 Fits to the baryon spectrum

This sub-section is focused on an analysis and fits to the experimental baryon masses as well as the baryon masses from LQCD calculations for the case of $SU(3)$. The validity of the mass relations: GMO, ES and GR are checked at different quark masses using the experiment and LQCD inputs as well as, using the fitted masses from the combined effective theory. The fits are basically performed in two approaches: individual fits to baryon masses corresponds to a given quark mass, and combined fits of baryon masses in a range of quark masses.

The mass formula for the fit is,

$$m_B = N_c m_0 + \frac{C_{HF}}{N_c} \hat{S}^2 - \frac{c_1}{\Lambda} \hat{\chi}_+ + \delta m_B^{1-loop}(\mu) - \frac{1}{\Lambda} \left(\frac{c_2}{2} \hat{\chi}_+^0 + \frac{h_2}{N_c^2} \hat{\chi}_+ \hat{S}^2 + \frac{h_3}{N_c} \hat{\chi}_+^0 \hat{S}^2 + \frac{h_4}{N_c} \tilde{\chi}_+^8 S^i G^{i8} \right), \quad (9.16)$$

where, $\delta m_B^{1-loop}(\mu)$ is the self-energy contributions to the masses which depends on the renormalization scale μ and the scale $\Lambda (= \mu = m_\rho$ considered throughout this work), and $\tilde{\chi}_+^8 S^i G^{i8} = 4B_0 m_8 \langle S^i G^{i8} \rangle$ ¹.

The input experimental masses and calculated LQCD baryon masses by Alexandrou *et.al* [37] can be combined into the Table(9.2). The LQCD simulations in Ref. [37] have been carried out for ten ensembles of dynamical twisted mass fermion gauge configurations at three different values of the inverse bare lattice coupling β , namely $\beta = 1.90, 1.95$ and 2.10 . The β values correspond to three different lattice spacings $a = 0.094, 0.082$ and 0.065 fm. Therefore, each ensemble can be identified by the lattice spacing a and the bare twisted light quark (u, d) mass μ_l , where as the renormalized strange quark mass m_s is determined using the physical mass of Ω^-

¹ A useful formula for the term proportional to h_4 is:
 $\langle S^i G^{i8} \rangle = \frac{1}{\sqrt{3}} \left(\frac{3}{4} \hat{I}^2 - \frac{1}{4} \hat{S}^2 - \frac{1}{48} N_c (N_c + 6) + \frac{1}{8} (N_c + 3) Y - \frac{3}{16} Y^2 \right) = \frac{1}{16\sqrt{3}} (12\hat{I}^2 - 4\hat{S}^2 + 3\mathcal{S}(2 - \mathcal{S}))$,
 where \mathcal{S} is the strangeness. This term is responsible for the tree-level mass splitting between Λ and Σ , and also it is identical to the result obtained in Ref. [119]

baryon. The quantity $R(m_l, m_s, a)$ defined in Ref. [120] of ETMC collaboration, for the quark mass ratio in terms of pion and kaon masses:

$$R(m_l, m_s, a) \equiv \frac{m_l}{m_s} \left(\frac{2M_K^2 - M_\pi^2}{M_\pi^2} \right), \quad (9.17)$$

with the Fig. (11) of Ref. [120] can be used to obtain the values for M_π and M_K for each ensemble as given in Table (9.3).

Table 9.2. Baryon masses : The first row corresponds to the physical measurements. The rest are the masses from LQCD calculations [37], each column corresponds to a specific lattice spacing (or β value) given in accordance with the Table (9.3).

M_π	M_K	M_N	M_Λ	M_Σ	M_Ξ	M_Δ	M_{Σ^*}	M_{Ξ^*}	M_Ω
139	497	938(3)	1116(3)	1189(3)	1315(3)	1228(3)	1383(3)	1532(3)	1672(3)
261	524	1102.0(18.3)	1232.9(39.4)	1310.3(43.5)	1333.1(35.6)	1490.9(83.4)	1566.9(67.8)	1613.9(53.9)	1657.5(60.9)
298	528	1092.1(23.5)	1234.3(39.4)	1292.4(43.1)	1329.4(34.9)	1456.0(86.3)	1537.2(67.4)	1586.9(54.5)	1656.2(64.8)
332	537	1140.7(13.0)	1249.6(40.2)	1338.1(43.1)	1342.2(36.9)	1492.3(83.5)	1592.0(67.5)	1613.3(60.4)	1680.8(63.7)
256	528	1070.6(14.1)	1231.4(36.4)	1306.7(39.9)	1363.2(31.2)	1517.8(74.9)	1593.8(60.8)	1637.9(50.4)	1711.1(53.5)
302	541	1145.8(11.4)	1261.0(35.6)	1318.0(38.5)	1366.2(32.0)	1515.2(75.0)	1578.7(61.0)	1612.6(50.2)	1692.4(54.4)
372	555	1204.9(3.9)	1306.3(35.1)	1358.0(39.3)	1374.8(32.2)	1562.1(74.0)	1633.2(59.8)	1660.9(48.7)	1709.3(54.0)
432	576	1276.4(10.0)	1332.8(35.8)	1390.9(37.8)	1374.6(34.5)	1601.9(73.1)	1638.2(60.0)	1663.3(48.3)	1693.1(53.6)
213	489	1031.0(12.5)	1179.8(28.7)	1252.2(30.8)	1327.2(25.0)	1407.4(59.8)	1522.2(47.0)	1597.3(38.0)	1681.6(41.8)
246	499	1072.1(21.5)	1215.7(29.4)	1277.5(32.4)	1328.2(25.8)	1448.4(63.2)	1538.0(48.6)	1581.9(39.5)	1648.4(43.7)
298	511	1103.8(20.8)	1221.6(29.1)	1278.3(32.0)	1329.0(25.3)	1448.4(60.9)	1529.4(49.7)	1588.5(40.2)	1674.0(43.4)

9.5.1 Individual fits : physically (experimentally) measured masses

The fit result for the physically observed baryons can be summarized as Table (9.4). Note that the large value of the low energy constant m_0 corresponds to the correlation between the spin-flavor singlet and the quark mass contribution. The extracted value of C_{HF} has a very good agreement with the experimental value of

$$m_\Delta - m_N.$$

Table 9.3. LQCD parameters and the values of M_π and M_K from Ref. [37].

β	a	$a\mu_l$	$m_l(\text{MeV})$	$m_s(\text{MeV})$	$R(m_l, m_s, a)$	M_π	M_K
1.90	0.0936(13)	0.003	12.796	92.4	0.979	260.7	523.751
		0.004	17.079	92.4	0.98	297.5	528.076
		0.005	21.327	92.4	0.976	332.3	537.375
1.95	0.0823	0.0025	11.947	92.4	0.972	255.8	527.901
		0.0035	16.726	92.4	0.982	301.8	540.918
		0.0055	26.248	92.4	0.984	371.6	555.24
		0.0075	35.769	92.4	0.994	431.6	576.349
2.10	0.0646	0.0015	9.327	92.4	0.965	212.8	488.953
		0.0020	12.407	92.4	0.976	245.5	499.152
		0.0030	18.602	92.4	0.979	298.4	511.071

Table 9.4. Fit results for the physically observed baryons (the baryon mass for a given spin, hyper-charge and iso-spin is given in the Eq. (9.16)).

$M_\pi = 139 \text{ MeV}$	m_0		C_{HF}	c_1	c_2	h_2	h_3	h_4
$M_K = 497 \text{ MeV}$	866.8(6)		290.7(8)	-2.291(3)	3.437(4)	0.102(4)	1.280(6)	1.762(5)
$\chi^2=1.16$	M_N	M_Λ	M_Σ	M_Ξ	M_Δ	M_{Σ^*}	M_{Ξ^*}	M_Ω
Physical Mass (MeV)	938±3	1116±3	1189±3	1315±3	1228±5	1383±3	1532±3	1672±3
Fitted Mass (MeV)	936.5	1118.2	1189.7	1313.5	1227.9	1383.4	1531.4	1672.2
			Δ_{GMO}	Δ_{ES1}	Δ_{ES2}	Δ_{GR}		
Exp.			31(8)	-6(6)	-9(6)	23(6)		
Th.			44	-7.3	-7.3	24		

9.5.2 Individual fits : LQCD baryon masses

Similar to the case with physically measured baryons, one can perform fits to each set of LQCD baryons corresponding to individual ensembles in LQCD. The fit results are shown in Table (9.5) with three main rows representing the three lattice spacings

(with ten ensembles) given in Table (9.3). There are several observations which can be made if one re-arranges the rows in the order of increasing pion mass.

- The C_{HF} is consistently increasing with the pion mass.
- The c_1 ($SU(3)$ breaking) is behaving uniformly for all ten ensembles.

The baryon masses obtained from the fits to individual LQCD ensembles are summarized in Table (9.6). Therefore, one can analyze the mass relations directly with LQCD masses as well as the fitted masses from the theory. The results are given in Table (9.7).

Table 9.5. Fit results of LECs to individual sets of baryon masses from LQCD (the baryon mass for a given spin, hyper-charge and iso-spin is given in the Eq. (9.16)).

χ^2	M_π	M_K	m_0	C_{HF}	c_1	c_2	h_3	h_4
0.716	261	524	597(4)	591(3)	-2.22(3)	3.32(4)	0.13(2)	1.63(5)
0.962	298	528	599(5)	606(3)	-2.26(3)	3.39(4)	0.14(2)	1.6(1)
0.695	332	537	632(4)	620(2)	-2.31(3)	3.46(4)	0.12(2)	1.7(1)
1.23	256	528	610(4)	589(3)	-2.26(2)	3.39(2)	0.15(2)	1.6(1)
0.935	302	541	632(3)	618(2)	-2.23(2)	3.35(2)	0.15(2)	1.54(5)
0.743	372	555	684(1)	643(1)	-2.31(3)	3.46(4)	0.15(2)	1.59(3)
0.382	432	576	746(3)	680(2)	-2.31(3)	3.46(4)	0.13(2)	1.65(5)
0.606	213	489	536(3)	548(2)	-2.20(2)	3.30(2)	0.12(2)	1.59(3)
1.198	246	499	555(4)	566(3)	-2.20(3)	3.30(4)	0.13(2)	1.59(5)
0.808	298	511	576(4)	589(3)	-2.25(3)	3.37(4)	0.12(2)	1.58(5)

Table 9.6. Baryon masses obtained from the fits to LQCD data. Each line contains a set of baryon masses corresponding to their pion mass scale from LQCD.

χ^2	M_π	M_K	M_N	M_Λ	M_Σ	M_Ξ	M_Δ	M_{Σ^*}	M_{Ξ^*}	M_Ω
0.716	261	524	1105.28	1210.04	1301.03	1345.55	1473.64	1572.23	1628.81	1643.39
0.962	298	528	1098.26	1208.32	1282.05	1342.99	1437.81	1539.30	1605.91	1637.64
0.695	332	537	1142.20	1228.03	1329.86	1354.33	1490.30	1578.80	1637.60	1666.71
1.23	256	528	1072.79	1209.12	1297.58	1373.98	1490.90	1601.01	1666.71	1688.01
0.936	302	541	1146.54	1250.10	1313.79	1372.09	1486.0	1584.25	1644.29	1666.11
0.743	372	555	1205.08	1284.51	1349.10	1387.14	1555.08	1628.57	1676.19	1697.96
0.384	432	576	1277.22	1316.89	1385.02	1384.47	1592.39	1641.10	1672.03	1685.18
0.606	213	489	1032.25	1169.67	1248.19	1332.24	1392.01	1523.65	1615.30	1666.96
1.198	246	499	1078.89	1196.63	1269.79	1337.99	1432.80	1536.17	1602.58	1632.03
0.808	298	511	1107.6	1210.42	1273.81	1334.64	1428.05	1533.53	1609.68	1656.5

Table 9.7. Deviations from the mass relations using LQCD data (in black)
Vs fitted masses (in blue) from the combined effective theory.

M_π	M_K	Δ_{GMO}	Δ_{GR}	Δ_{ES1}	Δ_{ES2}
261	524	139±98, 30	24±103, 12	-29±138, -42	-3±118, -42
298	528	152±100, 25	13±103, 6	-32±140, -35	20±121, -35
332	537	121±99, 21	17±107, 34	-78±140, 30	46±126, 30
256	528	133±89, 31	-12±94, -11	-32±125, -44	29±108, -44
302	541	77±87, 27	-14±94, 2	-30±125, 38	46±108, 38
372	555	118±86, 18	11±92, 10	-43±122, 26	21±106, 26
432	576	87±89, 13	41±92, 32	-11±122, -18	5±106, -18
213	489	75±71, 28	0±72, 8	-40±97, -40	9±83, -40
246	499	124±77, 26	-7±75, -2	-46±101, -37	23±86, -37
298	511	78±76, 21	8±76, 15	-22±101, 29	26±87, 29

9.5.3 Combined fits to the lattice QCD masses

The LQCD calculations facilitate the ability to analyze baryon masses corresponding to a range of quark masses. In order to eliminate the quark-mass-dependence from the LECs, one has to consider the baryon masses within a range of quark masses. The quark-mass-range chosen in this work is: $M_\pi^{\text{physical}} \leq M_\pi \lesssim 300 \text{ MeV}$, such that the convergence of the low energy expansion is preserved according to our observations. There are 11 sets of baryon masses in total (i.e. each baryon has 11 masses correspond to a range of $140 \lesssim M_\pi \lesssim 430 \text{ MeV}$), if one combines the LQCD results from Ref [37] and the empirical masses. A naive fit of LECs to all the 11 sets of baryon masses result in imperfect fits as well as unnatural LECs. This constraints the selection of baryon masses corresponding to a particular range of quark-masses. After some effort trying numerous combinations, the baryon masses which correspond to the range of $140 \text{ MeV} \leq M_\pi \lesssim 300 \text{ MeV}$ gives reasonably good fits with LECs which acquire natural sizes.

Let's first consider the baryon masses from LQCD which are corresponding to the range of $M_\pi \lesssim 300 \text{ MeV}$. This includes five sets of baryon masses (for the cases : $M_\pi = \{213, 246, 256, 261, 302\}$) i.e., 40 baryon masses in total. In the fitting, the number of degrees of freedom is 35 since the total number of fitting parameters is 6. The fit results are given in the first row of Table(9.8). Notice that the value of m_0 gets smaller since it acquires the absolute spin-flavor singlet contribution by detaching with the $SU(3)$ flavor singlet (quark mass) contribution to the low energy constant c_2 . μ_2 is also redundant in this case, as it is the same for the individual fits to LQCD masses. C_{HF} also obtained a smaller value since it is correlated with μ_{20} which is also correlated with c_2 since the counter term of h_3 contains a quark mass contribution. The value of c_1 which governs the $SU(3)$ breaking has not much deviated from the average value extracted from individual fits. This observation indicates

that the $SU(3)$ breaking is approximately invariant with respect to the quark mass.

As the second step in the combined fitting approach, the set of physical baryon masses are added to the existing set of baryon masses from LQCD which were considered in the fits corresponding to the first row of Table (9.8). Therefore, the number of degrees of freedom increases to 43. The fit result is given in the second row of Table (9.8). Notice that the considerable amounts of changes can be observed only from the LECs : m_0, C_{HF}, h_3 and h_4 . This means that, the addition of physical masses to the fit affects the contributions to the baryon masses from the spin-flavor singlet component and the hyperfine interaction. In addition to these observations of LECs, one can check the deviations from the mass relations. The analysis of mass relations with this second combined fit results are given in Table (9.9). The LEC μ_2 which enters in Δ_{GR} is best determined by fixing it using Δ_{GR} in the physical case, and then the rest of the LECs are determined by the overall fit. In this way, the deviations of the mass relations are one of the predictions of the effective theory, and can therefore be used as a test of LQCD calculations. At present the errors in the LQCD calculations are relatively large, and thus such a test is not yet very significant.

Table 9.8. Results for LECs : first row fit to LQCD octet and decuplet baryon masses [37] including results for $M_\pi \leq 300$ MeV, and second row including also the physical masses. Throughout the renormalization scale is $\mu = m_\rho$.

χ^2_{dof}	m_0	C_{HF}	c_1	c_2	h_3	h_4
0.58	168(3)	182(7)	-2.39(2)	-1.49(3)	1.16(3)	1.95(3)
0.98	154(2)	220(4)	-2.36(1)	-1.57(2)	1.30(3)	1.89(2)

Table 9.9. Deviations from mass relations in MeV.

Here, $\Delta_{ES1} = m_{\Xi^*} - 2m_{\Sigma^*} + m_{\Delta}$ and $\Delta_{ES2} = m_{\Omega^-} - 2m_{\Xi^*} + m_{\Sigma^*}$.

M_{π} [MeV]	M_K [MeV]	Δ_{GMO}		Δ_{GR}		Δ_{ES1}		Δ_{ES2}	
		Exp	Th	Exp	Th	Exp	Th	Exp	Th
139	497	31±42	46	23±30	38	-6±30	-14	-9±30	-14
213	489	75±70	33	0±72	29	-40±97	-11	9.2±83	-11
246	499	124±77	30	-7±75	25	-46±101	-11	23±86	-11
255	528	133±89	37	-12±94	26	-32±125	-14	29±108	-14
261	524	139±99	35	24±103	25	-29±138	-13	-3±119	-13
302	541	77±87	32	-14±94	23	-30±125	-13	46±108	-13

Using the fit results, one can plot the evolution of each baryon mass with respect to the pion mass as given in Fig. (9.4). The plot includes, the theoretical predictions with error-bands (in blue-green) and the masses from experiment + LQCD (in red). Regarding the theoretical prediction, the 67% confidence interval is represented by the light blue, and 95% confidence interval is represented by light green.

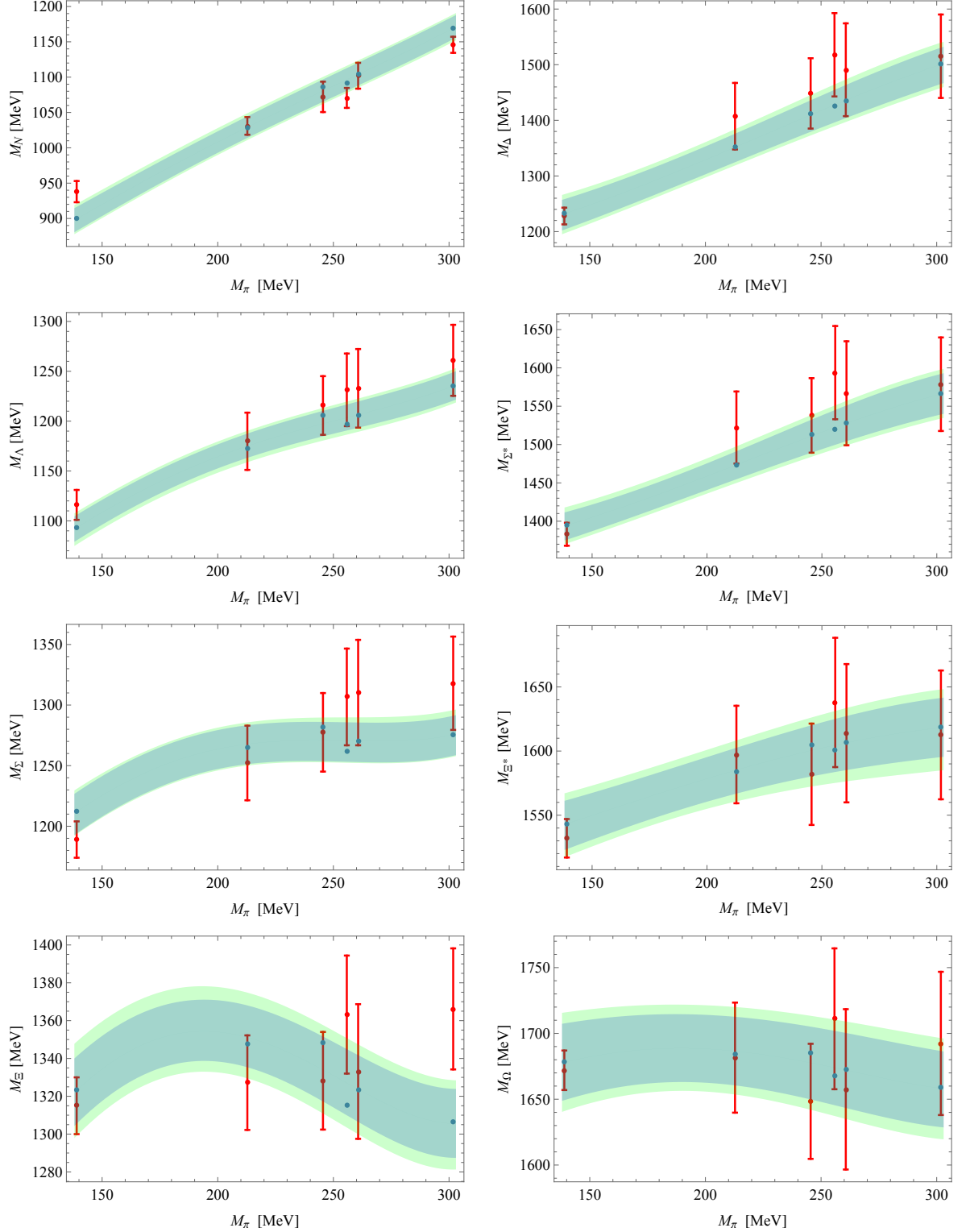


Figure 9.4. The evolution of baryon masses obtained from the combined fit result (second row of Table (9.8)) with respect to the pion mass. The 67% confidence interval is represented by the band of light blue, and 95% confidence interval is represented by the band of light green. The red points with error bars are the calculations from LQCD [37].

9.6 Predictions on sigma terms

From the baryon masses the σ -terms are derived according to the definition,

$$\sigma_{Bm_q} \equiv m_q \frac{\partial m_B}{\partial m_q} , \quad (9.18)$$

where, m_q has several choices, for example;

$$m_q = \left\{ \begin{array}{c} \hat{m} , \\ m_s , \\ m^0 = (2\hat{m} + m_s)/3 , \\ m^8 = 1/\sqrt{3}(\hat{m} - m_s) . \end{array} \right\} . \quad (9.19)$$

The m^0 and m^8 are $SU(3)$ singlet and octet components of the quark masses. Naturally the set of σ -terms will satisfy the same relations discussed above for the masses. These relations are exact at tree the tree level, and the deviations occur due to the loop corrections. The σ -terms associated with the same m_q are related via those relations and their deviations are calculable as described before for the masses. In addition to the GMO and ES relations one finds the following tree level $\mathcal{O}(\xi^3)$ relations,

$$\begin{aligned} \sigma_{Nm_s} &= \frac{m_s}{8\hat{m}} (-4(N_c - 1) \sigma_{N\hat{m}} + (N_c + 3) \sigma_{\Lambda\hat{m}} + 3(N_c - 1) \sigma_{\Sigma\hat{m}}) \\ \sigma_{\Lambda m_s} &= \frac{m_s}{8\hat{m}} (-4(N_c - 3) \sigma_{N\hat{m}} + (N_c - 5) \sigma_{\Lambda\hat{m}} + 3(N_c - 1) \sigma_{\Sigma\hat{m}}) \\ \sigma_{\Sigma m_s} &= \frac{m_s}{8\hat{m}} (-4(N_c - 3) \sigma_{N\hat{m}} + (N_c + 3) \sigma_{\Lambda\hat{m}} + (3N_c - 11) \sigma_{\Sigma\hat{m}}) \\ \sigma_{\Delta m_s} &= \frac{m_s}{8\hat{m}} (-4(N_c - 1) \sigma_{\Delta\hat{m}} - 5(N_c - 3)(\sigma_{\Lambda\hat{m}} - \sigma_{\Sigma\hat{m}}) + 4N_c \sigma_{\Sigma^*\hat{m}}) \\ \sigma_{\Sigma^* m_s} &= \frac{m_s}{8\hat{m}} (-(N_c - 3)(4 \sigma_{\Delta\hat{m}} + 5 \sigma_{\Lambda\hat{m}} - 5 \sigma_{\Sigma\hat{m}}) + 4(N_c - 2) \sigma_{\Sigma^*\hat{m}}). \end{aligned} \quad (9.20)$$

Several of these relations are poorly satisfied. The deviations are calculable and given by the non-analytic contributions to one-loop. It is easy to understand why these relations receive large corrections. The reason is that, they behave as $\mathcal{O}(p^3 N_c)$ in the large N_c limit. This implies that any tree level relation one may use to relate m_s and \hat{m} , thus the σ terms will receive in principle such large non-analytic deviations. In the physical case $N_c = 3$, those deviations are numerically large for the first, third,

and fourth relations above. This in particular affects the nucleon strangeness σ term, and thus indicates that its estimation from arguments based on tree level relations for an arbitrary N_c , is subject to important corrections such as for the nucleon- $\hat{\sigma}$ [121]. In terms of the octet components of the quark masses, in addition to GMO and ES relations one finds:

$$\sigma_{N m_8} = \frac{(N_c + 3) \sigma_{\Lambda m_8} + 3(N_c - 1) \sigma_{\Sigma m_8}}{4(N_c - 3)}, \quad (9.21)$$

$$\sigma_{\Delta m_8} = \frac{-5(N_c - 3) \sigma_{\Lambda m_8} + 5(N_c - 3) \sigma_{\Sigma m_8} + 4N_c \sigma_{\Sigma^* m_8}}{4(N_c - 3)}, \quad (9.22)$$

where it can be readily checked that they are well defined for $N_c \rightarrow 3$ as the numerators on the RHS are proportional to $(N_c - 3)$. These relations are violated as $\mathcal{O}(p^3 N_c^0)$ in the large N_c . For both relations in the limit $N_c \rightarrow \infty$ one finds $\text{LHS} - \text{RHS} = \frac{N_c}{128\pi} \left(\frac{\dot{g}_A}{F_\pi} \right)^2 (M_K - M_\pi)(M_K^2 - M_\pi^2) + \mathcal{O}(1/N_c)$. Thus they are not as precise as the GMO and ES relations. Finally, if the LEC constant h_2 vanishes, one has one extra tree-level relation related to Eq. (9.14), namely,

$$\sigma_{\Xi^* m_8} - \sigma_{\Sigma^* m_8} - (\sigma_{\Xi m_8} - \sigma_{\Sigma m_8}) = 0 \quad (9.23)$$

whose deviation behaves as $\mathcal{O}(1/N_c^2)$ in the large N_c limit, and thus expected to be very good.

9.7 Conclusions and discussion

There are some key observations extracted from the analysis of the baryon masses. Considering the aspect of fitting, the ξ -expansion works very well with all the physically measured ground-state baryon masses. Also, the fit results for the individual set of baryon masses corresponding to it's LQCD ensemble, shows that the theory works pretty well up to the quark mass scale around ~ 300 MeV. This can be directly observed by the theoretical predictions (see Fig. (9.4)) from the *combined* fit, which refers to the fit including all the baryon masses (physical+LQCD) up to ~ 300 MeV

quark mass scale.

Another important fact is that, the one-loop corrections to the self-energy includes the decuplet contributions in the loop-corrections. This improves the convergence of the expansion, which reflects in the good behavior of $SU(3)$ symmetry. For example, the GMO, ES mass relations are exact at the tree level for any arbitrary N_c and the deviations to those relations are from the loop corrections. These corrections are calculable and also behave as $\mathcal{O}(1/N_c)$, i.e., the mass relations become exact in the large N_c limit.

Moreover, the baryon masses from this combined approach allows one to determine the quark mass dependence to the baryon masses, i.e., in other words the baryon σ -terms. The idea of the *combined-fit* is to study the baryon masses on this aspect, because the LECs extracted from the combined fit are independent of the quark mass scale. Once the LECs are fixed from the combined fit, one can simply study the behavior of baryon masses with respect to quark masses. Therefore this framework can be used to predict the σ -terms with the corrections up to $\mathcal{O}(1/N_c)$ for all ground-state baryons. Also, this can address the ambiguity in the value of the nucleon- $\hat{\sigma}$ at the physical point ($M_\pi = 139$ MeV) with the corrections of $\mathcal{O}(1/N_c)$ which is the same for the case of GMO relation [121].

CHAPTER 10

BARYON CURRENTS (VECTOR AND AXIAL-VECTOR) FROM THE COMBINED APPROACH

10.1 Introduction

This chapter is focused on calculating the baryon vector currents and axial-vector currents. The notion of *baryon currents* were initially introduced by R. C. Hwa and J. Nuyts in Ref. [122]. On the basis of the quark model, one can construct the baryon currents as linear combinations of the products of three quarks. Then, using the canonical anti-commutation relations for the quarks, the equal-time commutation relations of the baryon currents. The $1/N_c$ expansion framework with the quark operators as the operator basis provides the framework to study the baryon spin-flavor structure [11–14]. Also, baryon decays play a crucial role on $SU(3)$ flavor symmetry breaking as well as the chiral $SU(3) \times SU(3)$ symmetry breaking [123]. Therefore, the combined effective framework can be used to study the spin-flavor-chiral symmetry and its breaking effects. At the tree-level, the u^{ia} : *chiral vielbein* in the LO Lagrangian in Eq. (8.13) contains the chiral currents and one can expand it to obtain the interaction vertices associated with the baryon currents as well as the meson-baryon-current interactions. Since the focus of this work is to calculate the one-loop corrections to the baryon currents, one also needs the meson Lagrangian in Eq. (7.95) (with covariant derivative fields D_μ instead of ∂_μ to include the external currents) in order to consider the currents entering to the loop through the GB propagator.

Hadronic weak currents possess the V-A structure of the weak interactions. In general, a hadronic weak current J_μ can be defined as,

$$J_\mu = V_\mu - A_\mu , \quad (10.1)$$

where,

$$\begin{aligned} V_\mu &= V_{ud}\bar{u}\gamma_\mu d + V_{us}\bar{u}\gamma_\mu s && : \text{Vector current} , \\ A_\mu &= V_{ud}\bar{u}\gamma_\mu\gamma_5 d + V_{us}\bar{u}\gamma_\mu\gamma_5 s && : \text{Axial-vector current} . \end{aligned} \quad (10.2)$$

V_{ud}, V_{us} are the elements of Cabibbo-Kobayashi-Maskawa matrix (or CKM matrix) [124, 125]. Therefore the matrix elements of V_μ and A_μ between the baryon states with same spin (denoted as B_1 and B_2) has the general forms [123] :

$$\langle B_2 | V_\mu | B_1 \rangle = V_{CKM} \bar{u}_{B_2}(p_2) \left[f_1(q^2) \gamma_\mu + \frac{f_2(q^2)}{M_{B_1}} \sigma_{\mu\nu} q^\nu + \frac{f_3(q^2)}{M_{B_1}} q_\mu \right] u_{B_1}(p_1) , \quad (10.3)$$

$$\langle B_2 | A_\mu | B_1 \rangle = V_{CKM} \bar{u}_{B_2}(p_2) \left[g_1(q^2) \gamma_\mu + \frac{g_2(q^2)}{M_{B_1}} \sigma_{\mu\nu} q^\nu + \frac{g_3(q^2)}{M_{B_1}} q_\mu \right] \gamma_5 u_{B_1}(p_1) , \quad (10.4)$$

where V_{CKM} represents the corresponding element of CKM matrix, $q \equiv p_1 - p_2$ is the momentum transfer, and u_{B_i} is the Dirac spinor of the i^{th} baryon. The vector (axial-vector) matrix element is characterized by the form factors $f_i(q^2)$ ($g_i(q^2)$), and the leading form factor can be denoted as $f_1(0) = g_V$ ($g_1(0) = g_A$).

In addition to the introduction, this chapter includes two more sections dedicated to vector currents, axial-vector currents including fit results to LQCD calculations [38].

10.2 Vector currents: charges

In this section the one-loop corrections to the vector current charges are calculated. The study is similar to that carried out in [123]. In the rest frame of a baryon with the presence of an external current, the dominant contribution to the matrix elements of the vector current is the corresponding charge, which is of $\mathcal{O}(\xi^0)$. The sub-leading terms are proportional to $\mathcal{O}(q/N_c)$, where q is the 4-momentum transfer through the external current. Therefore, $q \sim M_{B_1} - M_{B_2} \sim \mathcal{O}(p^2)$, where M_{B_i} is the rest-mass of the i^{th} baryon involve with the vector current.

At $q^2 = 0$, the baryon matrix elements for the vector current in the limit of exact $SU(3)$ symmetry are simply given by the matrix elements of the associated charge or $SU(3)$ generator T^a . According the the Ademollo-Gatto theorem (AGT) [126], the vector coupling constants to the first order in the symmetry-breaking interaction, are not renormalized. An application to this theorem is strangeness-violating leptonic decays of baryons and mesons. The theorem implies the amplitude of the vector currents in the limit $q^2 \rightarrow 0$ are uniquely predicted up to first order in symmetry breaking. In other words, the matrix elements of charge operator can deviate from the symmetry only to second order in symmetry breaking [127]. Therefore, at lowest order, the charges are simply given by the $SU(3)$ generators : T^a , and the one-loop corrections are UV finite. Since up to $\mathcal{O}(\xi^3)$ the AGT is satisfied, the corrections to the charges are unambiguously given at one-loop by the non-analytic contributions from the loops.

The one-loop diagrams are given in Fig. (10.1), and the corrections to the charges are obtained by evaluating the diagrams at $q \rightarrow 0$. In that limit the UV divergencies as well as the finite polynomial terms in quark masses and $\delta\hat{m}$ cancel in each of the

two sets of diagrams, $\{A+B\}$, and $\{C+D+E\}$, as required by the AGT. The results for the diagrams are the following:

$$\begin{aligned}
\{A\} &= -\frac{i}{2F_\pi^2} f^{abc} f^{bcd} T^d I(0, 1, M_b^2) \\
\{B\} &= \frac{i}{4F_\pi^2} f^{abc} f^{bcd} T^d (q_0^2 K(q, M_b, M_c) + 4q_0 K^0(q, M_b, M_c) + 4K^{00}(q, M_b, M_c)) \\
\{C\} &= \frac{1}{2} \{T^a, \delta \hat{Z}_{1-loop}\} \\
\{D\} &= i \left(\frac{\dot{g}_A}{F_\pi} \right)^2 \sum_{n_1, n_2} G^{ib} \mathcal{P}_{n_2} T^a \mathcal{P}_{n_1} G^{jb} \frac{1}{q_0 - \delta m_{n_2} + \delta m_{n_1}} \\
&\quad \times (H_{ij}(p_0 - \delta m_{n_1}, M_b) - H_{ij}(p_0 + q_0 - \delta m_{n_2}, M_b)) \\
\{E\} &= \left(\frac{\dot{g}_A}{F_\pi} \right)^2 f^{abc} \sum_n G^{ib} \mathcal{P}_n G^{jc} H_{ij0}(p_0 - \delta m_n, q, M_b, M_c), \tag{10.5}
\end{aligned}$$

where the integrals K , K^μ , $K^{\mu\nu}$, H_{ij} and H_{ij0} are given in Appendix C. Since the temporal component of the current can only connect baryons with the same spin, q_0 is equal to the $SU(3)$ breaking mass difference between them plus the kinetic energy transferred by the current, which are all $\mathcal{O}(p^2)$, and can be neglected: so one can take the limit $q_0 \rightarrow 0$ in the end. Diagram $\{D\}$ requires a careful handling of the limit in the cases when the denominator vanishes. The same is the case for diagram $\{F\}$ in the axial-vector currents in next section. The $U(1)$ baryon number current is used to check the calculation: only diagrams $C+D$ contribute, and as required cancel each other.

The UV divergent and polynomial pieces contributed by the diagrams in Fig. (10.1) can be explicitly calculated, and are given as follows.

$$\begin{aligned}
\{A\}^{\text{poly}} &= \frac{\lambda_\epsilon + 1}{(4\pi)^2} \frac{1}{2F_\pi^2} f^{abc} f^{bcd} M_b^2 T^d \\
\{B\}^{\text{poly}} &= -\frac{\lambda_\epsilon + 1}{(4\pi)^2} \frac{1}{2F_\pi^2} f^{abc} f^{bcd} T^d (M_b^2 + \frac{1}{6} \vec{q}^2) \\
\{C\}^{\text{poly}} &= \frac{1}{(4\pi)^2} \left(\frac{\dot{g}_A}{F_\pi} \right)^2 \frac{1}{2} \{ T^a, (\lambda_\epsilon + 1) M_b^2 G^{ib} G^{ib} - 2(\lambda_\epsilon + 2) G^{ib} [\delta\hat{m}, [\delta\hat{m}, G^{ib}]] \} \\
\{D\}^{\text{poly}} &= \frac{1}{(4\pi)^2} \left(\frac{\dot{g}_A}{F_\pi} \right)^2 \frac{1}{3} \sum_{n_1, n_2} G^{ib} \mathcal{P}_{n_2} T^a \mathcal{P}_{n_1} G^{ib} \frac{1}{q_0 - \delta m_{n_2} + \delta m_{n_1}} \\
&\quad \times \{ (p_0 - \delta m_{n_1}) (3(\lambda_\epsilon + 1) M_b^2 - 2(\lambda_\epsilon + 2)(p_0 - \delta m_{n_1})^2 - \{p_0 \rightarrow p_0 + q_0, \delta m_{n_1} \rightarrow \delta m_{n_2}\}) \} \\
&= \frac{1}{(4\pi)^2} \left(\frac{\dot{g}_A}{F_\pi} \right)^2 \frac{1}{3} \{ -3(\lambda_\epsilon + 1) M_b^2 G^{ib} T^a G^{ib} \\
&\quad + 2(\lambda_\epsilon + 2) ([\delta\hat{m}, [\delta\hat{m}, G^{ib}]] T^a G^{ib} + G^{ib} T^a [\delta\hat{m}, [\delta\hat{m}, G^{ib}]] - [\delta\hat{m}, G^{ib}] T^a [\delta\hat{m}, G^{ib}]) \} \\
\{E\}^{\text{poly}} &= -\frac{1}{(4\pi)^2} \left(\frac{\dot{g}_A}{F_\pi} \right)^2 \frac{i}{6} f^{abc} \sum_n G^{ib} \mathcal{P}_n G^{jc} \{ \lambda_\epsilon (2q^i q^j + q^2 g^{ij}) + q^2 g^{ij} \\
&\quad - 3 g^{ij} ((\lambda_\epsilon + 1)(M_b^2 + M_c^2) - (\lambda_\epsilon + 2)(\delta m_{in} - 2\delta m_n + \delta m_{out})^2) \} \\
&= -\frac{1}{(4\pi)^2} \left(\frac{\dot{g}_A}{F_\pi} \right)^2 \frac{i}{6} \{ ((2q^i q^j + q^2 g^{ij}) \lambda_\epsilon - q^2 g^{ij}) [T^a, G^{ib}] G^{jb} \\
&\quad + 3(\lambda_\epsilon + 1) M_b^2 [[T^a, G^{ib}], G^{jb}] - 3(\lambda_\epsilon + 2) ([T^a, G^{ib}], [\delta\hat{m}, [\delta\hat{m}, G^{jb}]] \\
&\quad + [[\delta\hat{m}, G^{ib}], [T^a, [\delta\hat{m}, G^{ib}]]]) \} ,
\end{aligned} \tag{10.6}$$

where in the evaluations one sets $p_0 \rightarrow \delta m_{in}$ and $p_0 + q_0 \rightarrow \delta m_{out}$. Combining the polynomial pieces and using that $[\delta\hat{m}, T^a] = [\delta\hat{m}, \hat{G}^2] = [\delta\hat{m}, G^{ib} T^a G^{ib}] = 0$, one finally obtains:

$$\begin{aligned}
\{A + B\}^{\text{poly}} &= -\frac{\lambda_\epsilon + 1}{(4\pi)^2} \frac{\vec{q}^2}{4F_\pi^2} T^a \\
\{C + D + E\}^{\text{poly}} &= \frac{\lambda_\epsilon - 3}{(4\pi)^2} \left(\frac{\dot{g}_A}{4F_\pi} \right)^2 \vec{q}^2 T^a
\end{aligned} \tag{10.7}$$

As required by the AGT, when $q \rightarrow 0$ the UV divergences and polynomial terms vanish for all the $SU(3)$ vector charges of the baryon spin-favor multiplet. The calculation of the finite non-analytic contributions has been carried out in previous work [123], and will not be revisited here.

The only counter term required is the one proportional to g_E in Eq. (8.15), where $\gamma_{g_E} = \frac{1}{(4F_\pi)^2}(4 - \dot{g}_A^2)$, and which provides the only unknown analytic contribution to the octet and decuplet charge radii up to the order of the calculation. More details will be presented elsewhere in a study of the vector current's form factors. In the context of the charge form factors, studies implementing the $1/N_c$ expansion for extracting the long distance charge distribution of the nucleon has been carried out in Refs. [128–131].

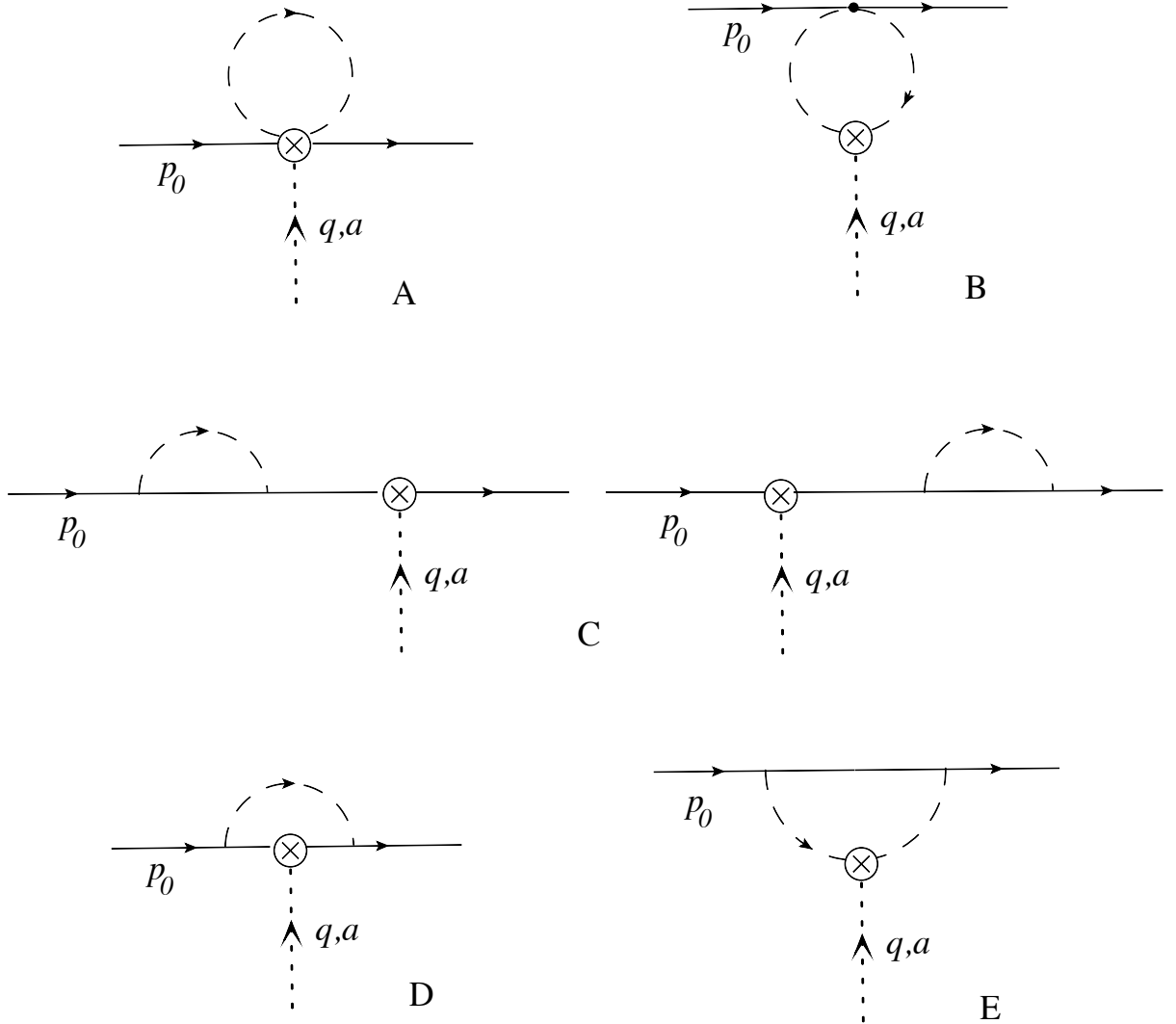


Figure 10.1. Diagrams contributing to the 1-loop corrections to the vector charges.

10.3 Axial couplings

In this section, the axial vector currents are studied to one-loop. At the tree level the axial vector currents have two contributions, namely the contact term and the GB pole ones, and reads:

$$A^{\mu a} = \dot{g}_A G^{ja} (g_j^\mu - \frac{q^\mu q_j}{q^2 - M_a^2}). \quad (10.8)$$

In the non-relativistic limit, or equivalently large N_c limit, the time component of the axial vector current is suppressed with respect to the spatial components. The couplings associated with the latter are analyzed below to $\mathcal{O}(\xi^2)$.

At the leading order the axial couplings are all given in by the coupling \dot{g}_A . For $N_c = 3$ one obtains: $F = \dot{g}_A/3$, $D = \dot{g}_A/2$, and the axial coupling in the decuplet baryons is $\mathcal{H} = \dot{g}_A/6$. The one-loop diagrams contributing at that order are shown in Fig.(10.2). The matrix elements of interest for the axial currents are $\langle \mathbf{B}' | A^{ia} | \mathbf{B} \rangle$ evaluated at vanishing external 3-momentum. The axial couplings are then defined by:

$$\langle \mathbf{B}' | A^{ia} | \mathbf{B} \rangle = g_A^{\mathbf{B}\mathbf{B}'} \frac{6}{5} \langle \mathbf{B}' | G^{ia} | \mathbf{B} \rangle. \quad (10.9)$$

The axial couplings defined here are $\mathcal{O}(N_c^0)$. The $\mathcal{O}(N_c)$ of the matrix elements of the axial currents is due to the operator G^{ia} . The factor 6/5 mentioned earlier is included so that g_A^{NN} at $N_c = 3$ exactly corresponds to the usual nucleon g_A , which has the value 1.2723 ± 0.0023 [39]. This definition of the axial couplings is convenient in the context of the $1/N_c$ expansion, as the differences between the different axial couplings are $\mathcal{O}(1/N_c^2)$.

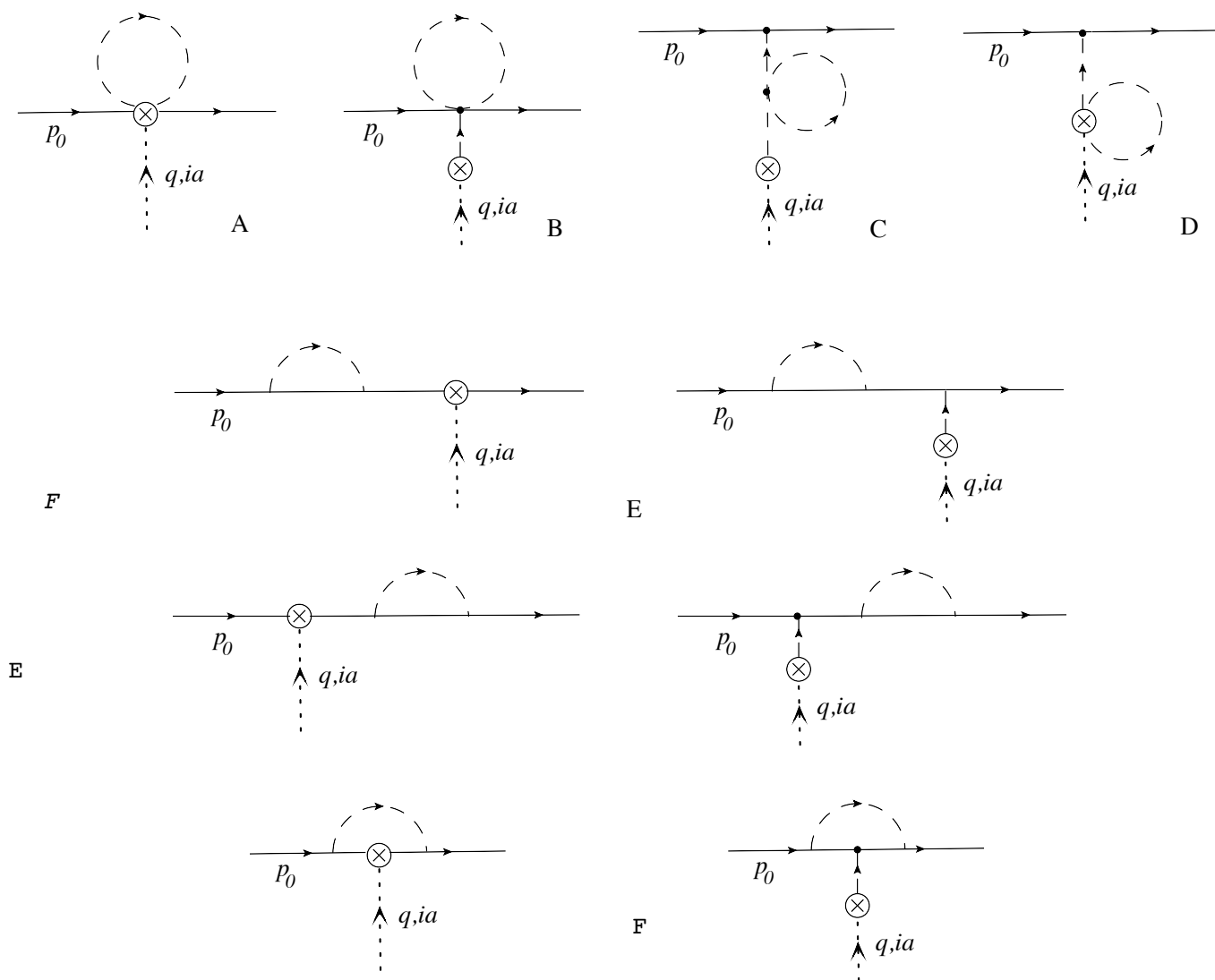


Figure 10.2. Diagrams contributing to the 1-loop corrections to the axial vector currents.

The results for the diagrams are the following:

$$\begin{aligned}
\{A\} &= -g_i^\mu \frac{\dot{g}_A}{2F_\pi^2} f^{abc} f^{cdb} G^{id} I(0, 1, M_b) \\
\{B\} &= \frac{\dot{g}_A}{6F_\pi^2} \frac{q^\mu q_i}{q^2 - M_a^2} f^{abc} f^{cdb} G^{id} I(0, 1, M_b) \\
\{C\} &= \frac{2\dot{g}_A}{3F_\pi^2} \frac{q^\mu q_i}{q^2 - M_d^2} f^{abc} f^{cdb} G^{id} I(0, 1, M_b) \\
\{D\} &= -\frac{\dot{g}_A}{3F_\pi^2} \frac{q^\mu q_i}{q^2 - M_a^2} f^{abc} f^{cdb} G^{id} I(0, 1, M_b) \\
\{E\} &= \frac{1}{2} \dot{g}_A (g_i^\mu - \frac{q^\mu q_i}{q^2 - M_a^2}) \{G^{ia}, \delta \hat{Z}_{1\text{-loop}}\} \\
\{F\} &= i(g_i^\mu - \frac{q^\mu q_i}{q^2 - M_a^2}) \dot{g}_A \left(\frac{\dot{g}_A}{F_\pi} \right)^2 \sum_{n_1, n_2} G^{jb} \mathcal{P}_{n_2} G^{ia} \mathcal{P}_{n_1} G^{kb} \frac{1}{q_0 - \delta m_{n_2} + \delta m_{n_1}} \\
&\quad \times (H_{jk}(p_0 - \delta m_{n_1}, M_b) - H_{jk}(p_0 + q_0 - \delta m_{n_2}, M_b)) . \tag{10.10}
\end{aligned}$$

The corresponding polynomial terms of these one loop contributions are:

$$\begin{aligned}
\{A\}^{\text{poly}} &= \frac{1}{(4\pi)^2} \frac{\dot{g}_A}{2F_\pi^2} (\lambda_\epsilon + 1) g_i^\mu f^{abc} f^{bcd} G^{id} M_b^2 \\
\{B\}^{\text{poly}} &= -\frac{1}{(4\pi)^2} \frac{\dot{g}_A}{6F_\pi^2} (\lambda_\epsilon + 1) \frac{q^\mu q_i}{q^2 - M_a^2} f^{abc} f^{bcd} G^{id} M_b^2 \\
\{C\}^{\text{poly}} &= -\frac{1}{(4\pi)^2} \frac{2\dot{g}_A}{3F_\pi^2} (\lambda_\epsilon + 1) \frac{q^\mu q_i}{q^2 - M_d^2} f^{abc} f^{bcd} G^{id} M_b^2 \\
\{D\}^{\text{poly}} &= \frac{1}{(4\pi)^2} \frac{\dot{g}_A}{3F_\pi^2} (\lambda_\epsilon + 1) \frac{q^\mu q_i}{q^2 - M_a^2} f^{abc} f^{bcd} G^{id} M_b^2 \\
\{E\}^{\text{poly}} &= \frac{1}{(4\pi)^2} \frac{1}{2} \dot{g}_A \left(\frac{\dot{g}_A}{F_\pi} \right)^2 (g_i^\mu - \frac{q^\mu q_i}{q^2 - M_a^2}) \tag{10.11}
\end{aligned}$$

$$\begin{aligned}
&\times \{G^{ia}, (\lambda_\epsilon + 1) M_b^2 G^{jb} G^{jb} - 2(\lambda_\epsilon + 2) G^{jb} [\delta \hat{m}, [\delta \hat{m}, G^{jb}]]\} \\
\{F\}^{\text{poly}} &= -\frac{1}{(4\pi)^2} \dot{g}_A \left(\frac{\dot{g}_A}{F_\pi} \right)^2 (g_i^\mu - \frac{q^\mu q_i}{q^2 - M_a^2}) \left((\lambda_\epsilon + 1) M_b^2 G^{jb} G^{ia} G^{jb} \right. \\
&\quad - \frac{2}{3} (\lambda_\epsilon + 2) (G^{jb} G^{ia} [\delta \hat{m}, [\delta \hat{m}, G^{jb}]] \\
&\quad \left. + [\delta \hat{m}, [\delta \hat{m}, G^{jb}]] G^{ia} G^{jb} - [\delta \hat{m}, G^{jb}] G^{ia} [\delta \hat{m}, G^{jb}]) \right) . \tag{10.12}
\end{aligned}$$

The conservation of the axial currents is readily checked in the chiral limit. At this point it is important to check the cancellation of the N_c power counting violating terms shown in the polynomial terms of diagrams E and F . Such terms cancel in the

sum, as it is easy to show using the results displayed in Appendix ?? for the axial vector currents. One obtains:

$$\begin{aligned}
\{E + F\}^{\text{poly}} &= \frac{1}{(4\pi)^2} \dot{g}_A \left(\frac{\dot{g}_A}{F_\pi} \right)^2 \left(g_i^\mu - \frac{q^\mu q_i}{q^2 - M_a^2} \right) \\
&\times \left((\lambda_\epsilon + 1) \frac{1}{6} B_0 (23 m^0 G^{ia} + \frac{11}{4} d^{abc} m^b G^{ic} + \frac{5}{3} m^a S^i) \right. \\
&+ (\lambda_\epsilon + 2) \frac{C_{HF}^2}{N_c^2} \left(\left(1 - \frac{N_c(N_c + 6)}{3} \right) G^{ia} + \frac{11}{6} (N_c + 3) S^i T^a \right. \\
&\left. \left. - \frac{8}{3} \{\hat{S}^2, G^{ia}\} - \frac{4}{3} S^i \{S^j, G^{ja}\} + \frac{11}{6} \hat{S}^2 G^{ia} \hat{S}^2 \right) \right) \quad (10.13)
\end{aligned}$$

The quark mass dependent UV divergencies are $\mathcal{O}(m_q/N_c)$, and the quark mass independent ones give a term proportional to G^{ia} , i.e., to the LO term but suppressed by a factor $1/N_c$, while the rest of the terms are $\mathcal{O}(1/N_c^2)$ or higher. The cancellation mechanism that eliminates the N_c counting violating terms must be rather subtle, as it required an explicit and lengthy calculation starting from Eq. (10.12)

In order to obtain the counter terms one uses the relations given in Appendix D. The counter terms are contained in the Lagrangians $\mathcal{L}_{\mathbf{B}}^{(2,3)}$, and the corresponding β -functions are the ones shown in Table(10.1). In addition to \dot{g}_A , there are seven LECs that are necessary to renormalize the axial vector couplings for generic N_c . For $N_c = 3$ the terms proportional to $C_{1,2,3}^A$ are linearly dependent and one is eliminated. At $N_c = 3$, after considering isospin symmetry, there are thirty four axial couplings associated with the axial currents mediating transitions in the spin-flavor multiplet of baryons. This means that there are twenty seven relations among those couplings that must be satisfied at the order of the present calculation. Such relations are straightforward to derive with the results provided here, and they should eventually become one good test for their LQCD calculations. It should be noted that in general the relations do dependent on N_c explicitly.

Table 10.1. β functions for counter terms contributing to the axial-vector currents.

LEC	$F_\pi^2 \beta$	LEC	$F_\pi^2 \beta / \Lambda^2$
\dot{g}_A	$\dot{g}_A^3 \frac{C_{HF}^2}{3}$	D_1^A	$-\frac{1}{48} \dot{g}_A (36 + 23 \dot{g}_A^2)$
C_1^A	$-\frac{11}{6} \dot{g}_A^3 C_{HF}^2 \frac{N_c+3}{N_c}$	D_2^A	$-\frac{5}{144} \dot{g}_A^3$
C_2^A	$\frac{1}{2} \dot{g}_A^3 C_{HF}^2 \frac{1-2N_c}{N_c}$	$D_3^A(d)$	$-\frac{1}{192} \dot{g}_A (36 + 11 \dot{g}_A^2)$
C_3^A	$\frac{8}{3} \dot{g}_A^3 C_{HF}^2$	$D_3^A(f)$	0
C_4^A	$\frac{8}{3} \dot{g}_A^3 C_{HF}^2$		

The one loop corrections to the axial currents are such that they do not contribute to the Goldberger-Treiman discrepancies (GTD) [132]. The discrepancies are given by terms in the Lagrangian of $\mathcal{O}(\xi^3)$, namely:

$$\mathcal{L}_{\mathbf{B}}^{(3)} = \cdots + i\mathbf{B}^\dagger (g_{GTD} [\nabla^i, \tilde{\chi}_-^a] G^{ia} + g_{GTD}^0 \partial^i \chi_-^0 S^i) \mathbf{B}. \quad (10.14)$$

As noted in [132] there are three LECs determining the spin 1/2 GTD in $SU(3)$. The $1/N_c$ expansion shows that those LECs are actually determined by the two shown above, which also determine the GTDs of the decuplet baryons.

The following observations are important: if one disregards the non-analytic contributions to the corrections to the axial couplings, it is observed that the corrections $\mathcal{O}(N_c)$ and $\mathcal{O}(N_c^0)$ to the matrix elements in $S = 1/2$ and $3/2$ baryons due to the counter terms are $\mathcal{O}(p^2)$, i.e., proportional to quark masses. On the other hand the terms independent of quark masses are $\mathcal{O}(1/N_c)$, i.e., spin symmetry breaking is suppressed $\mathcal{O}(1/N_c^2)$ with respect to the leading order. This indicates that the effects of spin-symmetry breaking are more suppressed than the $SU(3)$ symmetry breaking. It is important to note that at tree level NNLO the axial couplings satisfy N_c independent relations. For the case of the $\Delta Y = 0$ couplings within the baryon octet and

decuplet one finds in the $I = 1$ case the first relation below, and in the case of the $I = 0$ (η channel) one finds GMO and ES relations, namely:

$$\begin{aligned} \left(\frac{g_A}{g_V}\right)^{\pi\Delta+\frac{3}{5}\pi\Xi^*-\frac{8}{5}\pi\Sigma^*} &= 0, \\ 2(g_A^{\eta N} + g_A^{\eta\Xi}) - 3g_A^{\eta\Lambda} - g_A^{\eta\Lambda} &= 0, \\ g_A^{\eta\Sigma^*} - g_A^{\eta\Delta} = g_A^{\eta\Xi^*} - g_A^{\eta\Sigma^*} &= g_A^{\eta\Omega} - g_A^{\eta\Xi^*}. \end{aligned} \quad (10.15)$$

These relations are only violated by finite non-analytic terms. Additional relations are straightforward to derive for other couplings, such as those involving the $\Delta Y = \pm 1$ and the octet to decuplet off diagonal ones.

At LO and using $\left(\frac{g_A}{g_V}\right)^{\pi N} = 1.267 \pm 0.004$ for the nucleon, one obtains $\left(\frac{g_A}{g_V}\right)^{KN\Lambda} = 0.760$, $\left(\frac{g_A}{g_V}\right)^{KN\Sigma} = -0.253$, and $\left(\frac{g_A}{g_V}\right)^{K\Sigma\Xi} = \left(\frac{g_A}{g_V}\right)^{\pi N}$, to be compared with the ones obtained from semi-leptonic hyperon decays [133] 0.718 ± 0.015 , -0.340 ± 0.017 and 1.32 ± 0.20 respectively. The NLO $SU(3)$ breaking corrections are evidently necessary. On the other hand, the coupling $g_A^{N\Delta}$ is at LO equal to g_A , while its phenomenological value extracted from the width of the Δ assuming a vanishing GTD is equal to 1.235 ± 0.011 [116, 134], which shows a remarkably small breaking of the spin-symmetry. This seems to be in line with what was discussed above, namely that spin symmetry breaking is suppressed with respect to $SU(3)$ breaking by one extra order in $1/N_c$. In the following subsections the results for the axial couplings are confronted with recent LQCD calculations.

10.3.1 Fits to LQCD Results

LQCD calculations of axial couplings, in particular for the nucleon, have a long history. However, calculations involving hyperons, and including the decuplet baryons are very recent. Indeed, the first such calculations were carried out by C. Alexandrou et al [38], where the calculation of the axial couplings associated with the two neu-

tral $\Delta\mathcal{S} = 0$ currents were performed for transitions within the octet and within the decuplet baryons. They used twisted mass Wilson action adapted to 2+1+1 flavors (2-light quark flavors + strange flavor + charm flavor). The results show the recurring issue in LQCD calculations of axial couplings where the results come out between 5 and 10 % smaller than the physical value for the nucleon. Recent calculations of g_A^N have been able to give consistent results [135], but those calculations are still missing for hyperons and the baryon decuplet.

In this subsection the results [38], are fitted with the effective theory. The LECs that can be fitted with these results are: $g_A, C_1^A \dots$. In order to make a clear identification of the different couplings, it is convenient to define the couplings in a convenient way, which reflects the fact that the values of the axial couplings are approximately related by spin-flavor symmetry. It is then convenient to write the zero momentum transfer matrix elements of the axial currents as follows:

$$\langle B' | A^{ia} | B \rangle = \frac{6}{5} g_A^{aBB'} \langle B' | G^{ia} | B \rangle. \quad (10.16)$$

The results shown above for the UV divergencies of the one loop contributions imply that: $\delta g_A^{aBB'}(UV div)/g_A^{aBB'} = \mathcal{O}(C_{HF}/N_c) + \mathcal{O}(m_q/N_c)$. At LO, $g_A^{\pi NN} = g_A^N = 1.267$. The relations between the couplings $g_A^{aBB'}$ and the ones displayed in [38] are as follows:

$$\begin{aligned} \langle B_8 | A^{i=0\ 3} | B_8 \rangle &= \frac{1}{2} g_A^{B_8} \\ \langle B_{10} | A^{i=0\ 3} | B_{10} \rangle &= \frac{1}{6} g_A^{B_{10}} \\ \langle B_8 | A^{i=0\ 8} | B_8 \rangle &= \frac{1}{2\sqrt{3}} g_8^{B_8} \\ \langle B_{10} | A^{i=0\ 8} | B_{10} \rangle &= \frac{1}{6\sqrt{3}} g_8^{B_{10}} \end{aligned} \quad (10.17)$$

where $B_{8,10}$ is an octet (decuplet) baryon with spin projection +1/2, and the couplings on the RHS are those used in [38] and displayed in Tables (IV) and (V) of that

reference. The LQCD results are given for several π and K masses. The values of M_π for the different cases are given in Table (I) of [38], and the corresponding M_K is determined using the physical masses by the LO relation: $M_K^2 = M_{K_{\text{phys}}}^2 + \frac{1}{2}(M_\pi^2 - M_{\pi_{\text{phys}}}^2)$, which corresponds to keeping m_s fixed. While for general N_c the nine terms associated with the LECs in Table (10.1) are linearly independent, at $N_c = 3$ the term associated with C_2^A becomes linearly dependent with LO term, and thus its effects are absorbed into $\delta\dot{g}_A$. In the case of the LQCD results being fitted here there is an additional linear dependency, namely that of the term C_4^A which becomes linearly dependent with the term C_3^A . So the fit will involve seven NLO LECs in addition to \dot{g}_A . The results of the fits are shown in Table (10.2).

Table 10.2. LECs obtained by fitting to the LQCD results of Ref. [38]: here the choices are $\Lambda = m_\rho$ MeV and for the full NLO fit $\mu = m_\rho$ as well. The independence of the χ^2 on the choice of μ has been checked. In the NLO full fits \dot{g}_A is an input; three different reasonable values are included as example.

Fit	χ_{dof}^2	\dot{g}_A	$\delta\dot{g}_A$	C_1^A	C_2^A	C_3^A	C_4^A	D_1^A	D_2^A	D_3^A	D_4^A
LO	3.9	1.35	-	-	-	-	-	-	-	-	-
NLO Tree	0.91	1.42	-	-0.18	-	-	-	-	0.009	-	-
NLO Full	1.08	1.02	0.15	-1.11	0.	1.08	0.	-0.56	-0.02	-0.08	0.
	1.13	1.04	0.08	-1.17	0.	1.15	0.	-0.59	-0.02	-0.09	0.
	1.19	1.06	0.	-1.23	0.	1.21	0.	-0.62	-0.03	-0.09	0.

The LO fit, which involves only fitting the LO value of \dot{g}_A , shows a remarkably good approximation to the full set of the LQCD results. This is clearly aided by the very small dependency on M_π of the LQCD results. It also shows the very good approximate spin-flavor symmetry that relates axial couplings in the octet and decuplet. A fit where only tree contributions are included up to the NNLO gives a very precise description. Indeed, turning off some of the LECs as indicated in Ta-

ble (10.2) provides a consistent fit. Note that in this case $\delta\mathring{g}_A$, which is required to cancel an UV divergence proportional to the leading term, can be turned off, as it is only required when the loop contributions are included. The full NLO fit is more complicated. Although the implemented consistency with the $1/N_c$ expansion gives an important reduction of the non-analytic contributions, these are still significant. The most significant issue in this case becomes the determination of the LO \mathring{g}_A . If one fits it, then the fit naturally drives it down to small values, which suppress the non-analytic contributions. Such a situation is unrealistic, and therefore some strategy is needed. Here one finds what the origin of this problem resides: at one loop one needs to renormalize \mathring{g}_A via the counterterm proportional to $\delta\mathring{g}_A$, which is suppressed by one power in $1/N_c$. Fixing both the LO \mathring{g}_A and the counterterm would thus require information at different values of N_c , which is not accessible at present. One possible approach is to fix \mathring{g}_A to the value obtained with the LO fit, and fit the higher order LECs. This however fails because the resulting fit has too large a χ^2 . Another strategy is to input several different values of \mathring{g}_A , and determine an approximate range for it based on obtaining a χ^2 that is reasonable. Finally one can perform a different strategy, namely use the value for \mathring{g}_A obtained by matching to the deviation to the GMO relation, which can be used to give a value for \mathring{g}_A/F_π . If one does this, in the physical case one obtains that $\mathring{g}_A \sim 1.15$ if one uses $F_\pi = 93$ MeV. This however is not what one should use for the present LQCD results, since they extrapolate to too low of a value for g_A^N at the physical point. One would expect that in that case a correspondingly smaller value should be used, namely $\mathring{g}_A \sim 1.05$. The NLO fit with such an input for \mathring{g}_A is almost consistent, and is shown in Table (10.2). Ultimately, in order to have the LECs in BChPT $\times 1/N_c$ fully determined one needs a global analysis that involves LQCD calculations of a complete set of observables. This requires the LQCD determination of the quark mass dependencies of the observables, and also the possibility of results for different values of N_c , which is a more difficult task, but

which has already been initiated with the baryon masses for two flavors [113], and which has been analyzed with the effective theory [76].

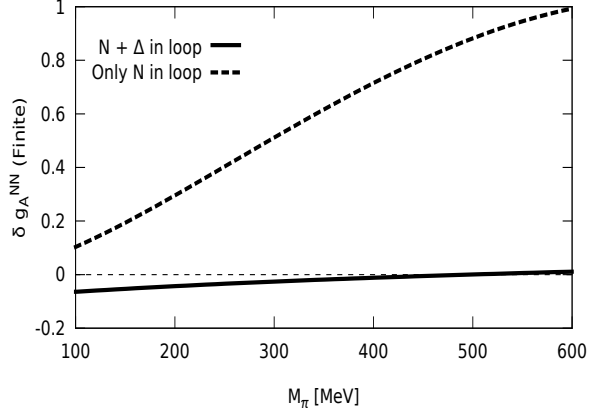


Figure 10.3. The effect of switching off the contribution of the Δ in the loops [36].

As illustration of the importance of including the decuplet in the effective theory, Fig.(10.3) shows the effect of removing it on the one-loop contributions. There is a dramatic cancellation between octet and decuplet contributions even at $N_c = 3$, without which the rather flat behavior of the axial couplings with M_π is virtually impossible to explain. This dramatic improvement in the behavior of the effective theory when it is made consistent with the $1/N_c$ expansion permeates other observables, such as the mass relations and vector charges discussed earlier, as well as virtually any other quantity, such as pion-nucleon scattering, Compton scattering, etc.

CHAPTER 11

CONCLUSIONS AND PERSPECTIVES

The qualitative idea of generalizing QCD from $SU(3)$ to $SU(N_c)$ by introducing N_c number of colors [10], has become a quantitative powerful tool with its development over a four decades. The application to baryons [15] with introducing large N_c power counting, and the discovery of the dynamical spin-flavor symmetry of baryons in the large N_c limit [11–14] made a substantial contribution for the advancement in the framework. This framework allows one to perform perturbative calculations in the low energy (non-perturbative) regime of QCD. In particular, in the baryonic sector the spin-flavor symmetry can be studied with its explicit breaking by the sub-leading $1/N_c$ corrections, via the construction of effective operators associated with the observables of interest [44]. The $1/N_c$ expansion is thus a very powerful effective theory in baryon phenomenology.

The initial focus of this thesis work was predominantly motivated by several facts. First, there are missing resonances in the lower lying excited baryon multiplets. Second, the availability of LQCD results on the lower-lying baryon multiplets contain a complete set of states, including the ground state and resonances corresponding to several different quark masses [28, 29]. Third, the successful application of the $1/N_c$ framework to the excited baryon multiplets: $[56, 0^+]$ (Roper multiplet) in Ref. [77], $[56, 2^+]$ in Ref. [25] and $[70, 1^-]$ in Refs. [21, 23, 58, 59] with the available baryon masses from experiment. The $1/N_c$ framework was simultaneously applied to both physical and LQCD baryon masses corresponding to the $[56, 0^+]$, $[56, 2^+]$, and $[70, 1^-]$ multiplets. The importance of this study is governed by the ability to extract the dynamics of the spin-flavor symmetry with its breaking in $SU(3)$, and the behavior effective operators with respect to the quark mass. The significance of this work is further

demonstrated by the predictions of lower-lying missing resonances in the physical case with higher precision, and the identification of undetermined quantum numbers (e.g. spin and parity) of some baryon states in the Particle Data Group [27, 136].

The main conclusions of this study on baryon masses in $1/N_c$ expansion can be summarized as follows. The leading contribution to the baryon masses in all considered multiplets is governed by the spin-flavor singlet operator and hyper-fine operator. The spin-orbit contribution is smaller compared to the spin-flavor singlet and hyper-fine contributions, and shows small variation with respect to the quark mass in each multiplet. The $SU(3)$ breaking operators are significant in magnitude near the physical quark mass, while the operators vanish at the $SU(3)$ symmetric point ($M_\pi \sim 700$ MeV). The fit results to physical baryon masses for each multiplet are in good agreement with the previous work [21, 23, 25, 58, 59, 77]. Fitting to LQCD results was a challenge due the ambiguity of identification of baryon states for a given spin. A model independent method was implemented, which tested the mass combinations with mass relations and identified reasonable combination of baryon masses to be fitted with the theory. Finally, the filtered baryon mass combinations from the mass relations constrained the operator coefficients to be fitted with a reasonable χ^2 value and natural size of the coefficients. Therefore, this methodology was successfully applied simultaneously to identify the baryon states corresponding to each multiplet, and yielded quality fit results to the LQCD spectrum.

The main focus of this thesis work was motivated by the combined approach of two effective theories, namely ChPT and $1/N_c$ expansion in baryon phenomenology. This framework was originally developed in Refs. [34, 35, 109, 137], such that the effective Lagrangian respects the chiral $SU(N_f) \times SU(N_f)$ symmetry in the chiral limit, and the contracted dynamical spin-flavor symmetry $SU(2N_f)$ in the large N_c limit.

The heavy baryon formalism of ChPT (HBChPT) is also assumed in this combined approach. One can expect a slower rate of convergence of the low energy expansion, because the expansion progresses in steps of $\mathcal{O}(p)$ rather than steps of $\mathcal{O}(p^2)$ in the conventional ChPT. The essence of this combined framework is making the link between the chiral expansion and the $1/N_c$ expansion. Due to the observation of non-commutativity of the two expansions [30], they are linked by considering the size of the baryon mass splitting of $\mathcal{O}(1/N_c)$, which is of $\mathcal{O}(p)$, the so called the ξ -expansion [36]. Therefore, having a systematic low energy expansion, including the chiral-spin-flavor symmetries combined together as an effective theory can be also considered as a powerful effective theory in baryon phenomenology.

There are some *key* observations from this work, which can be lead to a better understanding of baryon phenomenology. Because, this work concentrate on the implementation of this combined framework to calculate one-loop corrections to the ground state baryon masses, vector and axial-vector currents in the case of $SU(3)_{\text{flavor}}$, including an analysis with physical and LQCD results. It is worth noting that the decuplet degrees of freedom in the loops were taken into account to improve the convergence of the low energy expansion. One of the most important observations is the deviations from the GMO, ES, and GR mass relations, that are explicitly calculated from this framework to $\mathcal{O}(\xi^3)$. The deviations to GMO and ES relations behave as $\mathcal{O}(1/N_c)$, such that the $SU(3)$ symmetry breaking relations are exact in the large N_c limit. It is reasonable to suspect that the GR relation also has the same behavior, if one neglects the tree level counter term proportional to the LEC h_2 . The previous argument is supported by the fit results obtained by fixing $h_2 = 0$. Moreover, the fit results show that the combined framework works well in the case of $SU(3)_{\text{flavor}}$ in the range of small quark masses ($M_\pi \lesssim 300$ MeV). The main expectation of the combined fit to the baryon masses is to extract the LEC values which are independent of quark

mass, for the determination of baryon σ -terms [121].

It is clear the ξ -expansion framework can describe the LQCD results on baryon masses as well as axial couplings. For example, the mild behavior of the axial couplings with respect to the quark mass has been confirmed in the case of $SU(3)$. This completes the study of the combined framework in $SU(3)$ for the baryon masses, since the one-loop contributions were believed to be large in magnitude and have a small range of convergence. The smaller values in g_A^{NN} at the physical point is expected to be a LQCD issue rather than the problem of convergence of the effective theory, because the ξ -expansion is well behaved for g_A . Some possible sources of systematic errors in the extraction from LQCD might be finite volume effects and/or the effects from the three-point functions by excited states.

REFERENCES

- [1] W. Marciano and H Pagels. Quantum chromodynamics. *Physics Reports*, **36**:137, (1978).
- [2] M. Gell-Mann. Symmetries of baryons and mesons. *Phys. Rev.*, **125**:1067, (1962).
- [3] M. Gell-Mann. A schematic model of baryons and mesons. *Phys. Lett.*, **8**:214, (1964).
- [4] G Zweig. An $SU(3)$ model for strong interaction symmetry and its breaking; Version 2. (CERN-TH-412):80, (1964).
- [5] O. W. Greenberg. Spin and Unitary-Spin Independence in a Paraquark Model of Baryons and Mesons. *Phys. Rev. Lett.*, **13**:598, (1964).
- [6] M. Y. Han and Y. Nambu. Three-Triplet Model with Double $SU(3)$ Symmetry. *Phys. Rev.*, **139**:B1006, (1965).
- [7] D. J. Gross and F. Wilczek. Ultraviolet Behavior of Non-Abelian Gauge Theories. *Phys. Rev. Lett.*, **30**, (1973).
- [8] H. D Politzer. Reliable Perturbative Results for Strong Interactions? *Phys. Rev. Lett.*, **30**:1346, (1973).
- [9] S. Weinberg. Phenomenological Lagrangians. *Physica*, **A 96**:327, (1979).
- [10] G. 't Hooft. A Planar Diagram Theory for Strong Interactions. *Nucl. Phys.*, **B72**:461, (1974).
- [11] J. L. Gervais and B. Sakita. Large N QCD Baryon Dynamics: Exact Results from Its Relation to the Static Strong Coupling Theory. *Phys. Rev. Lett.*, **52**:87, (1984).

- [12] R. F. Dashen and A. V. Manohar. Baryon - pion couplings from large N_c QCD. *Phys. Lett.*, **B315**:425, (1993).
- [13] J. L. Gervais and B. Sakita. Large n Baryonic Soliton and Quarks. *Phys. Rev.*, **D30**:(1795), (1984).
- [14] R. F. Dashen and A. V. Manohar. $1/N_c$ corrections to the baryon axial currents in QCD. *Phys. Lett.*, **B315**:438, (1993).
- [15] E. Witten. Baryons in the $1/N_c$ Expansion. *Nucl. Phys.*, **B160**:57, (1979).
- [16] S. Okubo. Note on Unitary Symmetry in Strong Interactions. *Progress of Theoretical Physics*, **27**:949, (1962).
- [17] S. Coleman and S. L. Glashow. Electrodynamical properties of baryons in the unitary symmetry scheme. *Phys. Rev. Lett.*, **6**:423, (1961).
- [18] S. Coleman, S. L. Glashow, and D. J. Kleitman. Mass formulas and mass inequalities for reducible unitary multiplets. *Phys. Rev.*, **135**:B779, (1964).
- [19] E. E. Jenkins and R. F. Lebed. Naturalness of the Coleman-Glashow mass relation in the $1/N_c$ expansion: An update. *Phys. Rev.*, **D62**:077901, (2000).
- [20] F. Gürsey and L. A. Radicati. Spin and Unitary Spin Independence of Strong Interactions. *Phys. Rev. Lett.*, **13**:173, (1964).
- [21] J. L. Goity, C. L. Schat, and N. N. Scoccola. Negative parity 70-plet baryon masses in the $1/N_c$ expansion. *Phys. Rev.*, **D66**:114014, (2002).
- [22] J. L. Goity. $1/N_c$ countings in baryons. *Phys. Atom. Nucl.*, **68**:624, (2005).
- [23] C. L. Schat, J. L. Goity, and N. N. Scoccola. Masses of the 70- baryons in large N_c QCD. *Phys. Rev. Lett.*, **88**:102002, (2002).

- [24] J. L. Goity, C. Schat, and N. N. Scoccola. Decays of nonstrange negative parity baryons in the $1/N_c$ expansion. *Phys. Rev.*, **D71**:034016, (2005).
- [25] J. L. Goity, C. L. Schat, and N. N. Scoccola. Analysis of the $[56, 2^+]$ baryon masses in the $1/N_c$ expansion. *Phys. Lett.*, **B564**:83, (2003).
- [26] J. L. Goity and N. N. Scoccola. Decays of nonstrange positive parity excited baryons in the $1/N_c$ expansion. *Phys. Rev.*, **D72**:034024, (2005).
- [27] I. P. Fernando and J. L. Goity. Baryon spin-flavor structure from an analysis of lattice QCD results of the baryon spectrum. *Phys. Rev.*, **D91**:036005, (2015).
- [28] R. G. Edwards, J. J. Dudek, D. G. Richards, and S. J. Wallace. Excited state baryon spectroscopy from lattice QCD. *Phys. Rev.*, **D84**:074508, (2011).
- [29] R. G. Edwards, N. Mathur, D. G. Richards, and S. J. Wallace. Flavor structure of the excited baryon spectra from lattice QCD. *Phys. Rev.*, **D87**:054506, (2013).
- [30] T. D. Cohen and W. Broniowski. The Role of the delta isobar in chiral perturbation theory and hedgehog soliton models. *Phys. Lett.*, **B292**:5, (1992).
- [31] E. E. Jenkins and A. V. Manohar. Baryon chiral perturbation theory using a heavy fermion Lagrangian. *Phys. Lett.*, **B255**:558, (1991).
- [32] E. E. Jenkins and A. V. Manohar. Chiral corrections to the baryon axial currents. *Phys. Lett.*, **B259**:353, (1991).
- [33] E. E. Jenkins and A. V. Manohar. Baryon masses in chiral perturbation theory. *Nucl. Phys.*, **B368**:190, (1992).
- [34] R. Flores-Mendieta, E. E. Jenkins, and A. V. Manohar. $SU(3)$ symmetry breaking in hyperon semileptonic decays. *Phys. Rev.*, **D58**:094028, (1998).

- [35] R. Flores-Mendieta and C. P. Hofmann. Renormalization of the baryon axial vector current in large- N_c chiral perturbation theory. *Phys. Rev.*, **D74**:094001, (2006).
- [36] A. C. Cordón and J. L. Goity. Baryon masses and axial couplings in the combined $1/N_c$ and chiral expansions. *Phys. Rev. D*, **87**:016019, (2013).
- [37] C. Alexandrou, V. Drach, K. Jansen, C. Kallidonis, and G. Koutsou. Baryon spectrum with $N_f = 2 + 1 + 1$ twisted mass fermions. *Phys. Rev.*, **D90**:074501, (2014).
- [38] C. Alexandrou, K. Hadjiyiannakou, and C. Kallidonis. Axial charges of hyperons and charmed baryons using $N_f = 2 + 1 + 1$ twisted mass fermions. *Phys. Rev.*, **D94**:034502, (2016).
- [39] C. Patrignani et al. Review of Particle Physics. *Chin. Phys.*, **C40**:100001, (2016).
- [40] F Halzen and A. D. Martin. Quark and Leptons: An Introductory Course in Modern Particle Physics. John Wiley and Sons, (1984).
- [41] E. E. Jenkins. Large- N_c QCD. *Proceedings of Science*, **EFT09**:044, (2009).
- [42] F. E. Close. An Introduction to Quarks and Partons. Academic Press Inc., (1979).
- [43] D. Faiman and A. W. Hendry. Harmonic-oscillator model for baryons. *Phys. Rev.*, **173**:1720, (1968).
- [44] J. L. Goity. Large N_c limit of spin - flavor breaking in excited baryon levels. *Phys. Lett.*, **B414**:140, (1997).
- [45] F. Stancu. Group theory in subnuclear physics. *Oxford Stud. Nucl. Phys.*, **19**, (1996).

- [46] D. Pirjol and T. M. Yan. Excited baryons phenomenology from large N_c QCD. *Phys. Rev.*, **D57**:5434, (1998).
- [47] E. E. Jenkins and R. F. Lebed. Baryon mass splittings in the $1/N_c$ expansion. *Phys. Rev.*, **D52**:282, (1995).
- [48] A. V. Manohar. Large N QCD. In *Probing the standard model of particle interactions. Proceedings, Summer School in Theoretical Physics, NATO Advanced Study Institute, 68th session, Les Houches, France, July 28-September 5, 1997. Pt. 1, 2*, pages 1091–1169.
- [49] R. F. Dashen, E. E. Jenkins, and A. V. Manohar. Spin flavor structure of large N_c baryons. *Phys. Rev.*, **D51**:3697, (1995).
- [50] R. F. Dashen, E. E. Jenkins, and A. V. Manohar. The $1/N_c$ expansion for baryons. *Phys. Rev.*, **D49**:4713, (1994).
- [51] T. H. R. Skyrme. A non-linear field theory. *Proceedings of the Royal Society of London. Series A, Mathematical and Physical Sciences*, **260**:127, (1961).
- [52] A. V. Manohar. Equivalence of the chiral soliton and quark models in large N . *Nucl. Phys.*, **B248**:19, (1984).
- [53] E. E. Jenkins. LARGE- N_c BARYONS. *Annual Review of Nuclear and Particle Science*, **48**:81, (1998).
- [54] R. Dashen, E. E. Jenkins, and A. V. Manohar. Erratum: $1/N_c$ expansion for baryons. *Phys. Rev.*, **D51**:2489, (1995).
- [55] Markus A. L. and John M. R. Baryons from quarks in the $1/N$ expansion. *Nucl. Phys.*, **B426**:71, (1994).
- [56] M. A. Luty, J. March-Russell, and M. White. Baryon magnetic moments in a simultaneous expansion in $1/N$ and m_s . *Phys. Rev.*, **D51**:2332, (1995).

- [57] C. Carone, H. Georgi, and S. Osofsky. On spin independence in large N_c baryons. *Phys. Lett. B*, **322**:227, (1994).
- [58] C. E. Carlson, C. D. Carone, J. L. Goity, and R. F. Lebed. Operator analysis of $\ell = 1$ baryon masses in large N_c QCD. *Phys. Rev.*, **D59**:114008, (1999).
- [59] C. E. Carlson, C. D. Carone, J. L. Goity, and R. F. Lebed. Masses of orbitally excited baryons in large N_c QCD. *Phys. Lett.*, **B438**:327, (1998).
- [60] A. Walker-Loud, H. W. Lin, D. G. Richards, R. G. Edwards, M. Engelhardt, et al. Light hadron spectroscopy using domain wall valence quarks on an Asqtad sea. *Phys. Rev.*, **D79**:054502, (2009).
- [61] J. M. Bulava, R. G. Edwards, E. Engelson, J. Foley, B. Joo, et al. Excited State Nucleon Spectrum with Two Flavors of Dynamical Fermions. *Phys. Rev.*, **D79**:034505, (2009).
- [62] H. W. Lin et al. First results from 2+1 dynamical quark flavors on an anisotropic lattice: Light-hadron spectroscopy and setting the strange-quark mass. *Phys. Rev.*, **D79**:034502, (2009).
- [63] G. P. Engel, C.B. Lang, D. Mohler, and Andreas Schäfer. QCD with Two Light Dynamical Chirally Improved Quarks: Baryons. *Phys. Rev.*, **D87**:074504, (2013).
- [64] C. Alexandrou, T. Korzec, G. Koutsou, and T. Leontiou. Nucleon Excited States in $N_f = 2$ lattice QCD. *Phys. Rev.*, **D89**:034502, (2014).
- [65] M. S. Mahbub, W. Kamleh, D. B. Leinweber, P. J. Moran, and A. G. Williams. Structure and Flow of the Nucleon Eigenstates in Lattice QCD. *Phys. Rev.*, **D87**:094506, (2013).

- [66] M. S. Mahbub, W. Kamleh, D. B. Leinweber, P. J. Moran, and A. G. Williams. Low-lying Odd-parity States of the Nucleon in Lattice QCD. *Phys. Rev.*, **D87**:011501, (2013).
- [67] D. Pirjol and C. L. Schat. $1/N_c$ corrections to the $SU(4)$ symmetry for $L = 1$ baryons: The Three towers. *Phys. Rev.*, **D67**:096009, (2003).
- [68] E. G. de Urreta, J. L. Goity, and N. N. Scoccola. Global analysis of the negative parity non-strange baryons in the $1/N_c$ expansion. *Phys. Rev.*, **D89**:034024, (2014).
- [69] N. Matagne and Fl. Stancu. The $[56, 4^+]$ baryons in the $1/N_c$ expansion. *Phys. Rev.*, **D71**:014010, (2005).
- [70] N. Matagne and Fl. Stancu. Excited $[70, \ell^+]$ baryons in large N_c QCD. *Phys. Lett.*, **B631**:7, (2005).
- [71] N. Matagne and Fl. Stancu. Masses of $[70, \ell^+]$ Baryons in the $1/N_c$ Expansion. *Phys. Rev.*, **D74**:034014, (2006).
- [72] N. Matagne and Fl. Stancu. Highly excited negative parity baryons in the $1/N_c$ expansion. *Phys. Rev.*, **D85**:116003, (2012).
- [73] N. Matagne and Fl. Stancu. Baryon resonances in large N_c QCD. *Rev. Mod. Phys.*, **87**:211, (2015).
- [74] J. Beringer et al. Review of Particle Physics (RPP). *Phys. Rev.*, **D86**:010001, (2012).
- [75] E. E. Jenkins, A. V. Manohar, J. W. Negele, and A. Walker-Loud. A Lattice Test of $1/N_c$ Baryon Mass Relations. *Phys. Rev.*, **D81**:014502, (2010).

- [76] A. C. Cordon, T. DeGrand, and J. L. Goity. The N_c dependencies of baryon masses: Analysis with Lattice QCD and Effective Theory. *Phys. Rev.*, **D90**:014505, (2014).
- [77] C. E. Carlson and C. D. Carone. Predictions for decays of radially excited baryons. *Phys. Lett.*, **B484**:260, (2000).
- [78] N. Isgur and G. Karl. P Wave Baryons in the Quark Model. *Phys. Rev.*, **D18**:4187, (1978).
- [79] C. Jayalath, J. L. Goity, E. G. de Urreta, and N. N. Scoccola. Negative parity baryon decays in the $1/N_c$ expansion. *Phys. Rev.*, **D84**:074012, (2011).
- [80] S. R. Coleman, J. Wess, and B. Zumino. Structure of phenomenological Lagrangians. 1. *Phys. Rev.*, **177**:2239, (1969).
- [81] C. G. Callan, S. R. Coleman, J. Wess, and B. Zumino. Structure of phenomenological Lagrangians. 2. *Phys. Rev.*, **177**:2247, (1969).
- [82] S. Scherer. Introduction to chiral perturbation theory. *Adv. Nucl. Phys.*, **27**:277, (2003).
- [83] M. Gell-Mann and M. Lévy. The axial vector current in beta decay. *Il Nuovo Cimento (1955-1965)*, **16**:705, (1960).
- [84] J. Gasser and H. Leutwyler. Chiral Perturbation Theory to One Loop. *Annals Phys.*, **158**:142, (1984).
- [85] J. Gasser, M.E. Sainio, and A. Svarc. Nucleons with Chiral Loops. *Nucl. Phys.*, **B307**:779, (1988).
- [86] A. V. Manohar and H. Georgi. Chiral quarks and the non-relativistic quark model. *Nucl. Phys.*, **B234**:189, (1984).

- [87] C. Vafa and E. Witten. Restrictions on symmetry breaking in vector-like gauge theories. *Nucl. Phys.*, **B234**:173, (1984).
- [88] J. Gasser and H. Leutwyler. Chiral perturbation theory: Expansions in the mass of the strange quark. *Nucl. Phys.*, **B250**:465, (1985).
- [89] H. Leutwyler. On the Foundations of Chiral Perturbation Theory. *Annals of Physics*, **235**:165, (1994).
- [90] B. Borasoy. Introduction to Chiral Perturbation Theory. *Springer Proc. Phys.*, **118**:1, (2008).
- [91] M. Gell-Mann, R. J. Oakes, and B. Renner. Behavior of Current Divergences under $SU(3) \times SU(3)$. *Phys. Rev.*, **175**:2195, (1968).
- [92] A. Krause. Baryon Matrix Elements of the Vector Current in Chiral Perturbation Theory. *Helv. Phys. Acta*, **63**:3, (1990).
- [93] V. Bernard, N. Kaiser, J. Kambor, and Ulf-G. Meissner. Chiral structure of the nucleon. *Nucl. Phys.*, **B388**:315, (1992).
- [94] H. Pagels. Departures from Chiral Symmetry: A Review. *Phys. Rept.*, **16**:219, (1975).
- [95] S. Weinberg. Nonlinear realizations of chiral symmetry. *Phys. Rev.*, **166**:1568, (1968).
- [96] V. Bernard, N. Kaiser, and Ulf-G. Meissner. Chiral dynamics in nucleons and nuclei. *Int. J. Mod. Phys.*, **E4**:193, (1995).
- [97] P. J. Ellis and H. B. Tang. Pion nucleon scattering in a new approach to chiral perturbation theory. *Phys. Rev.*, **C57**:3356, (1998).

- [98] T. Becher and H. Leutwyler. Baryon chiral perturbation theory in manifestly Lorentz invariant form. *Eur.Phys.J.*, **C9**:643, (1999).
- [99] T. Fuchs, J. Gegelia, G. Japaridze, and S. Scherer. Renormalization of relativistic baryon chiral perturbation theory and power counting. *Phys. Rev.*, **D68**:056005, (2003).
- [100] T. R. Hemmert, B. R. Holstein, and J. Kambor. Systematic $1/M$ expansion for spin $3/2$ particles in baryon chiral perturbation theory. *Phys. Lett.*, **B395**:89, (1997).
- [101] T. R. Hemmert, B. R. Holstein, and J. Kambor. Chiral Lagrangians and delta(1232) interactions: Formalism. *J. Phys.*, **G24**:1831, (1998).
- [102] T. R. Hemmert, M. Procura, and W. Weise. Quark mass dependence of the nucleon axial vector coupling constant. *Phys. Rev.*, **D68**:075009, (2003).
- [103] N. Fettes and Ulf. G. Meissner. Pion - nucleon scattering in an effective chiral field theory with explicit spin $3/2$ fields. *Nucl. Phys.*, **A679**:629, (2001).
- [104] M. Procura, B. U. Musch, T. Wollenweber, T. R. Hemmert, and W. Weise. Nucleon mass: From lattice QCD to the chiral limit. *Phys. Rev.*, **D73**:114510, (2006).
- [105] C. Hacker, N. Wies, J. Gegelia, and S. Scherer. Including the Delta(1232) resonance in baryon chiral perturbation theory. *Phys. Rev.*, **C72**:055203, (2005).
- [106] V. Bernard, T. R. Hemmert, and Ulf-G. Meissner. Infrared regularization with spin $3/2$ fields. *Phys. Lett.*, **B565**:137, (2003).
- [107] V. Bernard, T. R. Hemmert, and Ulf-G. Meissner. Chiral extrapolations and the covariant small scale expansion. *Phys. Lett.*, **B622**:141, (2005).

- [108] M. Procura, B. U. Musch, T. R. Hemmert, and W. Weise. Chiral extrapolation of g_A with explicit Delta(1232) degrees of freedom. *Phys. Rev.*, **D75**:014503, (2007).
- [109] E. E. Jenkins. Chiral Lagrangian for baryons in the $1/N_c$ expansion. *Phys. Rev.*, **D53**:2625, (1996).
- [110] Ph. Hagler. Hadron structure from lattice quantum chromodynamics. *Phys. Rept.*, **490**:49, (2010).
- [111] Z. Fodor and C. Hoelbling. Light Hadron Masses from Lattice QCD. *Rev. Mod. Phys.*, **84**:449, (2012).
- [112] C. Alexandrou. Hadron Structure in Lattice QCD. *Prog.Part.Nucl.Phys.*, **67**:101, (2012).
- [113] T. DeGrand. Lattice baryons in the $1/N_c$ expansion. *Phys. Rev.*, **D86**:034508, (2012).
- [114] S. Weinberg. The Quantum theory of fields: Foundations. *Cambridge University Press, New York*, **Vol. 1**, (1995).
- [115] S. Weinberg. Effective chiral Lagrangians for nucleon - pion interactions and nuclear forces. *Nucl. Phys.*, **B363**:3, (1991).
- [116] A. C. Cordon and J. L. Goity. Baryon Masses and Axial Couplings in the Combined $1/N_c$ and Chiral Expansions. *Phys. Rev.*, **D87**:016019, (2013).
- [117] M. E. Peskin and D. V. Schroeder. An Introduction to Quantum Field Theory. Westview Press, (1995).
- [118] T. D. Cohen. Chiral and large- N_c limits of quantum chromodynamics and models of the baryon. *Rev. Mod. Phys.*, **68**:599, (1996).

- [119] N. Matagne and Fl. Stancu. Matrix elements of $SU(6)$ generators for baryons at arbitrary N_c . *Phys. Rev.*, **D73**:114025, (2006).
- [120] N. Carrasco et al. Up, down, strange and charm quark masses with $N_f = 2+1+1$ twisted mass lattice QCD. *Nucl. Phys.*, **B887**:19, (2014).
- [121] J. M. Alarcón, I. P. Fernando, and J. L. Goity. *In preparation*.
- [122] R. C. Hwa and J. Nuyts. Commutation Relations of Baryon Currents. *Phys. Rev.*, **151**:1215, (1966).
- [123] R. Flores-Mendieta and J. L. Goity. Baryon vector current in the chiral and $1/N_c$ expansions. *Phys. Rev.*, **D90**:114008, (2014).
- [124] N. Cabibbo. Unitary symmetry and leptonic decays. *Phys. Rev. Lett.*, **10**:531, (1963).
- [125] M. Kobayashi and T. Maskawa. CP-Violation in the Renormalizable Theory of Weak Interaction. *Progress of Theoretical Physics*, **49**:652, (1973).
- [126] M. Ademollo and R. Gatto. Nonrenormalization theorem for the strangeness-violating vector currents. *Phys. Rev. Lett.*, **13**:264, (1964).
- [127] R. F. Lebed and M. Suzuki. Current algebra and the ademollo-gatto theorem in spin-flavor symmetry of heavy quarks. *Phys. Rev.*, **D44**:829, (1991).
- [128] C. Granados and C. Weiss. Chiral dynamics and peripheral transverse densities. *JHEP*, **01**:092, (2014).
- [129] C. Granados and C. Weiss. Light-front representation of chiral dynamics with Δ isobar and large- N_c relations. *JHEP*, **06**:075, (2016).

- [130] J. M. Alarcón, A.N. Hiller Blin, M.J. Vicente Vacas, and C. Weiss. Peripheral transverse densities of the baryon octet from chiral effective field theory and dispersion analysis. *Nuclear Physics*, **A964**:18, (2017).
- [131] J. M. Alarcón and C. Weiss. Nucleon form factors in dispersively improved Chiral Effective Field Theory II: Electromagnetic form factors. *arXiv*, **1710.06430**, (2017).
- [132] J. L. Goity, R. Lewis, M. Schvellinger, and L. Z. Zhang. The Goldberger-Treiman discrepancy in $SU(3)$. *Phys. Lett.*, **B454**:115, (1999).
- [133] N. Cabibbo, E. C. Swallow, and R. Winston. Semileptonic hyperon decays. *Ann. Rev. Nucl. Part. Sci.*, **53**:39, (2003).
- [134] A. C. Cordon and J. L. Goity. Nucleon and Delta axial-vector couplings in $1/N_c$ - Baryon Chiral Perturbation Theory. *arXiv*., **1303.2126**, (2013).
- [135] E. Berkowitz et al. An accurate calculation of the nucleon axial charge with lattice QCD. *arXiv*, **1704.01114**, (2017).
- [136] I. P. Fernando and J. L. Goity. Predictions for Excited Strange Baryons. In *Mini-Proceedings: Workshop on Physics with Neutral Kaon Beam at JLab (KL2016): Newport News, VA, USA, February 1-3, 2016*, pages 75–82, (2016).
- [137] R. Flores-Mendieta, C. P. Hofmann, E. Jenkins, and A. V. Manohar. Structure of large N_c cancellations in baryon chiral perturbation theory. *Phys. Rev.*, **D62**:034001, (2000).

APPENDICES

APPENDIX A

SPIN-FLAVOR ALGEBRA AND OPERATOR BASES

The $4N_f^2 - 1$ generators of the spin-flavor group $SU(2N_f)$ consist of the three spin generators S^i , the $N_f^2 - 1$ flavor $SU(N_f)$ generators T^a , and the remaining $3(N_f^2 - 1)$ spin/flavor generators G^{ia} .

In representations with N_c indices (baryons), the generators G^{ia} have matrix elements $\mathcal{O}(N_c)$ on states with $S = \mathcal{O}(N_c^0)$. A contracted $SU(6)$ algebra is defined by the generators $\{S^i, I^a, X^{ia}\}$, where $X^{ia} = G^{ia}/N_c$. In large N_c , the generators X^{ia} become semiclassical as $[X^{ia}, X^{jb}] = \mathcal{O}(1/N_c)$, while having matrix elements $\mathcal{O}(1)$ between baryons.

The symmetric irrep of $SU(6)$ with N_c Young boxes decomposes into the following $SU(2)_{\text{spin}} \times SU(3)$ irreps: $[S, (p, q)] = [S, (2S, \frac{1}{2}(N_c - 2S))]$, $S = 1/2, \dots, N_c/2$ (assume N_c is odd). The baryon states are then denoted by: $|SS_3, YII_3\rangle$. Clearly the spin S of the baryons determines its $SU(3)$ irrep.

In $SU(3)$ for a given irrep given (p, q) , the range of hypercharge is:

$$Y_{\min}(p, q) = -\frac{2p+q}{3} \leq Y \leq Y_{\max}(p, q) = \frac{p+2q}{3} \quad (\text{A.1})$$

It is convenient to define:

$$\begin{aligned} \bar{Y}(p, q) &= Y_{\max}(p, q) - q \\ \bar{Y}'(p, q) &= Y_{\min}(p, q) + q. \end{aligned} \quad (\text{A.2})$$

One has that $\bar{Y} > \bar{Y}'$ if $p > q$, and viceversa. The possible isospin values for a given Y are as follows:

$$\begin{aligned}
\text{if } p \geq q: I(Y) &= \begin{cases} \text{if } Y \geq \bar{Y}: & \frac{1}{2}(p - Y_{\max} + Y), \dots, \frac{1}{2}(p + Y_{\max} - Y) \\ \text{if } \bar{Y}' \leq Y < \bar{Y}: & \frac{1}{2}(p - Y_{\max} + Y), \dots, \frac{1}{2}(p + Y_{\max} + Y - 2\bar{Y}) \\ \text{if } Y_{\min} \leq Y < \bar{Y}': & \frac{1}{2}(q + Y_{\min} - Y), \dots, \frac{1}{2}(q + Y - Y_{\min}) \end{cases} \\
\text{if } q \geq p: I(Y) &= \begin{cases} \text{if } Y \geq \bar{Y}': & \frac{1}{2}(p - Y_{\max} + Y), \dots, \frac{1}{2}(p + Y_{\max} - Y) \\ \text{if } \bar{Y} \leq Y < \bar{Y}': & \frac{1}{2}(p + 2\bar{Y}' - Y_{\max} - Y), \dots, \frac{1}{2}(p + Y_{\max} - Y) \\ \text{if } Y_{\min} \leq Y < \bar{Y}: & \frac{1}{2}(q + Y_{\min} - Y), \dots, \frac{1}{2}(q + Y - Y_{\min}) \end{cases}
\end{aligned}$$

with this, one can easily builds the content of ground state baryons for arbitrary N_c .

A.1 Matrix elements of spin-flavor generators

According to the Wigner-Eckart theorem, the matrix element of a generic $SU(2)_{\text{spin}} \times SU(3)$ tensor operator $O_{\tilde{R}\tilde{Y}\tilde{I}_3}^{\ell\ell_3}$ between baryon states of the form $\begin{vmatrix} S & S_3 \\ R & YII_3 \end{vmatrix}$ will be given in terms of reduced matrix elements (RMEs) and $SU(3)$ Clebsch-Gordan (CG) coefficients as,

$$\begin{aligned}
\left\langle \begin{vmatrix} S' & S'_3 \\ R' & Y'I'I'_3 \end{vmatrix} \middle| O_{\tilde{R}\tilde{Y}\tilde{I}_3}^{\ell\ell_3} \middle| \begin{vmatrix} S & S_3 \\ R & YII_3 \end{vmatrix} \right\rangle &= \frac{1}{\sqrt{2S'+1}\sqrt{\dim R'}} \langle SS_3, \ell\ell_3 | S'S'_3 \rangle \\
&\times \sum_{\gamma=1,2} \langle S', R' || O_{\tilde{R}}^{\ell} || S, R \rangle_{\gamma} \left\langle \begin{vmatrix} R & \tilde{R} \\ YII_3 & \tilde{Y}\tilde{I}\tilde{I}_3 \end{vmatrix} \middle| \begin{vmatrix} R' & \\ Y'I'I'_3 & \end{vmatrix}_{\gamma} \right\rangle_{\gamma},
\end{aligned} \tag{A.3}$$

where, R is the irrep of $SU(3)$ to which the state belongs, and ℓ is the angular momentum in the spherical basis.

Matrix elements of the spin-flavor generators between baryon states in the spin-flavor symmetric representation are then given by:

$$\begin{aligned}
\left\langle \begin{array}{c} S' \ S'_3 \\ Y' I' I'_3 \end{array} \left| S^m \right| \begin{array}{c} S \ S_3 \\ Y I I_3 \end{array} \right\rangle &= \delta_{SS'} \delta_{YY'} \delta_{II'} \delta_{I_3 I'_3} \sqrt{S(S+1)} \langle S S_3, 1m \mid S' S'_3 \rangle \\
\left\langle \begin{array}{c} S' \ S'_3 \\ Y' I' I'_3 \end{array} \left| T^{yii_3} \right| \begin{array}{c} S \ S_3 \\ Y I I_3 \end{array} \right\rangle &= \delta_{SS'} \delta_{S_3 S'_3} \frac{1}{\sqrt{\dim(2S, \frac{1}{2}(N_c - 2S))}} \langle S \parallel T \parallel S \rangle \\
&\quad \times \left\langle \begin{array}{c} (2S, \frac{1}{2}(N_c - 2S)) \\ Y \ I \ I_3 \end{array} \begin{array}{c} (1, 1) \\ yii_3 \end{array} \left| \begin{array}{c} (2S, \frac{1}{2}(N_c - 2S)) \\ Y' \ I' \ I'_3 \end{array} \right\rangle_{\gamma=1} \\
\left\langle \begin{array}{c} S' \ S'_3 \\ Y' I' I'_3 \end{array} \left| G_{yii_3}^m \right| \begin{array}{c} S \ S_3 \\ Y I I_3 \end{array} \right\rangle &= \frac{\langle S S_3, 1m \mid S' S'_3 \rangle}{\sqrt{2S'+1} \sqrt{\dim(2S, \frac{1}{2}(N_c - 2S))}} \sum_{\gamma} \langle S' \parallel G \parallel S \rangle_{\gamma} \\
&\quad \times \left\langle \begin{array}{c} (2S, \frac{1}{2}(N_c - 2S)) \\ Y \ I \ I_3 \end{array} \begin{array}{c} (1, 1) \\ yii_3 \end{array} \left| \begin{array}{c} (2S, \frac{1}{2}(N_c - 2S)) \\ Y' \ I' \ I'_3 \end{array} \right\rangle_{\gamma} \tag{A.4}
\end{aligned}$$

where the reduced matrix elements are (here $p = 2S$, $q = \frac{1}{2}(N_c - 2S)$):

$$\begin{aligned}
\langle S \parallel T \parallel S \rangle &= \text{sign}(q - 0^+) \sqrt{\dim(p, q) C_2(p, q)} \\
&= \text{sign}(N_c - 2S - 0^+) \\
&\quad \times \frac{\sqrt{(2S+1)(N_c - 2S+2)(N_c + 2S+4)(N_c(N_c+6) + 12S(S+1))}}{4\sqrt{6}} \\
\langle S' \parallel G \parallel S \rangle_{\gamma=1} &= \begin{cases} \text{if } S = S' + 1 : & -\frac{\sqrt{(4S^2-1)((N_c+2)^2-4S^2)((N_c+4)^2-4S^2)}}{8\sqrt{2}} \\ \text{if } S = S' - 1 : & -\frac{\sqrt{(4S(S+2)+3)(N_c-2S)(N_c-2S+2)(N_c+2S+4)(N_c+2S+6)}}{8\sqrt{2}} \\ \text{if } S = S' : & \text{sign}(N_c - 2S - 0^+) \frac{(N_c+3)(2S+1)\sqrt{S(S+1)(N_c-2S+2)(N_c+2S+4)}}{\sqrt{6N_c(N_c+6)+12S(S+1)}} \end{cases} \\
\langle S' \parallel G \parallel S \rangle_{\gamma=2} &= -\delta_{SS'} \frac{(2S+1)\sqrt{(N_c-2S)(N_c+2S+6)((N_c+2)^2-4S^2)((N_c+4)^2-4S^2)}}{8\sqrt{2}\sqrt{N_c(N_c+6)+12S(S+1)}} \tag{A.5}
\end{aligned}$$

A.2 Bases of spin-flavor composite operators

Here the bases of 2- and 3-body spin-flavor operators along with important operator relations relevant to this work are given. There are operator relations which are valid for matrix elements in the symmetric irrep of $SU(6)$. The first ones are relations for 2-body operators [49], and are shown in Table. (A.1).

Table A.1. 2-body identities for the $SU(6)$ generators acting on the irreducible representation $(N_c, 0, 0, 0, 0, 0)$.

Relation	$SU(2)_{\text{spin}} \times SU(3)$
$2\hat{S}^2 + 3\hat{T}^2 + 12\hat{G}^2 = \frac{5}{2}N_c(N_c + 6)$	$(\ell = 0, \mathbf{1})$
$d^{abc}\{G^{ia}, G^{ib}\} + \frac{2}{3}\{S^i, G^{ic}\} + \frac{1}{4}d^{abc}\{T^a, T^b\} = \frac{2}{3}(N_c + 3)T^c$	$(0, \mathbf{8})$
$\{T^a, G^{ia}\} = \frac{2}{3}(N_c + 3)S^i$	$(1, \mathbf{1})$
$\frac{1}{3}\{S^i, T^a\} + d^{abc}\{T^b, G^{ic}\} - \epsilon^{ijk}f^{abc}\{G^{jb}, G^{kc}\} = \frac{4}{3}(N_c + 3)G^{ia}$	$(1, \mathbf{8})$
$-12\hat{G}^2 + 27\hat{T}^2 - 32\hat{S}^2 = 0$	$(0, \mathbf{1})$
$d^{abc}\{G^{ib}, G^{ic}\} + \frac{9}{4}d^{abc}\{T^b, T^c\} - \frac{10}{3}\{S^i, G^{ia}\}$	$(0, \mathbf{8})$
$4\{G^{ia}, G^{ib}\}^{\mathbf{27}} = \{T^a, T^b\}^{\mathbf{27}}$	$(0, \mathbf{27})$
$d^{abc}\{T^b, G^{ic}\} = \frac{1}{3}(\{S^i, T^a\} - \epsilon^{ijk}f^{abc}\{G^{jb}, G^{kc}\})$	$(1, \mathbf{8})$
$\epsilon^{ijk}\{G^{ja}, G^{kb}\}^{\mathbf{10}+\bar{\mathbf{10}}} = (f^{acd}d^{bce}\{T^d, G^{ie}\})^{\mathbf{10}+\bar{\mathbf{10}}}$	$(1, \mathbf{10} + \bar{\mathbf{10}})$
$\{G^{ia}, G^{ja}\}^{\ell=2} = \frac{1}{3}\{S^i, S^j\}^{\ell=2}$	$(2, \mathbf{1})$
$d^{abc}\{G^{ia}, G^{jb}\}^{\ell=2} = \frac{1}{3}\{S^i, G^{ja}\}^{\ell=2}$	$(2, \mathbf{8})$

The following identities follow from these relations:

from the $(0, \mathbf{1})$ relations:

$$\begin{aligned}
 \hat{G}^2 &= \frac{1}{4} \left(\frac{3}{4}N_c(N_c + 6) - \frac{5}{3}S^2 \right) \\
 \hat{T}^2 &= \frac{1}{4} \left(\frac{N_c(N_c + 6)}{3} + 4\hat{S}^2 \right),
 \end{aligned} \tag{A.6}$$

from the $(0, \mathbf{8})$ relations:

$$\begin{aligned}
 d^{abc}\{G^{ib}, G^{ic}\} &= \frac{3}{4}(N_c + 3)T^a - \frac{7}{6}\{S^i, G^{ia}\} \\
 d^{abc}\{T^b, T^c\} &= -\frac{(N_c + 3)}{3}T^a + 2\{S^i, G^{ia}\},
 \end{aligned} \tag{A.7}$$

and from the $(1, \mathbf{8})$ relations:

$$\begin{aligned}
 \epsilon_{ijk}f_{abc}\{G^{ia}, G^{jb}\} &= (S^kT^c - (N_c + 3)G^{kc}) \\
 d^{abc}\{T^a, G^{ib}\} &= 2d^{abc}T^aG^{ib} = \frac{1}{3}(S^iT^c + (N_c + 3)G^{ic}) \\
 f^{abc}\{T^b, G^{ic}\} &= \epsilon^{ijk}\{S^j, G^{ka}\},
 \end{aligned} \tag{A.8}$$

while the rest of the identities are explicit in Table (A.1). Making use of these relations, the basis of 2-body operators can be chosen to be as shown in Table (A.2).

Table A.2. 2-body basis operators.

2-body operator	(ℓ, \mathbf{R})
\hat{S}^2	$(0, \mathbf{1})$
$\{S^i, S^j\}^{\ell=2}$	$(2, \mathbf{1})$
$\{S^i, T^a\}$	$(1, \mathbf{8})$
$\{S^i, G^{ia}\}$	$(0, \mathbf{8})$
$\epsilon^{ijk}\{S^j, G^{ka}\}$	$(1, \mathbf{8})$
$\{S^i, G^{ja}\}^{\ell=2}$	$(2, \mathbf{8})$
$\{T^a, G^{ib}\}^{\mathbf{10}+\bar{\mathbf{10}}}$	$(1, \mathbf{10} + \bar{\mathbf{10}})$
$\{T^a, T^b\}^{\mathbf{27}}$	$(0, \mathbf{27})$
$\{G^{ia}, G^{jb}\}^{(2, \mathbf{27})}$	$(2, \mathbf{27})$
$\{T^a, G^{ib}\}^{\mathbf{27}}$	$(1, \mathbf{27})$

Making use of the basis of 2-body operators, some lengthy work leads to building the basis of 3-body operators $\ell = 0, 1$. That basis is displayed in Table A.3:

Table A.3. Operators of interest in the 3-body basis up to $\ell = 1$.

3-body operator	(ℓ, \mathbf{R})
$T^a \hat{S}^2$	$(0, \mathbf{8})$
$\{T^a, \{S^i, G^{ib}\}\}^{\mathbf{10}+\bar{\mathbf{10}}}$	$(0, \mathbf{10} + \bar{\mathbf{10}})$
$\{T^a, \{S^i, G^{ib}\}\}^{\mathbf{27}}$	$(0, \mathbf{27})$
$S^i \hat{S}^2$	$(1, \mathbf{1})$
$\{T^a, \{T^b, T^c\}^{\mathbf{27}}\}$	$(0, \mathbf{8} \otimes \mathbf{27})$
$S^i \{T^a, T^b\}^{\mathbf{27}}$	$(1, \mathbf{27})$
$\{S^j, \{G^{ia}, G^{jb}\}^{(2, \mathbf{27})}\}$	$(1, \mathbf{27})$
$\{\hat{S}^2, G^{ia}\}$	$(1, \mathbf{8})$
$\epsilon^{ijk}\{S^j, \{T^a, G^{kb}\}\}^{\mathbf{10}+\bar{\mathbf{10}}}$	$(1, \mathbf{10} + \bar{\mathbf{10}})$
$\epsilon^{ijk}\{S^j, \{T^a, G^{kb}\}\}^{\mathbf{27}}$	$(1, \mathbf{27})$
$\{G^{ia}, \{T^b, T^c\}^{\mathbf{27}}\}$	$(1, \mathbf{8} \otimes \mathbf{27})$
$\{G^{ia}, \{S^j, G^{jb}\}\}$	$(1, \mathbf{8} \otimes \mathbf{8})$

APPENDIX B

BUILDING BLOCKS FOR THE EFFECTIVE LAGRANGIANS

In the symmetric representations of $SU(6)$ the baryon spin-flavor multiplet consists of the baryon states in the $SU(3)$ irreps ($p = 2S, q = \frac{1}{2}(N_c - 2S)$), where S is the baryon spin. This permits a straightforward implementation of the non-linear realization of chiral $SU_L(3) \times SU_R(3)$ on the spin-flavor multiplet. The baryon spin-flavor multiplet is given by the field \mathbf{B} , where the fields have well defined spin, and therefore also are in irreps of $SU(3)$.

Defining as usual the Goldstone Boson fields π^a , $a = 1, \dots, 8$, through the unitary parametrization $u = \exp(i\frac{\pi^a T^a}{F_\pi})$ (note that in the fundamental representation $T^a = \lambda^a/2$, with λ^a the Gell-Mann matrices), for any isospin representation one defines a non-linear realization of chiral symmetry according to [80, 81]:

$$(L, R) : u = u' = R u h^\dagger(L, R, u) = h(L, R, u) u L^\dagger, \quad (\text{B.1})$$

where (L, R) is a $SU_L(3) \times SU_R(3)$ transformation. This equation defines h , and since h is a $SU(3)$ transformation itself, it can be written as $h = \exp(ic^a T^a)$. The chiral transformation on the baryon multiplet \mathbf{B} is then given by:

$$(L, R) : \mathbf{B} = \mathbf{B}' = h(L, R, u) \mathbf{B}. \quad (\text{B.2})$$

On the other hand, spin-flavor transformations of interest are the contracted ones, namely those generated by $\{S^i, I^a, X^{ia} = \frac{1}{N_c} G^{ia}\}$. While the isospin transformations act on the pion fields in the usual way, and the spin transformations must be performed along with the corresponding spatial rotations. The transformations generated by X^{ia} are defined to only act on the baryons.

The effective baryon Lagrangian can be expressed in the usual way as a series of terms which are $SU_L(3) \times SU_R(3)$ invariant (upon introduction of appropriate sources; see for instance [82] for details). The fields in the effective Lagrangian are the Goldstone Bosons parametrized by the unitary $SU(3)$ matrix field u and the baryons given by the symmetric $SU(6)$ multiplet \mathbf{B} .

The building blocks for the effective theory consist of low energy operators composed in terms of the GB fields, derivatives and sources (chiral tensors), and spin-flavor composite operators (spin-flavor tensors). The low energy operators are the usual ones, namely:

$$\begin{aligned} D_\mu &= \partial_\mu - i\Gamma_\mu, \quad \Gamma_\mu = \Gamma_\mu^\dagger = \frac{1}{2}(u^\dagger(i\partial_\mu + r_\mu)u + u(i\partial_\mu + \ell_\mu)u^\dagger), \\ u_\mu &= u_\mu^\dagger = u^\dagger(i\partial_\mu + r_\mu)u - u(i\partial_\mu + \ell_\mu)u^\dagger, \\ \chi &= 2B_0(s + ip), \quad \chi_\pm = u^\dagger\chi u^\dagger \pm u\chi^\dagger u, \\ F_L^{\mu\nu} &= \partial^\mu\ell^\nu - \partial^\nu\ell^\mu - i[\ell^\mu, \ell^\nu], \quad F_R^{\mu\nu} = \partial^\mu r^\nu - \partial^\nu r^\mu - i[r^\mu, r^\nu], \end{aligned} \quad (\text{B.3})$$

where D_μ is the chiral covariant derivative, s and p are scalar and pseudo-scalar sources, and ℓ_μ and r_μ are gauge sources. It is convenient to define the $SU(3)$ singlet and octet components of χ^\pm using the fundamental $SU(3)$ irrep, namely:

$$\begin{aligned} \chi_\pm^0 &= \frac{1}{3}\langle\chi_\pm\rangle \\ \tilde{\chi}_\pm &= \chi - \chi_\pm^0 = \tilde{\chi}_\pm^a \frac{\lambda^a}{2} \end{aligned} \quad (\text{B.4})$$

Displaying explicitly the quark masses,

$$\chi_+ = 4B_0\mathcal{M}_q + \dots \quad (\text{B.5})$$

The three quark mass combinations, namely $SU(3)$ singlet, isosinglet, and isotriplet are respectively defined to be:

$$m^0 = \frac{1}{3}(m_u + m_d + m_s), \quad m^8 = \frac{1}{\sqrt{3}}(m_u + m_d - 2m_s), \quad m^3 \equiv (m_u - m_d). \quad (\text{B.6})$$

The spin-flavor operators were discussed in Appendix A.

The leading order equations of motion are used in the construction of the higher order terms in the Lagrangian, namely, $iD_0\mathbf{B} = (\frac{C_{HF}}{N_c}S(S+1) + \frac{c_1}{2\Lambda}\hat{\chi}_+)\mathbf{B}$, and $\nabla_\mu u^\mu = \frac{i}{2}\chi_-$.

APPENDIX C

LOOP INTEGRALS

The one loop integrals needed in this work are provided here. The definition $\widetilde{d^d k} \equiv d^d k / (2\pi)^d$ is used. The scalar and tensor one-loop integrals are:

$$\begin{aligned}
I(n, \alpha, \Lambda) &\equiv \int \widetilde{d^d k} \frac{k^{2n}}{(k^2 - \Lambda^2)^\alpha} = i(-1)^{n-\alpha} \frac{1}{(4\pi)^{\frac{d}{2}}} \frac{\Gamma(n + \frac{d}{2})\Gamma(\alpha - n - \frac{d}{2})}{\Gamma(\frac{d}{2})\Gamma(\alpha)} (\Lambda^2)^{n-\alpha+\frac{d}{2}} \\
I^{\mu_1, \dots, \mu_{2n}}(\alpha, \Lambda) &\equiv \int \widetilde{d^d k} \frac{k_{\mu_1} \cdots k_{\mu_{2n}}}{(k^2 - \Lambda^2)^\alpha} = i(-1)^{n-\alpha} \frac{1}{(4\pi)^{\frac{d}{2}}} \frac{1}{4^n n!} \frac{\Gamma(\alpha - n - \frac{d}{2})}{\Gamma(\alpha)} (\Lambda^2)^{n-\alpha+\frac{d}{2}} \\
&\quad \times \sum_{\sigma} g_{\mu_{\sigma_1} \mu_{\sigma_2}} \cdots g_{\mu_{\sigma_{2n-1}} \mu_{\sigma_{2n}}} \tag{C.1} \\
&= \frac{1}{4^n n!} \frac{\Gamma(\frac{d}{2})}{\Gamma(n + \frac{d}{2})} I(n, \alpha, \Lambda) \sum_{\sigma} g_{\mu_{\sigma_1} \mu_{\sigma_2}} \cdots g_{\mu_{\sigma_{2n-1}} \mu_{\sigma_{2n}}} ,
\end{aligned}$$

where σ are the permutations of $\{1, \dots, 2n\}$.

The Feynman parametrizations needed when heavy propagators are in the loop are as follows:

$$\begin{aligned}
\frac{1}{A_1 \cdots A_m B_1 \cdots B_n} &= 2^m \Gamma(m+n) \int_0^\infty d\lambda_1 \cdots d\lambda_m \int_0^1 d\alpha_1 \cdots d\alpha_n \delta(1 - \alpha_1 - \cdots - \alpha_n) \\
&\quad \times \frac{1}{(2\lambda_1 A_1 + \cdots + 2\lambda_m A_m + \alpha_1 B_1 + \cdots + \alpha_n B_n)^{m+n}} , \tag{C.2}
\end{aligned}$$

where the A_i are heavy particle static propagators denominators, and the B_i are relativistic ones.

The integration over a Feynman parameter λ is of the general form:

$$J(C_0, C_1, \lambda_0, d, \nu) \equiv \int_0^\infty (C_0 + C_1(\lambda - \lambda_0)^2)^{-\nu+\frac{d}{2}} d\lambda , \tag{C.3}$$

which satisfies the recurrence relation:

$$\begin{aligned}
J(C_0, C_1, \lambda_0, d, \nu) &= \frac{-\lambda_0(C_0 + C_1\lambda_0^2)^{1-\nu+\frac{d}{2}} + (3+d-2\nu)J(C_0, C_1, \lambda_0, d, \nu-1)}{(d-2\nu+2)C_0}, \\
J(C_0, C_1, \lambda_0, d, \nu) &= C_0 \frac{d-\nu}{d-2\nu+1} J(C_0, C_1, \lambda_0, d, \nu+1) + \frac{\lambda_0}{d-2\nu+1} (C_0 + C_1\lambda_0^2)^{\frac{d}{2}-\nu}.
\end{aligned} \tag{C.4}$$

Integrals with factors of λ in the numerator are obtained by using,

$$\begin{aligned}
J(C_0, C_1, \lambda_0, d, \nu, n=1) &\equiv \int_0^\infty (\lambda - \lambda_0)^{n=1} (C_0 + C_1(\lambda - \lambda_0)^2)^{-\nu+\frac{d}{2}} d\lambda \\
&= -\frac{1}{2C_1(\frac{d}{2}+1-\nu)} (C_0 + C_1\lambda_0^2)^{\frac{d}{2}+1-\nu},
\end{aligned} \tag{C.5}$$

and the recurrence relations

$$J(C_0, C_1, \lambda_0, d, \nu, n) = \frac{1}{C_1} (J(C_0, C_1, \lambda_0, d, \nu-1, n-1) - C_0 J(C_0, C_1, \lambda_0, d, \nu, n-2)). \tag{C.6}$$

For convenience in some of the calculations for the currents, one defines:

$$\tilde{J}(C_0, C_1, \lambda_0, d, \nu, n) \equiv J(C_0, C_1, \lambda_0, d, \nu, n) + \lambda_0 J(C_0, C_1, \lambda_0, d, \nu). \tag{C.7}$$

For the calculations in this work the following integrals are needed at $d = 4 - 2\epsilon$:

$$\begin{aligned}
J(C_0, C_1, \lambda_0, d, 3) &= \frac{1}{\sqrt{C_0 C_1}} \left(\frac{\pi}{2} + \arctan(\lambda_0 \sqrt{\frac{C_1}{C_0}}) \right), \\
J(C_0, C_1, \lambda_0, d, 2) &= \frac{1}{d-3} (\lambda_0 (C_0 + C_1\lambda_0^2)^{\frac{d}{2}-2} + (d-4)C_0 J(C_0, C_1, \lambda_0, d, 3)), \\
J(C_0, C_1, \lambda_0, d, 1) &= \frac{1}{d-1} (\lambda_0 (C_0 + C_1\lambda_0^2)^{\frac{d}{2}-1} + (d-2)J(C_0, C_1, \lambda_0, d, 2)).
\end{aligned} \tag{C.8}$$

C.1 Specific integrals

Here a summary of relevant one-loop integrals for the calculations in this work is provided for the convenience of the reader.

1) Loop integrals involving only relativistic propagators

$$\begin{aligned}
I(0, 1, M) &= -\frac{i}{(4\pi)^{\frac{d}{2}}} \Gamma(1 - \frac{d}{2}) M^{d-2} \\
I(0, 2, M) &= \frac{i}{(4\pi)^{\frac{d}{2}}} \Gamma(2 - \frac{d}{2}) M^{d-4} \\
I(1, 1, M) &= \frac{i}{(4\pi)^{\frac{d}{2}}} \frac{d}{2} \Gamma(-\frac{d}{2}) M^d \\
I(1, 2, M) &= -\frac{i}{(4\pi)^{\frac{d}{2}}} \frac{d}{2} \Gamma(1 - \frac{d}{2}) M^{d-2} \\
K(q, M_a, M_b) &\equiv \int \widetilde{d^d k} \frac{1}{(k^2 - M_a^2 + i\epsilon)((k+q)^2 - M_b^2 + i\epsilon)} = \int_0^1 d\alpha I(0, 2, \Lambda(\alpha)) \\
K^\mu(q, M_a, M_b) &\equiv \int \widetilde{d^d k} \frac{k^\mu}{(k^2 - M_a^2 + i\epsilon)((k+q)^2 - M_b^2 + i\epsilon)} = \int_0^1 d\alpha (\alpha - 1) q^\mu I(0, 2, \Lambda(\alpha)) \\
K^{\mu\nu}(q, M_a, M_b) &\equiv \int \widetilde{d^d k} \frac{k^\mu k^\nu}{(k^2 - M_a^2 + i\epsilon)((k+q)^2 - M_b^2 + i\epsilon)} \\
&= \int_0^1 d\alpha ((1 - \alpha)^2 q^\mu q^\nu I(0, 2, \Lambda(\alpha)) + \frac{g^{\mu\nu}}{d} I(1, 2, \Lambda(\alpha))), \tag{C.9}
\end{aligned}$$

where:

$$\Lambda(\alpha) = \sqrt{\alpha M_a^2 + (1 - \alpha) M_b^2 - \alpha(1 - \alpha) q^2}$$

2) Loop integrals involving one heavy propagator

$$\begin{aligned}
H(p^0, M) &\equiv \int \widetilde{d^d k} \frac{1}{(p^0 - k^0 + i\epsilon)(k^2 - M^2 + i\epsilon)} \\
&= \frac{2i}{(4\pi)^{\frac{d}{2}}} \Gamma(2 - \frac{d}{2}) J(M^2 - p^{02}, 1, p^0, d, 2) \\
H^{ij}(p^0, M) &\equiv \int \widetilde{d^d k} \frac{k^i k^j}{(p^0 - k^0 + i\epsilon)(k^2 - M^2 + i\epsilon)} \\
&= -\frac{i}{(4\pi)^{\frac{d}{2}}} g^{ij} \Gamma(1 - \frac{d}{2}) J(M^2 - p^{02}, 1, p^0, d, 1) \tag{C.10} \\
H^{ij\mu}(p^0, M_a, M_b, q) &\equiv \int \widetilde{d^d k} \frac{k^i (k+q)^j (2k+q)^\mu}{(p^0 - k^0 + i\epsilon)(k^2 - M_a^2 + i\epsilon)((k+q)^2 - M_b^2 + i\epsilon)} \\
&= i \frac{4}{(4\pi)^{\frac{d}{2}}} \int_0^1 d\alpha \left\{ -\frac{1}{2} \Gamma(3 - \frac{d}{2}) q^i q^j \alpha(1 - \alpha) \right. \\
&\quad \times \left((1 - 2\alpha) q^\mu J(C_0, C_1, \lambda_0, d, 3) - 2 g^{\mu 0} \tilde{J}(C_0, C_1, \lambda_0, d, 3, 1) \right) \\
&\quad + \Gamma(2 - \frac{d}{2}) \left(-(1 - 2\alpha) g^{ij} q^\mu + 2(\alpha g^{\mu i} q^j - (1 - \alpha) g^{\mu j} q^i) \right) J(C_0, C_1, \lambda_0, d, 2) \\
&\quad \left. + 2 g^{ij} g^{\mu 0} \tilde{J}(C_0, C_1, \lambda_0, d, 2, 1) \right\},
\end{aligned}$$

where:

$$\begin{aligned}
C_0 &= \alpha M_a^2 + (1 - \alpha) M_b^2 - p^{02} - 2(1 - \alpha) p^0 q^0 - (1 - \alpha)(\alpha q^2 + (1 - \alpha) q^{02}) \\
C_1 &= 1 \\
\lambda_0 &= p^0 + (1 - \alpha) q^0.
\end{aligned} \tag{C.11}$$

Computing the polynomial pieces of the integrals, one obtains:

$$\begin{aligned}
H(p^0, M)^{\text{poly}} &= \frac{i}{(4\pi)^2} 2p^0 (\lambda_\epsilon + 2) \\
H^{ij}(p^0, M)^{\text{poly}} &= \frac{i}{(4\pi)^2} \frac{p^0}{3} ((3M^2 - 2p^{02}) \lambda_\epsilon + 7M^2 - \frac{16}{3} p^{02}) \\
H^{ij0}(p^0, M_a, M_b, q)^{\text{poly}} &= \frac{i}{6(4\pi)^2} ((2q^i q^j + q^2 g^{ij}) \lambda_\epsilon + q^2 g^{ij} - 3(\lambda_\epsilon + 1)(M_a^2 + M_b^2) g^{ij} \\
&\quad + 3(\lambda_\epsilon + 2)(2p^0 + q^0)^2 g^{ij}),
\end{aligned} \tag{C.12}$$

where the UV divergency is given by the terms proportional to $\lambda_\epsilon \equiv 1/\epsilon - \gamma + \log 4\pi$, where $d = 4 - 2\epsilon$.

APPENDIX D

USEFUL OPERATOR REDUCTION FORMULAS

The reductions of multi-body spin-flavor operators which appear in the polynomial contributions of the one-loop corrections to the self-energy and the currents require some lengthy work, and are therefore provided here. The reductions are only valid for matrix elements between states in the totally symmetric irrep of $SU(6)$.

1. Self-energy:

$$\begin{aligned}
[[\delta\hat{m}, G^{ia}], G^{ia}] &= \frac{C_{HF}}{N_c} \left(\frac{7}{2} \hat{S}^2 - \frac{3}{8} N_c(N_c + 6) \right) \\
[[\delta\hat{m}, [\delta\hat{m}, G^{ia}]], G^{ia}] &= \left(\frac{C_{HF}}{N_c} \right)^2 (4\hat{S}^4 - (N_c(N_c + 6) - 18)\hat{S}^2 - \frac{3}{2} N_c(N_c + 6)) \\
[[\delta\hat{m}, [\delta\hat{m}, [\delta\hat{m}, G^{ia}]]], G^{ia}] &= \left(\frac{C_{HF}}{N_c} \right)^3 (36\hat{S}^4 - (5N_c(N_c + 6) - 36)\hat{S}^2 - 3N_c(N_c + 6)) \\
M_a^2 G^{ia} G^{ia} &= 2B_0 \left(m^0 \hat{G}^2 + m^a \left(-\frac{7}{24} \{S^i, G^{ia}\} + \frac{3}{16} (N_c + 3) T^a \right) \right) \\
M_a^2 [[\delta\hat{m}, G^{ia}], G^{ia}] &= 4 \frac{C_{HF}}{N_c} B_0 \left(\frac{8}{3} m^0 \hat{S}^2 + \frac{5}{12} m^a \{S^i, G^{ia}\} \right) - 4M_a^2 G^{ia} G^{ia}
\end{aligned} \tag{D.1}$$

2. Vector currents:

$$\begin{aligned}
G^{ia}[\delta\hat{m}, [\delta\hat{m}, G^{ia}]] &= \left(\frac{C_{HF}}{N_c}\right)^2 \left(\frac{3}{4}N_c(N_c+6) + \left(\frac{1}{2}N_c(N_c+6) - 9\right)\hat{S}^2 - 2\hat{S}^4\right) \\
[\delta\hat{m}, G^{ia}][\delta\hat{m}, G^{ia}] &= -G^{ia}[\delta\hat{m}, [\delta\hat{m}, G^{ia}]] \\
G^{ib}T^a[\delta\hat{m}, [\delta\hat{m}, G^{ib}]] &= -[\delta\hat{m}, G^{ib}]T^a[\delta\hat{m}, G^{ib}] \\
&= \left(\frac{C_{HF}}{N_c}\right)^2 \left(3(N_c+3)S^i G^{ia} + \left(\frac{3}{4}(N_c(N_c+6) - 6) \right. \right. \\
&\quad \left. \left. + \frac{1}{2}(N_c(N_c+6) - 30)\hat{S}^2 - 2\hat{S}^4\right)T^a\right) \\
[[T^a, G^{ib}], [\delta\hat{m}, [\delta\hat{m}, G^{ib}]]] &= -[[T^a, [\delta\hat{m}, G^{ib}]], [\delta\hat{m}, G^{ib}]] \\
&= 2[\delta\hat{m}, G^{ib}]T^a[\delta\hat{m}, G^{ib}] - \{T^a, [\delta\hat{m}, G^{ib}][\delta\hat{m}, G^{ib}]\} \\
f^{abc}f^{bcd}M_b^2T^d &= 6B_0(m^0T^a + \frac{1}{4}d^{abc}m^bT^c) \\
M_b^2G^{ib}T^aG^{ib} &= 2B_0\left(m^0(\hat{G}^2 - \frac{9}{8})T^a \right. \\
&\quad \left. + \frac{1}{2}m^b\left(\frac{1}{2}\{T^a, \frac{3}{8}(N_c+3)T^b - \frac{7}{24}S^iG^{ib}\} - \frac{3}{4}d^{abc}T^c\right)\right) \\
M_b^2[[T^a, G^{ib}], G^{ib}] &= \frac{9}{2}B_0\left(m^0T^a + \frac{1}{4}m^bd^{abc}T^c\right)
\end{aligned} \tag{D.2}$$

3. Axial-vector currents:

$$\begin{aligned}
G^{jb}G^{ia}[\delta\hat{m}, [\delta\hat{m}, G^{jb}]] + h.c. &= \left(\frac{C_{HF}}{N_c}\right)^2 \left(\frac{3}{2}N_c(N_c+6)G^{ia} + \left(\frac{1}{2}N_c(N_c+6) - 14\right)\{\hat{S}^2, G^{ia}\} \right. \\
&\quad \left. - \{\hat{S}^2, \{\hat{S}^2, G^{ia}\}\} + \frac{3}{2}(N_c+3)S^iT^a + 2S^iS^jG^{ja}\right) \\
[\delta\hat{m}, G^{jb}]G^{ia}[\delta\hat{m}, G^{jb}] &= \left(\frac{C_{HF}}{N_c}\right)^2 \left(-\frac{1}{2}\left(3 + \frac{1}{2}N_c(N_c+6)\right)G^{ia} \right. \\
&\quad + \frac{1}{2}\left(13 - \frac{1}{2}N_c(N_c+6)\right)\{\hat{S}^2, G^{ia}\} + \frac{1}{2}\{\hat{S}^2, \{\hat{S}^2, G^{ia}\}\} \\
&\quad \left. - \frac{5}{4}(N_c+3)S^iT^a\right) \\
f^{acd}f^{bcd}M_c^2G^{ib} &= 6B_0(m^0\delta^{ab} + \frac{1}{4}m^cd^{abc})G^{ib} \\
M_b^2G^{jb}G^{ia}G^{jb} &= \frac{1}{2}\{G^{ia}, M_b^2G^{jb}G^{jb}\} - \frac{B_0}{12}(23m^0G^{ia} \\
&\quad + m^b\left(\frac{5}{3}\delta^{ab}S^i + \frac{11}{4}d^{abc}G^{ic}\right))
\end{aligned} \tag{D.3}$$

VITA

ISHARA PRIYASAD FERNANDO

301, Saint Thomas Drive, Apt E, Newport News, VA 23606, 757-405-4706, ishara@jlab.org

Education

Doctor of Philosophy (December, 2017)
Physics
Hampton University

Bachelor of Science (October, 2010)
Physics
University of Colombo

Publications and Presentations

1. I. P. Fernando and J. L. Goity, “Predictions for Excited Strange Baryons”, Workshop on Physics with Neutral Kaon Beam at JLab (KL2016) Mini-Proceedings. arXiv:1604.02141 [hep-ph](<https://arxiv.org/abs/1604.02141>): pg. 75-82.
2. I. P. Fernando and J. L. Goity, “Baryon spin-flavor structure from an analysis of lattice QCD results of the baryon spectrum”, Phys. Rev. D **91**, 036005(2015)
<http://journals.aps.org/prd/pdf/10.1103/PhysRevD.91.036005>
3. C. Albertus, E. Ruiz Arriola, I. P. Fernando, J. L. Goity, “Heavy Baryons in the large N_c limit”, Phys. Lett. B **750**, 331-337(2015)
<http://www.sciencedirect.com/science/article/pii/S0370269315007054>
4. K. A. I. L. Wijewardena Gamalath, M. A. I. P. Fernando, “Strain Distributions in Group IV and III-V Semiconductor Quantum Dots”, International Letters of Chemistry, Physics and Astronomy, Vol. 7, pp. 36-48, Sep. 2013
<https://www.scipress.com/ILCPA.7.36>
5. “Baryon masses in $1/N_c$ expansion”
Guest colloquium lecture - University of Peradeniya, Sri Lanka. (June 22, 2016)
6. “An analysis of baryon Masses in $1/N_c$ expansion”
Guest colloquium talk - Hampton University. (February 9th, 2017)
7. “Baryon masses in ChPT combined with $1/N_c$ expansion” Poster competition (1st Place), Users’ Group Meeting - at Jefferson Lab, Newport News, VA. (June 19-21, 2017)